

Some pages of this thesis may have been removed for copyright restrictions.

If you have discovered material in AURA which is unlawful e.g. breaches copyright, (either yours or that of a third party) or any other law, including but not limited to those relating to patent, trademark, confidentiality, data protection, obscenity, defamation, libel, then please read our [Takedown Policy](#) and [contact the service](#) immediately

**OCULAR BIOMETRIC CORRELATES OF EARLY- AND LATE-ONSET
MYOPIA**

Justine Harper
Doctor of Philosophy

Aston University, Birmingham
February 2001

This copy of the thesis has been supplied on condition that anyone who consults it is understood to recognise that its copyright rests with its author and that no quotation from the thesis and no information derived from it may be published without proper acknowledgement.

Aston University
Ocular Biometric Correlates of Early- and Late-Onset Myopia
Justine Harper
Doctor of Philosophy
February 2001

Summary

Myopia is a refractive condition and develops because either the optical power of the eye is abnormally great or the eye is abnormally long, the optical consequences being that the focal length of the eye is too short for the physical length of the eye. The increase in axial length has been shown to match closely the dioptric error of the eye, in that a 1mm increase in axial length usually generates 2 to 3D of myopia.

The most common form of myopia is early-onset myopia (EOM) which occurs between 6 to 14 years of age. The second most common form of myopia is late-onset myopia (LOM) which emerges in late teens or early twenties, at a time when the eye should have ceased growing. The prevalence of LOM is increasing and research has indicated a link with excessive and sustained nearwork. The aim of this thesis was to examine the ocular biometric correlates associated with LOM and EOM development and progression.

Biometric data was recorded on 50 subjects, aged 16 to 26 years. The group was divided into 26 emmetropic subjects and 24 myopic subjects. Keratometry, corneal topography, ultrasonography, lens shape, central and peripheral refractive error, ocular blood flow and assessment of accommodation were measured on three occasions during an 18-month to 2-year longitudinal study. Retinal contours were derived using a specially derived computer program.

The thesis shows that myopia progression is related to an increase in vitreous chamber depth, a finding which supports previous work. The myopes exhibited hyperopic relative peripheral refractive error (PRE) and the emmetropes exhibited myopic relative PRE. Myopes demonstrated a prolate retinal shape and the retina became more prolate with myopia progression. The results show that a longitudinal, rather than equatorial, increase in the posterior segment is the principal structural correlate of myopia. Retinal shape, relative PRE and the ratio of axial length to corneal curvature have been indicated, in this thesis, as predictive factors for myopia onset and development.

Data from this thesis demonstrates that myopia progression in the LOM group is the result of an increase in anterior segment power, owing to an increase in lens thickness, in conjunction with posterior segment elongation. Myopia progression in the EOM group is the product of a long posterior segment, which over-compensates for a weak anterior segment power. The weak anterior segment power in the EOM group is related to a combination of crystalline lens thinning and surface flattening.

The results presented in this thesis confirm that posterior segment elongation is the main structural correlate in both EOM and LOM progression. The techniques and computer programs employed in the thesis are reproducible and robust providing a valuable framework for further myopia research and assessment of predictive factors.

Key Words: myopia, retinal contour, biometry, peripheral refraction

Acknowledgements

I would like to sincerely thank my supervisor, Professor Bernard Gilmartin, for his expert guidance, advice and support throughout my time at Aston. I would also like to thank my associate supervisor, Dr Mark Dunne, for his unfailing enthusiasm and whose computer program and assistance has been essential for the project.

Special thanks go to friends, students and colleagues at Aston University, too numerous to mention them all, for their help and contributions to the project as either subjects or advisors. I would specifically like to thank Dr Fiona Baker simply for being a good friend.

I would like to extend my gratitude to Mr Chris Knight for his extensive reworking and adaptation of the *RetinaFit* computer program.

Many thanks to Bausch and Lomb for their supply of contact lenses and to the College of Optometrists for their travel grant.

To my husband Robert, my Mum, Dad and Sean. Thankyou for your love, support and for wanting me to succeed. Especially for Rob for still wanting to marry me even through the trials and tribulations associated with writing this thesis.

CONTENTS

Summary	2
Acknowledgements	3
Contents	4
List of tables	8
List of figures	10
List of appendices	12
1 EYE DEVELOPMENT AND REFRACTIVE ERROR	13
1.1 Development of refractive error	13
1.2 Growth of the eye	18
1.3 Emmetropization	21
1.3.1 Active emmetropization and nurture	22
1.3.2 Passive emmetropization and nature	23
1.3.3 Clear retinal image models	24
1.4 Myopia development	25
1.4.1 Classification of myopia	27
1.4.2 Prevalence of myopia	29
1.4.3 Progression of myopia	35
1.5 Animals models of myopia	37
1.6 Summary	41
2 LATE-ONSET MYOPIA	42
2.1 Prevalence	42
2.1.1 Gender differences	44
2.2 Progression	44
2.3 Ocular biometric correlates	47
2.4 Accommodation	51
2.4.1 Possible mechanisms for myopia development	53
2.5 Vergence and myopia	55
2.5.1 The near phoria and myopia development	55
2.6 Summary	56
3 PERIPHERAL REFRACTION	57
3.1 Ocular aberrations	57
3.2 Peripheral astigmatism in human eyes	59
3.2.1 Classification of peripheral astigmatism	60
3.2.2 Refractive error and the skiagram	63
3.3 Peripheral astigmatism in schematic eyes	64
3.3.1 Modelling peripheral astigmatism using schematic eyes	65
3.4 Retinal contour	66
3.5 Summary	67
3.6 Aims and objectives of the thesis	68
4 INSTRUMENTATION AND SUBJECTS	69
4.1 Subjects	69
4.2 Biometry measurements	70
4.2.1 Measurement of refractive error	70
4.2.1a Infra-red optometers	71

	4.2.1b The Canon Autorefractometer R-1	72
	4.2.1c Mode of operation	73
	4.2.2 Peripheral refraction	74
	4.2.3 A-scan ultrasound	75
	4.2.4 Keratometry	77
	4.2.5 Topographic corneal mapping system	78
	4.2.6 Measurement of accommodation	79
	4.2.7 Measurement of convergence	80
	4.2.8 Accommodative response	80
	4.2.9 Scheimpflug videography	81
	4.2.10 Ocular blood flow tonograph	83
4.3	Drugs instilled for experimental procedures	85
5	OCULAR BIOMETRIC CORRELATES OF EARLY- AND LATE-ONSET MYOPIA	86
5.1	Introduction	86
5.2	Retinal shape assessment	86
5.3	Guide to abbreviations	88
5.4	Purpose	89
5.5	Methods	89
5.6	Results	92
	5.6.1 Validity and repeatability	92
	5.6.2 Cross-sectional analysis	93
	5.6.3 Longitudinal analysis	101
5.7	Discussion	109
5.8	Summary	114
6	CORNEAL SHAPE IN EMMETROPIA AND MYOPIA	115
6.1	Introduction	115
6.2	Corneal assessment	115
6.3	Corneal curvature	117
6.4	Evaluation of corneal curvature	117
6.5	Purpose	119
6.6	Methods	120
6.7	Results	121
	6.7.1 Validity and repeatability	121
	6.7.2 Cross-sectional analysis	122
	6.7.3 Longitudinal analysis	128
6.8	Discussion	130
6.9	Summary	133
7	OCULAR COMPONENT ANALYSIS AND RETINAL SHAPE	135
7.1	Introduction	135
7.2	Retinal shape	135
7.3	Vergence contributions to emmetropia and myopia	136
7.4	Purpose	137
7.5	Method	138
7.6	Results	140
	7.6.1 Validity and repeatability	140
	7.6.2 Relative PRE	141

	7.6.3	Ocular component analysis by vergence contribution	143
	7.6.4	Retinal contour in myopia onset and progression	149
7.7		Discussion	150
7.8		Summary	154
8		ACCOMMODATION IN EMMETROPIA AND MYOPIA	155
8.1		Introduction	155
8.2		Assessment of accommodation	155
8.3		Purpose	157
8.4		Method	157
8.5		Results	159
	8.5.1	Validity and repeatability	159
	8.5.2	Amplitude of accommodation	160
	8.5.3	Accommodative error index	163
	8.5.4	Accommodation response gradient	165
8.6		Discussion	166
8.7		Summary	169
9		OCULAR BLOOD FLOW IN EMMETROPES AND MYOPES	170
9.1		Introduction	170
9.2		Pulsatile ocular blood flow	170
	9.2.1	The Ocular Blood Flow Tonograph (OBF tonograph)	171
9.3		Purpose	171
9.4		Method	172
9.5		Results	174
9.6		Discussion	177
9.7		Summary	180
10		CRYSTALLINE LENS ASSESSMENT IN EMMETROPIA AND MYOPIA USING THE SCHEIMPFLUG CAMERA	181
10.1		Introduction	181
10.2		The Scheimpflug Principle	181
10.3		Derivation of lens surface curvature	183
10.4		Purpose	184
10.5		Method	184
10.6		Results	186
	10.6.1	Validity and repeatability	186
	10.6.2	Lens surface shape	186
10.7		Discussion	189
10.8		Summary	192
11		GENERAL DISCUSSION	
11.1		Classification of myopia	193
11.2		Predictive factors for myopia onset and progression	194
11.3		Cross-sectional analysis of biometric correlates in emmetropia and myopia	195
11.4		Cross-sectional analysis of biometric correlates in early- and late-onset myopia	198
11.5		Longitudinal ocular biometric changes in myopia onset and progression	199
11.6		Future work	202

References

204

Appendices

226

LIST OF TABLES

TABLE		PAGE
1.1	A summary of previous literature on axial dimensions of the infants eye (Redrawn from Wood, Mutti and Zadnik (1996)).	18
1.2	A summary of previous literature on the corneal power of the infant eye. (redrawn from Wood, Mutti and Zadnik (1996)).	19
1.3	Coefficients of correlation (r) of refractive error with optical components: Data from seven studies. Redrawn from Goss and Grosvenor (1999).	27
1.4	Prevalence of myopia from birth to the later adult years, from various studies. (Redrawn from Goss and Grosvenor (1999) and Zadnik and Mutti (1998)).	30
1.5	Prevalence of myopia by occupation. Redrawn from Rosenfield and Gilmartin (1998).	34
2.1	Comparison of data reported for the three cross-sectional studies: emmetropes (EMM) and early adult-onset myopes (EAOM). Redrawn from Grosvenor (1994).	48
2.2	Mean changes (+SD) in spherical equivalent refractive error and its components during 3-year longitudinal study, for subjects in each of 3 refractive groups. Redrawn from Grosvenor and Scott (1993).	50
2.3	Correlations between changes in spherical equivalent refractive error and changes in refractive components, for subjects in each of the 3 refractive error groups. Redrawn from Grosvenor and Scott (1993).	50
5.1	Values of validity.	92
5.2	Bias and limits of agreement for repeatability of ocular component measurements on two separate occasions.	93
5.3	Correlation matrix relating subjective (es) and objective (esc) refractive error with vitreous chamber depth (vd) for the right eye on all three occasions (n=50).	94
5.4	Correlation matrix relating subjective (es) and objective (esc) refractive error with anterior chamber depth (acd) for the right eye on all three occasions (n=50).	95
5.5	Correlation matrix relating subjective (es) and objective (esc) refractive error with lens thickness (lt) for the right eye on all three occasions (n=50).	95
5.6	Correlation matrix relating subjective (es) and objective (esc) refractive error with axial length to corneal curvature (al/k) for the right eye on all three occasions (n=50).	96
5.7	Correlation matrix relating subjective (es) and objective (esc) refractive error to retp and retr for the right eye on all three occasions (n=50).	97
5.8	Correlation matrix relating subjective (es) and objective (esc) refractive error to paf for the right eye on two occasions (n=50).	98
5.9a	Mean parameter values for emmetropic subjects, for right eye only on first and final visit.	98
5.9b	Mean parameter values for myopic subjects, for right eye only on first and final visit.	99
5.10	t test probability (p value) for comparison of parameter means in emmetropes and myopes.	99
5.11a	Mean parameter values for early-onset myopic subjects, for right eye on first and final visit.	100
5.11b	Mean parameter values for late-onset myopic subjects, for right eye on first and final visit.	100
5.12	t test probability (p value) for comparison of parameter means in early- and late-onset myopes.	101
5.13a	Results of stepwise multiple regression of final state of refraction (es3 and esc3).	102
5.13b	Results of stepwise multiple regression of final state of refraction (es3 and esc3). Mean data.	104
5.13c	Results of stepwise multiple regression of final state of refraction (es3 and esc3). Reduced parameter data.	105
5.13d	Parameter frequency according to step location. All the different situations are included.	106
5.14	Results of stepwise multiple regression of final state of refraction (es3 and esc3) using early-and late-onset myopia data.	107
5.15a	Results of stepwise multiple regression for difference in refractive error (es3-1 and esc3-1).	108

5.15b	Parameter frequency according to step location.	108
5.16	Results of stepwise multiple regression for difference in refractive error (es3-1). Early- and late-onset myopes only.	109
6.1	Values of validity.	121
6.2	Bias and limits of agreement for repeatability of ocular component measurements on two separate occasions.	122
6.3	Central corneal curvature for all subjects, right and left eyes and on all 3 visits.	122
6.4	Correlation coefficient values (r) for all subjects, at all visits, right and left eye separated, for both keratometry and corneal topography.	124
6.5a	Central corneal curvature for emmetropic subjects, right and left eyes on all 3 occasions.	125
6.5b	Central corneal curvature for myopic subjects, right and left eyes on all 3 occasions.	125
6.6	t Test probability (p value) for comparison of keratometric corneal curvatures in emmetropes and myopes. Right eye only.	126
6.7	Corneal shape (p-value) for right and left eyes over 3 visits.	127
6.8	Mean corneal shape in emmetropes and myopes, right and left eyes on 3 visits.	127
6.9	t test probability (p value) for comparison of corneal shape (p-value) in emmetropes and myopes. Right eye only.	128
6.10	Numerical change in variables over an 18-month to 2-year period. Emmetropes n = 26, myopes n = 24.	128
7.1	Values of validity (n=50).	140
7.2	Repeatability measurements for parameters (n=30).	141
7.3	Percentages of relative myopia found in emmetropes and relative hyperopia found in myopes in nasal and temporal meridians.	142
7.4	The dioptric values of relative PRE for emmetropes and myopes both nasally and temporally.	143
7.5	The calculated mean vergence contributions, retinal shape indicators (r_0 and ρ) and indices for predicting myopia progression (paf and a/k) in emmetropia, late- and early-onset myopia. Mean and standard deviations are shown. All powers are expressed in dioptres and distances in millimeters.	144
7.6	ANOVA and post hoc results to compare emmetrope, late- and early-onset myopia means for each parameter.	145
7.7	The calculated change in mean vergence contributions and retinal shape indicators (r_0 and ρ) in progressing emmetropia, late- and early-onset myopia. Mean and standard deviations are shown. All powers are expressed in dioptres and distances in millimeters.	146
8.1	Values of validity.	159
8.2	Values of repeatability.	159
9.1	Mean and standard deviations for refractive error, axial length, intraocular pressure, pulse amplitude, pulse volume and ocular blood flow measured with the OBF Tonograph.	174
9.2	ANOVA and post hoc results to compare emmetrope, late- and early-onset myopia means for each parameter.	177
10.1	Values of validity for lens curvature calculations.	186
10.2	Values of repeatability for lens curvature calculations.	186
10.3	Anterior and posterior lens surface parameters and lens thickness (\pm S.D.) in emmetropes and myopes.	188
10.4	Change in anterior and posterior lens surface parameters and lens thickness (\pm S.D.) in progressive late-onset (LOM prog) and progressive early-onset (EOM prog) myopes. Right eyes only (Lom prog n = 7 and Eom prog n = 8).	189

LIST OF FIGURES

FIGURE		PAGE
1.1	(a) Distribution of corneal radius. (b) Distribution of anterior chamber depth. (c) Distribution of lens power. (d) Distribution of axial length. (e) Distribution of refractive error. Distributions a – c fit a normal distribution while d and e do not (after Stenström, 1946).	15
1.2	Distribution of refractive error in new-borns. Re-drawn from data by Cook and Glasscock (1951)	17
1.3	The distribution of refractive errors. X-axis, refraction (D); y-axis, number of subjects. After Sorsby et al. (1961).	22
1.4	Myopia prevalence with age (criterion for myopia is 0.50D or greater). After Grosvenor (1987).	28
1.5	Percentage of eyes showing a hyperopic or myopic shift of $\geq 0.25D$ or no shift ($\leq 0.12D$) in SPEQ between the entrance and third academic year examinations (2.5 year period) for 994 eyes. Redrawn from O'Neal and Cannon (1987).	32
1.6a	Childhood myopia progression. Data from five males. After Goss and Winkler (1983).	36
1.6b	Childhood myopia progression. Data from five females. After Goss and Winkler (1983).	36
2.1a	Example of adult stabilization of myopia. 5 subjects and each symbol represents the refractive error (D) in the principal meridian nearest horizontal in the right eye. After Goss et al. (1985).	45
2.1b	Example of adult continuation of myopia progression. 4 subjects and each symbol represents the refractive error (D) in the principal meridian nearest horizontal. Re-drawn from Goss et al. (1985).	46
2.1c	Example of adult acceleration of myopia progression. 3 subjects and each symbol represents the refractive error (D) in the principal meridian nearest horizontal. Re-drawn from Goss et al. (1985).	46
3.1	Tangential image shell (T) and sagittal image shell (S) formed by an oblique ray bundle (O). After Dunne (1995).	58
3.2a	Showing the peripheral refraction types A and B. After Ferree et al. (1931).	61
3.2b	Showing three type C eyes. After Ferree et al. (1932).	61
4.1	Static 'single-shot' recording through 4 pupil diameters illustrating the change in waveform. The charts demonstrate the difficulty in locating the peak position in small pupils. After Winn et al. (1989).	74
4.2	Canon Autorefractometer R-1. Arc fitted for taking measurements of peripheral refraction.	74
4.3	Omega Ultrasound (Storz).	77
4.4	Eyesys 2000 Corneal Topography System.	79
4.5	Scheimpflug camera (Marcher instruments).	82
4.6	Schematic drawing of the OBF tonograph in contact with the cornea. After Hosking et al. (2000).	84
5.1	Vitreous chamber depth plotted against refractive error for the right eye on the first visit (n=50).	94
5.2	The ratio of axial length to corneal curvature (a/k) plotted against subjective refractive error for the right eye on the 1 st visit (n=50).	96
5.3	A tally chart of parameters plotted against frequency of occurrence	106
6.1	Schematic illustration of ellipsoids	119
6.2	Keratometric central corneal curvature plotted against refractive error for the right eye on the first visit (n = 50).	123
6.3	Corneal topography central corneal curvature plotted against refractive error for the right eye on the first visit (n = 50).	123
6.4	Keratometric corneal curvature plotted against vitreous chamber depth. Right eye (n = 50).	124
6.5a	Keratometric central corneal curvature plotted against refractive error in emmetropes, for the right eye, on the first visit (n = 26).	125
6.5b	Keratometric central corneal curvature plotted against refractive error in myopes, for the right eye, on the first visit (n = 24).	126

6.6	Change in refractive error, over an 18-month to 2-year period, plotted against change in keratometric corneal curvature. Myopes only, right eye (n = 24).	129
6.7	Change in refractive error, over an 18-month to 2-year period, plotted against change in corneal shape. Right eye only (n = 50).	130
7.1	Formation of vergence contributions through the eye.	136
7.2a	Subjective refractive error plotted against relative PRE at 35° in the nasal meridian. Right eye only (n=50).	141
7.2b	Subjective refractive error plotted against relative PRE at 35° in the temporal meridian. Right eye only (n=50).	142
7.3	The initial paf values plotted against the change in refractive error over the study period (n = 100).	147
7.4	Initial al/k ratios plotted against the change in refractive error over the study period. N = 100.	148
7.5	Mean retinal contour for a -3.00D myope derived from 5 separate set of peripheral refraction measurements. Error bars represent ±SEM.	149
7.6	Retinal contours plotted for progressive emmetropes (n = 8), progressive late-onset myopes (n = 10) and progressive early- onset myopes (n = 10) at initial and final visits. Negative equatorial coordinates represent the nasal retina and positive the temporal retina.	150
8.1	Amplitude of accommodation plotted against refractive error (n = 50).	160
8.2	Mean amplitudes of accommodation in emmetropes (Emm), early-onset myopes (EOM) and late-onset myopes (LOM). Error bars represent ±1 SEM.	161
8.3	Mean amplitudes of accommodation for the stable emmetropic group (Emm1), progressing emmetropic group (Emm2), stable myopic group (Myo1) and progressing myopic group (Myo2). Error bars represent ±1 SEM.	162
8.4	Accommodative error index plotted against refractive error (n = 45).	163
8.5	Mean accommodative error indices in emmetropes (Emm), early-onset myopes (EOM) and late-onset myopes (LOM). Error bars represent ±1 SEM.	163
8.6	Mean accommodative error index plotted against progressive late-onset myopes (LOM prog) and progressive early-onset myopes (EOM prog). Error bars represent ±1SEM.	164
8.7	Accommodation response gradients plotted for emmetropes (Emm), stable myopes (Myo1) and progressive myopes (Myo2). Error bars represent ±1 SEM.	165
9.1	Intraocular pressure plotted against refractive error for all right eyes (n = 48).	174
9.2	Pulse amplitude plotted against refractive error for all right eyes.	175
9.3	Pulse volume plotted against refractive error for all right eyes.	175
9.4	Ocular blood flow plotted against refractive error for all right eyes.	176
10.1	The Scheimpflug Rule	182
10.2	Image obtained using the Scheimpflug camera (after Harper, 1999).	182
10.3	Refractive error plotted against asphericity for the anterior lens surface. Right eye only (n = 48).	187
10.4	Refractive error plotted against apical radius for the anterior lens surface. Right eye only (n = 48).	187
11.1	Retinal contours plotted for progressive emmetropes (n = 8), progressive late-onset myopes (n = 10) and progressive early- onset myopes (n = 10) at initial and final visits. Negative equatorial coordinates represent the nasal retina and positive the temporal retina.	199

LIST OF APPENDICES

1	Biometric measurements	227
2	Recruitment letters	230
3	University Ethical Committee forms and consent forms	233
4	Calculations and computer programs relating to the thesis	240
5	Statistical analysis	253
6	Data relating to corneal curvature and shape	259
7	Data relating to peripheral refractive error, retinal curvature and retinal shape	262
8	Data relating to accommodation	265
9	Data relating to intraocular pressure and ocular blood flow	266
10	Data relating to crystalline lens curvature and shape	267
11	ARVO abstract	268
12	Ocular volume	269

CHAPTER 1

EYE DEVELOPMENT AND REFRACTIVE ERROR

Introduction

The aetiology of myopia has instigated a great deal of interest over many years and has been the focus of numerous research studies. A high proportion of the literature discussed in this chapter reflects the many theories proposed for the development and causes of myopia. Special interest has been given to a particular classification of myopia: late-onset myopia.

1.1 Development of refractive error

Emmetropia is a refractive state of the eye whereby, when accommodation is relaxed, the image of an object at infinity is sharply focused on the retina. The mechanism of emmetropization co-ordinates the development of the various ocular components of the eye, i.e. corneal curvature, anterior chamber depth, crystalline lens and vitreous depth, to produce emmetropia (Sorsby, 1967). Emmetropization is a product of an active mechanism, which regulates the growth of one or more ocular parameters through a feedback response based on the quality of the retinal image.

In the absence of emmetropia the eye has a refractive error and this is often termed ametropia. Ametropia is a refractive state of the eye in which, when accommodation is relaxed, the image of an object at infinity is not sharply focused on the retina and this produces an indistinct retinal image. Ametropia can be categorised into three types: myopia, hypermetropia and astigmatism. Myopia is a refractive condition and when accommodation is relaxed, the image from a distant object is focused in front of the retina. In contrast, images from distant objects are focused behind the retina in hypermetropia. Astigmatism is a refractive condition in which the image of a point object is not a single point but separated into two usually perpendicular lines at different distances from the optical system.

McBrien and Barnes (1984) reviewed three major theories for emmetropization and ametropia: the biological-statistical theory, the use-abuse theory and the theory of emmetropization.

Biological-statistical theory

According to Sorsby *et al.* (1957) and Sorsby (1967) ametropia can develop in two ways, these are: -

Correlation ametropia - all the ocular component values lie within the normal range of emmetropic values. Ametropia arises when there appears to be a lack of correlation between the ocular components. This form of ametropia produces the majority of refractive errors within the range of +6 to -4D implying that the correlation between components is at fault and not the components themselves.

Component ametropia - occurs when the value of one particular component falls outside the normal emmetropic range. Eyes with a high refractive error are generally a result of component ametropia and, in the majority of cases, it is due to an abnormal axial length. See figure 1.1 that illustrates the distribution of certain ocular components.

Use-abuse theory

A longitudinal study by Young (1977) found a correlation between the amount of time spent reading and myopia. The study revealed that continual accommodation and nearwork disturbed the normal response characteristics of the ciliary muscle, giving temporary changes in lens thickness, which eventually induced an increase in vitreous depth leading to a myopic refractive error.

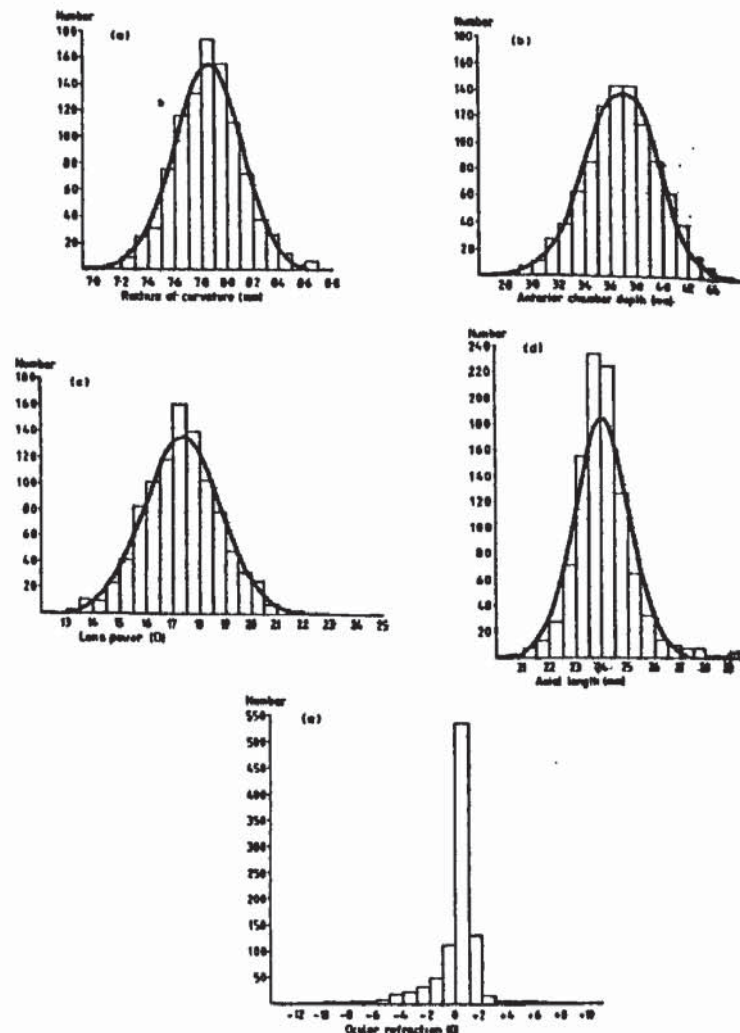


Figure 1.1 (a) Distribution of corneal radius. (b) Distribution of anterior chamber depth. (c) Distribution of lens power. (d) Distribution of axial length. (e) Distribution of refractive error. Distributions a – c fit a normal distribution while d and e do not (after McBrien and Barnes, 1984).

Theory of emmetropization

Van Alphen (1961) carried out a detailed statistical study of the component values of refraction using data compiled by Stenstrom (1946). See figure 1.1.

Analysis of the components revealed three factors associated with emmetropia and ametropia. The factors were:-

1. *Size* – loadings in corneal curvature and axial length. Independent of refraction, larger eyes would have flatter corneae.
2. *Stretch* – loadings in axial length, anterior chamber depth and lens power. Predicts that larger eyes have deeper anterior chambers and flatter lenses.
3. *Derailment* – loadings in all variables. Associated with the resistance offered to the intraocular pressure by the ciliary muscle-choroid layer.

Van Alphen suggested that the size factor of the eye was not important when determining refraction but the stretch factor was important. Scleral stretch would increase axial length. The ciliary muscle-choroid layer would stretch, displacing the iris lens diaphragm posteriorly which would result in a deeper anterior chamber depth and would also flatten the crystalline lens. Traditionally, only parasympathetic receptors had been recognized on the ciliary muscle, but in 1965, van Alphen *et al.*, noted the presence of both alpha- and beta-receptors whilst testing adrenergic blocking drugs on animal intraocular muscle tissue. Similarly, van Alphen (1976) found sympathetic receptors on human tissue. A number of investigators produced evidence for inhibition of accommodation using sympathetic nervous system agonists, i.e. sympathomimetics (Graves, 1926; Cogan, 1937; Biggs *et al.*, 1959; Heath, 1936 and van Alphen, 1961). Further research by Gilmartin (1986) and Gilmartin *et al.* (1992) detected sympathetic innervation, on the ciliary muscle, in the form of two subclasses of inhibitory adrenoceptors, i.e. beta-2 and alpha-1 inhibitory receptors. High densities of alpha-2 adrenergic receptors, predominately of the alpha-2A subtype, have been recently found in the human ciliary body and iris (Bylund and Chacko, 1999). Van Alphen proposed that emmetropization was under the control of the ciliary muscle-choroid layer and was dependent upon the autonomic nervous system. A closed loop, negative feedback model was used to describe emmetropia which implied that hypermetropia was a result of excess parasympathetic innervation during ocular growth and myopia a result of excess sympathetic innervation. Cortical and subcortical centres control the ciliary muscle tonus and maintain emmetropia. Ametropia is produced when factors interfere with this emmetropization mechanism. In a review, Gilmartin (1986), discusses the concept of dual innervation of the ciliary muscle during accommodation and concludes that although there is evidence to suggest that the autonomic nervous system and accommodation plays an important role in emmetropization, genetics and hereditary cannot be ignored.

Cross sectional and longitudinal studies

In 1951, Cook and Glasscock researched the development of refractive error in 100 neonate eyes following the use of atropine. The mean refractive error was found to be +1.50D. The majority of neonates were hypermetropes: 57% showing hypermetropia to +4D and a further 18% between +4D and +12D. The remaining 25% were myopes with refractive errors up to -12D. Cook and Glasscock suggested either poor cycloplegia or

prematurity as explanations for the high percentage of myopic infants. Between 17% and 63% of the subjects presented with greater than 1D of astigmatism. The majority of this astigmatism was against-the-rule. See Figure 1.2 below.

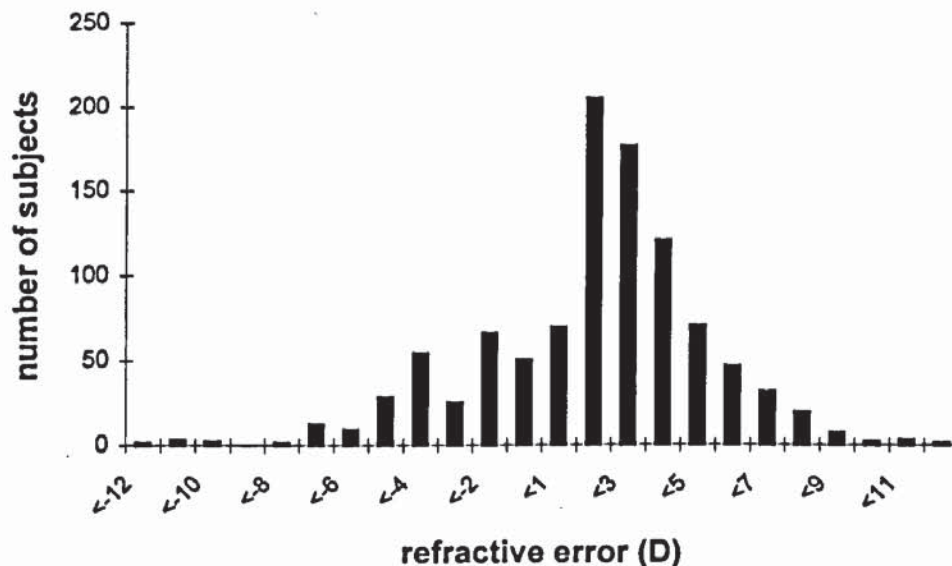


Figure 1.2 Distribution of refractive error in new-born infants. Re-drawn from data by Cook and Glasscock (1951).

A further study by Mohindra (1977) developed the technique of non-cycloplegic near retinoscopy, to eliminate the use of cycloplegic drugs, and refracted 400 full-term infants between birth and 5 years of age. A Gaussian distribution of refractive error with a range of -14 to +12D was found for infants aged 0 to 4 weeks and by the age of 2.5 to 5 years the range had reduced from -3 to +4D. A longitudinal study to determine refractive error in 210 newborn infants was investigated by Thompson (1987). At birth almost 80% of the infants had 1D or more of hypermetropia with the average spherical equivalent refractive error being +2.75D (sd \pm 2.60). Thompson found that the range of refractive errors at birth was -4.50 to +9.75D and by 1 year of age the range of refractive errors had reduced to -2.25 to +4D. A number of studies on this subject conclude that there is a large spread of refractions during the first 3 years of life, possibly owing to the fact that eye growth is most rapid during this period and ocular parameters have not yet reached adult proportions.

In 1995, Saunders *et al.* studied the rate of emmetropization in human infants. Using Mohindra's near retinoscopy technique, they refracted 22 infants during the first 6 months of life and then again between 12 and 17 months. The investigators discovered that emmetropization occurred more rapidly in infants with high refractive errors.

1.2 Growth of the eye

Most ocular components undergo rapid change between birth and 3 years of age. During the first five years the vitreous depth increases by 3 to 4mm, anterior chamber depth by 1mm, axial length by 4 to 5mm and the cornea loses between 5 and 10D of power. There is a decrease in ocular power over the first year of life. The reduction in axial length, the decline in corneal power and the crystalline lens change can usually account for this power decrease. See table 1.1 for a summary of the axial dimensions of the infant eye.

Table 1.1 A summary of previous literature on axial dimensions of the infant eye (Redrawn from Wood, Mutti and Zadnik (1996)).

Author	Year	n	Age	ACD (mm)	LT (mm)	AL (mm)
Gernet	1964	36	1-5 days	2.9	3.4	17.1
Luyckx	1966	52	4-7 days	2.6	3.7	17.6
Larsen	1971a,b,d	80	1-5 days	2.4	4.0	16.6
Fledelius	1992	25	37-43 weeks (gestational age)	2.6	3.8	17.3

ACD – anterior chamber depth; AL – axial length; LT – lens thickness.

Axial length

On average, the eye at birth is 18mm long. Many newborns are hypermetropic owing to the lack of compensation from the cornea and lens for the short axial length. By 3 years of age the axial length has increased to approximately 22 to 23mm Sorsby *et al.* (1961). Between the ages of 3 to 13 years, the eye increases in length by just 1mm. Erickson (1991) showed that an increase in axial length of just 1mm results in a myopic shift of approximately 2 to 3D. An increase in axial length of 5mm during infancy should induce a myopic shift of 10 to 15D but this is not normally observed indicating a compensatory power change in the other ocular components. An average adult eye is approximately 24mm in axial length with a range from 20 to 29.5mm (Stenström, 1946).

Corneal curvature

The majority of all post-natal corneal growth occurs within the first few years of life and the cornea of a child is steeper than that of a neonate by approximately 3 to 5D (Sorsby *et al.*, 1961). The mean corneal radius of curvature of 19 infants aged 3 to 18 months was found to be 7.76mm, ranging from 7.35 to 8.46mm (Wood *et al.*, 1996). Mean corneal power was found to be 43.5D. However, Inagaki *et al.* (1985) found infant corneal curvatures to be steeper. They measured the corneal radius of curvature in 22 infants, at the gestation age of 37-43 weeks, and found the mean radius of curvature to be 7.05mm.

Zadnik *et al.* (1993) reported that corneal power varied by only 0.75D in 530 children aged between 6 and 12 years. If corneal power does not change with age, yet axial length increases, the eye must remain emmetropic due to a reduction in crystalline lens power and possibly a change in the lens refractive index. Fledelius (1982) investigated the changes in corneal radius of curvature in a longitudinal study of 67 low birth-weight subjects aged 10 to 18 years. He found at both 10 and 18 years of age the corneal radius ranged from 7.5mm to 8.5mm. See table 1.2 for a literature summary on the corneal power of the infant eye.

Table 1.2 A summary of previous literature on the corneal power of the infant eye. (redrawn from Wood, Mutti and Zadnik (1996)).

Author	Year	n	Age	Corneal power (D)
York and Mandell	1969	8	0-3 months	47.75
Mandell	1967	5	4-15 days	48.80
Inagaki	1986	11	14 days	47.00
Insler et al.	1987	19	39 weeks (gestational age)	46.98

There appears to be some lack of consensus between investigators as to when the cornea stops growing and at what point it reaches adult dimensions. Research by Gordon and Donzis (1985) and Atkinson *et al.* (1980) propose that the majority of corneal growth occurs in the first two years of life with minimal growth after this time. Stenström (1946) and Sorsby *et al.* (1957) both agree that by 3 years of age the corneal radius of curvature has reached adult proportions, whereas, Fledelius and Stubgaard (1986) suggest that the cornea does not reach an adult level until 5 years of age.

A cross-sectional investigation on corneal curvature in 454 subjects, aged between 5 and 80 years of age, revealed a shift from with-the-rule astigmatism, in very young subjects, to against-the-rule astigmatism in older subjects and an increase in oblique astigmatism with age (Fledelius and Stubgaard, 1986). In association, Gwiazda *et al.* (1993a), discovered that children with a negative spherical equivalent, in the first 6 months of infancy, in conjunction with either no astigmatism or against-the-rule astigmatism were more likely to be myopic at school age than children with infantile with-the-rule astigmatism. The study also revealed that children with against-the-rule astigmatism developed myopia early in life than children without any astigmatism. The presence of against-the-rule astigmatism, in infancy, could be used as a predictive factor for development of ametropia (Hirsch, 1964).

Anterior chamber depth

Studies have shown that the anterior chamber depth increases from birth as the eye grows. However, the increase in anterior chamber depth is not a major factor in refractive error development (Goss and Erickson, 1990). A maximum anterior chamber depth of 3 to 4mm is reached by approximately 15 years of age (Sorsby and Leary, 1970).

Crystalline lens

Gordon and Donzis (1985) calculated the refractive power of the crystalline lens and found the mean lens power to be 34.4D in a full-term newborn eye and 18.8D in an adult eye. The equivalent crystalline lens power decreases by approximately 8D during the first year-and-a-half of life and continues to decrease in to the school years. By early adulthood the lens power had stabilized.

Although new fibres are continually being added to the crystalline lens, it either maintains its thickness or undergoes thinning during the first few years of life (Larsen, 1971d). Measurements of crystalline lens parameters in 19 infants, aged 3 to 18 months, were calculated by Wood, Mutti and Zadnik (1996) using previously reported values of ocular dimensions (Larsen, 1971a, b, c and d). The investigators calculated the mean anterior lens radius to be 8.7mm and the posterior lens radius to be 5.6mm. They concluded that the gradient refractive index of the lens must increase during infancy owing to the lens radii values being higher (flatter lens curvature) than values traditionally accepted for infant schematic eyes.

With age, the crystalline lens becomes thicker and the radius of curvature of the anterior and posterior lens surfaces become steeper (Brown, 1974). Typically, these changes in the lens parameters would induce a myopic shift in the refractive error. However, this increase in myopia with age does not generally occur suggesting the involvement of a compensatory mechanism; this is often termed the 'lens paradox' (Pierscionek and Chan, 1989). Hemenger *et al.* (1995) proposed that the compensatory mechanism was a reduction in the gradient refractive index of the lens.

1.3 Emmetropization

Emmetropization is a mechanism which co-ordinates the development of certain ocular components to prevent ametropia and to produce emmetropia. Emmetropia is dependent upon optimum correlation between the corneal radii of curvature, the crystalline lens surface radii, thickness and refractive index, the refractive indices of the ocular media and anterior and posterior chamber depths. For emmetropia to exist there must be a co-ordinated relationship between these ocular components so that the focal length of the optics is conjugate with the axial length of the eye.

According to Cook and Glasscock (1951) the average refractive error at birth is approximately 2D of hyperopia and is considered to show normal distribution (see figure 1.1). Thompson (1987) measured the refractive error in 210 newborn infants during their first week of life and found that approximately 80% of the infants had 1D or more of hypermetropia (see §1.1). However, further research by Mohindra and Held (1981), using a near-retinoscopy refraction technique on 72 infants, found the average refractive error to be slightly myopic at birth with a shift towards emmetropia by 6 months of age. The investigators suggested that the amount of myopia found might be artificially high owing to the use of a non-cycloplegic technique.

Results obtained under cycloplegic conditions were found to shift from myopia or emmetropia, in the first few months after birth, to more hyperopic readings by 6 months of age (Abrahamsson and Sjostrand, 1992; Wood and Hodi, 1992 and Wood *et al.*, 1995).

The eye grows during the first 6 months resulting in a rapid change in the refractive error. As a result, both the myopic and hyperopic refractive errors decrease which produces a more leptokurtotic distribution by 12 months of age (see figure 1.3). The shift towards an increasingly emmetropic state can be attributed to the

'emmetropization' of ocular structures. Emmetropization occurs during the first 4-5 years and adult-like distributions of refractive error can be found by 6 years of age (Mohindra and Held, 1977).

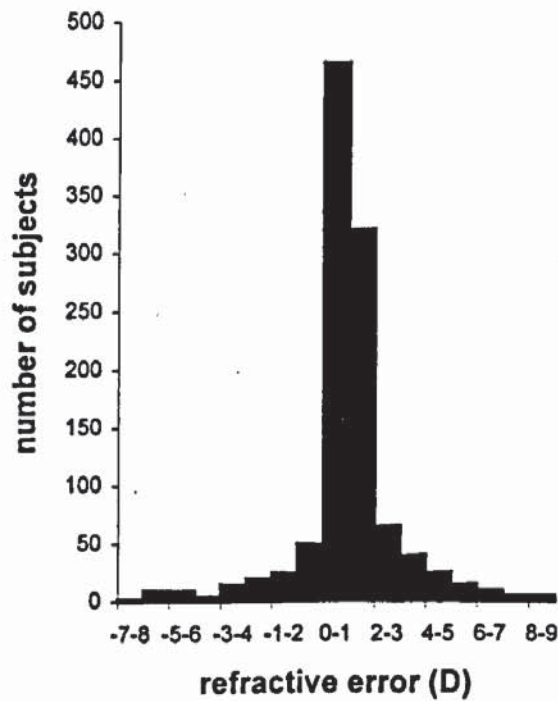


Figure 1.3 The distribution of refractive errors. X-axis, refraction (D); y-axis, number of subjects. After Sorsby *et al* (1961).

Most infantile astigmatism is corneal (Howland and Sayles, 1985). Astigmatism reduces during the period of emmetropization and is often completely eliminated by 5 years of age suggesting that there is also emmetropization of astigmatic errors (Gwiazda *et al.*, 1993a).

1.3.1 Active emmetropization and nurture

The model of emmetropization suggests that the eye is a 'smart organ'. The eye grows and the axial length increases to compensate for the eye's focal length. Evidence for active emmetropization can be obtained from animal experiments (Irving *et al.*, 1992; Irving *et al.*, 1995; Schmid and Wildsoet, 1997; Schaeffel *et al.*, 1988; Wallman and Adams, 1987; Wallman, 1991 and Wildsoet and Wallman, 1995). Irving *et al* (1992) induced ametropia in chick eyes by introducing positive and negative lenses. The chick eye reduced hyperopic blur by growing rapidly whereas the myopic blur was reduced by an increase in the choroidal thickness. The increase in retinal thickness pushes the eye

forward thereby making the eye shorter. Human refractive error studies by Cheng *et al.* (1992) did not show any changes in the choroidal thickness although there is currently growing concern over the extrapolation of animal data to humans proposing inhibition of natural emmetropization with early intervention of prescription lenses (Hung *et al.*, 1995 and Wildsoet, 1997). In a recent study, Smith *et al.* (1999) investigated the effect of unilateral form deprivation in adolescent macaque monkeys. The onset of deprivation was between 3.7 and 5 years of age, which corresponds to 15 to 20 human years; a stage in life where normal axial growth is complete. Prior to form deprivation the monkeys were isometric with matched axial dimensions between the two eyes, yet after 71 to 80 weeks of form deprivation the deprived eyes had become relatively more myopic and exhibited a correlating increase in vitreous chamber depth. The conclusion of the study is that ocular growth is a vision dependent mechanism.

Numerous human studies have reported on the effect of near addition lenses to reduce the progression of myopia. A number of studies comparing either +1D or +2D reading addition in flat-top bifocal form or single vision lenses have been unsuccessful in their attempt to slow myopia progression, particularly when the subjects presented with exophoria at near (Grosvenor *et al.*, 1987; Goss, 1986 and Roberts and Banford, 1967). However, progression rates of myopia were reduced by approximately 0.25D per year when the subjects used bifocal lenses and presented with esophoria at near. Gwiazda *et al.* (1999) found AC/A ratios to be elevated in myopic children. Young myopes presenting with an esophoria underaccommodate at near and relax their accommodation to maintain single binocular vision. Blurred near work, owing to the reduction in accommodation, could result in a myopic shift as shown in animal experiments.

1.3.2 Passive emmetropization and nature

The model proposes that the eye can alter the rate of change of its optics according to changes in its growth. The focal length of the eye changes in response to its size and shape. Passive emmetropization suggests that there is an inborn relationship between eye size and its optics.

Hofstetter (1969) proposed that any eye could be emmetropic, regardless of its size, provided that eye growth occurs in such a way to allow proportionate increase in corneal radii and axial length. Hofstetter's model of proportional growth only shows weak association in human eyes. The eye at birth is 18mm long. By 3 years of age the

axial length has increased to 23mm (Sorsby *et al.*, 1961). Between the ages of 3 to 13 years, the eye increases in length by just 1mm. Erickson (1991) showed that an increase in axial length of just 1mm results in a myopic shift of approximately 2 to 3D. An increase in axial length of 5mm during infancy should induce a myopic shift of 10 to 15D but this is not normally observed suggesting a power change in the other ocular components. A flattening of the lens and increased anterior chamber depth must compensate for the increase in the axial length. The increase in axial length is not counteracted by a change in corneal power due to the cornea having already reached adult values by early infancy (Wood, Mutti and Zadnik, 1996).

1.3.3 Clear retinal image models

Van Alphen (1961) proposed that both the attainment and maintenance of emmetropization was dependent on clear retinal images from each eye and achieved by a closed-loop control mechanism based on the autonomic innervation characteristics of the ciliary muscle-choroid layer (see §1.1). Van Alphen depicted the eye as a self-focusing mechanism, controlled by local and higher centres, in which blurred images control and alter the axial length to account for total refractive power, thereby producing emmetropia.

Medina and Fariza (1993) proposed the existence of a first-order feedback system for emmetropization, whereas Wallman (1991) presented a two-loop feedback model in which the accommodative system and the emmetropization system work in unison to adjust the optical power of the eye to its length.

Degradation and defocus of the retinal image and how they influence the growth of the eye in both animal and human studies are of great importance. Generally, a number of parameters are not fully considered in experimental myopia studies and may have an impact on the results. Flitcroft (1999) devised a computer model to examine the impact of a variety of parameters including habitual viewing distance, ocular refraction, oculomotor performance and spatial sensitivity of the retinal elements when lenses are placed infant of a primate eye. He suggests that both optical and neurophysiological factors must be taken into consideration when comparing the response to lens defocus experiments in both primates and chick eyes.

Emmetropization can be summarised using a dual intersecting feedback loop hypothesis where genetically programmed ocular growth is altered by blur received from the relationship between accommodation and vergence. The shift in refractive error from

emmetropia to myopia may be the result of an intricate mechanism including genetics and environment (Goss *et al.*, 1988). See §1.4.2.

1.4 Myopia development

Myopia is a refractive condition resulting in blurred distance vision. When accommodation is relaxed, the images from distant objects are focused in front of the retina producing an indistinct retinal image. Myopia develops because either the optical power of the eye is abnormally great or the eye is abnormally long, such that, the focal length of the optics of the eye is too short for the physical length of the eye. Erickson (1991) found the amount of myopic error to be directly related to an increase in axial length, or more specifically, to an increase in the vitreous chamber depth.

During the first 4-5 years there is a large decrease in ocular power and a shift towards emmetropia. Gordon and Donzis (1985) analysed the ocular parameter changes, in a cross-sectional study, of 148 eyes ranging from premature newborns to 36 year-old adults. Axial length increases rapidly during the first 2 years of life. During the following year the rate of growth slows to approximately 0.4mm/year with no significant increase in axial length detected after 10 years of age. Although there is a lack of consensus between investigators as to when the cornea stops growing, Gordon and Donzis suggest that the corneal power decreases during the first 6 months with no significant reduction in corneal power after this point in time. Lens power decreases by 8D during the first 18 months of life and continues to decrease, at a slower rate, into the early teenage years. Paradoxically, myopia usually develops after the age of 6, which coincides with a period of relatively slow ocular growth (Zadnik *et al.*, 1993 and Larsen, 1971a, b, c and d). The shift towards myopia can be attributed to an increase in axial length of the eye, which has not been compensated for by either a decrease in lens power or corneal power.

Correlation Studies

Numerous studies have investigated the relationships between refractive error and axial length, corneal power, lens power and anterior chamber depth (see table 1.3). A significant and negative correlation exists between refractive error and axial length (or vitreous chamber depth). A small negative correlation was found between corneal power and refractive error. No significant correlation was found between lens power

and refraction. The negative sign indicates that a more minus refractive error, i.e. myopia, is associated with a greater axial length.

Comparison studies

Many studies have shown that myopic eyes are associated with greater axial lengths, or vitreous chamber depths, compared to emmetropic eyes (McBrien and Adams, 1997; Curtin, 1985 and Sorsby *et al.*, 1962a). Corneal curvature and power varies greatly in both emmetropes and myopes. The majority of investigators found corneal curvature to be steeper and corneal power greater in myopes compared to emmetropes (Curtin, 1985; Sorsby *et al.*, 1957; Grosvenor and Scott, 1991; Scott and Grosvenor, 1993 and Goss *et al.*, 1997). Sheridan (1955) used comparison phakometry to compare the anterior crystalline lens radius between myopic and emmetropic eyes and found no statistically significant difference between myopes and emmetropes. Goss *et al.* (1997) did not find a significant difference in lens power between emmetropes and myopes, measured by phakometry in their study of 176 young adults, although the results did reveal a slight shift towards a flatter posterior lens surface curvature in myopes.

Table 1.3 Coefficients of correlation (r) of refractive error with optical components: Data from seven studies. Redrawn from Goss and Grosvenor (1999).

<i>Study</i>	<i>Sample (n=)</i> <i>age (yrs)</i> <i>country</i>	<i>Axial length</i> <i>(mm)</i>	<i>Power of anterior</i> <i>corneal surface</i> <i>(D)</i>	<i>Crystalline lens</i> <i>power (D)</i>
Stenström (1948a, b)	1000 20-35 Sweden	-0.76	-0.18	0.00
Ohno (1956)	495 14-16 Japan	-0.6	-0.11	+0.39
van Alphen (1961)a	194 <50 Great Britain	-0.77	-0.3	+0.28
Araki (1961)	295 9-56 Japan	-0.77	-0.17	+0.02
Garner <i>et al.</i> (1990)	904 7-17 Malaysia	-0.77	-0.12	+0.30
Goss <i>et al.</i> (1990)	1286 6-40 several data sources	Males:-0.74 Females:-0.76	Males: -0.14 Females: -0.07	- -
Goss <i>et al.</i> (1997)	176 20-44 Oklahoma	-0.71b	-0.28	+0.08

a. Using data from Sorsby *et al.* (1957)

b. Correlation of refractive error with vitreous depth.

1.4.1 Classification of myopia

Different systems of classification of myopia have been attempted by a number of authors and have tended to reflect the vast number of aetiological conditions associated with myopia or the progression of myopia.

Duke-Elder (1949) classified myopia as either simple, as a result of the normal biological distribution, or degenerative. Donders (1864) suggested three categories in which to classify myopia according to progression: stationary myopia, temporarily progressive myopia and permanently progressive myopia. Refractive error distribution and correlation versus component ametropia have also been utilised as categories for

myopia classification (Sorsby *et al.*, 1957; Hirsch, 1950 and Borish, 1970). The problem associated with most classification systems is where cut-off values should lie in order to provide a specific category. Age of onset has been proposed as a simplified way of classifying myopia (Grosvenor, 1987 and Curtin, 1985). Grosvenor examined the prevalence of myopia in British and American populations at birth, in childhood, during the school years and adult years. The prevalence data was used to derive the following categories: -

1. *Congenital myopia*. Present at birth, persists through infancy and manifests by 5 to 6 years of age.
2. *Youth-onset myopia*. The most common type of myopia. Onset occurs around 6 years of age and persists throughout the teenage years.
3. *Early adult-onset myopia*. Onset occurs after physical maturity and ordinarily between 20 and 40 years of age.
4. *Late adult-onset myopia*. This form of myopia presents after 40 years of age and generally progresses in later life. Late adult-onset myopia is often associated with crystalline lens changes, i.e. nuclear sclerosis.

Figure 1.4 shows a graphical representation of the prevalence of myopia with age. The advantages of this classification system proposed by Grosvenor are that no assumptions are made regarding the aetiology of the myopia and the data and cut-off values can be easily checked.

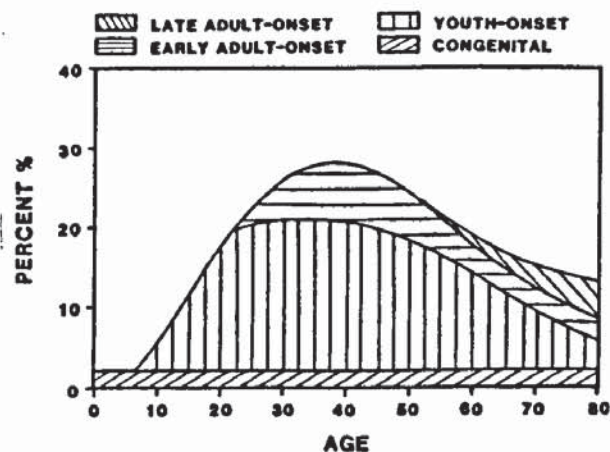


Figure 1.4 Myopia prevalence with age (criterion for myopia is 0.50D or greater). After Grosvenor, 1987.

1.4.2 Prevalence of Myopia

The prevalence of myopia is dependent upon a number of factors: age, education, social and economic status, occupation, gender, ethnicity, genetics and time reading and performing close work.

Age

A high prevalence of myopia has been found in newborns and high myopic refractive errors are common in premature babies of low-birth-weight (Linfield, 1993). Cook and Glasscock (1951) ascertained that 25% of Caucasian neonates were myopic following a cycloplegic investigation using atropine. The results obtained by Goldschmidt (1969) were similar to those of Cook and Glasscock, although Mohindra and Held (1981) found 50% of newborns to be myopic. Fledelius (1981) proposed that the high prevalence of myopia in newborns was a result of the steep cornea found in the immature eye. Mean refractive error reduces towards emmetropia during the first 12 months of life and only 1-2% of the population remain myopic by 5 to 7 years of age (Hirsch, 1964; Blum *et al.*, 1959; Laatikainen and Erkkila, 1980 and Mantyjarvi, 1983). See table 1.4 for selected studies on myopia prevalence with age.

Many children enter school as emmetropes and leave as myopes. A second episode of myopia, often termed youth-onset myopia, occurs around 6 to 7 years of age. The amount of myopia gradually increases during the school years resulting in 25% of Western populations exhibiting myopia by late teens.

The number of myopic subjects reaches a peak between the ages of 18 to 40 years with approximately 30 to 35% of Western populations suffering with myopia.

After the age of 45, some myopes experience a decrease in the amount of myopia and occasionally encounter a shift from myopia to hyperopia (Hirsch, 1958). However, a small percentage of subjects encounter a myopic shift, owing to the appearance of nuclear cataracts, which is frequently termed late-onset myopia.

Table 1.4. Prevalence of myopia from birth to the late adult years. Data from various studies. (Redrawn from Goss and Grosvenor (1999) and Zadnik and Mutti (1998)).

<i>Age (yrs)</i>	<i>Study</i>	<i>Subject</i>	<i>Criterion</i>	<i>Prevalence (%)</i>
Birth	Cook & Glasscock (1951)	Caucasian	any myopia	24
Birth	Goldschmidt (1969)	Danish	any myopia	25
Birth	Mohindra & Held (1981)	Boston, USA	any myopia	50
5-6	Hirsch (1952)	Los Angeles	-1D or more	1
6	Blum et al. (1959)	Orinda, CA	-0.5D or more	2
6	Hirsch (1964)	Ojai, CA	-0.5D or more	2
7-8	Laatikainen & Erkkila (1980)	Finnish	-0.5D or more	2
7	Mantjarvi (1983)	Finnish	-0.25D or more	1
12-17	Sperduto et al. (1983)	USA		23.9
13-14	Hirsch (1952)	Los Angeles	-0.25D or more	23
14-15	Laatikainen & Erkkila (1980)	Finnish	-0.5D or more	22
15	Mantjarvi (1983)	Finnish	-0.25D or more	23
20-30	Borish (1970)	several sources	greater than -0.50D	22
30-40				16
45-49	Hirsch (1958)	Optometric patients	-1.13D or more	7

Gender

A number of researchers have studied the connection between myopia and gender. Peckham *et al.* (1977) and Pendse *et al.* (1951) investigated the relationship between gender and refractive error in junior-school aged children and found no significant correlation. However, Hirsch (1952) detected a greater myopic refractive error in boys

compared to girls aged 5 to 6 years of age although, by 14 years of age the number of myopic females exceeded that of the males. Sperduto *et al.* (1983) found a higher prevalence of myopia in females than in males in a national survey of 14,147 US citizens. The study also revealed differences in prevalence between age groups. Between the ages of 25-34 years, the investigators found 27.8% of females to be myopic and only 20.2% of males. No marked gender differences were observed after the age of 35. The different amounts of myopia prevalence are likely to be a result of the early onset of puberty in females compared to males with no significant gender distinction being noted after the body has ceased growing (Goss and Winkler, 1983).

Intelligence and education

Intelligence, success at school and increasing nearwork demands have frequently been specified as causative factors for myopia. Both Young (1963) and Grosvenor (1970) reported that myopes were more successful at school and received higher grades compared to non-myopes. In an earlier study, Young (1955) observed a small statistically significant correlation between myopia and the subject's IQ and nearwork in a cross-sectional analysis of 6 to 17 year-olds. Complications arise when the amount of nearwork has to be examined separately from intelligence and achievement. When the individual effects of intelligence and nearwork are considered, the findings suggest that achievement, rather than nearwork, has the stronger relationship with myopia progression (Ashton, 1985).

Ethnicity

Extremely high prevalences of myopia have been reported in Southeast Asia. In a study of 18-year-old Taiwanese subjects, 75% were found to be myopic and half had myopic refractive errors in the magnitude of 3D or more (Lin *et al.*, 1988b). The high prevalence of myopia is a growing concern in many Asian countries with reports of 55 to 58% of 12-year-olds in Hong Kong presenting with myopic refractive errors (Edwards, 1998. Cited by Goss and Grosvenor, 1999).

Interestingly, myopia prevalence has also increased in Arctic regions. Young *et al.* (1969) investigated the prevalence of myopia in Eskimo populations. Only a very small percentage of Eskimo parents and grandparents were found to be myopic, whereas almost half of the children of school age had myopic refractive errors. The proposed

explanations for this dramatic increase in myopia are changes in diet, environment, e.g. lighting and the addition of education and schooling.

Occupation and near work demands

A number of studies have associated myopia prevalence with particular occupations and near work demands. Certain occupations require the employee to perform a task at a relatively close working distance and often for a sustained period of time. As early as 1813, Ware reported that many officers in the Queen's guard were myopic whilst the incidence of myopia in the foot guards was relatively low. Data on refractive error from military staff has always been popular with researchers owing to the differences in near work demands between the ranks. Kinney *et al.* (1980) detected an increase in myopia development in Navy submariners, compared to National Guardsmen, over a 3.5 year period. Using previous ocular examination records for students at the United States Air Force Academy, O'Neal and Connon (1987), detected a statistically significant myopic shift of $-0.50D$ or more in 21.3% of the hyperopes, 25% of the emmetropes and 55.1% of the myopes. The researchers suggested that the myopic shift could be related to the intensive educational program and near work environment. See Figure 1.5 showing the percentage of eyes having a shift in refractive error over a 2.5 year period.

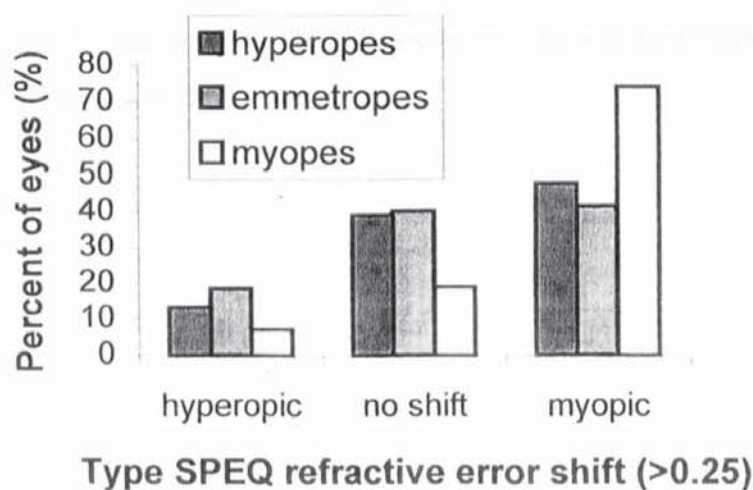


Figure 1.5 Percentage of eyes showing a hyperopic or myopic shift of $\geq 0.25D$ or no shift ($\leq 0.12D$) in SPEQ (spherical equivalent) between the entrance and third academic year examinations (2.5 year period) for 994 eyes. Redrawn from O'Neal and Connon (1987).

Adams and McBrien (1992) and McBrien and Adams (1997) investigated the refractive and biometric changes found in clinical microscopists aged 21 to 63 years. Over a 2-year period, 39% of emmetropic eyes underwent a myopic shift (mean change of $-0.58D \pm 0.04D$) and 48% of myopes progressed by 0.37D or more (McBrien and Adams, 1997). The effects of sustained near work have also been examined in a study of 870 Jewish teenagers aged 15 to 18 years (Zylbermann *et al.*, 1993). A significantly higher prevalence and degree of myopia was revealed in 193 Orthodox Jewish males compared to non-Orthodox. The study habits of Orthodox Jews are intensive comprising long periods of sustained near vision, frequent changes in accommodation, various sizes of print read and in association with a swaying motion. See table 1.5 for prevalence of myopia by occupation.

The introduction of the visual display unit (VDU) and its effect on near vision demand has evoked two recent studies (Mutti and Zadnik, 1996 and Cole *et al.*, 1996). In a longitudinal study by Cole, Maddocks and Sharpe, the VDU users were found to be more myopic by 0.35D than the non-VDU users although the difference was not statistically significant. Similarly, in a review paper, Mutti and Zadnik could find no evidence to suggest that myopia onset or progression was associated with VDU use. There appears to be some agreement between researchers regarding myopia incidence and certain occupations and the majority of studies are longitudinal as this allows differentiation between the non-myopes who progress towards myopia and the myopes who simply become more myopic.

Table 1.5 Prevalence of myopia by occupation. Redrawn from Rosenfield and Gilmartin (1998).

<i>Study</i>	<i>Source</i>	<i>No of patients</i>	<i>Gender and School</i>	<i>Age range (yrs)</i>	<i>Prevalence of myopia (%)</i>
Midelfart <i>et al.</i> 1992	Norwegian Medical students	140		22-26 (presumably)	50.3
Zylberman <i>et al.</i> 1993	Jewish Students	224	Girls, general schools	14-18	31.7
		278	Girls, Orthodox schools		36.2
		175	Boys, general schools		27.4
		193	Boys, Orthodox schools		81.3
Adams and McBrien, 1992	Clinical microscopists	251		21-63	71.0

Inheritance and genetics

Genes are the basic units of hereditary and are responsible for relaying characteristics from parent to child. Genes can exist in alternative forms called alleles that determine which aspect of the characteristic is shown. A heterozygous organism requires two different alleles to control a particular feature but the aspect of the feature will be determined by the dominant allele. A homozygous organism requires two identical alleles to control a particular feature and these may be either dominant or recessive. Heritability is the statistical study of polygenic and multifactorial inheritance. Polygenic inheritance describes variations in appearance by one or more pairs of genes, whereas, multifactorial inheritance accounts for environmental and random variation as well as gene variation between relatives. Goss *et al.* (1988) analysed data from Sorsby *et al.* (1962b) and found heritability values for refractive error to be between 0 and 0.87 with the majority of values within the range of 0.4 to 0.7. Also, in the same study by Sorsby, refractive error showed greater agreement in uniovular twins, than in biovular twins, illustrating the presence of genetic contribution in refractive error development. Low myopia has been studied by a small number of authors (Borish, 1970; Goldschmidt, 1968 and Wold, 1949). Goldschmidt concluded that refraction could not be determined by a single gene, owing to the number of embryologic layers, and must be multifactorial in nature with a high dependence upon environmental factors. Animal experimentation has also indicated that the near-vision environment can induce myopia. Young (1961) placed nine monkeys in restraining chairs, which prevented vision

beyond 20 inches, and found that six of the animals became more myopic by an average of 0.75D after 1 year of confinement. Goldschmidt (1968) suggested that the several classifications of myopia were a result of a number of genetic patterns and, although there is still some uncertainty as to the exact mode of inheritance, myopia appears to develop from the complex behaviour of genetics and environment.

1.4.3 Progression of myopia

Myopia can be present at birth and can also appear during the adult years but the majority of myopia commences in childhood. This type of myopia is often termed youth-onset myopia (Grosvenor, 1987) and once it is detected, it generally increases. Youth-onset myopia originates around 6 years of age and continues throughout the teenage years. Axial elongation of the vitreous chamber has been indicated as the ocular component responsible for the increase in myopia (Sorsby and Leary, 1970). Defining the onset of myopia becomes important when investigating the prevalence or incidence of myopia and different investigators use different definitions. Garner *et al.* (1990) and Edwards and Brown (1996) used a spherical equivalent of $-0.50D$ whereas Rosenfield and Gilmartin (1987b) defined myopia as a spherical equivalent refraction of greater than $-0.50D$. Goss and Winkler (1983) studied 299 patient records with a minimum of 4 refractions recorded between the ages of 6 and 24 years. The requirement for myopia was at least $-0.50D$. The investigators found that the average age of cessation of myopia progression was 15.25 years in females and 16.66 years in males and these are the approximate ages for the end of the adolescent growth spurt. Goss and Cox (1985) described various parameters of myopia progression using a linear regression model. The data was collected for 559 patients, from five optometric practices, where at least 4 examinations had been completed between the ages of 6 and 24 years. The majority of patients were Caucasian. Mean rate of myopia progression for girls was $-0.43D$ per year ($n=145$) and $-0.40D$ per year for boys ($n=158$), although, myopia tends to cease earlier in females compared to males. The study also concluded that development of myopia at an early age normally indicates a high amount of myopia in the future, a finding also reported in studies by Fledelius (1981), Goss (1990) and Grosvenor *et al.* (1987). See figures 1.6a and b for graphs of childhood myopia progression in relation to gender.

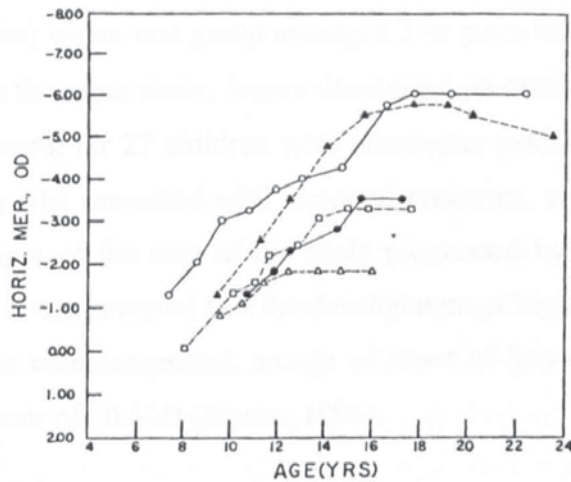


Figure 1.6a Childhood myopia progression. Data from five males. After Goss and Winkler, 1983

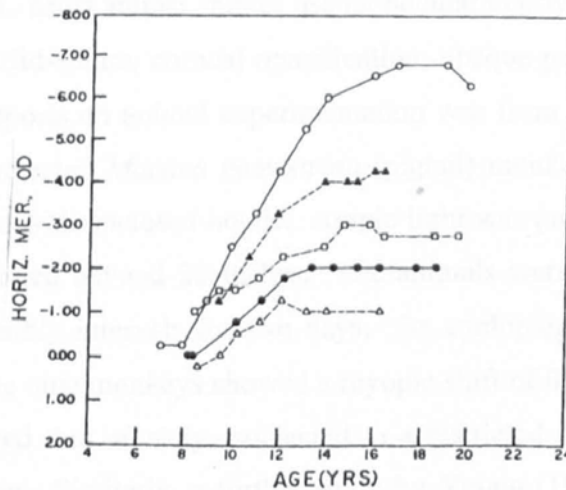


Figure 1.6b Childhood myopia progression. Data from five females. After Goss and Winkler, 1983.

Mean myopia progression rates for the United States and Europe have been found to vary between -0.30 to -0.60 D per year (Goss, 1984; Goss, 1990; Goss, 1994; Baldwin *et al.*, 1969; Mantyjarvi, 1985; Grosvenor *et al.*, 1987 and Jensen, 1991).

Higher myopia progression rates have often been related to time spent reading and under-taking nearwork. A three year longitudinal study by Parssinen *et al.* (1989), in Finland, examined myopic children aged 9 to 11 years and analysed the relationship between refraction and nearwork. The results indicated a weak, but statistically significant, correlation between change in refraction and time spent reading. However, a similar experiment by Jensen (1991) did not find a significant difference when comparing myopia progression, over a 2 year period, between Danish schoolchildren

(aged 9 to 12 years) where one group averaged 2 or more hours reading a day and one group did not. In the same study, Jensen discovered an average myopic progression of $-1.32D$, over 2 years, for 27 children with intraocular pressure higher than 16mmHg. Also, 28 children who presented with temporal crescents, which are normally seen in pathological myopia, at the start of the study progressed by $-1.39D$ in 2 years. In a proceeding study it was revealed that the development of high myopia was correlated to the age of myopia commencement; an age of onset of less than 7 years resulted in a mean refractive error of $-6.60D$ (Jensen, 1995).

1.5 Animal models of myopia

Animal models can provide valuable information on the mechanisms that induce myopia development and permit further investigation into the process of emmetropization. Most animal studies use monocular deprivation techniques to achieve myopia, such as lid-suture, corneal opacification, opaque goggles and occlusion. One of the earliest reports on animal experimentation was from Young (1961). He placed nine randomly selected *Macaca nemestrina* (pigtail) monkeys, aged 4 to 6 years, in restraining chairs with enclosed hoods. Ample light was provided under the hoods but vision was restricted beyond 20 inches. The animals were returned to their cages at biweekly or monthly intervals for two days. On cycloplegic refraction, it was found that six out of the nine monkeys showed a myopic shift of $0.75D$ after six months. The experiment proved that monkeys subjected to a restricted visual environment became myopic over time. Similarly, a further study by Young (1963) concluded that young monkeys reared in a restricted visual space also became myopic and the degree of myopia was dependent upon age of onset, restricted viewing conditions and the level of illumination.

Studies involving form deprivation techniques

Chickens have often been used as experimental animals in myopia and emmetropization studies owing to the fast development of the eyes. Chickens, in a similar way to humans, demonstrate emmetropization and tend to be hyperopic at birth. Chick eyes also exhibit a wide distribution of refractive errors at birth and this variability in refraction narrows with eye development and age (Wallman *et al.*, 1981). However, results obtained through experimentation with chick eyes cannot be directly related to human eyes because the chick eye has both corneal and lenticular accommodation and

the ciliary muscle is striated rather than smooth (Trollo and Wallman, 1987). The mechanism of emmetropization in chick eyes was demonstrated by Wallman and Adams (1987) and Hodos and Kuenzel (1984). The investigators restricted the frontal visual field of chicks, at hatching, using hemispherical occluders for 2, 4 or 6 weeks. The chicks were deprived of form-vision in the nasal visual field, which induced severe myopia. The temporal retina was not affected. The myopic change was found to be a result of axial elongation of the vitreous chamber. Chick eyes are more susceptible to form deprivation at a young age but the capability declines with age. Wallman and Adams also discovered that the chick eyes recovered from the myopia once the restriction had been removed and elongation of the vitreous chamber had ceased. The rate of recovery was related to the amount of myopia induced and inversely related to age. The increase in axial length appears to be the main structural parameter for myopia production (Christensen and Wallman, 1991 and Smith *et al.*, 1987) although, Hodos and Kuenzel (1984) suggest that myopia is a result of both axial and equatorial growth of the vitreous chamber.

Smith *et al.* (1987) reviewed the effects of form deprivation on the refractive state of the rhesus monkey. One eye was sutured closed for a period exceeding 18 months, at various ages ranging from 26 days to 25 months. Longer axial lengths and higher myopic/less hyperopic refractive errors were found in the animals that were monocularly treated at an early age. McBrien and Norton (1992) assessed the ocular dimension changes that occurred in Tree shrews on monocular visual deprivation. The animals were monocularly deprived, due to lid suturing, from the initial day of eye opening for periods of 15, 30, 45, 60 and 75 days. After 75 days, the visually deprived eyes not only showed high degrees of myopia and increased vitreous chamber depth, but also corneal flattening, thinner crystalline lenses and a shallower anterior chamber depth. Contrary to the findings in the avian study by Wallman and Adams (1987), the Tree shrews did not recover from the induced vitreous chamber elongation.

More pertinent to this thesis is the work of Smith *et al.* (1999) who investigated formed deprivation myopia in adolescent monkeys. The rhesus monkeys were aged between 3.7 and 5 years, which corresponds to approximately 15 to 20 human years. Unilateral form deprivation was produced, in four monkeys, by surgically fusing the eyelids of one eye. The eyes were isometric at onset and assessed after 71 to 80 weeks of form deprivation. All four eyes became relatively more myopic than the fellow non-treated eye (mean anisometropia $-2.03 \pm 0.78D$). The investigators also noted an increase in

vitreous chamber depth of $0.55 \pm 0.31\text{mm}$ and axial length of $0.49 \pm 0.35\text{mm}$. The findings show that myopia and ocular growth occur in 'teenage' monkeys when subjected to form deprivation. The results suggest that the same vision-dependent mechanisms that induce myopia in monkeys could be found in human school-age children.

Diseases associated with visual image degradation and form deprivation in human children, i.e. ptosis, lid hemangiomas, cataract, optic atrophy, macular dystrophy, retinopathy of prematurity and retinitis pigmentosa, have been found to disrupt the emmetropization process and generate axial myopia (Robb, 1977; Hoyt *et al.*, 1981 and Nathan *et al.*, 1985).

Studies involving lens induced defocus

The chick eye has been found to respond to lens induced defocus. Wildsoet and Wallman (1992) produced hyperopia, in 3-day-old chicks, by fixing a -15D lens in front of one eye. The cycloplegic refraction, after just 4.5 days, revealed a compensatory myopic shift in refractive error with a mean difference between the two eyes of -8D . A compensatory axial increase in the vitreous chamber depth was found on examination using ultrasound. Conversely, eyes made myopic with the introduction of a $+15\text{D}$ lens produced a hyperopic shift with a mean difference of $+14\text{D}$ between the two eyes. Ultrasonic measurement showed a compensatory shortening of the vitreous chamber depth. Irving *et al.* (1992) concluded that the decrease in the vitreous chamber depth was a result of an increase in the choroidal thickness (choroidal accommodation). The increase in choroidal thickness pushes the eye forward thereby making the eye shorter. Wildsoet and Wallman (1992), suggest that choroidal thickness changes are temporary and the choroid slowly returns to normal after emmetropia has been achieved and as the sclera begins to compensate. Further experimentation, by Wallman *et al.* (1992), showed that chick eyes made locally myopic by form deprivation, resulted in local choroidal response to the myopic region of the retina. An accommodative feedback loop has often been proposed as an explanation for eye growth control (van Alphen, 1961 and Medina and Fariza, 1993). Unfortunately, the theory of an accommodative feedback loop can not fully justify the local myopia that occurs with partial deprivation and the local retina changes that are associated. Further investigation has found evidence to support this argument. The elimination of accommodation or links to accommodation have not prevented form deprivation myopia, recovery or lens-induced

defocus (Troilo and Wallman, 1991; Wildsoet and Wallman, 1992 and Wildsoet and Pettigrew, 1988). The retina is able to carry information regarding retinal image quality, has close links with the sclera and choroid and contains a number of different substances and growth factors, therefore, making it a suitable location for local eye growth control (Ehinger, 1982). A study by Cheng *et al.* (1992) found no indication for the presence of choroidal thickening in human eyes, although, further investigation may be warranted on this subject considering the suggestion that full correction of refractive errors and hyperopic defocus could enhance eye growth.

Astigmatism

The presence of astigmatism in childhood is frequently associated with spherical ametropia later in life (Ehrlich *et al.*, 1995; Gwiazda *et al.*, 1993a and Hirsch, 1964). Ehrlich *et al.* suggest that the uncorrected astigmatism produces a type of image degradation, which disrupts the normal emmetropization process, and instigates form deprivation myopia. Many risk factors must be considered when searching for an explanation for the development of myopia in humans and animal studies have been useful in assessing the risk associated with uncorrected astigmatism. Smith *et al.* (1997), cited Rosenfield and Gilmartin (1998), found minimal corneal or refractive astigmatism in normal infant monkeys at 3 weeks old. A cylindrical spectacle lens was introduced in front of one or both of the eyes of the monkey to stimulate uncorrected astigmatism without changing the location of the circle of least confusion (+1.50/-3.00×180). Compared to the control monkeys, the cylinder-reared monkeys showed little or no reduction in hyperopia and, in some cases, an increase in the amount of hyperopia with age. A small number of monkeys showed a significant degree of myopia and monocularly cylinder-reared monkeys demonstrated anisometropia. Notable changes towards a normal, isometropic refractive error were found when the cylindrical lenses were removed from one or both eyes. The results indicate that the presence of uncorrected astigmatism alters the emmetropization process and causes ametropia.

Animal experiments provide us with a solid stage on which to base our theories on the mechanisms that generate emmetropia and ametropia. However, it must always be assumed that the results from animal experiments cannot be successfully extrapolated to

to humans owing to the significant differences evident between subjects and environments.

1.6 Summary

- Myopia is a common condition found in Western populations and especially in Southeast Asian populations.
- The prevalence of myopia in Western populations is close to 25% by late-teens and reaches a peak of 30-35% between the ages of 18 to 40 years. The prevalence of myopia in Chinese and Taiwanese populations is around 60 to 75%.
- Myopia also appears to be more prevalent in females compared to males.
- Mean progression rates for myopia in young subjects is approximately -0.50D per year but values vary depending on the research study.
- The main structural correlate of myopia is an increase in axial length, and more specifically an increase in the posterior vitreous chamber.
- The aetiology of myopia is not yet fully understood but various factors have been implicated: hereditary and genetics, nearwork demands, nutrition and increased intraocular pressure. Animal studies in myopia and emmetropization have provided some insight into myopia development. Results from the animal studies suggest that emmetropization is an active process which is capable of detecting and adjusting for retinal defocus. However, animal studies have a limited use and the results cannot always be extrapolated to humans.
- All cross-sectional research into the subject of myopia is valid, but clearly longitudinal studies involving human subjects are required to determine possible risk factors and to further our understanding of myopia development.

CHAPTER 2

LATE-ONSET MYOPIA

Introduction

There are a vast number of articles, in United States and European journals, since 1812, on the subject of myopia. A number of articles have been written on the subject of youth-onset (early-onset) myopia but only a relatively small number of articles are aimed at the subject of early adult-onset (late-onset) myopia. By late-teens, approximately 25% of Western industrial populations exhibit myopia. Previous myopia studies have shown that myopia occurs when there is a breakdown in the co-ordinated relationship between the ocular components. Erickson (1991) found the amount of myopia to be directly related to an increase in axial length, or more specifically, to an increase in the vitreous chamber depth. Eye growth ceases by 14 years of age (Sorsby *et al.*, 1961 and Sorsby and Leary, 1970) and it is around this time that youth-onset myopia often stabilizes (Grosvenor, 1994).

The second most common form of myopia is late-onset. This form of myopia appears in late teens or early to middle twenties at a time when physical maturity has been reached (Grosvenor, 1987). Late-onset myopia constitutes 8 to 10% of the myopic population in the Western world and appears to be increasing (Fledelius, 1995a). Investigation has found no clear evidence for the hereditary basis of late-onset myopia. Late-onset myopia appears to develop at time when normal eye growth has presumably ceased (Goldschmidt, 1968). For that reason, what physiological changes must be occurring for there to be a myopic shift in refractive error during this period and what are the associated causative factors?

2.1 Prevalence

Approximately 30 to 35% of Western populations suffer with myopia between the ages of 18 to 40 years, an increase of 5-10% from late-teens (Grosvenor, 1987). Refractive error studies in Southeast Asia report much higher prevalence of myopia in the order of 62% in Hong Kong schoolchildren between the ages of 8 to 19 years (Lam *et al.*, 1999) and over 75% of Taiwanese schoolchildren by 18 years of age (Lin *et al.*, 1988a and 1988b). Aboriginal populations have a lower prevalence rate for myopia (Grosvenor, 1994).

The majority of myopic subjects develop myopia between the ages of 6 to 15 years (early-onset myopia). However, another category of myopia exists: late-onset myopia. This form of myopia develops between the ages of 18 to 40 years and represents 8 to 10% of the total myopic population, although a prevalence of approximately 25% has been proposed by Fledelius (1995a).

The focus of many late-onset myopia studies is subjects aged between 17 and 25 years. A strong association has been detected between myopia onset and progression and intensive near work demands (McBrien and Adams, 1997; Adams and McBrien, 1992 and Midelfart *et al.*, 1992). With this criteria in mind, college, university and military academy students are probably the most vulnerable and accessible groups for investigation.

Septon (1984) found that 75% of 2nd year Optometry students reported having a myopic refractive error. Further investigation revealed that myopia onset occurred at three separate age groups: ages 8 to 9 years, 12 to 13 years and 19 years. A recent longitudinal study involving 100 females and 92 males, enrolled in a university engineering program, was completed by Kinge and Midelfart (1999). The refractive errors were measured, under cycloplegic conditions, at the beginning and end of a three-year study program. The mean age of the students was 20.6 years. The prevalence of myopia at entrance was 48% with an increase in prevalence to 65% after 3 years. Of subjects who were emmetropic at the start of the study, 59% became myopic. The results show that there is a reasonably high prevalence of myopia in university students and myopia can progress over the duration of study period.

In a study of British army recruits between 18 and 22 years of age, Sorsby *et al.* (1960) found an 11% myopia prevalence, whereas Goldschmidt (1968), estimated a 14% prevalence rate of myopia in Swedish army recruits. O'Neal and Connon (1987) conducted a retrospective study, on 497 cadets aged 17 to 21 years, at the United States Air-Force Academy. Refractive error examination records were analysed, over a period of 2.5 years, during the intensive educational program. At entrance to the Academy, 37.3% of cadets were hyperopic, 18.5% emmetropic and 44.2% were myopic by $-0.25D$ or more. A myopic shift in the spherical equivalent refractive error was noted in a number of subjects over the assessment period. A clinically significant myopic shift of $-0.50D$ or more was seen in 21.3% of hyperopes, 25% of emmetropes and 55.1% of myopes. The results demonstrate a similar trend to those found by Kinge and Midelfart

(1999) whereby an increase in prevalence and progression of myopia can be seen during a 2.5 to 3 year program of concentrated nearwork.

2.1.1 Gender Differences

Sperduto *et al.* (1983) examined gender differences in myopia prevalence and progression using data from a sample of subjects aged from 1 to 74 years of age. Prior to 35 years of age, a higher proportion of female subjects suffered with myopia compared to males. After 35 years of age the prevalence rates for the two sexes were similar (see §1.4.2). In a specific study to assess the relationship between gender and refractive error, Pendse *et al.* (1951), found no significant difference in refractive error for males and females at 18 years of age.

2.2 Progression

Grosvenor (1977) calculated myopia progression between the ages of 20 and 40 years using a survey of previous optometric records. The initial subjects, who were myopic at 20 years of age, showed an increase in myopia of approximately 1.00D over the 20 years duration (-0.05D change per year). Grosvenor (1987) categorised myopia under four distinct headings to enable simple classification of myopia according to age. However, this classification system is frequently difficult to apply to the early adult-onset category owing to the lack of knowledge regarding dates of myopia onset and rate of myopia progression from childhood. Goss *et al.* (1985) collected refractive error data from five optometry practices in central United States in an attempt to define three basic patterns to help characterise the classification of late-onset myopia. The longitudinal study consisted of 559 myopic patients, of which 116 cases were used to compare myopia progression in childhood and during the early adult years. The subjects were aged between 6 and 24 years. The investigators determined the following three basic patterns:

- 1) *Adult stabilization* – stabilization of myopia in young adulthood after the progression of myopia during childhood. Adult stabilization was found in 87% of female subjects and 68% of male subjects.
- 2) *Adult continuation* – the rate of myopia progression in young adulthood is slower than that found in childhood. This pattern was found in 13% of females and 25% of males.

- 3) *Adult acceleration* – the rate of myopia progression in young adulthood is faster than that found in childhood or a previously emmetropic subject has onset of myopia. No female subjects presented with this pattern and only 6% of male subjects.

On further analysis of the data, Goss *et al.* (1985) observed myopia progression rates of between -0.05 and -0.20D per year for the adult continuation subjects and the adult acceleration subjects. See figures 2.1a to c for examples of basic patterns of myopia progression.

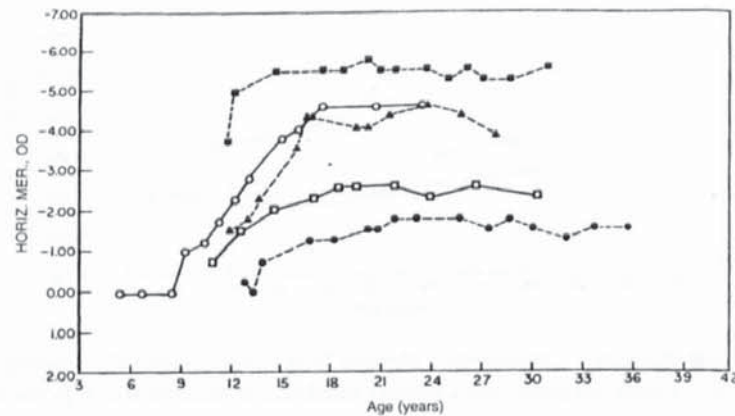


Figure 2.1a Example of adult stabilization of myopia. 5 subjects and each symbol represents the refractive error (D) in the principal meridian nearest horizontal in the right eye. After Goss *et al.*, 1985.

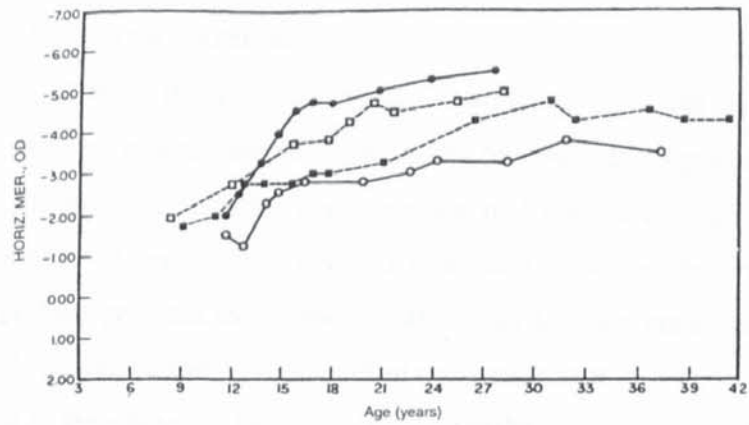


Figure 2.1b Example of adult continuation of myopia progression. 4 subjects and each symbol represents the refractive error (D) in the principal meridian nearest horizontal. Re-drawn from Goss *et al.*, 1985

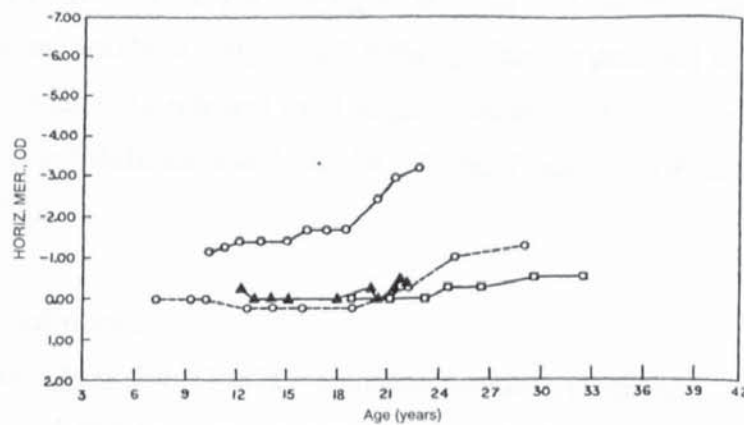


Figure 2.1c Example of adult acceleration of myopia progression. 3 subjects and each symbol represents the refractive error (D) in the principal meridian nearest horizontal. Re-drawn from Goss *et al.*, 1985

Myopia progression rates of between -0.05 and -0.20D per year have been found in previous studies (Grosvenor, 1977 and Goss *et al.*, 1985). A recent 3 year investigation into myopia progression, by Kinge and Midelfart (1999), revealed a mean refractive error increase from $-0.64 \pm 2.18\text{D}$ to $-1.21 \pm 2.30\text{D}$. Fifty-nine percent of eyes, that were initially emmetropic, became myopic, 73% of myopic eyes progressed further, with at least -0.37D change, and 8% of hyperopic eyes became myopic. The results indicated a definite shift towards myopia in university students and suggest that adults participating in study may develop myopia or renew myopia progression. The results obtained from the studies mentioned here justifies the use of a longitudinal investigation, rather than cross-sectional, for further research in this particular field of interest.

2.3 Ocular biometric correlates

Examination of adult myopia, as with any form of myopia, can be filled with inherent problems which makes comparison between studies impracticable. Interstudy variations, methods of refraction, age, gender and race can be difficult to standardise. Research into adult myopia has resulted in a number of conclusions being reached for the onset and progression of myopia in adulthood and the underlying ocular biometric changes, which induce the myopic shift in refractive error.

Eye growth is complete by 14 years of age (Sorsby *et al.*, 1961 and Sorsby and Leary, 1970). Goldschmidt (1968) deduced that a sudden onset or progression of myopia in adulthood must be a result of increased corneal or lens power, rather than an increase in vitreous depth or axial length, owing to the fact that the eye has stopped growing. However, it has also been suggested that the eye has the potential to resume growth and that vitreous chamber depth and axial length increase could produce the myopic shift in refractive error (McBrien and Millodot, 1987a; Fledelius, 1995a and Simensen and Thorud, 1994).

Cross sectional studies

McBrien and Millodot (1987a) compared ocular component dimensions in 30 emmetropes and 30 late-onset myopes, who were both age and sex matched. Data was analysed for the left eye only. The most statistically significant parameter, related to late-onset myopia, was vitreous chamber elongation. Late onset myopes were also found to have significantly deeper anterior chambers and thinner crystalline lenses. No correlation was found in corneal curvature measures. Similar results were found in a later study by Bullimore *et al.* (1992) on accommodative responses and ocular biometric characteristics in emmetropes, early-onset and late-onset myopes. A significant difference in mean vitreous chamber depth and axial length was noted between emmetropes and late-onset myopes. The mean vitreous chamber depth of the emmetrope group was $16.89 \pm 0.85\text{mm}$ compared to $18.24 \pm 1.16\text{mm}$ for the late-onset myope group. Contrary to the results of McBrien and Millodot (1987a), no significant differences were found between the groups for anterior chamber depth or lens thickness. The two research projects reviewed here have found a definite correlation between late-onset myopia and vitreous chamber elongation, although, in a comparable study by Grosvenor and Scott (1991), no significant differences were detected between the mean vitreous chamber depth or axial length when comparing the ocular biometric parameters

in emmetropes and late-onset myopes. The authors did, however, find the cornea to have a higher refracting power in early adult-onset myopes than in emmetropes. See table 2.1 for data comparison among studies.

Table 2.1 Comparison of data reported for the three cross-sectional studies: emmetropes (EMM) and early adult-onset myopes (EAOM). Redrawn from Grosvenor (1994).

	<i>McBrien and Millodot (1987)</i>		<i>Grosvenor and Scott (1991)</i>		<i>Bullimore et al. (1992)</i>	
	EMM	EAOM	EMM	EAOM	EMM	EAOM
Number of subjects	30	30	18	23	14	14
Mean age (yrs)	Students from university		21.5	22.4	21.7	21.1
Mean sph equiv refr (D)	+0.17	-1.29	+0.36	-1.42	-0.08	-2.18
Mean corneal power (D)	42.72	42.72	<u>42.80</u>	<u>43.92²</u>	42.92	42.94
Mean ant ch depth (mm)	3.78	4.05 ²	3.63	3.73	3.57	3.58
Mean lens thickness (mm)	<u>3.63</u>	<u>3.46¹</u>	3.59	3.60	3.79	3.68
Mean vitr ch depth (mm)	<u>16.35</u>	<u>17.07²</u>	16.24	16.43	<u>16.89</u>	<u>18.24³</u>
Mean axial length (mm)	<u>23.76</u>	<u>24.58²</u>	23.46	23.75	<u>24.25</u>	<u>25.49³</u>

Shared underlining denotes a statistically significant difference: 1 indicates $p < 0.05$, 2 indicates $p < 0.01$, 3 indicates $p < 0.001$.

Sorsby *et al.* (1957) and Sorsby *et al.* (1961) hypothesized that emmetropia was a result of balanced refractive contributions by several ocular components. The term ‘inflatable globe’ was used to describe the strong relationship between globe length and refractive power and globe length and corneal refractive power. The authors intimated that an increased globe size is compensated for by a flatter corneal curvature and decreased globe size by a steeper corneal curvature. Koretz *et al.* (1995) assessed the relationship among age-dependent ocular biometric variables, which contribute to emmetropia and ametropia, in the adult human eyes. Manifest refraction, keratometry and A-scan ultrasonography were determined in 185 unaccommodated right eyes in subjects aged 18 to 70 years. The cohort consisted of 2 hyperopes, 47 myopes and 136 emmetropes. Koretz, Rogot and Kaufman found that anterior segment length increased significantly with increasing globe length in emmetropes but not in ametropes. The findings indicated an ‘inflatable anterior segment’ in association with the traditional ‘inflatable globe’ as a mechanism for emmetropization. However, this increased separation between the lens and cornea with increasing globe size was not evident in adult human myopia.

Longitudinal studies

Kent (1963) reported longitudinal data on his brother and showed that keratometric measurements changed and corneal power increased as myopia progressed from onset at 22 years of age. Longitudinal refraction and keratometry data from patient files have shown corneal steepening and corneal power increase during young adult myopia progression (Goss *et al.*, 1985 and Goss, 1987). Using linear regression, Goss (1987), calculated the rates of myopia progression and the rates of corneal power change. Longitudinal records of 37 patients were assessed where the selection criteria for the young adult myopia group required 3 or more eye examinations, to include refractive error and keratometry readings, at 18 years of age or older. The results indicated that an increase in myopia was correlated with anterior surface corneal steepening in young adults and the correlation was greater along the vertical corneal meridian compared to the horizontal meridian. Although the correlations were significant, the amounts of corneal steepening were low, therefore the authors concluded that the cornea could not be the exclusive contributor in myopia progression.

Refractive error and associated ocular component changes were investigated in a 3-year longitudinal prospective study by Grosvenor and Scott (1993). The cohort consisted of 29 youth-onset myopes, 26 early adult-onset myopes and 24 emmetropes. During the 3-year period, mean spherical equivalent refraction shifted towards myopia for all three refractive error groups. All three groups showed refractive error change to be significantly correlated with changes in vitreous chamber depth and axial length. Owing to the high standard deviations, the authors could not significantly correlate any other ocular parameters with the increase in myopia over the 3 years. In summary, there is no clear evidence to suggest that myopia onset or progression is a consequence of an increase in corneal or crystalline lens power in the absence of axial elongation. See table 2.2 for mean changes in refraction and components and table 2.3 for correlation coefficients between refraction and components.

Table 2.2 Mean changes (\pm SD) in spherical equivalent refractive error and its components during 3-year longitudinal study, for subjects in each of 3 refractive groups. Redrawn from Grosvenor and Scott (1993)

	<i>Youth-onset myopes</i>	<i>Early adult-onset myopes</i>	<i>Emmetropes</i>
Sph equiv refr error (D)	-0.26 (0.52)	-0.18 (0.40)	-0.15 (0.87)
Corneal power (D)	+0.01 (0.22)	-0.05 (0.13)	+0.02 (0.20)
Lens power (D)	-0.24 (0.66)	-0.36 (0.52)	-0.40 (0.87)
Ant chamber depth (mm)	+0.05 (0.09)	+0.04 (0.07)	+0.03 (0.08)
Lens thickness (mm)	+0.04 (0.09)	+0.05 (0.07)	+0.07 (0.08)
Vitr chamber depth (mm)	+0.09 (0.22)	+0.11 (0.19)	+0.06 (0.26)
Axial length (mm)	+0.18 (0.21)	+0.20 (0.18)	+0.16 (0.26)

Table 2.3 Correlations between changes in spherical equivalent refractive error and changes in refractive components, for subjects in each of the 3 refractive error groups. Redrawn from Grosvenor and Scott (1993).

	<i>Youth-onset myopes</i>	<i>Early adult-onset myopes</i>
Corneal power	-0.32	-0.13
Lens power	+0.06	0.00
Ant chamber depth	-0.09	+0.04
Lens thickness	+0.12	+0.24
Vitr chamber depth	-0.67*	-0.77*
Axial length	-0.64*	-0.73*

* significant at the 5% level of confidence ($p < 0.05$)

As mentioned previously, myopia can be associated with closework and excessive nearwork demands. Hence, McBrien and Adams (1997) investigated adult-onset and adult-progression of myopia in a particular occupational group – clinical microscopists. The sample population consisted of 251 subjects, aged 21 to 63 years. Refraction and ocular dimensions were recorded on four occasions over a 2-year period. Refractive error was measured subjectively and objectively in conjunction with keratometer and A-scan ultrasonography measurements. Sixty-one percent of subjects presented with myopia on initial questioning and 36% of these myopic subjects reported myopia onset after entry into the occupation. Of eyes initially emmetropic at the start of the study, 39% shifted in refractive error towards myopia by greater than 0.37D. The shift was associated with an elongation of the vitreous chamber. No change was noted in corneal curvature, lens thickness or anterior chamber depth. Forty-eight percent of initially

myopic subjects progressed further into myopia by 0.37D or more during the 2-years. Again, an increase in depth of the vitreous chamber can account for the myopic shift. The most recent longitudinal study on young adults demonstrates a refractive change of $-0.52 \pm 0.45\text{D}$, over a 3-year term, with an accompanying increase in vitreous chamber depth of $0.27 \pm 0.30\text{mm}$ and change in lens thickness of $0.07 \pm 0.10\text{mm}$ (Kinge *et al.*, 1999).

There appears to be conclusive evidence from both cross-sectional and longitudinal studies that myopia develops and progresses during the early adult years due to an uncompensated vitreous chamber elongation, with little or no change in the other ocular components, except for possibly corneal refractive power.

2.4 Accommodation

Accommodation is the term used to describe the mechanism, within the eye, which allows rapid change in refracting power to enable objects to be focused on the retina. Nearwork has been implicated in the aetiology of myopia (McBrien and Millodot, 1986a). As yet, no clear link exists between nearwork and the increase in axial length, which is associated with myopia. During accommodation there is deformation of the crystalline lens which produces an increase in the dioptric power of the eye. Myopia is a result of excessive ocular refractive power, with respect to axial length; hence, it is not unreasonable to associate myopia with accommodation.

Various researchers have attempted to correlate accommodation differences with refractive error to show whether myopia develops as a result of an abnormal accommodative system or if the accommodative system undergoes a change owing to a myopic shift in refractive error. Higher amplitudes of accommodation have been found in low myopes compared with high myopes and both myopic groups have been found to have higher amplitudes of accommodation than emmetropes and hyperopes (McBrien and Millodot, 1986a and Maddock *et al.*, 1981). McBrien and Millodot (1986b) assessed accommodative response in four refractive groups and reported a reduced mean gradient for the accommodative stimulus-response function in late-onset myopes compared to emmetropes and early-onset myopes. However, the accommodative responses of emmetropes, early-onset myopes and late-onset myopes did not significantly differ, in a study by Abbott *et al.* (1998), but a reduced accommodative response was noted in the progressing myopes. Abbott, Schmid and Strang used three

different techniques to measure the accommodation stimulus-response curves in adult myopes and emmetropes. The most significant results were achieved by presenting a series of negative lenses to the subject whilst viewing a distant target. The results indicated a link between myopia progression in adults and inaccurate accommodation. The stable myopes demonstrated accommodation responses similar to those of emmetropes.

Tonic accommodation

Tonic accommodation is also described as the resting or passive state of accommodation. Tonic accommodation occurs in the absence of a stimulus, i.e. either in a situation of complete darkness or when the eye is gazing at a bright empty field. During these conditions, the eye tends to focus at an intermediate point rendering the emmetropic eye slightly myopic by approximately 0.50 to 1.00D. Tonic accommodation reflects the balance between parasympathetic and sympathetic innervation to the ciliary muscle (Rosenfield *et al.*, 1993). Conflicting results have been found between investigators for measurements of tonic accommodation, especially when considering late-onset and progressing myopes. Rosenfield and Gilmartin (1987b) and Rosenfield and Gilmartin (1987c) found low dioptric levels of tonic accommodation in late-onset myopes. In a longitudinal study, Jiang (1995) followed forty-four college students over 2 to 3 years. At recruitment, 33 subjects were emmetropes and 11 subjects were late-onset myopes. Six, initially emmetropic subjects became myopic over the duration of the study and showed higher values of mean dark-focus and AC/A ratios than for the subjects who remained emmetropic. Interestingly, seven of the late-onset myopes, displayed lower mean dark-focus values than the subjects who remained emmetropic. In a similar study, Adams and McBrien (1993) noted no significant difference between the initial values of tonic accommodation (dark focus) in subjects who remained emmetropic and those who became myopic over the 2-year study period. In contrast to the results of Jiang (1995), 49% of subjects developed lower tonic accommodation levels in association with a myopic shift in refractive error.

Strang *et al.* (2000) found no difference when assessing open-loop accommodation response positions in emmetropes and early and late-onset myopes. However, the investigators did record different response positions according to experimental set-up. A significant variation in open-loop accommodation was found when measurements were taken in darkness (DA) and using a pinhole pupil (PA). The data revealed the PA

values to be higher than the DA values in all three refractive groups. Similar results were found by Gray *et al.* (1998) when assessing open-loop accommodation using three different methods of opening the loop.

Accommodative adaptation

Tonic accommodation levels differ before and after periods of sustained nearwork (Ebenholtz, 1983; Fisher *et al.*, 1987; Gilmartin and Bullimore, 1987; Rosenfield and Gilmartin, 1988 and Owens and Wolf-Kelly, 1987). Accommodative adaptation demonstrates the shift in accommodation that is detected before and after a sustained near task (Rosenfield, 1994). Immediately following a near-vision task, emmetropes show greater adaptation compared to late-onset myopes (Gilmartin and Bullimore, 1991).

2.4.1 Possible mechanisms for myopia development

Retinal defocus

It has been suggested that a defocused retinal image could be a precursor to axial elongation. To reduce a blur circle on the retina, the eye could, conceivably, adjust its location to minimise the distortion. Animal studies have been used to demonstrate the effects of retinal image degradation (see § 1.5). Irving *et al.* (1992) used positive and negative lenses to induce myopic and hyperopic refractive errors in chick eyes owing to the compensatory growth mechanisms. Although it has been shown that humans do not have the same compensatory growth mechanisms as chicks (Mutti and Zadnik, 1995), retinal defocus is present during a sustained near-vision task or following task completion and could possibly induce ocular biometric changes. For axial elongation to be induced by retinal defocus, the crucial period of image degradation must be either during a period of sustained near-vision or immediately after the near-task has been completed. Subjects presenting with reduced accommodative adaptation generally demonstrate a greater lag of accommodation to a near stimulus (Rosenfield and Gilmartin, 1998). It has also been found that transient periods of retinal defocus can occur after sustained nearwork. Rosenfield *et al.* (1992) detected a transient increase in accommodation of 0.20D after sustained nearwork and Ong and Cuiffreda (1995) observed an increase of >1.00D. Findings suggest that retinal defocus is more likely to instigate myopia development during the course of near-vision, rather than immediately

after the period of near-vision, owing to the reduced accommodative response found in subjects prior to myopia onset (Portello and Rosenfield, 1997).

Intraocular pressure

Higher intraocular pressure values have been found in myopic eyes compared to non-myopic eyes (Edwards and Brown, 1993). One hypothesis for axial elongation in myopia is that the eye stretches as a result of the intraocular pressure exerting forces upon the sclera and forcing it outwards (Pruett, 1988). Stansbury (1948) proposed that myopia was a result of increased intraocular pressure during periods of accommodation. However, research has shown that intraocular pressure decreases during accommodation (Mauger *et al.*, 1984). Further examination, using animals (monkeys), has revealed an increase in vitreous chamber pressure with accommodation which decreases when accommodation is relaxed (Young and Leary, 1991). Owing to the lack of agreement between researchers, further investigation is required in order to confirm the proposal that myopia development is associated with increased intraocular pressure and accommodation.

Accommodation and retinal stretch

It has been implied that axial elongation in myopia is produced by forces acting upon the sclera during accommodation. In young subjects, the ora serrata progresses forward by approximately 0.05mm for each dioptre of accommodation (Moses, 1981). Enoch (1975) designed a model, which generated a retinal shift of 0.5mm for 10D of accommodation. As a result of the shift, the surface area of the retina increased by 2.4%. Yet, it still remains uncertain as to how the forward movement of the retina and choroid influences a change in the sclera to permit axial elongation in the posterior pole.

Eye elongation during accommodation was assessed using partial coherence interferometry (Findl *et al.*, 1997). The partial coherence interferometer (PCI) allows non-invasive axial length measurements to be recorded with a precision of greater than 5 μ m. During maximum accommodation the axial length increased by $11 \pm 2.1\mu$ m in emmetropes and $5 \pm 1.9\mu$ m in myopes. The posterior lens pole was also found to move posteriorly by $70 \pm 39\mu$ m during maximum accommodation. The results and authors imply that axial elongation during accommodation could be a contributing factor to the development and progression of myopia.

2.5 Vergence and myopia

Ocular vergence, during sustained near vision, may be implicated in the aetiology of myopia. Goss (1991) collected retrospective data from a group of children before and after the onset of myopia, and for a group of children who remained emmetropic. The subjects were aged between 6 and 15 years. The mean near-point heterophoria was measured and found to be 1.0^Δ esophoria for the 'became myopic' group and 2.0^Δ exophoria for the 'remained emmetropic' group. The difference was significant. Heterophoria data was measured in relation to myopia progression in subjects less than 17 years of age (Roberts and Banford, 1967). The mean rate of myopia progression was greatest amongst those subjects presenting with esophoria at near (0.48D/y; n=167), while the lowest progression rates were found in those subjects presenting with heterophoria between orthophoria and 4^Δ exophoria (0.39D/y; n=105).

Accommodative convergence and myopia

Rosenfield and Gilmartin (1987b) assessed accommodative convergence in groups of emmetropes, early- and late-onset myopes. Accommodation was induced using stimuli of 3.0, 3.9 and 4.6D and measured using an objective infrared autorefractor. Concomitant vergence changes were determined using a Maddox rod and tangent scale. The data revealed greater accommodative convergence and higher response AC/A ratios in early-onset myopes compared to the other two groups. In a further study, Rosenfield and Gilmartin (1987a), found both myopic groups to have greater amounts of accommodative convergence compared to the emmetropic group. In a longitudinal study of 2-3 years, Jiang (1995) monitored AC/A ratios in 33 emmetropes and 11 myopes. Seven out of 11 myopes had increases in myopia and six initially emmetropic subjects developed myopia during the study. The response AC/A ratio was significantly higher in the progressing myopes compared to the stable emmetropes. Also the response AC/A ratio was higher in 'became myopic' group compared to the stable emmetropes.

2.5.1 The near phoria and myopia development

Previous studies have shown an association between myopia and esophoria at near (Goss, 1991; Goss and Jackson, 1996b and Goss and Jackson, 1996a) and myopia and accommodative convergence (Rosenfield and Gilmartin, 1987a and Rosenfield and Gilmartin, 1987b). The esophoria at near could be a result of increased accommodative

response which produces excess accommodative convergence. However, Scheiman and Wick (1994) found higher lags of accommodation in subjects with near-esophorias. A high lag of accommodation at near and reduced accommodative response will produce hyperopic defocus, which, according to a number of researchers, may initiate axial elongation and induce myopia (Goss and Wickham, 1995; Hung *et al.*, 1995 and Wallman and McFadden, 1995).

2.6 Summary

- The most common form of myopia is youth-onset, which occurs around 6 years of age. The second most common form of myopia is late-onset, which appears in late-teens or early to middle twenties at a time when physical maturity has been reached.
- Early adult-onset myopia accounts for 8 to 10% of the myopic population in the Western world and appears to be increasing.
- Mean adult myopia progression rates are approximately -0.05 to -0.20D per year, but vary according to the research study.
- Normal eye growth is complete by 14 years of age yet axial length appears to be the main biometric correlate associated with the onset and progression of myopia in adults.
- Sustained nearwork, excessive nearwork demands and visual display unit use have been implicated in the development of myopia in adults. Various researchers have attempted to correlate accommodation differences with refractive error to show whether myopia develops as a result of an abnormal accommodative system or if the accommodative system undergoes a change owing to a myopic shift in refractive error. Inaccurate accommodation, reduced accommodative response and varying tonic accommodation levels prior and post sustained nearwork have all been implicated as causes for adult-onset myopia.
- Possible mechanisms for myopia development are retinal defocus, increased intraocular pressure and accommodation induced retinal stretch.
- A longitudinal study of adult-onset and progression of myopia, involving the measurement of a number of biometric parameters in association with accommodation measurements and techniques to assess retinal shape, is justified in order to assess the changes analogous with a myopic shift in refractive error.

CHAPTER 3

PERIPHERAL REFRACTION

Introduction

Research has indicated a relationship between ametropia and the type and amount of peripheral refraction. Peripheral refraction has been classified into categories depending upon the size of the interval of Sturm and change in astigmatism with varying degrees of eccentricity. Measurement of peripheral refraction, in conjunction with a number of other ocular biometric readings, permits the derivation of retinal contour. The retinal contour can be used as a tool to describe in greater detail the shape of the retina both in ametropia and in subjects where the amount of ametropia is changing over time.

This chapter has been added to review background literature in order to explain the related thought-processes behind the retinal contour program (RetinaFit), devised by Dr Mark Dunne. The chapter also discusses the classification of peripheral refraction in relation to central refraction.

3.1 Ocular aberrations

An aberration is an optical fault in which rays from a single point object do not form a precise point image after passing through the optical system. Refracting systems are subject to a number of aberrations and these can effect the quality and resolution of an image. The eye is no exception and the image produced is influenced by spherical aberration, chromatic aberration, coma, oblique astigmatism, field curvature and distortion (Charman, 1983). Young (1801) was the first to recognise that light striking the cornea and lens at an oblique angle could cause astigmatism. In the eye, astigmatism can occur due to the toroidal shape of the anterior and posterior corneal surfaces or crystalline lens, by subluxation of the crystalline lens or by light entering the eye at an oblique angle. In the peripheral field, objects are imaged by obliquely incident rays of light which are limited principally by the pupil. Rays in the plane of oblique incidence converge first and produce tangential line foci. Rays travelling at right angles to the plane of oblique incidence converge to produce sagittal line foci. Light enters the eye from all directions and when an object is placed at a set distance, foci arising from

pencils of light lie on two curved surfaces referred to as the tangential and sagittal image shells and located half way between them is the circle of least confusion (Dunne, 1995). The space between the sagittal and tangential foci is called the interval of Sturm whose magnitude represents the peripheral astigmatism. In a typical human eye these image shells fall either side of the retina (Ferree *et al.*, 1931 and Millodot, 1981) and owing to their shape are often described as the teacup and saucer. The position of the sagittal and tangential line foci, with respect to the retina, change with variation in field angle (see figure 3.1). As the field angle increases, the tangential image shell falls progressively further in front of the retina and becomes increasingly myopic. Consequently, the sagittal image shell falls further behind the retina and becomes increasingly hyperopic.

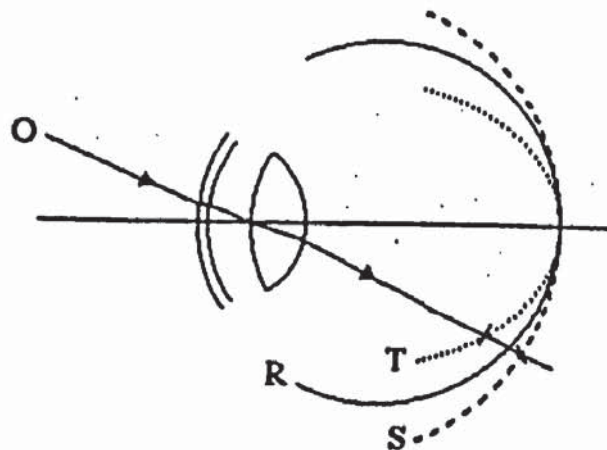


Figure 3.1 Tangential image shell (T) and sagittal image shell (S) formed by an oblique ray bundle (O). After Dunne (1995).

Optometers and retinoscopes have been used to measure peripheral refraction and research has been carried out in human eyes (Ferree *et al.*, 1931; Millodot, 1981 and Dunne *et al.*, 1987) and in schematic eyes (Dunne and Barnes, 1987; Le Grand, 1967 and Lotmar, 1971). Millodot and Lamont (1974) measured peripheral refraction subjectively, to an eccentricity of 60° , using spherical lenses. The final measurement was ascertained with the use of a bracketing technique whilst the subjects viewed a distant Landolt C. The researchers found close agreement between the results obtained by the subjective method and those found by an objective method (Zeiss coincidence refractometer) for the same subjects. Skiascopy was the term used by Ferree *et al.*

(1931) for retinoscopy and peripheral astigmatism is generally represented as a 'skiagram'.

3.2 Peripheral astigmatism in human eyes

Parent (1881, cited in Le Grand (1967)) was the first researcher to measure peripheral astigmatism in human eyes. The astigmatism was measured using retinoscopy at eccentricities of 15° and 45° along the horizontal meridian. Parent recorded astigmatism of 0.50D at 15° and 2.75D at 45° describing an increase in astigmatism at a greater degree of eccentricity. Millodot (1981) assessed peripheral refraction in 62 eyes, horizontally from 60° nasally to 60° temporally, using a refractometer. He concluded that the amount of astigmatism increased progressively towards the periphery in 91% of eyes examined and the type of astigmatism differed significantly between myopes, near-emmetropes and hyperopes.

Rempt *et al.* (1971); Millodot and Lamont (1974) and Millodot (1981) did not investigate peripheral refraction under cycloplegic conditions, whereas, Logan *et al.* (1995) used two drops of 1% tropicamide HCl, with instillation separated by an interval of 5 minutes, to induce cycloplegia. Millodot and Lamont (1974) used a refractometer to measure peripheral refraction and ascertained that without cycloplegia, relaxation of accommodation was very difficult and produced instability within the visual system. However, Millodot (1981) again declined the use of cycloplegia, when assessing the effect of ametropia on the peripheral refraction, owing to the peripheral aberrations induced by the enlarged pupil. Ferree *et al.* (1931) concluded that the prolonged fixation, found during measurement of peripheral refraction, resulted in a myopic shift in refractive error and this tendency towards myopia was observed either with or without cycloplegia. Logan *et al.* (1995) used a Canon R-1 autorefractor to measure peripheral refraction under the influence of cycloplegia. The cycloplegia prevented changes in accommodation and provided pupil dilation. Without pupil dilation, the signal returning from the eye to the Canon R-1 AutoRef becomes attenuated as the pupil diameter approaches the minimum limiting level (Winn *et al.*, 1989).

3.2.1 Classification of peripheral astigmatism

Ferree *et al.* (1931) and Ferree *et al.* (1932) assessed peripheral refraction in twenty-one eyes using a Zeiss refractometer. Measurements were taken at either 5° or 10° intervals, both nasally and temporally along the horizontal meridian, to a maximum of 60°. The following three types were classified from the results: -

1. Type A – the *horizontal* meridian became *more myopic* with increasing eccentricity and the *vertical* meridian *more hyperopic*. The interval of Sturm varied between subjects with the average type A subject presenting with approximately 6.00D of astigmatism nasally and 4.50D temporally at 50°. Twelve eyes exhibited peripheral refraction type A.
2. Type B – the eye became *less myopic* in the *horizontal* meridian and *more hyperopic* in the *vertical* meridian, with increasing eccentricity. Only small intervals of Sturm were noted and the average type B eye demonstrated approximately 1.00D of astigmatism nasally and 1.50D temporally at an eccentricity of 50°. Six eyes exhibited peripheral refraction type B.
3. Type C – the peripheral refraction was asymmetrical and the interval of Sturm was found to be significantly different between the nasal and temporal meridia. Three eyes exhibited peripheral refraction type C.

Ferree *et al.* (1932) assumed that the asymmetry between nasal and temporal halves was an effect of an asymmetrical eyeball, asymmetry in the position of the lens about the anteroposterior plane of the eye or both. See figure 3.2a, which depicts an average type A and type B eye and 3.2b which shows three type C eyes.

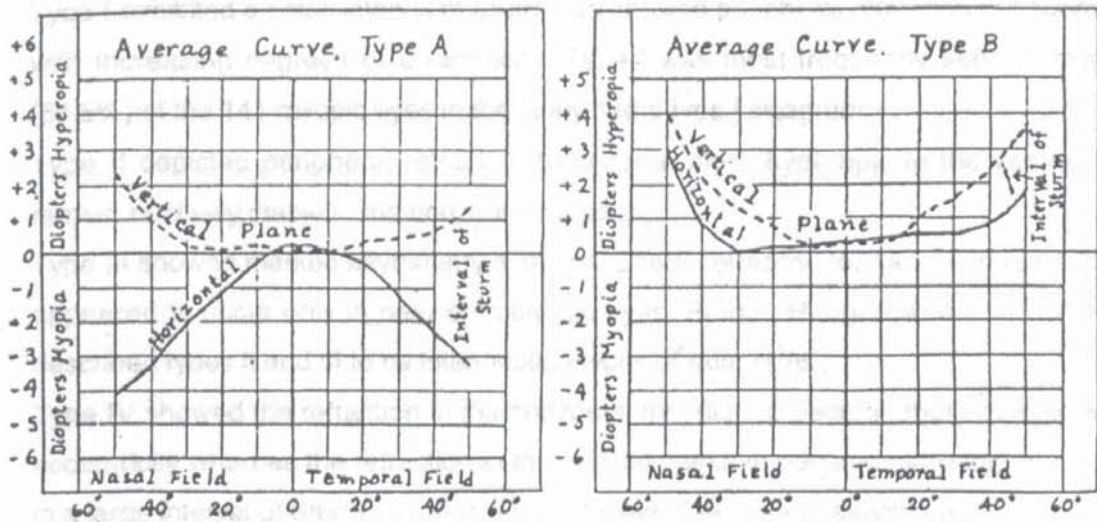


Figure 3.2a Showing the peripheral refraction types A and B. After Ferree *et al.* (1931)

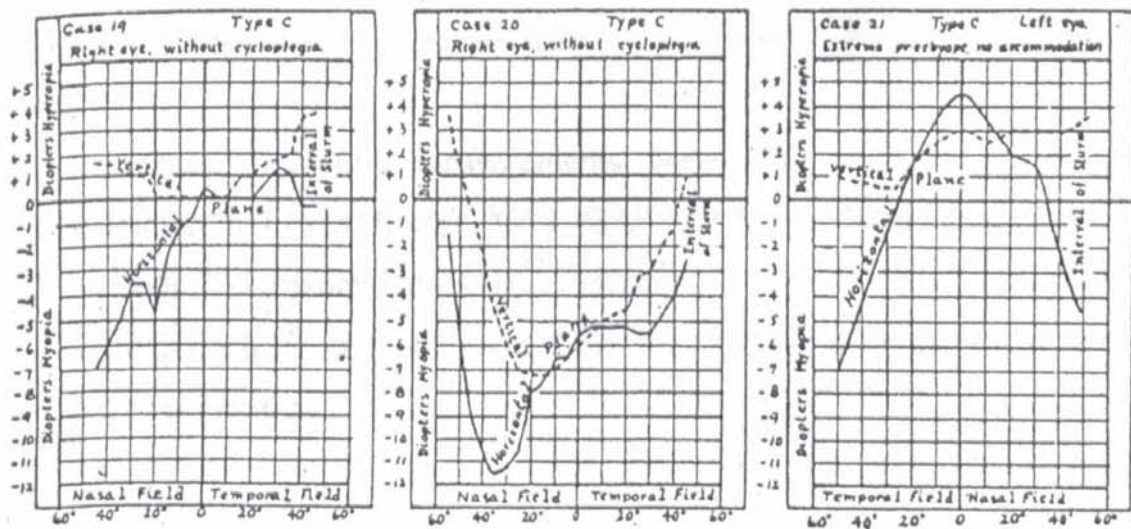


Figure 3.2b Showing three type C eyes. After Ferree *et al.* (1932).

Peripheral refraction was measured, using retinoscopy, in 422 pilots in a study to determine whether the shape of a skiagram could be correlated to the central refractive error (Rempt *et al.*, 1971). Measurements were taken along the horizontal meridian at 0° , 20° , 40° and 60° and occasionally at 10° , 30° and 50° . The results were represented diagrammatically and termed skiagrams.

The investigators discovered 5 classifications of skiagram, which are: -

1. Type I – exhibited a small interval of Sturm and showed *peripheral refraction* to become *less myopic* with increasing degrees of eccentricity. The type I skiagram was frequently seen in myopic eyes (64.5%).
2. Type II – found *peripheral refraction* to become increasingly *hyperopic* in the *vertical* meridian and remain comparatively *stable* in the *horizontal* meridian.
3. Type III – *peripheral refraction* exhibited distinct *asymmetry* between the nasal and temporal meridia. This skiagram only appeared in emmetropic eyes.
4. Type IV – refraction in the *horizontal* meridian became increasingly *myopic* with eccentricity. Refraction in the *vertical* meridian became increasingly *hyperopic* with eccentricity. Subjects presenting with this skiagram demonstrated high degrees of peripheral astigmatism. Over 50% of all eyes examined showed a type IV skiagram and 62.2% of emmetropic eyes.
5. Type V – existed only in hyperopic eyes. The *peripheral refraction* became less *hyperopic* with eccentricity.

Peripheral refraction measurements were also attempted along the vertical meridian in 7 eyes (Rempt *et al.*, 1971). In 4 eyes the skiagram was symmetrical in both the horizontal and vertical meridia. The other 3 eyes exhibited asymmetry in both the horizontal and vertical meridia, but less asymmetry was noted along the vertical meridian.

Millodot and Lamont (1974) measured peripheral refraction in 3 subjects using retinoscopy, refractometry and a subjective method of refraction. Readings were taken along the horizontal meridian in the temporal field, at 10° intervals, out to 60°. Retinoscopy readings were found to be unreliable beyond an eccentricity of 50°, although, all three techniques demonstrated satisfactory qualitative agreement in measuring peripheral refraction. These findings cast some doubt on the accuracy of the measurements obtained by Rempt *et al.* (1971) when measuring peripheral refraction, by retinoscopy, at eccentricities beyond 50°.

3.2.2 Refractive error and the skiagram

Many candidates are rejected when entering the air force or commercial air training programmes due to the detection or possible development of myopia. Hoogerheide *et al.* (1971) observed the refractive development of 214 pilots, over a number of years, to assess the risk of myopia progression and onset. The skiagram classification, designed by Rempt *et al.* (1971), was used to describe the peripheral refraction. The initial skiagram was compared to the final refractive error. Forty percent of the 28 pilots who were initially hyperopic and showed a myopic shift in refractive error, but remained either emmetropic or hyperopic, had type I skiagrams. Nine hyperopic pilots became myopic and 45% belonged to the type I group. Seventeen emmetropic pilots became myopic and 77% again conform to type I. The type IV skiagram was found in 66% of emmetropic and hyperopic pilots where no myopic shift in refractive error was apparent. Rempt *et al.*, also found type II and V eyes which they considered intermediate forms. Hoogerheide *et al.*, found that type II eyes were represented by a flatter tangential image shell compared to the sagittal and were found in emmetropic and myopic eyes. Conversely, the type V eyes had a flatter sagittal image shell compared to the tangential and were present in emmetropic and hyperopic eyes.

Type I was the most commonly found skiagram in myopic eyes. Type I resemble the type B eyes described by Ferree *et al.* (1931). According to the results, Hoogerheide *et al.* (1971) concluded that the skiagram could be used as an indicator to predict whether a subject may have a myopic shift in refractive error.

Millodot (1981) studied the relationship between peripheral refraction and ametropia in both eyes of 32 subjects, varying in age from 18 to 57 years. Using an objective optometer (Topcon refractometer), Millodot measured central and peripheral refractive error along the horizontal axis, nasally and temporally, to 60° eccentricity. The subjects were divided, by spherical equivalent refractive error, into three groups: 30 myopic eyes (range -1.00D to -7.87D), 13 near-emmetropic eyes (range -0.99D to +0.74D) and 19 hyperopic eyes (range +0.75D to +4.50D). Millodot found that the amount of astigmatism increased steadily with eccentricity in 91% of eyes and this amount is nearly independent of the central refraction. Ferree *et al.* (1931) would describe these eyes as type A. The astigmatism was found to be constant cross the horizontal plane in 5 eyes (type B) and asymmetric between nasal and temporal fields in 9 eyes (type C).

The study also found differences in the type of astigmatism in relation to ametropia. On average, the centrally emmetropic eyes exhibited mixed astigmatism towards the periphery, the centrally myopic eyes exhibited compound myopic astigmatism and the centrally hyperopic eyes exhibited compound hyperopic astigmatism (except in the far periphery).

3.3 Peripheral astigmatism in schematic eyes

Theoretical values for peripheral astigmatism can be achieved using schematic eyes. A schematic eye is a theoretical optical model of an eye, retaining average dimensions of the human eye but excluding the complications. There are many schematic eyes, derived by a number of authors, as no single model can approximate all eyes owing to the gradient index nature of the crystalline lens, dimension changes with age and asymmetries within the ocular system.

The majority of schematic eyes are represented as small-angle paraxial models with a limited number of optical surfaces and homogeneous optical media. The first model produced by Listing (1851. Cited in Bennett and Rabbetts, 1989) became the basis for subsequent schematic eyes. The most commonly used schematic eyes are those derived by Gullstrand in 1909. Gullstrand's No.1 schematic eye had six refracting surfaces with a high index homogeneous nucleus (1.406) surrounded by a lower index cortex (1.386). Data was provided for both an unaccommodated version and accommodated version of the eye. Gullstrand's No.2 eye is a simplified schematic eye which consists of a single-surface cornea and a 'thin' crystalline lens.

Paraxial models are unable to predict ocular aberrations away from the optical axis. Modern schematic eye designs have included aspheric corneal surfaces, different refractive indices within the system and occasionally aspheric lenticular surfaces (Lotmar, 1971 and Drasdo and Fowler, 1974).

Theoretical values for peripheral astigmatism

Le Grand (1967) used a three-surfaced schematic eye to calculate peripheral astigmatism and examined how it varied with eccentricity. The astigmatism was determined along the horizontal meridian, in 10° intervals, both nasally and temporally. The hypothetical values ranged from 0D at 0° eccentricity to 11.29D nasally and 7.52D temporally at an eccentricity of 50°. The calculated values for astigmatism, obtained by Le Grand, appear to be considerably greater than those acquired experimentally, e.g.

results obtained from Ferree *et al.* (1931), Rempt *et al.* (1971) and Millodot (1981). Le Grand suggested that the lack of agreement between the theoretical and experimental amounts of astigmatism was a result of either peripheral flattening of the cornea and posterior crystalline lens surface or the gradient structure of the lens. However, it must also be noted that Le Grand based his calculations on an emmetropic schematic eye with spherical surfaces and homogeneous refractive indices. More realistic values for peripheral astigmatism were calculated by Lotmar (1971) using a schematic eye with aspheric surfaces, although the peripheral astigmatism was still of a higher order than that found experimentally. Lotmar concluded that the difference found between empirical and theoretical values was a result of peripheral flattening of the cornea or variations in the refractive index or curvature of the crystalline lens which gives rise to a reduction in peripheral astigmatism. Millodot and Lamont (1974) pursued the idea by assessing peripheral astigmatism in subjects where the aspheric cornea was fitted with a spherical contact lens. Unfortunately, no significant difference was found with or without the contact lens.

3.3.1 Modelling peripheral astigmatism using schematic eyes

Determining exact complex ocular parameters is extremely difficult; yet, these properties govern peripheral refraction. The interval of Sturm depends upon the power of the whole system. The tangential foci are mainly influenced by power and the sagittal foci are mainly influenced by retinal curvature (Dunne, 1995).

Dunne and Barnes (1987) assessed peripheral astigmatism in a schematic eye by adjusting the crystalline lens curvature and the refractive index. The peripheral astigmatism was modelled in a four-surfaced schematic eye, with an homogeneous lenticular refractive index, to match that of peripheral astigmatism found in real eyes. Pupil size, central refraction and biometry measurements from real eyes were used, although the lens parameters did not correlate exactly with those of real eyes. Low amounts of peripheral astigmatism were found difficult to model, which often occurs in many myopic eyes. To correct for these low values of peripheral astigmatism, Dunne and Barnes had to use unrealistically flat aspheric lenticular surfaces. When the model was used to produce the correct amount of peripheral astigmatism, an over correction of the spherical aberration resulted. Lotmar (1971) also found an overestimation of spherical aberration when modelling peripheral astigmatism. Dunne and Barnes concluded that both spherical aberration and peripheral astigmatism could not be

concurrently modelled in schematic eyes. However, further work by Dunne and Barnes (1990) calculated peripheral astigmatism in schematic eyes by modelling peripheral refraction previously measured in eyes where the optical surface parameters were known. Measured ocular component data in conjunction with a computer program designed by Leary and Young (1968) was used to derive a three-surfaced schematic eye. With this technique, Dunne and Barnes discovered that peripheral astigmatism could be modelled to produce results that corresponded with the upper limits of experimental data to eccentricities of at least 40°. Their calculations indicated that aspheric surfaces and monoincidental crystalline lens parameters could be used to model peripheral astigmatism adequately.

3.4 Retinal contour

A number of investigators have suggested that different classifications of peripheral astigmatism are related to ametropia and a variety of retinal shapes (Charman and Jennings, 1982 and Ferree and Rand, 1933). Dunne *et al.* (1987) devised a model to correlate peripheral astigmatism with retinal shape. The retinal shape was then used to describe ametropia. An elliptical retinal surface model, with a constant equatorial radius, produced values and types of peripheral astigmatism found experimentally.

Further work, by Dunne (1995), led to the development of a computer program to determine retinal contour utilising measurements of central refraction, peripheral refraction, keratometry and A-scan ultrasound from real eyes. The program used formulae derived by Royston *et al.* (1989) and Bennett (1988b) to create a three-surfaced schematic model of the eye. Peripheral refraction can be measured at various eccentricities. The computer program adjusts the asphericity of the cornea until the calculated values of peripheral astigmatism match the measured values. The retinal curvature can then be adjusted until the calculated sagittal refractive error matches the measured value. Co-ordinates for the retinal contour are then expressed for each eccentricity measured. Dunne also evaluated the inherent errors arising from the computing scheme's methods of compensating for unmeasured human ocular complications, e.g. gradient index structure of the crystalline lens and its surface asphericity, varying pupil apertures and ocular surface misalignment and toricity. Fortunately, the computed retinal contours were only mildly affected by the inherent errors. Other investigators have used laser Doppler interferometry (LDI) to measure

retinal shape *in vivo* (Hitzenberger, 1991 and Schmid *et al.*, 1994), high resolution magnetic resonance imaging (Cheng *et al.*, 1992) and computed tomography (Wang *et al.*, 1994) to give a cross-sectional image of the eye.

3.5 Summary

- The human eye exhibits peripheral astigmatism.
- Peripheral astigmatism is influenced by the ocular components and can be classified according to the pattern of horizontal and vertical foci.
- Peripheral astigmatism has been measured in eyes with various central refractive errors and it has been suggested that one particular pattern of peripheral astigmatism, the type I or type B eye, may be indicative of myopia. It then follows that this pattern of astigmatism may reveal the type of biometric characteristics that accompany myopia. This link has not yet been thoroughly explored, especially in association with the onset and progression of myopia. One particular aspect exploited in this thesis is retinal contour and its relationship with emmetropia and myopia.

3.6 Aims and objectives of the thesis

There has been a large amount of research on the subject of myopia, especially youth-onset myopia. Youth-onset myopia occurs around the age of 6 and continues throughout the teenage years. By the late-teens, approximately 25% of Western populations exhibit myopia with an even greater percentage found in Southeast Asian countries.

The second most common form of myopia is early adult-onset (late-onset). This form of myopia appears in the late teens or middle twenties at a time when physical maturity has been reached and the eye, in theory, should have ceased growing. Late-onset myopia constitutes 8 to 10% of the myopia population in the Western world and appears to be increasing. An explanation for late-onset of myopia is still unclear. The majority of studies on this subject have been cross-sectional with the exception of a small number of longitudinal studies.

Previous studies have indicated significant correlation between late-onset myopia and particular ocular parameters, i.e. axial length and its allied constituents and keratometry. Sustained near work and changes in the accommodative and vergence systems have been indicated as possible causative factors for myopia onset. The aim of this thesis is to investigate the ocular biometric correlates associated with late-onset myopia and will include assessment of retinal shape and possible causative factors. A number of parameters will be assessed, including A-scan ultrasound, keratometry, corneal topography, accommodative stimulus-response, *in vivo* crystalline lens measurement (Scheimpflug camera), parental history, near work demands, central refractive error, peripheral refraction and ultimately retinal contour, to enable further understanding of how these parameters contribute to late-onset myopia.

One particular area of interest is that of peripheral astigmatism and retinal contour. The type I classification of peripheral astigmatism has previously been linked to the myopic eye (Hoogerheide *et al.*, 1971) and the prolate retinal shape, associated with myopia, has been demonstrated in a cross-sectional study of anisometropia (Logan, 1997). The longitudinal assessment of central and peripheral refraction in this study will, hopefully, provide a way of predicting myopia in subjects and will illustrate the change in retinal shape with myopia onset and progression.

CHAPTER 4

INSTRUMENTATION AND SUBJECTS

4.1 Subjects

The subjects comprise 2 groups: emmetropes and myopes. Hyperopes were not included in the experiment. The cohort consisted of 50 subjects, aged 16 to 26 years (mean age 20.36 ± 2.73), of Caucasian, Indian sub-continent and East-African Asian origin. The subjects were divided into 23 males and 27 females. The majority of subjects were recruited from the Optometry undergraduate course at Aston University. A small number of subjects ($n = 4$) were recruited from other schools within Aston University and through colleagues.

Subjects were excluded from the study if they presented with the following: -

1. Hypermetropia - where the spherical equivalent refraction is greater than +0.50D
2. Astigmatism greater than -2.00D
3. Strabismus or amblyopia
4. Gas permeable or hard contact lens wearers
5. Ocular disease
6. Systemic disease that may influence the results.
7. Prescribed medication that may influence the results.

Nine subjects were habitual soft contact lenses wearers.

Thirty-five subjects were examined on 3 occasions over a 2-year period and the remainder were examined on 3 occasions over an 18-month period. At initial examination, the group was divided into 26 emmetropic subjects and 24 myopic subjects. Emmetropes were defined as subjects with a spherical equivalent refractive error of -0.24 to $+0.50$ D. Myopes were defined as subjects with a spherical equivalent refractive error of -0.25 D or greater.

All biometric data and refractive history for subjects are provided in Appendix 1. *Considerable time was spent attempting to recruit children and young adolescents, aged 7 to 15 years, for the study. Letters were sent to schools and Scout groups to encourage children to get involved but unfortunately the recruitment failed due to lack*

of interest and parental consent. Copies of the letters sent to schools and parents can be found in appendix 2.

Ethical approval was acquired from Aston University HSEC prior to the onset of the study and informed consent was obtained from all subjects proceeding experimental testing. Details of ethical approval can be found in appendix 3.

4.2 Biometry measurements

A series of measurements were required, including oculomotor balance tests, according to the rationale presented in previous chapters. At all 3 visits the subjects participated in the following: -

1. Full subjective refraction (checked using +1.00D blur test) and eye examination
2. Objective central refraction (Canon R-1 Autorefractometer)
3. Objective peripheral refraction (Canon R-1 Autorefractometer)
4. A-scan ultrasonography (Storz Omega)
5. Keratometry (Rodentstock)
6. Corneal topography (EyeSys 2000)
7. Assessment of accommodation
8. Oculomotor balance assessment
9. Scheimpflug photography.

On the final visit, measurements were taken of intraocular pressure and ocular blood flow and subjects were questioned regarding their family history, refractive history and approximate number of hours spent working at near. The same person (Justine Harper, GOC registered Ophthalmic Practitioner) took all measurements.

The subjective and objective refractions were obtained after instillation of 2 drops of 1% tropicamide HCl (*Minims*[®], Chauvin Pharmaceuticals, Kent, U. K.) to each eye with a 5-minute interval between drops to achieve mydriasis and cycloplegia. Drug dosage was 2 drops of approximately 30µl per eye. Mydriasis and the depth of cycloplegia were monitored by assessing pupil response to light and amplitude of accommodation.

4.2.1 Measurement of refractive error

Subjective and objective measurements of refractive error were a central part of this study. The subjective refractive error was recorded for each subject, at each visit, to

allow comparison with previous refractions undertaken by the subject's own optometrist. The experimental design required the use of an objective method of measuring refractive error to allow the stimuli to be presented to the subjects at a range of different distances and locations from the eye. Five refractive error readings were taken at each stimulus distance. All refractive error measurements were converted from sphere, cylinder and axis into an equivalent mean sphere value using a computer program, written by Dr Mark Dunne, in *Quickbasic*. Previous investigation on instrumentation and experimental set-up for measurement of peripheral refraction indicated the Canon R-1 to be the autorefractor of choice (Logan, 1997). The Canon R-1 infrared autorefractor provides a binocular open-view extending 18° vertically and 50° horizontally.

4.2.1a Infrared optometers

An optometer is an instrument that measures refractive error and is being used increasingly in general optometric practice. Objective optometers use an optical system within the instrument to determine the vergence of light reflected from a subject's retina. Objective optometers are divided into non-electronic instruments, e.g. Zeiss Jena Coincidence Refractionometer (designed by Hartinger in 1951) and electronic instruments, e.g. Canon Autorefractor (Canon Europa, Holland 1981). Collins (1937. Cited in Bennett and Rabbetts, 1989), designed the first electronic optometer. The instrument worked by assessing the quality of the retinal image. The basic features of the Collins optometer were utilised in subsequent optometers, e.g. the *Dioptron*.

Electronic optometers fall into three main classes according to their mode of operation, these are: -

1. *Analysis of image quality* - based on the principle of grating focus
2. *Retinoscopic scanning* – based on the principle of retinoscopy
3. *Scheiner disc refraction* – based on the Scheiner disc principle of refraction

The majority of electronic optometers use infrared radiation (IR) as it cannot be seen by the human eye, rather than visible light, to prevent subject distraction when ascertaining the refractive error. Infrared radiation also reduces the risk of pupil constriction and accommodation, which is another disadvantage of bright visible light. Pupil constriction results in an increase in depth-of-focus, which may induce accommodative

changes (Ward and Charman, 1985). The principle of the grating focus is the most commonly employed method for assessing refractive error in electronic optometers. A grating target is illuminated by IR light and is imaged on the retina. The image reflected back from the retina is passed through a mask to detect the intensity. As the optimum focus of the retinal image is approached, the intensity of the reflected IR light increases. The optometer used for objective refraction in this thesis was the Canon Autorefractometer R-1. The instrument uses IR light and the grating focus principle.

4.2.1b The Canon Autorefractometer R-1

The Canon R-1 Autorefractometer was introduced in 1981 by Canon Europa, Holland. The instrument provides objective, static refractive error measurements and is unique in design. The Canon possesses a binocular open-view field extending 18° vertically and 50° horizontally. The open-field of view was a clear advantage over other commercially available instruments, allowing subjects to fixate in a number of different locations and so reduce instrument myopia (Hennessey, 1975). This particular feature has established the Canon as a research instrument permitting measurement of accommodation response and objective measurement of ocular response to stimuli at varying distances from the eye.

A video camera transmits a magnified image of the subject's eye to a monitor, which assists in alignment of the instrument and in checking the subject's fixation. A stationary internal ring is projected, in conjunction with the first Purkinje image from the subject's eye, for alignment purposes.

In normal mode of operation, the grating focus propels a lens along a carrier until the output voltage reaches a maximum and the time taken to achieve this is computed. The Canon has three sets of detectors, each separated by 60°, and computes a spherocylindrical refractive finding by applying a sine curve. The Canon can be modified to provide continuous recordings of refractive error measurements (Pugh and Winn, 1988). These modifications allow the focusing system to be disabled and set manually to allow the output voltage from any one of the three detectors to be examined continuously. In continuous mode, the refractive error measurements are directly related to the magnitude of the output signal. Modification of the Canon in this way has enabled measurement of microfluctuations in accommodation (Gray *et al.*, 1993 and Gray *et al.*, 2000) and dynamic measurements of accommodative response (Culhane and Winn, 1999).

The manufacturers claim an operating range of $\pm 15.00D$ for spherical power and $\pm 7.00D$ for cylindrical power. Power increments are in $0.12D$ steps and the cylinder axes in 1° steps. The single-shot measurement operation is complete in 0.2 sec and a spherocylindrical measure of the subject's refractive error is displayed on the monitor. The results can be printed onto heat sensitive paper or directly transferred to a computer. The Canon R-1 Autorefractor has not been commercially available for a number of years, but recently an instrument using a similar open-view design, but different image processing features, has been introduced (Shin-Nippon SRW-500 autorefractor, Grafton Optical, U.K.).

4.2.1c Mode of operation

The Canon R-1 images a square-wave grating on the subject's retina while focusing lenses traverse along the optical axis of the measurement trolley. When the retinal image is optimally in focus, the photodetectors deliver maximum output. The time taken for this sequence of events to occur is then converted to a dioptric value of refractive error. There are three sets of photodetectors present in the Canon. The photodetectors measure concurrently in three meridians separated by 60° . The signal is converted into a d.c. voltage waveform. The relative location of the maximum voltage peak from each photodetector occurs for the position of best focus of reflected beam on the detector masks. Algorithms, described by Matsumura *et al.* (1983), provide calculation of refractive error through the spherocylindrical measurements.

All IR optometers have a limiting pupil diameter. The Canon has a specified minimum limiting pupil diameter of 2.9mm in the static mode. A minimum limiting pupil diameter of 3.8mm is required for continuous readings (Winn *et al.*, 1989). The Canon is pupil independent, in its static mode of operation, for pupil diameters greater than 2.9mm. Refractive error is calculated from the respective peak photodetector outputs derived from relative location rather than magnitude. If the pupil diameter is less than 2.9mm, the signal returning from the eye is too attenuated and a reliable measurement of refractive error cannot be achieved. The Canon is unable to locate the position of maximum output for the three photodetectors, for reduced pupil diameters, resulting in an error reading (see figure 4.1).

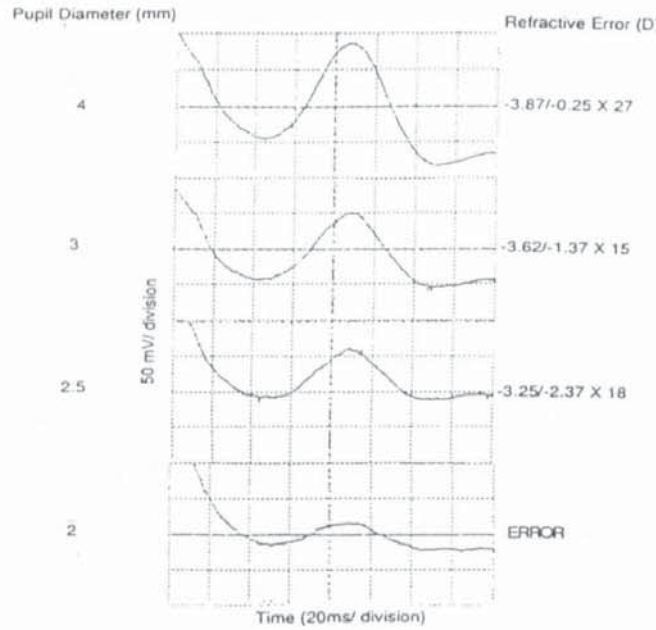


Figure 4.1 Static 'single-shot' recording through 4 pupil diameters illustrating the change in waveform. The charts demonstrate the difficulty in locating the peak position in small pupils. After Winn *et al.* (1989).

4.2.2 Peripheral refraction

Peripheral refraction was measured using the Canon R-1 Autoref for this study. An accessory, in the shape of an arc, was placed horizontally on top of the main body of the instrument at a distance of 50 cm from the subject's eyes (see figure 4.2).

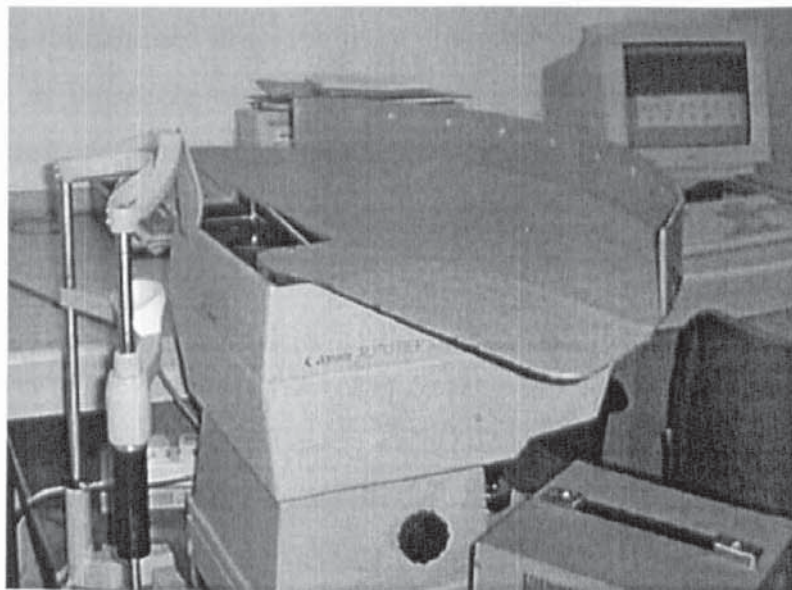


Figure 4.2 Canon Autoref R-1. Arc fitted for taking measurements of peripheral refraction.

The fixation targets were alternate yellow and orange spots set horizontally at 5° intervals around the arc to a maximum of 35° both nasally and temporally. Five refractive error readings were taken at each eccentricity. The data from the Canon was transmitted automatically to a personal computer via an interface (designed and distributed by Steve Spadafore, Franklin and Marshall College, Lancaster, USA). The interface was connected to the printer port of the Canon. A computer program, originally written in *Quickbasic* for the Apple Macintosh, devised by Dr Mark Dunne uses the refractive error data plus tangential keratometry readings and A-scan ultrasonography to produce X and Y co-ordinates to create the retinal contour. As computational speed of the original computer program was very slow, a final year computer science student from Aston University, Chris Knight, transferred the program to PC (under supervision) as part of his final year dissertation. The full computer program for PC is available on CD-ROM. See appendix 4.

4.2.3 A-scan ultrasound

A-scan ultrasound has been used extensively to measure ocular dimensions and is also employed in intraocular lens power calculations. Ultrasonic waves are produced by applying electrical energy to a small transducer. The transducer is located within a probe which is placed on the eye. The electrical energy generates a short pulse which is termed the Piezo-electrical effect. As the pulse voltage varies in polarity, the Piezo-electric crystal expands and contracts rapidly and vibrations are produced. The electrical energy is transformed into longitudinal sound waves. These sound waves are partially reflected by interfaces where there is a change in density, or elasticity, of the medium of the ocular components. The reflected vibration is called an echo.

The two methods of ultrasound most commonly used in ophthalmic applications are time-amplitude (A-scan) and intensity modulated (B-scan). A-scan ultrasonography is one-dimensional and is considered the most accurate mode for taking linear measurements within the eye. B-scan ultrasonography is two-dimensional and can map a transverse section of the eye by scanning.

The frequency of the sound waves is typically 10 –20 MHz which is above the range of human audibility. A lower frequency results in better penetration of the ocular media. High frequencies give better resolution but poor penetration. High frequency can also cause ocular injury. The amplitudes of the reflected echoes are recorded as micro-voltages and displayed on a storage oscilloscope. Echoes are recorded from the anterior

corneal surface, the anterior and posterior crystalline lens surfaces and the internal posterior surface of the eye. The echo from the internal posterior surfaces of the eye consists of a series of reflections resulting from the different layers of the retina. The time taken for the ultrasonic wave to be reflected and return to its point of origin is converted to distance (in millimeters), using the assumed velocities of sound in the ocular media. The Storz Omega assumes the value of velocity through the ocular media to be 1550m/s. Storey (1982) states an accuracy of $\pm 0.1\text{mm}$ for axial length measurement using the A-scan ultrasound and Bennett and Rabbetts (1989) suggest accuracy within $\pm 0.1\text{mm}$ to $\pm 0.2\text{mm}$ relating to possible errors of 0.25D and 0.50D in refractive error calculation.

Ultrasound was measured using a Storz Omega Compu-Scan Biometric Ruler (Storz International, St. Louis, USA). The instrument has a solid probe and a focused 10MHz transducer and takes a series of 512 readings in 0.5s. The relatively fast sampling time reduces the effects of eye movements (see figure 4.3).

The A-scan probe was initially sterilised with an alcohol swab (*Seton Healthcare*, England) before use with each subject. Unfortunately, the protocol for ultrasonography had to be adjusted towards the end of the study owing to the introduction of guidelines regarding variant Creutzfeldt-Jacob Disease (vCJD) and contact with the eye¹.

¹ Disposable tips were not available for the instrument at the time of study. Ultrasonography continued on subjects showing a myopic shift in refractive error only. Future projects of this nature would benefit from the new non-contact IOL Master (Zeiss Instruments) which uses partial coherent interferometric techniques to measure axial length, with resolution of $\pm 0.01\text{mm}$.



Figure 4.3 Omega Ultrasound (Storz).

Topical instillation of 1 drop of 0.4% benoxinate HCl (*Minims*[®], Chauvin) produced corneal anaesthesia in around 30 seconds to allow contact of the probe with the subject's eye. During ultrasonography, the subjects had reduced accommodation and dilated pupils owing to the previously induced cycloplegia (2 drops of 1% tropicamide HCl). A distant spotlight or Snellen letter have been found to be the optimum fixating conditions for obtaining accurate measurements (Steele *et al.*, 1992). The subjects were instructed to fixate a spotlight at 4m. While the subject was fixating the spotlight, the hand-held probe was placed gently onto the central portion of the cornea. A minimum of 10 measurements was taken on each eye and the probe was removed from the eye between each measurement. The instrument has a menu option to reject any measurements with a standard deviation of 0.1mm or greater; this option was employed.

4.2.4 Keratometry

Keratometry is a technique used to obtain measurements of the radii of curvature of the anterior surface of the cornea. The principle of the keratometer is based on the reflection of the image from the anterior corneal surface, the first Purkinje image, of an illuminated pattern (mires) of known size. The corneal radius of curvature can be calculated once the size of both the mires and the images are known. The radius of curvature can be measured along the two principle meridians and the amount of corneal

astigmatism present is the algebraic difference between these two radii. Most keratometers measure over an annular area of approximately 3mm diameter (Bennett and Rabbetts, 1989). The central radius of curvature is measured between two points on either side of the keratometer axis and it is assumed that the surface between these two points is spherical. However, the normal cornea flattens in the periphery and is aspheric (Bennett, 1988a).

The keratometer has a calibrated doubling device, that allows both mire points to be made coincident, which facilitates the measurement of this separation and hence the corneal radius that is directly proportional to it. This method has the advantage of making the results relatively independent of small eye movements.

The keratometry measurements were obtained using a Rodenstock keratometer. This instrument has variable doubling, a divided objective aperture and is a 2-position keratometer allowing the mires to be rotated to measure along separate meridians. Focusing errors are eliminated owing to a secondary objective system mounted in front of the doubling system, which produces a real image of the telescope entrance pupil.

The keratometer was calibrated at regular intervals with ball bearings of known diameter. Three readings were taken along the 2 principle meridians of each eye and the results averaged to give a mean. A short computer program, written in *Quickbasic* by Dr Mark Dunne, provided a tangential value of corneal curvature. See appendix 4.

4.2.5 Topographic Corneal Mapping System

Corneal topography instruments have become increasingly popular in the clinical environment. They can be used for determining the corneal refractive power, corneal shape changes due to contact lens wear, detection and diagnosis of keratoconus and to assess changes after refractive surgery and corneal graphs (Douthwaite *et al.*, 1999).

Most corneal topography instruments are based on the placido disc and keratoscope. A keratoscope is an instrument for inspecting the front surface of the cornea. It consists of alternate black and white concentric rings. The pattern of the rings is reflected from the cornea to provide a qualitative evaluation of the anterior corneal surface. Computer-assisted photokeratometry is an advanced version of keratometry and the instruments are generally known as corneal topography systems. One commercially available instrument is the *EyeSys 2000* Corneal Analysis System (Spectrum Ophthalmic, U.K.).

Keratometers are used to assess central corneal curvature and topographers are used to measure corneal curvature off the visual axis. Computerised corneal topography systems are used to assess corneal curvature both centrally and peripherally and can provide a more comprehensive description of corneal curvature and shape. The computer algorithms produce a map of the corneal surface. A colour coding system is applied to the map to indicate different corneal powers. Blue denotes low corneal power and red indicates high corneal power (Maguire *et al.*, 1987). The instrument also provides the major K readings along the main astigmatic meridians and an indication of peripheral corneal flattening in the form of a shape-factor, i.e. ρ -value. The *EyeSys* system provides a number of different corneal mapping options depending upon how the images and data need to be displayed. The *EyeSys* Corneal Analysis System has been used to evaluate corneal curvature, power and shape in this thesis (see figure 4.4). The *EyeSys* calibration was checked on a regular basis using the 6.13mm (55.06D) calibration sphere and calibration program provided with the *EyeSys* system.



Figure 4.4 Eyesys 2000 Corneal Topography System.

4.2.6 Measurement of accommodation

Accommodation is the term used to describe the mechanism, within the eye, which allows rapid change in refracting power to enable objects to be focused on the retina. The young eye is able to change its refractive power predominantly by alteration in anterior curvature of the crystalline lens via ciliary smooth muscle contraction.

Amplitude of accommodation is the maximum amount of accommodation an eye can exert. Amplitudes were measured subjectively using a RAF near-point rule which had been modified to read to the nearest 0.50D. The subjects observed a high contrast, black-on-white near-point card, with N5 print. The distance correction was in place before measurements began and the push-up method was used to assess the amplitude of accommodation. The RAF rule was placed on the subject's cheeks and the near-point card was held, at eye level, at a distance of 50cm from the subject. The near-point card was slowly moved in towards the subject. The subjects were asked to locate the position of first, slight, sustained blur of the target, as suggested by Rosenfield (1997), at which point the amplitude of accommodation was read from the RAF rule. This measurement was repeated three times. Monocular and binocular measurements were taken. The amplitude of accommodation declines from approximately 14D at age 10 to 0.50D at age 60. The average 20 year-old subject should have approximately 12D of accommodation.

4.2.7 Measurement of convergence

The near point of convergence is described as the nearest point where the lines of sight intersect when the eyes converge to the maximum. This point is approximately 8cm from the spectacle plane in a normal subject. The RAF near-point rule was used in the assessment of convergence in this thesis. The subjects were asked to observe the high contrast vertical black line on the near-point card. The push-up method was used to determine when the line doubled. The position of the card marked the near point of convergence. Unlike the decline in accommodative power with age there is no systematic decrease in convergence (Bennett and Rabbetts, 1989).

4.2.8 Accommodative response

Accommodation is a response to an out-of-focus retinal image. Measurement of the accommodative amplitude alone provides information regarding the maximum potential accommodative response, rather than the actual response to a stimulus. Some subjects may show a tendency to overaccommodate for near targets, rather than exhibiting the typical lag of accommodation (Rosenfield, 1997). The accommodation system has been implicated in myopia development, although, the true nature of the relationship remains unclear (see §2.4). The accommodation stimulus response-curve was measured with the Canon R-1 Autorefractor for this thesis.

As mentioned previously (see §4.2.1c) the minimum pupil diameter required for the Canon to calculate an accurate refractive error reading is 2.9mm. In young eyes near vision tasks normally cause a reduction in pupil diameter as accommodative demand increases. This reduction in pupil diameter limits the accommodative demand that can be imposed on subjects. If the accommodation level produces an associated pupil constriction of less than the limiting level of the instrument, an error reading will be recorded by the Canon. Appropriate selection of subjects and accommodative stimuli, in conjunction with reduced ambient lighting levels, were used in the present study to maintain pupil diameters above 2.9mm. Changes in stimuli were generated by physically moving the target, in real space, along the subject's midline in order to simulate naturalistic viewing conditions as demonstrated previously by Abbott *et al.* (1998) and Baker *et al.* (1998). Accommodative stimuli were located at viewing distances of 6, 3, 2, 1, 0.50, 0.33, 0.25 and 0.20m. The target luminance was set at 35cd/m². Six readings were taken at each stimulus location. Targets comprised high contrast, black-on-white Snellen acuity optotypes ranging from 6/60 to 6/6. Subjects were instructed to view an individual optotype in the lowest line of letters that they were able to see clearly. All subjects were either emmetropes or wore corrective contact lenses. All data was entered into an Excel spreadsheet to produce a single figure index for accommodative response (Chauhan and Charman, 1995).

4.2.9 Scheimpflug videography

In 1896, Theodor Scheimpflug developed the first camera to provide wide-angle photographs called 'eye of the fly'. Scheimpflug photography is a valuable technique for assessment of the anterior chamber of the eye. The Scheimpflug principle allows imaging of the anterior chamber, with minimal distortion, using a unique camera design and slit beam.

If the object plane is tilted with respect to the optical axis and the image plane is perpendicular to the optical axis, then the image produced will be unfocused. The image plane must be tilted to give a focused image. The amount of tilt is determined by the Scheimpflug principle. The optical axis of the camera is arranged to be at an angle of 45° to the optical axis of the slit beam. In accordance with the Scheimpflug principle, the lens plane, object plane and image plane must be co-incident to supply a focused image along the entire image plane. A camera using the Scheimpflug principle must have a lens and film plane that can be tilted separately. However, it must be noted that

although the image is focused along the plane, the magnification is not constant along the entire plane owing to different locations of the plane being at different distances from the lens.

There are a number of commercially available instruments on the market. The CASE-S (computerised anterior segment evaluation) instrument designed by Marcher Enterprises (Hereford, England) was used for *in vivo* anterior segment analysis in this thesis (see figure 4.5). The CASE-S comprises a CCD camera linked to a desktop computer. The CCD image plane is tilted to obtain a focused image. The slit beam and camera are separated by 45° to provide a sagittal section through the cornea and lens. The computer displays the images on screen as a matrix of 512x512 picture elements (pixels) and uses a 256 grey-scale range. Digitised images are saved and transferred to frame store for further analysis.

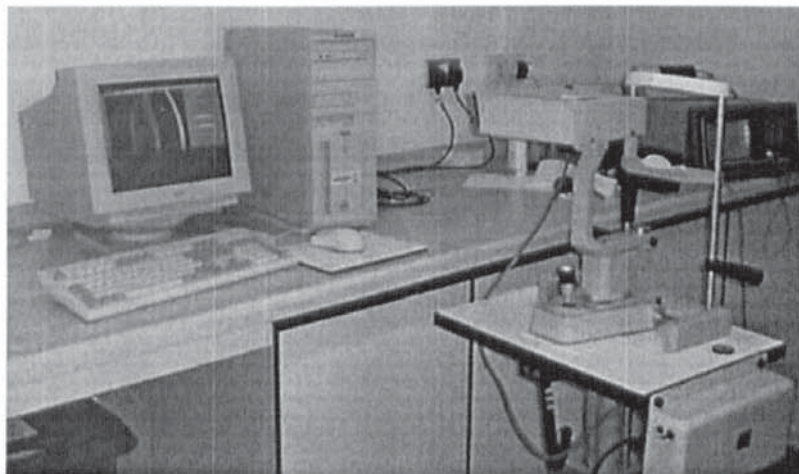


Figure 4.5 Scheimpflug camera (Marcher instruments).

For an accurate and reproducible section of the eye to be generated, the slit beam must pass along the optical axis of the eye. The CASE-S uses green and red (for right and left) patient fixation lights and a sensor to detect light reflected from the cornea to achieve alignment of the system. The CASE-S possesses an image analysis program which identifies the anterior and posterior corneal surfaces and the anterior and posterior crystalline lens surfaces and provides curvature measurements for these surfaces. The program can also supply linear measurements of the corneal thickness, anterior chamber depth and lens thickness. The analysis program positions three points along each surface, draws an arc through the points and supplies a spherical curvature reading. Unfortunately, the cornea and crystalline lens surfaces are aspherical, not

spherical. An alternative custom analysis program was used (*Extract*, written by Daniel Harris, Aston University, 1997) which provided accurate positioning of points along the corneal and lens surfaces and further manipulation of the data produced asphericity values.

Five images were taken for each eye. Mydriasis was achieved by instillation of 1% tropicamide HCl (*Minims*[®], Chauvin).

4.2.10 Ocular blood flow tonograph

The ocular blood flow (OBF) tonography system (OBF Labs, Cleverton, U. K.) is an objective method of measuring ocular blood flow. Blood enters the eye via the ophthalmic artery and consists of two components: the pulsatile component (which varies with the arterial pulse) and a steady continuous component. The OBF measures pulsatile choroidal blood flow. The pulsatile flow represents 75 to 85% of the total choroidal blood flow and the choroidal blood flow represents 80 to 95% of the total blood flow to the eye (Riva *et al.*, 1994; Langham *et al.*, 1989 and Hosking *et al.*, 2000). The high percentage of pulsatile flow present in the choroid provides a reliable parameter for evaluation of choroidal circulation.

The POBF consists of a pneumotonometer and a computerised analysis system. A continuous measurement of intraocular pressure (IOP) can be made using the pneumotonometer. The instrument obtains 200 IOP measurements per second over a number of heartbeats and has a resolution of 0.01 mmHg. In addition to measuring IOP, the instrument also calculates the blood flow through the eye in microlitres per second.

The pneumatic probe consists of a piston, a sensor and a silastic membrane disposable tip. A continuous flow of air circulates within the pneumotonometer and forces the piston forward. Airflow at the tip is constant and forces the membrane to bow outwards. When the tip is applied to the anaesthetised cornea it flattens the membrane and raises the pressure within the pneumotonometer sensor. The sensor automatically alters the pressure on the piston and the amount of alteration is dependent upon the IOP. Changes within the sensor are recorded and interpreted by the computer software (see figure 4.6).

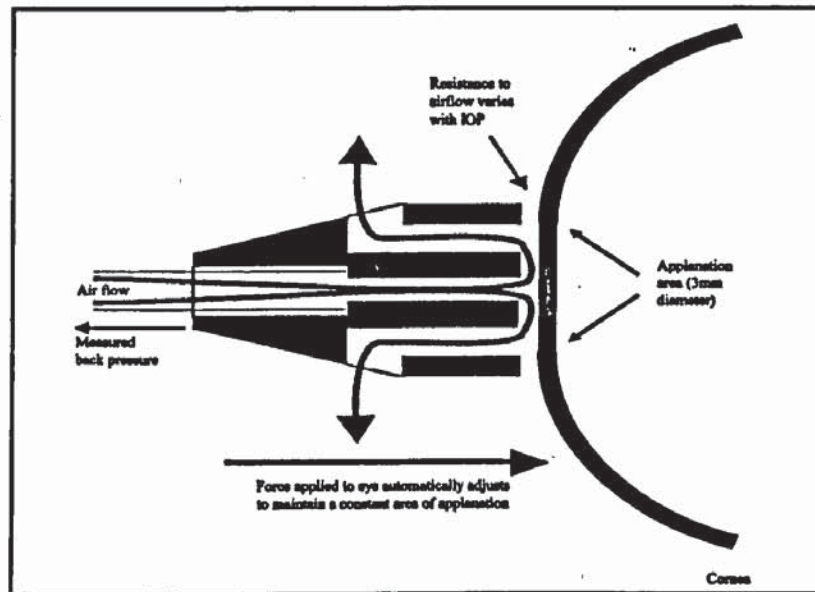


Figure 4.6 Schematic drawing of the OBF tonograph in contact with the cornea. After Hosking *et al.* (2000).

The pulsatile choroidal blood flow is calculated from: -

1. the pulsatile variations in IOP
2. the heart rate
3. the pulse volume

Unfortunately certain assumptions have to be made before calculation of the OBF can be made, these are: -

1. the outflow of blood from the eye is non-pulsatile and steady in flow
2. the blood vessels do not collapse
3. blood does not reflux
4. the IOP is registered correctly and is transferred into a volume measurement (Krakau, 1992).

Glaucoma, diabetes and other pathology of the retina, optic nerve head and choroid have been linked to impaired OBF measurements (Geyer *et al.*, 1999; Langham *et al.*, 1991 and Langham and Kramer, 1990). In relation to myopia, James *et al.* (1991) has indicated that choroidal circulation is reduced in eyes with long axial lengths. A recent study by Silver and Geyer (2000) has examined the pressure-volume relationship for a

living human eye, which relates changes in intraocular pressure to changes in intraocular volume.

4.3 Drugs instilled for experimental procedures

Cycloplegia and mydriasis was achieved by instilling two drops of 1% tropicamide HCl (Chauvin, *Minims*[®]). The drops were separated by a 5-minute interval as proposed by Egashira *et al.* (1993) in their study of cycloplegia in children. Dilation and cycloplegia was required to obtain peripheral refraction measurements, subjective refraction and Scheimpflug images. Ultrasound assessment was performed under cycloplegia to prevent measurement errors arising from lens thickness changes on accommodation. Benoxinate HCl (Chauvin, *Minims*[®]) was the topical anaesthetic used for ultrasonography and OBF.

CHAPTER 5

OCULAR BIOMETRIC CORRELATES OF EARLY- AND LATE-ONSET MYOPIA

5.1 Introduction

There have been a large number of biometric studies that have documented the association between the refractive state and ocular dimensions (see Chapters 1 and 2). The prevalence of myopia in developed countries is reported to be between 25% and 30% with much higher levels recorded in South-east Asia. Myopia can be classified by age of onset and further classified according to myopia progression (see § 2.2). Late-onset myopia, or early adult-onset myopia as it is also known, is characterised by the emergence of myopia after 15 years-of-age. The late-onset myopia group is of particular interest because the growth of the eye is considered to be complete by the age of 13 to 14 years and the majority of individuals refractive error stabilises around 14 to 15 years-of-age (Sorsby *et al.*, 1961 and Sorsby and Leary, 1970).

An abundance of cross-sectional and longitudinal studies exist on the subject of myopia but only a correspondingly low number report on the topic of late-onset myopia (see § 2.3). Previous research has indicated that both early-onset myopia and late-onset myopia is a result of an uncompensated increase in the vitreous chamber depth. Corneal curvature steepening has also been related to the development of myopia. The role of the cornea, in the ratio between axial length and corneal radius, has been indicated as a risk factor in the development of myopia (Grosvenor 1988 and 1994).

5.2 Retinal shape assessment

Calculation of retinal contour

The RetinaFit program, derived by Dunne (1995), produces X and Y co-ordinates to create a retinal contour for each subject. The retinal contour can be represented graphically by plotting a graph of the X and Y co-ordinates and related to the length of the eye by plotting the co-ordinates against axial length.

The retina is aspheric in shape and a simple way to describe the retinal contour is to use the equation for a conic constant. The equation is:

$$y^2 = 2r_0x - \rho x^2$$

where,

r_0 = retinal radius of curvature at the apex

ρ = ρ -value and represents the amount of peripheral flattening

The following ρ -values are used to describe various ellipses: -

$\rho > 1$ oblate (steepens in the periphery)

$\rho = 1$ circle

$0 < \rho < 1$ prolate (flattens in periphery)

$\rho = 0$ parabola

$\rho < 0$ hyperbola.

A graph of X against Y^2 can be plotted. By fitting and a 2nd order polynomial through the points, values can be obtained for retinal apical radius ($2r_0$) and retinal asphericity (ρ).

The peripheral astigmatic factor

The mean amount of astigmatism was calculated at the corresponding nasal and temporal eccentricities. A graph was plotted of eccentricity against mean peripheral astigmatism and a 2nd order polynomial fitted through the points to obtain a value called the 'peripheral astigmatic factor' (paf). The area under the curve represents the total amount of astigmatism. However, the increase in astigmatism from zero into the periphery is of primary interest, rather than the total amount of astigmatism present, so the graph was normalised. The paf was calculated using a mathematical application: integration. The equation for a 2nd order polynomial is:

$$y = ax^2 + bx + c$$

The equation for integration is:

$$\int_0^{35} ax^2 + bx + c dx$$

c can be ignored (normalised) and the equation for paf is:

$$\text{paf} = a(35^3)/3 + b(35^2)/2$$

Where,

a = value obtained from graph with 2nd order polynomial fitted

b = value obtained from graph with 2nd order polynomial fitted

35 = maximum eccentricity

The paf was calculated for both eyes on all subjects on the initial and final visits.

5.3 Guide to abbreviations

A number of abbreviations have been used in this chapter. The key below provides the descriptions for the abbreviations:

- all data = emmetropes and myopes assessed together.
- emms = emmetropes only (−0.24 to +0.50D)
- myos = myopes only (−0.25D or greater)
- es = subjective refractive error (D)
- esc = objective refractive error using the Canon R-1 Autorefractometer (D)
- both eyes = right and left eyes evaluated together
- R = right eye only
- L = left eye only
- al = axial length (mm)
- vd = vitreous chamber depth (mm)
- acd = anterior chamber depth (mm)
- lt = lens thickness (mm)
- k = corneal radius of curvature (mm)
- EyeSysk = corneal radius of curvature measured with the EyeSys (mm)
- EyeSysp = corneal asphericity
- al/k = ratio of axial length to corneal radius (mm)
- retp = retinal asphericity (calculated using the RetinaFit computer program)
- retr = retinal apical radius (mm. Calculated using the RetinaFit computer program)
- paf = peripheral astigmatic factor

5.4 Purpose

The aim of this chapter is to study the ocular biometric correlates of myopia, paying particular attention to the late-onset myopia group and the progressing myopia group. The correlates will be examined both cross-sectionally and longitudinally to provide further understanding of how these parameters contribute to myopia progression and myopia onset in young adults. It is hoped that the results will support the results of previous investigators, while providing some new information relating to causative and predictive factors. Basic regression statistics and corresponding correlations will be applied to the data in conjunction with a more advanced form of regression analysis: stepwise multiple regression.

5.5 Methods

Subjects

The cohort consisted of 26 emmetropic subjects and 24 myopic subjects. The myopic group was also sub-divided into early-onset myopes (n = 14) and late-onset myopes (n = 10) and the emmetropic group was sub-divided into stable emmetropes (n = 22) and emmetropes that progressed into late-onset myopia (n = 4). The subjects ranged in age between 16 and 26 years and were divided into 23 males and 27 females.

Thirty-five subjects were examined on 3 occasions over a 2-year period and the remainder were examined on 3 occasions over an 18-month to 2-year period. Both right and left eye were examined (see §4.1). Corrected visual acuity was at least 6/6 in each eye. At the initial examination the mean emmetropic subjective refractive error was $+0.24 \pm 0.24D$ and mean myopic subjective refractive error was $-2.08 \pm 1.57D$.

Experimental procedure

A large number of measurements were taken on all subjects and used in analysis for this chapter. The same examiner obtained all the measurements. These measurements include: -

1. Full subjective refraction (checked using +1.00D blur test) and eye examination
2. Objective central refraction (Canon Autorefr)
3. Objective peripheral refraction (Canon Autorefr)
4. A-scan ultrasonography (Storz Omega)
5. Keratometry (Rodenstock)
6. Corneal topography (EyeSys 2000)

Subjective refraction (see § 4.2.1).

The subjective refractive error was found at each visit on all subjects and obtained after instillation of 2 drops of 1% tropicamide HCl (*Minims*[®], Chauvin) with a 5-minute interval between drops to achieve cycloplegia. A 4m logMar chart was used to record the visual acuity and refractive error. The subjects were asked to sit in a chair located 4m from the chart whilst trial lenses were placed before their eyes until an end-point was reached. The final refraction was checked using the +1.00D blur test. All refractive error measurements were converted from sphere, cylinder and axis into equivalent mean sphere using a specially designed computer program, written by Dr Mark Dunne in *Quickbasic*.

Objective central refraction (see §4.2.1)

Central and peripheral refractive error measurements were taken using the Canon R-1 Autorefractometer. Two drops of 1% tropicamide induced mydriasis and cycloplegia, as mentioned in above paragraph. The subjects were instructed to place their chin on the chinrest and their forehead against the forehead bar. A strap was placed around the head to restrict head movement but not eye movement. The subject's left eye was covered with an occluder whilst the right eye viewed a distant object. Five central refractive error readings were taken on each eye.

Objective peripheral refraction (see § 4.2.2)

An arc was placed on top of the main body of the Canon R-1 to allow peripheral refractive error measurements to be taken. Horizontal fixation targets were set at 5° intervals to a maximum of 35° both nasally and temporally. Five readings were taken at each eccentricity. The data was transferred to a personal computer, in conjunction with keratometry and A-scan ultrasound measurements, and entered into a specially devised computer program called RetinaFit, written by Dr Mark Dunne for Macintosh and modified for PC by Chris Knight. A printout of the computer program can be found in Appendix 4. The data was then manipulated in a number of ways to achieve different values including retinal contour and the peripheral astigmatic factor (PAF).

A-scan ultrasonography (see § 4.2.3.)

The A-scan probe was sterilised with an alcohol wipe (*Medi-swab*[®], Seton Healthcare, England) before use on each subject. One drop of 0.4% benoxinate HCl (*Minims*[®], Chauvin) was instilled to each eye to induce corneal anaesthesia. The subject's pupils were dilated and accommodation was reduced owing to prior instillation of 2 drops of 1% tropicamide HCl. The probe was placed gently onto the cornea of one eye and ten measurements were taken while subjects fixated a distant spotlight with the alternate eye. Measurements were taken on both eyes in all subjects at all three visits.

Keratometry (see § 4.2.4)

Keratometry measurements were taken on all subjects at all three visits using a Rodenstock keratometer. Three measurements of corneal radius of curvature and axis were obtained along the two principal meridians for both eyes. Prior to taking the measurements, the subjects were positioned comfortably on the keratometer and the eyepiece focused in accordance to manufacturers guidelines.

The keratometer was calibrated using a precision 7.8mm spherical steel ball. The instrument was calibrated at regular intervals by the author or a member of the Optometry Division technical staff. See chapter 6 which describes the evaluation of corneal curvature in more depth.

Corneal topography (see §4.2.5)

Corneal topography was measured at each visit by using the *EyeSys 2000* Corneal Analysis System. Subject name, gender and date of birth were entered into the program database before corneal image capture and analysis. The subjects were instructed to place their chin on the chinrest and place their forehead against the browbar and asked to fixate a green flashing central light within the placido rings. To eliminate any nose shadow, the subject was advised to turn their head slightly so that the eye being captured faces the instrument directly. The videokeratoscope aligns itself with the eye automatically and a continuous video image of the eye is generated on a monitor. The image is adjusted until the pupil is centred within the central box. The subject is asked to blink and open their eye as wide as possible while the image is captured. The procedure was repeated three times on each eye at each visit.

The EyeSys 2000 was calibrated at regular intervals using the program and calibration sphere provided (55.06D). Also see chapter 6 which describes the evaluation of the cornea in more detail.

5.6 Results

5.6.1 Validity and repeatability

Validity refers to how close the measurement is to the truth. Ocular component studies typically neglect issues of repeatability. Repeatability is particularly important in longitudinal studies and can be described as 'the ability of a measurement to be duplicated on an intersession basis and an interobserver basis' (Zadnik *et al.*, 1992).

Three keratometry and corneal topography readings were taken on each eye at each visit. Ten ultrasound measurements were taken on each eye at each visit. Validity is designated in this study as the average standard deviation, over the three readings, for all subjects. See table 5.1 for validity values.

Table 5.1 Values of validity

<i>Instrument</i>	<i>Measurement</i>	<i>Validity</i>
Rodenstock keratometer	Radius of curvature (mm)	±0.02 (n=50)
EyeSys 2000 corneal topographer	Radius of curvature (mm)	±0.01 (n=50)
EyeSys 2000 corneal topographer	Asphericity value (ρ)	±0.02 (n=50)
Storz Omega ultrasound	Axial length (mm)	±0.09 (n=50)
Storz Omega ultrasound	Vitreous depth (mm)	±0.10 (n=50)
Storz Omega ultrasound	Anterior chamber depth (mm)	±0.05 (n=50)
Storz Omega ultrasound	Lens thickness (mm)	±0.03 (n=50)

Thirty eyes were analysed to provide values of repeatability. Repeatability is assessed on 2 separate measurement occasions (see appendix 5 for statistics review). The time separation between measurements was approximately 6 months with minimal refractive error change (less than or equal to $\pm 0.25D$) in the subjects over this period. The repeatability was assessed by calculating the numeric difference between values obtained on 2 separate occasions and subsequent analysis of the distribution as described by Zadnik *et al.* (1992). See table 5.2 for repeatability results.

Table 5.2 Bias and limits of agreement for repeatability of ocular component measurements on two separate occasions.

<i>Instrument</i>	<i>Measurement</i>	<i>Bias</i>	<i>Standard deviation</i>	<i>95% Limits of Agreement</i>
Keratometer	Radius of curvature (mm)	-0.01	0.03	-0.07 to 0.05
EyeSys 2000	Radius of curvature (mm)	0.00	0.03	-0.06 to 0.06
EyeSys 2000	ρ value	0.00	0.05	-0.10 to 0.10
Omega ultrasound	Axial length (mm)	0.14	0.19	-0.23 to 0.51
Omega ultrasound	Vitreous depth (mm)	0.20	0.16	-0.11 to 0.51
Omega ultrasound	Anterior chamber depth (mm)	-0.06	0.13	-0.31 to 0.19
Omega ultrasound	Lens thickness (mm)	0.01	0.09	-0.17 to 0.19
Subjective RX	Equivalent sphere (D)	-0.01	0.10	-0.21 to 0.19
Objective RX (Canon)	Equivalent sphere (D)	-0.06	0.29	-0.63 to 0.51

5.6.2 Cross-sectional analysis

Figure 5.1 shows a strong negative correlation between refractive error and vitreous chamber depth, for the right eye on the first visit and using the subjective refractive error data ($r = 0.64$, $p < 0.002$). The negative correlation indicates that an increasingly myopic refractive error is related to an increasingly long vitreous chamber depth. Similar correlations were found between subjective refractive error (es) and vitreous chamber depth (vd) for the right eye on all three occasions. Also, results were obtained for the objective central refraction (esc) plotted against vitreous depth (vd). See table 5.3 for correlation coefficients. Results for the left eye are comparable to the right.

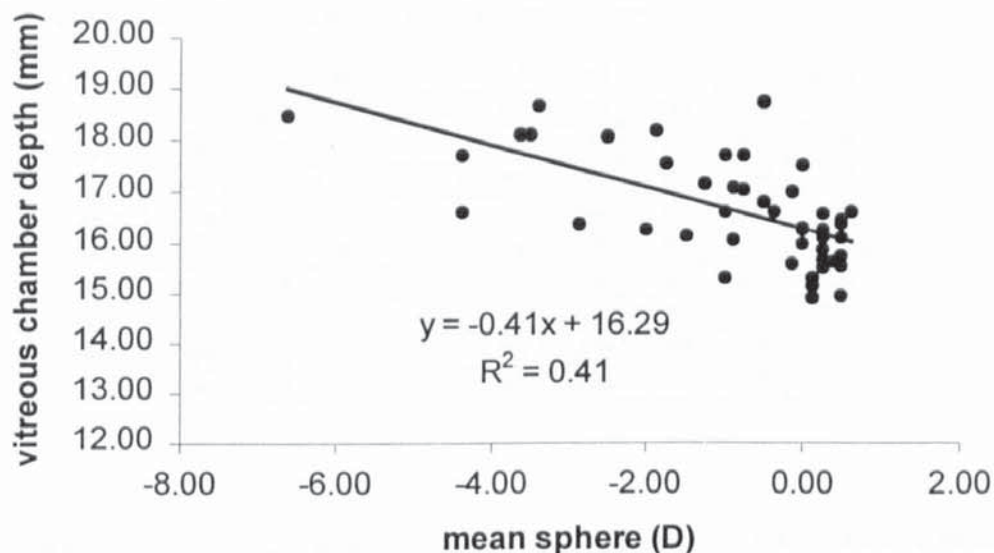


Figure 5.1 Vitreous chamber depth plotted against refractive error for the right on the first visit (n=50).

Table 5.3 Correlation matrix relating subjective (es) and objective (esc) refractive error with vitreous chamber depth (vd) for the right eye on all three occasions (n=50).

	es1	es2	es3	esc1	esc2	esc3	vd1	vd2	vd3
es1	1.000	.990	.987	.974	.967	.607	-.639	-.689	-.688
es2	.990	1.000	.995	.974	.973	.626	-.643	-.683	-.687
es3	.987	.995	1.000	.971	.968	.634	-.656	-.693	-.700
esc1	.974	.974	.971	1.000	.980	.648	-.642	-.684	-.682
esc2	.967	.973	.968	.980	1.000	.636	-.667	-.699	-.707
esc3	.607	.626	.634	.648	.636	1.000	-.565	-.450	-.471
vd1	-.639	-.643	-.656	-.642	-.667	-.565	1.000	.943	.960
vd2	-.689	-.683	-.693	-.684	-.699	-.450	.943	1.000	.978
vd3	-.688	-.687	-.700	-.682	-.707	-.471	.960	.978	1.000

Insignificant weak negative correlations were found between refractive error (es and esc) and anterior chamber depth (acd) for right eye on all three occasions (see table 5.4). The results were similar for the left eye. A negative correlation suggest that an increasingly myopic refractive error is related to a deeper anterior chamber depth.

Table 5.4 Correlation matrix relating subjective (es) and objective (esc) refractive error with anterior chamber depth (acd) for the right eye on all three occasions (n=50).

	es1	es2	es3	esc1	esc2	esc3	acd1	acd2	acd3
es1	1.000	.990	.987	.974	.967	.607	-.143	-.084	-.181
es2	.990	1.000	.995	.974	.973	.626	-.130	-.105	-.174
es3	.987	.995	1.000	.971	.968	.634	-.120	-.116	-.174
esc1	.974	.974	.971	1.000	.980	.648	-.169	-.140	-.177
esc2	.967	.973	.968	.980	1.000	.636	-.118	-.081	-.160
esc3	.607	.626	.634	.648	.636	1.000	-.148	-.378	-.296
acd1	-.143	-.130	-.120	-.169	-.118	-.148	1.000	.453	.504
acd2	-.084	-.105	-.116	-.140	-.081	-.378	.453	1.000	.699
acd3	-.181	-.174	-.174	-.177	-.160	-.296	.504	.699	1.000

Table 5.5 Correlation matrix relating subjective (es) and objective (esc) refractive error with lens thickness (lt) for the right eye on all three occasions (n=50).

	es1	es2	es3	esc1	esc2	esc3	lt1	lt2	lt3
es1	1.000	.990	.987	.974	.967	.607	-.021	.132	.163
es2	.990	1.000	.995	.974	.973	.626	-.004	.151	.174
es3	.987	.995	1.000	.971	.968	.634	.009	.160	.190
esc1	.974	.974	.971	1.000	.980	.648	.015	.180	.191
esc2	.967	.973	.968	.980	1.000	.636	.004	.189	.207
esc3	.607	.626	.634	.648	.636	1.000	.522	.266	.243
lt1	-.021	-.004	.009	.015	.004	.522	1.000	.664	.656
lt2	.132	.151	.160	.180	.189	.266	.664	1.000	.881
lt3	.163	.174	.190	.191	.207	.243	.656	.881	1.000

Table 5.5 shows the correlation matrix for refractive error and lens thickness for the right eye only. At the first visit the correlations are weak and either negative (es) or positive (esc). Over the three visits the correlations become stronger and positive. The results indicate that by the third visit there is a positive correlation, e.g. the objective refractive error data, ($r = 0.24$, $p = 0.05$) suggesting that as the amount of myopia increases the lens becomes thinner.

A significant negative correlation can be found between refractive error and the ratio of axial length to corneal curvature (al/k) for the right eye at the first visit ($r = 0.79$, $p < 0.002$). See figure 5.2. The ratio has been reported in previous literature to be a risk factor for the development of myopia (Grosvenor, 1988 and Grosvenor and Scott, 1994).

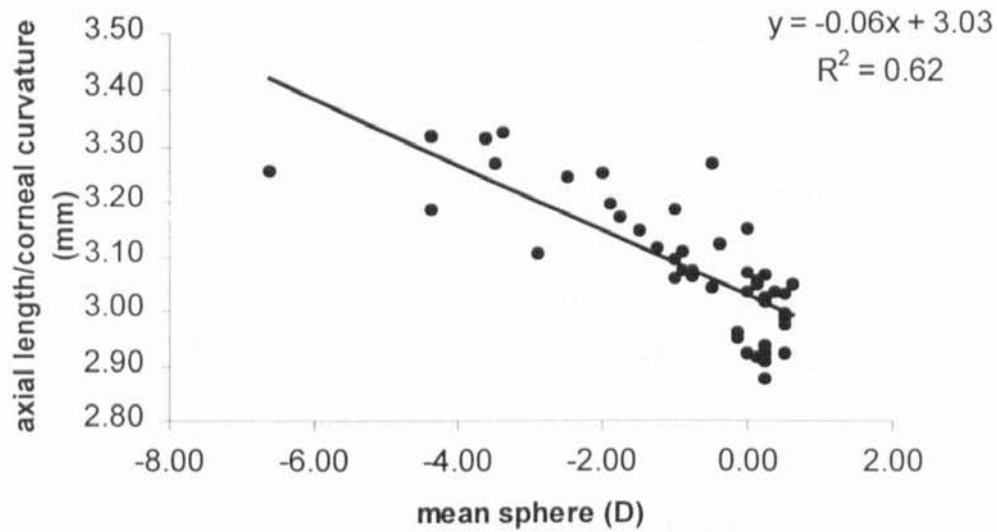


Figure 5.2 The ratio of axial length to corneal curvature (al/k) plotted against subjective refractive error for the right eye on the 1st visit (n=50).

The correlations for refractive error (es and esc) plotted against al/k for the right eye can be found in table 5.6. Similar results are evident for the left eye.

Table 5.6 Correlation matrix relating subjective (es) and objective (esc) refractive error with axial length to corneal curvature (al/k) for the right eye on all three occasions (n=50).

	es1	es2	es3	esc1	esc2	esc3	a/k1	a/k2	a/k3
es1	1.000	.990	.987	.974	.967	.607	-.787	-.768	-.801
es2	.990	1.000	.995	.974	.973	.626	-.803	-.777	-.813
es3	.987	.995	1.000	.971	.968	.634	-.798	-.777	-.809
esc1	.974	.974	.971	1.000	.980	.648	-.789	-.766	-.790
esc2	.967	.973	.968	.980	1.000	.636	-.789	-.750	-.790
esc3	.607	.626	.634	.648	.636	1.000	-.501	-.522	-.540
a/k1	-.787	-.803	-.798	-.789	-.789	-.501	1.000	.945	.956
a/k2	-.768	-.777	-.777	-.766	-.750	-.522	.945	1.000	.955
a/k3	-.801	-.813	-.809	-.790	-.790	-.540	.956	.955	1.000

An insignificant positive correlation was discovered between corneal curvature and refractive error and between corneal shape and refractive error. These results can be found in greater detail in §6.7.2.

The retinal shape can be summarised by its asphericity (retp) and the retinal curvature by its apical radius (retr). The values described will be reviewed in greater detail in chapter 7. Table 5.7 displays the correlations between refractive error (es and esc) and

retp and retr for the right eye on all three visits. The relationships are somewhat confusing, in that, the initial correlations between both retp and retr with refractive error are weak and positive, yet, over the two subsequent visits, the correlations become negative. At the initial visit, the correlations demonstrate that an increase in myopic refractive error is related to a reduction in retp and in retr (flatter conic curve in periphery and apical retinal steepening). However, the correlations for the two subsequent visits show that an increase in myopic refractive error is related to an increase in retp and in retr (steeper conic curve in periphery and apical retinal flattening).

Table 5.7 Correlation matrix relating subjective (es) and objective (esc) refractive error to retp and retr for the right eye on all three occasions (n=50).

	es1	es2	es3	esc1	esc2	esc3	retp1	retp2	retp3	retr1	retr2	retr3
es1	1.000	.990	.987	.974	.967	.607	.084	-.050	-.134	.161	-.038	-.111
es2	.990	1.000	.995	.974	.973	.626	.081	-.055	-.118	.157	-.046	-.088
es3	.987	.995	1.000	.971	.968	.634	.070	-.076	-.126	.146	-.069	-.106
esc1	.974	.974	.971	1.000	.980	.648	.136	-.096	-.188	.201	-.094	-.158
esc2	.967	.973	.968	.980	1.000	.636	.091	-.038	-.133	.151	-.047	-.102
esc3	.607	.626	.634	.648	.636	1.000	.066	-.111	-.196	.055	-.181	-.183
retp1	.084	.081	.070	.136	.091	.066	1.000	.137	-.098	.951	.242	.056
retp2	-.050	-.055	-.076	-.096	-.038	-.111	.137	1.000	.505	.172	.912	.550
retp3	-.134	-.118	-.126	-.188	-.133	-.196	-.098	.505	1.000	-.082	.542	.900
retr1	.161	.157	.146	.201	.151	.055	.951	.172	-.082	1.000	.309	.101
retr2	-.038	-.046	-.069	-.094	-.047	-.181	.242	.912	.542	.309	1.000	.699
retr3	-.111	-.088	-.106	-.158	-.102	-.183	.056	.550	.900	.101	.699	1.000

The peripheral astigmatic factor (paf) describes the amount of astigmatism present at each angle of eccentricity, for each eye, using an objective method to collect the data. In summary, it is the area under a graph of eccentricity plotted against astigmatism. Table 5.8 exhibits the correlations between refractive error (es and esc) and paf for the right eye on the first and final visits.

There is a moderately significant negative correlation between refractive error and paf at the initial visit ($p < 0.1$) indicating that an increase in the myopic refractive error is related to an increase in paf. However, at the final visit the relationship has changed to reveal a weak positive correlation so that an increase in the myopic refractive error is related to a decrease in paf. This relationship is explained further in the longitudinal analysis (stepwise multiple regression).

Table 5.8 Correlation matrix relating subjective (es) and objective (esc) refractive error to paf for the right eye on two occasions (n=50).

	es1	es2	es3	esc1	esc2	esc3	paf1	paf3
es1	1.000	.990	.987	.974	.967	.607	-.175	.152
es2	.990	1.000	.995	.974	.973	.626	-.207	.105
es3	.987	.995	1.000	.971	.968	.634	-.180	.129
esc1	.974	.974	.971	1.000	.980	.648	-.234	.161
esc2	.967	.973	.968	.980	1.000	.636	-.215	.139
esc3	.607	.626	.634	.648	.636	1.000	-.249	.134
paf1	-.175	-.207	-.180	-.234	-.215	-.249	1.000	.302
paf3	.152	.105	.129	.161	.139	.134	.302	1.000

Analysis of parameters in emmetropes and myopes

Tables 5.9a and b show the mean parameter values and their standard deviations for emmetropes and myopes, right eye only.

The data is separated out to enable parameter means to be compared between emmetropes and myopes. A simple 2-tailed, unmatched *t test* can be used to compare the means and results can be seen in table 5.10. See appendix 5 for explanation of *t test*.

Table 5.9a Mean parameter values for emmetropic subjects, for right eye only on first and final visit.

<i>Parameter</i>	<i>Visit 1</i>	<i>Visit 3</i>
Refractive error ¹ (D)	0.26±0.21	0.28±0.25
Refractive error ² (D)	0.08±0.46	-0.13±0.15
Axial length (mm)	23.44±0.54	23.49±0.50
Vitreous depth (mm)	16.00±0.60	16.19±0.56
Ant. Chamber depth (mm)	3.77±0.15	3.61±0.22
Lens thickness (mm)	3.69±0.22	3.68±0.21
Corneal curvature ³ (mm)	7.85±0.22	7.83±0.22
Axial length/cornea (mm)	2.99±0.06	3.00±0.06

1 subjective refractive error; 2 objective refractive error; 3 keratometry.
± 1 SD. N=26.

Table 5.9b Mean parameter values for myopic subjects, for right eye only on first and final visit.

<i>Parameter</i>	<i>Visit 1</i>	<i>Visit 3</i>
Refractive error ¹ (D)	-2.05±1.54	-2.29±1.55
Refractive error ² (D)	-1.98±1.39	-1.77±1.80
Axial length (mm)	24.76±0.89	24.76±0.82
Vitreous depth (mm)	17.32±0.92	17.43±0.89
Ant. Chamber depth (mm)	3.84±0.18	3.78±0.16
Lens thickness (mm)	3.60±0.37	3.55±0.25
Corneal curvature ³ (mm)	7.80±0.25	7.79±0.25
Axial length/cornea (mm)	3.18±0.09	3.18±0.08

1 subjective refractive error; 2 objective refractive error; 3 keratometry.
± 1 SD. N=24.

Table 5.10 *t* test probability (p value) for comparison of parameter means in emmetropes and myopes.

<i>Parameter p values</i>	<i>Visit 1</i>	<i>Visit 3</i>
Axial length (mm)	<u>9.87*10⁻⁸</u>	<u>4.17*10⁻⁸</u>
Vitreous depth (mm)	<u>3.40*10⁻⁷</u>	<u>5.26*10⁻⁷</u>
Ant. Chamber depth (mm)	0.13	<u>0.003</u>
Lens thickness (mm)	0.3	<u>0.04</u>
Corneal curvature ³ (mm)	0.57	0.79
Axial length/cornea (mm)	<u>1.02*10⁻¹⁰</u>	<u>5.05*10⁻¹¹</u>

Underlined values show $p < 0.05$ and are significant.

Parameter analysis in early- and late-onset myopes

Tables 5.11a and b show the mean parameter values and their standard deviations for early- and late-onset myopes, right eye only.

Table 5.11a Mean parameter values for early-onset myopic subjects, for right eye on first and final visit.

<i>Parameter</i>	<i>Visit 1</i>	<i>Visit 3</i>
Refractive error ¹ (D)	-2.95±1.45	-3.19±1.45
Refractive error ² (D)	-2.73±1.37	-2.69±1.31
Axial length (mm)	24.95±0.83	24.95±0.79
Vitreous depth (mm)	17.52±0.88	17.72±0.80
Ant. Chamber depth (mm)	3.83±0.21	3.75±0.18
Lens thickness (mm)	3.59±0.44	3.49±0.25
Corneal curvature ³ (mm)	7.73±0.21	7.72±0.23
Axial length/cornea (mm)	3.23±0.07	3.23±0.06

1 subjective refractive error; 2 objective refractive error; 3 keratometry.
± 1 SD. N= 14.

Table 5.11b Mean parameter values for late-onset myopic subjects, for right eye on first and final visit.

<i>Parameter</i>	<i>Visit 1</i>	<i>Visit 3</i>
Refractive error ¹ (D)	-0.79±0.26	-1.03±0.35
Refractive error ² (D)	-0.92±0.30	-1.22±0.36
Axial length (mm)	24.50±0.91	24.48±0.77
Vitreous depth (mm)	17.04±0.90	17.03±0.87
Ant. Chamber depth (mm)	3.85±0.13	3.83±0.13
Lens thickness (mm)	3.61±0.23	3.62±0.23
Corneal curvature ³ (mm)	7.90±0.26	7.90±0.24
Axial length/cornea (mm)	3.10±0.06	3.10±0.04

1 subjective refractive error; 2 objective refractive error; 3 keratometry.
± 1 SD. N=10

A two-tailed, unmatched *t* test was applied to compare the means of the parameters in early- and late-onset myopes, right eye. See table 5.12.

Table 5.12 *t* test probability (p value) for comparison of parameter means in early- and late-onset myopes.

<i>Parameter p values</i>	<i>Visit 1</i>	<i>Visit 3</i>
Axial length (mm)	0.24	0.17
Vitreous depth (mm)	0.29	0.07
Ant. Chamber depth (mm)	0.85	0.24
Lens thickness (mm)	0.90	0.21
Corneal curvature ³ (mm)	0.11	0.09
Axial length/cornea (mm)	<u>4.7*10⁻⁴</u>	<u>6.52*10⁻⁶</u>

Underlined values show $p < 0.05$ and are significant.

5.6.3 Longitudinal analysis

Final state of refractive error

To assess how the different parameters (x variables) relate to the subject's final state of refraction, a stepwise multiple regression analysis was employed (see table 5.13a). The statistical test was applied for a number of different situations. Explanation of this statistical test can be found in appendix 5.

The data was analysed in a number of different situations to reveal whether distinct relationships existed between the ocular parameters and the final state of refractive error and to take into consideration the effects of right and left eye data from the same subject. Generally, for statistical analysis, only one eye is assessed. However, there may be inherent interocular differences that need to be investigated further and, therefore, both eyes have been examined separately for this thesis. Table 5.13b displays the results of stepwise multiple regression where the mean data has been used, i.e. the right and left eye data has been summed and divided by two.

Statisticians suggest a ratio of 5 to 10 subjects per parameter for this type of analysis. The groups can be divided into emmetropes and myopes and sub-divided into right and left eyes, i.e. the myopic group, right eye contains 12 subjects only. This group does not contain an adequate number of subjects for a successful stepwise multiple regression analysis. To alleviate the problem, the analysis was repeated but with a reduced number of parameters (see table 5.13c).

Table 5.13a Results of stepwise multiple regression of final state of refraction (es3 and esc3).

<i>Final rx</i>	<i>Y variable</i>	<i>X variables</i>	<i>R</i>	<i>R²</i>	<i>F</i>	<i>P</i>	<i>% variance</i>
all data	es3	al/k3	0.47	0.22	26.86	<0.0001	22
es		lt2	0.52	0.27	17.78	<0.0001	5
both eyes		vd1	0.56	0.31	13.99	<0.0001	3.9
		k1	0.59	0.34	12.21	<0.0001	3.5
		retr1	0.61	0.37	13.44	<0.0001	2.2
all data	esc3	al/k3	0.66	0.44	74.93	<0.0001	44
esc		vd1	0.69	0.47	42.68	<0.0001	3
both eyes		lt3	0.72	0.51	32.76	<0.0001	4
		lt1	0.76	0.58	32.39	<0.0001	7
all data	es3	al3	0.51	0.23	13.81	0.0006	23
es		paf1	0.65	0.39	14.21	<0.0001	16
R							
all data	es3	al/k3	0.54	0.29	19.13	<0.0001	29
es							
L							
all data	esc3	vd1	0.54	0.29	16.18	0.0002	29
esc		k1	0.64	0.42	13.84	<0.0001	13
R		lt1	0.69	0.48	11.56	<0.0001	6
		lt3	0.83	0.68	19.98	<0.0001	20
		al/k3	0.85	0.72	18.59	<0.0001	4
all data	esc3	al/k3	0.79	0.63	80.17	0.0001	63
esc		acd3	0.83	0.68	49.72	0.0001	5
L		k1	0.86	0.74	43.54	<0.0001	6
		lt3	0.88	0.78	39.43	<0.0001	4
		retr1	0.9	0.8	35.32	<0.0001	2
emms	es3	vd1	0.33	0.11	6.29	0.0015	11
es		paf3	0.49	0.24	7.89	0.0011	13
both eyes							
emms	esc3	al/k1	0.54	0.21	12.96	0.0007	21
esc		retp3	0.54	0.29	9.9	0.0002	8
both eyes							
emms	es3	lt2	0.47	0.22	6.2	0.0208	22
es							
R							
emms	es3	al1	0.41	0.17	4.88	0.037	17
es		paf3	0.57	0.33	5.66	0.01	16
L							

Cont...

<i>Final rx</i>	<i>Y variable</i>	<i>X variables</i>	<i>R</i>	<i>R²</i>	<i>F</i>	<i>P</i>	<i>% variance</i>
emms	esc3	al/k2	0.51	0.26	7.55	0.0118	26
esc							
R							
myo	es3	al/k3	0.65	0.42	33.75	<0.0001	42
es		lt3	0.76	0.58	31.51	<0.0001	16
both eyes		paf1	0.83	0.68	31.15	<0.0001	10
		vd3	0.87	0.76	33.55	<0.0001	8
		paf3	0.9	0.8	34.54	<0.0001	4
myo	esc3	al/k3	0.63	0.4	30.43	<0.0001	40
esc		lt3	0.76	0.58	31.44	<0.0001	18
both eyes		paf1	0.84	0.7	33.76	<0.0001	12
		vd3	0.88	0.78	38.59	<0.0001	8
		retr3	0.91	0.84	42.76	<0.0001	6
myo	es3	al/k3	0.64	0.41	10.9	0.0045	41
es		lt3	0.83	0.69	16.74	0.0002	28
R		paf3	0.88	0.78	16.65	<0.0001	9
		vd2	0.93	0.86	19.38	<0.0001	8
myo	es3	al/k3	0.64	0.41	15.29	0.0008	41
es		paf1	0.74	0.54	12.4	0.0003	13
L		lt3	0.81	0.65	12.55	<0.0001	11
		al1	0.86	0.74	13.83	<0.0001	9
		Age	0.9	0.82	16.01	<0.0001	8
myo	esc3	paf1	0.57	0.34	7.74	0.0133	34
esc		al1	0.79	0.63	12.67	0.0006	29
R		lt3	0.9	0.81	19.57	<0.0001	18
		lt2	0.92	0.85	19.09	<0.0001	4
myo	esc3	al/k3	0.65	0.42	15.88	0.0006	42
esc		paf1	0.75	0.56	13.3	0.0002	14
L		lt3	0.83	0.69	14.48	<0.0001	13
		vd3	0.88	0.77	16.15	<0.0001	8
		retp3	0.93	0.87	23.89	<0.0001	10

Table 5.13b Results of stepwise multiple regression of final state of refraction (es3 and esc3). Mean data.

<i>Final rx</i>	<i>Y variable</i>	<i>X variables</i>	<i>R</i>	<i>R²</i>	<i>F</i>	<i>P</i>	<i>% variance</i>
all data	es3	vd3	0.324	0.12	6.34	0.0152	12
es		EyeSysk3	0.81	0.66	45.62	<0.0001	54
r+l mean		lt3	0.88	0.78	53.07	<0.0001	12
		al/k3	0.9	0.81	45.46	<0.0001	3
		retr1	0.92	0.84	46.27	<0.0001	3
all data	esc3						
esc		0					
r+l mean							
emms	es3	retr3	0.41	0.17	4.86	0.0373	17
es							
r+l mean							
emms	esc3	al/k1	0.49	0.24	7.52	0.0113	24
esc							
r+l mean							
myo	es3	al/k3	0.65	0.42	16.01	0.0006	42
es		acd3	0.79	0.62	16.86	<0.0001	20
r+l mean		lt2	0.83	0.69	15.11	<0.0001	7
		paf3	0.9	0.8	19.15	<0.0001	11
		vd2	0.94	0.85	27.67	<0.0001	5
		retp1	0.94	0.89	28.31	<0.0001	4
myo	esc3	al/k3	0.51	0.26	7.63	0.0113	26
esc		paf1	0.67	0.45	8.41	0.0021	19
r+l mean		EyeSysk1	0.75	0.56	8.4	0.0008	11
		al1	0.84	0.71	11.49	<0.0001	15
		vd2	0.87	0.76	11.54	<0.0001	5
		lt1	0.9	0.81	12.3	<0.0001	5
		lt3	0.93	0.87	19.04	<0.0001	6
		retr3	0.95	0.91	27.16	<0.0001	4

Table 5.13c Results of stepwise multiple regression of final state of refraction (es3 and esc3). Reduced parameter data.

<i>Final rx</i>	<i>Y variable</i>	<i>X variables</i>	<i>R</i>	<i>R²</i>	<i>F</i>	<i>P</i>	<i>% variance</i>
emms	es3	lt3	0.41	0.17	4.56	0.0442	17
es							
R (reduced)							
emms	es3	al1	0.41	0.17	4.88	0.037	17
es		paf3	0.57	0.33	5.66	0.01	16
L (reduced)							
emms	esc3	al/k1	0.5	0.25	7.47	0.0122	25
esc							
R (reduced)							
emms	esc3	al/k1	0.38	0.14	4.04	0.0559	14
esc							
L (reduced)							
myo	es3	al/k3	0.64	0.41	10.9	0.0045	41
es		lt3	0.83	0.69	16.74	0.0002	28
R (reduced)		paf3	0.88	0.78	16.65	<0.0001	9
		vd3	0.92	0.85	18.26	<0.0001	7
		EyeSysk3	0.96	0.92	26.27	<0.0001	7
		acd1	0.97	0.95	42.57	<0.0001	3
		retr3	0.99	0.98	55.42	<0.0001	2
		EyeSysk1	0.99	0.99	71.48	<0.0001	1
myo	es3	al/k3	0.64	0.41	15.29	0.0008	41
es		paf1	0.74	0.54	12.4	0.0003	13
L (reduced)		lt3	0.81	0.65	12.55	<0.0001	11
		al1	0.86	0.74	13.83	<0.0001	9
		Age	0.9	0.82	16.01	<0.0001	8
myo	esc3	paf1	0.57	0.33	7.74	0.0133	33
esc		al1	0.79	0.63	12.67	0.0006	30
R (reduced)		lt3	0.9	0.81	19.57	<0.0001	18
myo	esc3	al/k3	0.65	0.42	15.88	0.0006	42
esc		paf1	0.75	0.56	13.3	0.0002	14
L (reduced)		lt3	0.83	0.69	14.48	<0.0001	13
		vd3	0.88	0.77	16.15	<0.0001	8
		retp3	0.93	0.87	23.89	<0.0001	10

A tally chart of parameter occurrence, throughout the number of different situations, can be seen in figure 5.3

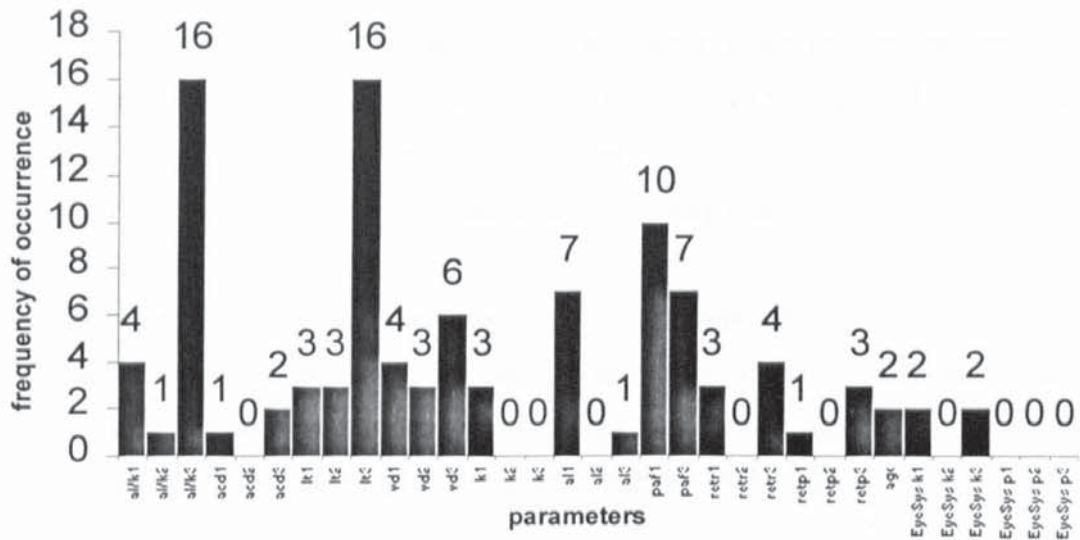


Figure 5.3 A tally chart of parameters plotted against frequency of occurrence.

Table 5.13d Parameter frequency according to step location. All the different situations are included.

Parameter	Step1	Step2	Step3	Step4	Step5	Step6	Step7	Step8
al/k1	4							
al/k2	1							
al/k3	14			1	1			
lt1			1	1			1	
lt2	1	1	1					
lt3	1	4	8	2			1	
vd1	2	1	1					
vd2				1	2			
vd3	1			5				
k1		1	1	1				
al1	2	2		3				
al3	1							
paf1	2	6	2					
paf3		3	2	1	1			
acd1						1		
acd3		2						
retr1					2	1		
retr3	1				2			1
retp1						1		
retp3		1			2			
Age					2			
EyeSysk1			1					1
EyeSysk3		1			1			

The results of the stepwise multiple regression provides an indication as to which parameters are significant and which parameters have minimal influence. The first step is the most important and generally generates the strongest relationship with the dependent variable (final state of refractive error). The parameters that have a weaker

relationship are arranged in descending step order. Occasionally, the *StatView* analysis program has difficulty in deciding on one parameter when two parameters are both closely linked with the dependent variable. This problem is displayed as an unusually high percentage variance at a lower step location.

Table 5.13d exhibits the parameter frequency in the step order.

Final state of refractive error for early- and late-onset myopes

The same stepwise regression analysis was applied to data for early- and late-onset myopes only. The summary can be found in table 5.14. Both eyes were used to increase the subject number and allow more parameters to be added.

Table 5.14 Results of stepwise multiple regression of final state of refraction (es3 and esc3) using early- and late-onset myopia data.

<i>final rx</i>		<i>Y variable</i>	<i>X variables</i>	<i>R</i>	<i>R²</i>	<i>F</i>	<i>P</i>	<i>% variance</i>
late myo		es3	acd3	0.52	0.27	6.71	0.0184	27
es								
both								
late myo		esc3	retr3	0.51	0.26	6.36	0.0213	26
esc			acd3	0.66	0.43	6.49	0.08	17
both								
early myo		es3	al3	0.53	0.28	10.33	0.0035	28
es			retr3	0.63	0.4	8.21	0.0018	12
both								
early myo		esc3	0					
esc								
both								

Predictive factors in myopia

An alternative way of assessing the relationship between myopia and the associated parameters, is to examine the longitudinal change in parameter values. The difference in each parameter was found by subtracting the value from the initial visit from that of the final visit. The change in refractive error was calculated in the same way ($3^{rd} - 1^{st}$). The analysis examines the connection between parameter change and refractive error change and indicates which parameters might be predictive factors for myopia onset and progression (see table 5.15a)

Table 5.15a Results of stepwise multiple regression for difference in refractive error (es3-1 and esc3-1).

<i>Difference</i>	<i>Y variable</i>	<i>X variables</i>	<i>R</i>	<i>R²</i>	<i>F</i>	<i>P</i>	<i>% variance</i>
myo	es3-1	retp 3-1	0.29	0.09	4.29	0.0439	9
es		lt 3-1	0.44	0.2	5.54	0.0071	11
both eyes							
myo	esc3-1	retp 3-1	0.41	0.17	9.54	0.0034	17
esc		lt 3-1	0.49	0.24	7.17	0.002	7
both eyes							
myo	es3-1	acd 3-1	0.62	0.38	9.12	0.0086	38
es							
L							
myo	esc3-1	EyeSys 3-1	0.52	0.27	5.55	0.0325	27
esc							
L							

Owing to the lack of significant stepwise results, a certain number of situations are not included in the summary. Emmetropes were not included in the analysis as longitudinal the refractive error change was minimal. The mean right and left eye data has also not been included as the results were very similar to those shown above (table 5.15a). No significant steps were evident using a reduced number of parameters, so this has also not been included.

The table below (5.15b) displays parameter popularity according to step location.

Table 5.15b Parameter frequency according to step location.

	<i>Step1</i>	<i>Step2</i>	<i>Step3</i>	<i>Step4</i>
EyeSysp 3-1	1			
acd 3-1	1			
retp 3-1	2			
lt 3-1		2		

Predictive factors in early- and late-onset myopia

The myopic group can be sub-divided in early- and late-onset myopes. The purpose of this analysis is to evaluate any differences in predictive factors between the groups. See table 5.16 for the summary of the results.

Table 5.16 Results of stepwise multiple regression for difference in refractive error (es3-1). Early- and late-onset myopes only.

Difference	Y variable	X variables	R	R ²	F	P	% variance
late myo	es3-1	acd 3-1	0.47	0.24	5.56	0.0299	24
es		retp 3-1	0.65	0.42	6.17	0.0097	18
both		retr 3-1	0.74	0.54	6.31	0.005	12
late myo	esc3-1	retp 3-1	0.54	0.29	7.47	0.0137	29
esc		lt 3-1	0.7	0.49	8.22	0.0032	20
both							
early myo	es3-1	lt 3-1	0.38	0.14	4.3	0.0481	14
es							
both							
early myo		al 3-1	0.74	0.55	15.04	<0.0001	18
esc							
both							

5.7 Discussion

Cross-sectional

A strong negative correlation was found between refractive error and vitreous chamber depth ($r = 0.64$, $p < 0.002$). Similar results were found on all three visits and the correlation strengthens with time. This strong negative correlation is unsurprising as it has long been accepted that myopia is related to an increase in the vitreous chamber depth (Erickson, 1991; McBrien and Adams, 1997; Curtin, 1985; Sorsby *et al.*, 1962b; McBrien and Millodot, 1987a; Fledelius, 1995b; Simensen and Thorud, 1994; Bullimore *et al.*, 1992; Grosvenor and Scott, 1993 and Kinge *et al.*, 1999). The refractive error shifted towards myopia, for the cohort of emmetropes and myopes, by $-0.10 \pm 0.28D$ (right eye only) over the 18-month to 2-year period. The strong correlation between refractive error and vitreous chamber depth might be a result of the increasing myopic refractive error over the examination period.

An insignificant negative correlation was detected between refractive error and anterior chamber depth on all three visits. Stenström (1946) observed a moderate negative correlation between refractive error and anterior chamber depth in adults aged 20 to 35 years, thereby implying that myopes have deeper anterior chambers. Larsen (1971a) also discovered a significant negative correlation in a group of 12 year old girls. However, Scott and Grosvenor (1993) developed structural models of emmetropic and myopic eyes and concluded that all other refractive components contributed to a myopic

refractive error except the anterior chamber depth. No significant correlation was found between changes in refractive error and changes in anterior chamber depth over a three-year period, in a study by Grosvenor and Scott (1993), although baseline cross-sectional data did indicate deeper anterior chambers in early-onset myopes compared to emmetropes. Lens thickness must also be considered, as this parameter will affect the biometric measurement of anterior chamber depth and make data interpretation difficult.

Between the ages of 6 to 10 years the crystalline lens becomes thinner and decreases its power which opposes the theory of the development of myopia (Zadnik *et al.*, 1995). It appears that myopic eyes tend to have thinner lenses (Fledelius, 1995a). The results of this study reveal a very weak positive and negative correlation ($escl$ and esl respectively) at the initial visit but at subsequent visits the correlation becomes positive and significant and are, therefore, in agreement with other investigators.

The ratio of axial length to corneal radius of curvature (al/k) provides an index to describe axial elongation (Grosvenor, 1988 and Grosvenor and Scott, 1994). The ratio for an emmetropic eye is very close to 3.0. A greater ratio is expected for a myopic eye and a lower ratio is expected for a hyperopic eye. The results of the current study indicate a strong negative correlation between refractive error and al/k on all three visits suggesting that an increasingly myopic eye has a greater al/k ratio.

Insignificant positive correlations were exhibited between corneal curvature and refractive error and corneal shape and refractive error. Further discussion can be found in a separate chapter dedicated to the cornea in emmetropia and myopia (see chapter 6).

The results for retinal shape and retinal radius are inconclusive. The correlations are weak and change from being positive at the initial visit to being negative at the two subsequent visits. Initially, the retinal asphericity and retinal radius reduce with increasing myopia, indicating a flattening of the conic curve as we move away from the vertex in conjunction with apical retinal steepening. At the two subsequent visits the retinal asphericity value and retinal radius increase with increasing myopia indicating a steepening of the conic curve as we move away from the vertex in conjunction with apical retinal flattening. This discrepancy may be explained by the high variance in

retinal contour measurements. The data may be more beneficial when evaluating the retinal shape in separate emmetropic and myopic groups.

A fairly significant correlation exists between refractive error and the peripheral astigmatic factor. The relationship is negative at the initial visit and positive at the final visit indicating a decrease in the paf with myopia over time. Rempt *et al.* (1971) classified eyes according to the amount of peripheral astigmatism present and their skiagrams. The Type I eye exhibits a small interval of sturm at high degrees of eccentricity (low paf) and is often associated with a myopic eye.

Parameter differences in emmetropes and myopes

The results indicate that mean axial length for the myopes is different to mean axial length for the emmetropes on both visits. As expected and previously discussed, the mean axial length of the myopic group is significantly longer than the emmetropic group. Similar results can be found for vitreous depth. Again, myopes tend to have longer vitreous chamber depths compared to emmetropes.

The mean anterior chamber depth was not found to be significantly different between emmetropes and myopes on the first visit, but was found to be significantly different on the third visit. On the final visit it is apparent that the mean anterior chamber depth is greater for the myopes compared to the emmetropes.

No significant difference between lens thickness means can be found on the first visit, although, a significant difference can be found on the final visit. The myopes have a significantly thinner crystalline lens. Consequently, this may be related to the measurements obtained for anterior chamber depth, in that, a thinner lens would produce a deeper anterior chamber depth.

A significant difference in means was found between emmetropes and myopes when assessing the axial length to corneal curvature ratio (al/k). The means were significantly different at both visits with the myopes demonstrating a higher ratio than the emmetropes. As discussed earlier, these results can be expected.

Parameter differences in early- and late-onset myopes

No significant differences in means were found for anterior chamber depth, vitreous depth, axial length or corneal curvature between the early- and late-onset myopic groups, at either the first or final visit. No significant difference in means was noted in vitreous depth although the early-onset myopes have a longer vitreous depth compared to the late-onset myopes at the final visit.

A significant difference in al/k means between early- and late-onset myopes was found at both the initial and final visit. The higher al/k ratio in early-onset myopes is a result of longer axial lengths and slightly steeper corneal radii compared to the late-onset myopes.

Longitudinal analysis – final state of refractive error

The final state of refractive error stepwise multiple regression analysis utilised data collected on the final visit and represented the maximum myopic refractive errors achieved by the subjects. The most common parameters to show a relationship with the final state of refractive error were the ratio of axial length to corneal curvature on the final visit (al/k_3) and lens thickness on the final visit (lt_3). A strong negative correlation is present between refractive error and al/k_3 indicating an increase in al/k_3 with an increase in the myopic refractive error. There is also a moderate positive correlation between refractive error and lt_3 suggesting an increase in the myopic refractive error is related to crystalline lens thinning.

The parameter located at step1, in a stepwise multiple regression analysis, is the most important factor and has the strongest relationship with the final state of refractive error. The parameters with weaker relationships are arranged in descending step order. Undoubtedly, al/k_3 has the strongest relationship with the final state of refractive error and is located at the step1 position 14 times throughout the various situations. lt_3 is a common parameter but only located at step1 once. Other parameters that have a strong relationship with the final state of refractive error are vitreous depth (vd_1), axial length (al_1) and the peripheral astigmatic factor (paf_1).

Longitudinal analysis – final state of refractive error for early- and late-onset myopes

The retinal apical radius on the final visit (retr3) is related to the final state of refractive error in both early- and late-onset myopes. Anterior chamber depth, on the final visit (acd3), is the main correlate with refractive error for the late-onset myopes and axial length, on the final visit (al3), is the main correlate with refractive error for early-onset myopes.

Predictive factors in myopia

The purpose of this analysis was to assess which parameters changed alongside a change in refractive error, or more specifically a myopic shift in refractive error. The most common parameters to change with a myopic shift in refractive error are retinal asphericity (retp3-1) and lens thickness (lt3-1). The parameters with the strongest relationships are anterior chamber depth (acd3-1), corneal shape (EyeSysp3-1) and retinal asphericity (retp3-1). Both retp3-1 and acd3-1 demonstrate a positive relationship with change in refractive error. EyeSysp3-1 has a negative relationship with change in refractive error. According to these results we can conclude that a myopic shift in refractive error is related to a flattening of the peripheral retina, a reduction of the anterior chamber depth and steepening of the peripheral cornea. Primarily, these observations appear unusual but they are applicable for longitudinal change only, i.e. although myopes tend to have deeper anterior chambers than emmetropes, a myopic shift in refractive error in myopes is associated with a shallowing of the anterior chamber.

Predictive factors in early- and late-onset myopia

Myopic progression in late-onset myopes is allied with a change in anterior chamber depth (acd3-1) and a change in retinal shape (retp3-1). A myopic shift in refractive error is related to a shallowing of the anterior chamber depth and a flattening of the peripheral retina. Myopic progression in early-onset myopes is associated with a longer axial length and crystalline lens change.

Future analysis - Hotelling's T squared statistic

In multiple regression statistics the primary consideration is which X variables are most important in predicting or explaining Y. However, when the Xs are correlated two Xs may be associated with the Y. Hotelling (1940, *Ann Math Stat.* 11:271) devised a test to

investigate whether X_1 is a better predictor of Y than X_2 alone. This statistical test could be used in future analysis of this data (Snedecor and Cochran, Statistical Methods, 1980).

5.8 Summary

- Cross-sectional analysis shows a strong negative correlation between refractive error and vitreous chamber depth (vd) indicating that a myopic eye is associated with a long vitreous chamber depth.
- A weak negative correlation is evident between refractive error and the anterior chamber depth (acd).
- On the final visit a positive correlation can be found between refractive error and lens thickness (lt). This suggests that a more myopic eye has a thinner lens.
- A t test can be applied to the data to analyse whether the parameter means are significantly different in emmetropes and myopes. Significantly greater means in al, vd and al/k measurements were found in the myopic group.
- A t test was also applied to analyse parameter means in early- and late-onset myopes. Early-onset myopes were found to have a greater value of al/k compared to the late-onset myopes.
- A final state of refractive error stepwise multiple regression analysis was employed to assess the link between the parameters and refractive error at the final visit. Al/k ratio (final visit) has the strongest relationship with the final state of refractive error. Other parameters with strong relationships to refractive error are vd (initial visit), al (initial visit) and the peripheral astigmatic factor (paf).
- Acd (final visit) has the strongest relationship with the final state of refractive error in late-onset myopes and al (final visit) has the strongest association in early-onset myopes.
- Using a predictive stepwise multiple regression analysis, we can conclude that a myopic shift in refractive error is related to a flattening of the peripheral retina, a thinning of the anterior chamber depth and a steepening of the peripheral cornea.
- Myopic progression in late-onset myopes is associated with a reduction in the anterior chamber depth (possibly due to increased lens thickness) and peripheral retinal flattening. Early-onset myopia progression is mainly related to an increase in axial length.

CHAPTER 6

CORNEAL SHAPE IN EMMETROPIA AND MYOPIA

6.1 Introduction

The cornea is the principal refracting surface of the eye, having a power of approximately 42D (over two-thirds of the total power of the eye). Notable changes in ocular power thus occur as a result of minor changes in the corneal curvature.

Keratometers are the most widely used instruments to measure anterior corneal radii of curvature. The corneal radius is determined by the separation of two reflected mires which represent an object, of known size and position, imaged by the anterior convex surface of the cornea, i.e. Purkinje image I. The main limitation of the instrument is that it generally only measures the central 3mm portion of the cornea and this curvature is assumed to be spherical. Keratometry measurements are less accurate beyond the 3mm central portion owing to the aspheric character of the peripheral cornea.

Myopia develops because either the optical power of the eye is too great for its length or the eye is abnormally long. As the cornea contributes a large proportion of the total ocular power of the eye, it might be assumed that the cornea plays a part in the development of myopia. A number of studies have researched the role of the cornea in emmetropia and myopia, both cross-sectionally and longitudinally and in both children and adults (see Chapters 2 and 3). The purpose of this chapter is to analyse the corneal curvature and topography data obtained by traditional keratometry methods and a semi-automated method (*EyeSys 2000* Corneal Analysis System) in both emmetropes and myopes, with the emphasis on late-onset myopia.

6.2 Corneal Assessment

Central corneal radius of curvature

The traditional method of measuring the corneal radius of curvature is keratometry (see §4.2.4). There are a number of commercially available instruments, e.g. Rodenstock, Zeiss, Bausch and Lomb and Javal-Schiötz. Automated keratometers are also available, e.g. Humphrey and Canon. The unique design of the auto-keratometers provides a measure of corneal curvature by either projecting a ring mire of collimated light onto

the cornea (Canon design) or projecting three beams of near infrared light onto the cornea in a triangular pattern (Humphrey). Photo-sensor systems are used to detect the light patterns and calculate corneal radius of curvature.

The accuracy of a keratometric reading depends largely on the accommodation of the observers eye and instrument setup, i.e. correct focusing of the mires and eyepiece (Littman, 1951. Cited in Clark, 1973). Stone (1962) suggested an accuracy of $\pm 0.4\text{mm}$ for corneal radius measurements and Clark (1973) indicated an accuracy of $\pm 0.015\text{mm}$ when using a conventional two-mire keratometer.

Charman (1972) estimated the precision of a two mire keratometer to be approximately $\pm 0.04\text{mm}$.

Corneal contour

The corneal contour can be examined using a keratoscope. The simplest form of the keratoscope is the hand-held Placido disc which consists of alternating black and white concentric rings. The device permits visual inspection of the central 4 to 6mm diameter corneal area. Measurement of the virtual concentric target ring images, in one or more semi-meridians, provides information about the corneal shape. The ring images appear elliptical when marked corneal astigmatism is present. Distorted reflections are a result of keratoconus, corneal scarring or surface irregularities. The main disadvantage of the keratoscope is that it must be held normal to the line of sight, if not, a false indication of corneal contour is produced.

A more popular device than the keratoscope is the photokeratoscope which is attached to a camera and provides instant quantitative information over a large area of the cornea in all meridians. By determining the size of the image and the size of the object, corneal topography can be assessed, the theory being the same as that for the keratometer.

The recent development of computer-assisted photokeratoscopes has provided detailed mapping and analysis of the cornea. Two commercially available instruments are the TMS-1 (Computer Anatomy Inc., New York, USA.) and the *EyeSys 2000* Corneal Analysis System (EyeSys Labs., Houston, USA). The instruments are generally known as corneal topography systems and measure corneal curvature and assess corneal contour both centrally and peripherally (see §4.2.5).

6.3 Corneal curvature

There is no consensus between researchers as to when the cornea reaches adult proportions and stops growing. Two, three and five years-of-age have all been suggested as possible ages for when the cornea reaches adult dimensions (see §1.2). The corneal radius of curvature shows minimal change after it has reached adult values and shows a constant value in the second to third decade of life. The majority of other ocular components continue to grow throughout childhood and tend to stabilize in early adulthood (see §1.2).

Stenström (1946) investigated the variation and correlation of optical components in human eyes. In his cross-sectional study of adults aged 20 to 35 years, he found the mean corneal curvature of all the subjects to be 7.86mm with a range of 7.00 to 8.65mm. The mean corneal radius of curvature for males was found to be 7.90mm and 7.77mm for females. In a study to assess the corneal topography of 98 subjects, using the *EyeSys* videokeratoscope, Douthwaite *et al.* (1999) found the group average apical radius to be 7.93mm horizontally and 7.78mm vertically. The group average ρ -value was 0.76 horizontally and 0.82 vertically.

6.4 Evaluation of corneal curvature

Keratometry

The measurements of corneal radii of curvature are generally expressed in millimeters (mm). The results can also be transformed into corneal dioptric power readings by assuming that the cornea is a single surface with a refractive index of 1.336. The following formula is used to convert the corneal radii of curvature into corneal power (D): -

$$cp = 1000(n-1)/r$$

where,

cp = corneal power (D)

n = corneal refractive index

r = corneal radius of curvature (mm)

Corneal topography

The *EyeSys 2000* Corneal Analysis System provides detailed maps of the corneal contour using a specialised series of algorithms. The system provides many different analysis programs and advanced diagnostics depending upon the examiner's

requirements. The most popular analysis programs for clinicians are those designed for contact lens fitting and dioptric power mapping of the corneal surface. The corneal contour is represented by a map and a colour-coding scheme is applied to relate information regarding power and curvature. Measurements generated by the corneal mapping programs include simulated keratometry readings, dioptric power measurements at specific points on the cornea, astigmatic axis location and pupil contour. The numerical map generates information concerning corneal curvature and corneal eccentricity (e). The cornea is not spherical, but aspheric, and can be described as an ellipse. The eccentricity value can be used to describe the corneal asphericity (ρ). The ρ -value is often referred to as the shape factor to illustrate the amount of asphericity present on the cornea. The formula that relates eccentricity to the shape factor is,

$$\rho = 1 - e^2$$

The equation to describe a conic constant is as follows: -

$$y^2 = 2r_0x - \rho x^2$$

where,

r_0 = radius of curvature at the apex

ρ = ρ -value and represents the amount of peripheral flattening

The following ρ -values are used to describe various ellipses:-

$\rho > 1$ oblate (steepens in periphery)

$\rho = 1$ sphere

$0 < \rho < 1$ prolate (flattens in the periphery)

$\rho = 0$ parabola

$\rho < 0$ hyperbola.

Figure 6.1 shows the shape of the prolate ellipse (PE) and oblate ellipse (OE) in comparison with a circle (C).

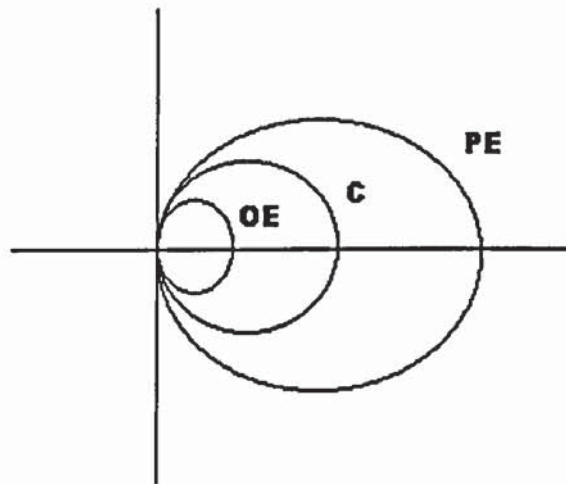


Figure 6.1 Schematic illustration of ellipsoids.

6.5 Purpose

A number of research studies have found corneal curvature to be steeper and corneal power to be greater in the myopic eye compared to the emmetropic eye (Curtin, 1985; Sorsby *et al.*, 1957; Grosvenor and Scott, 1991; Scott and Grosvenor, 1993 and Goss *et al.*, 1997). However, Scott and Grosvenor, paradoxically found corneal radius of curvature to be positively correlated to vitreous chamber depth and Stenström (1946) indicated that corneal curvature was positively correlated to axial length. These results imply that flatter corneas are associated with longer eyes, yet, an elongated vitreous chamber depth is generally related to a more myopic eye.

There appears to be a lack of agreement between investigators as to the role of the cornea in late-onset myopia. There is no conclusive evidence from either cross-sectional or longitudinal studies as to the true role of the cornea in myopia onset and progression in young adults.

6.6 Methods

Subjects

The cohort consisted of 26 emmetropic subjects and 24 myopic subjects. The myopic group was also sub-divided into early-onset myopes (n = 14) and late-onset myopes (n = 10) and the emmetropic group was sub-divided into stable emmetropes (n = 22) and emmetropes that progressed into late-onset myopia (n = 4). The subjects ranged in age between 16 and 26 years and were divided into 23 males and 27 females.

Thirty-five subjects were examined on 3 occasions over a 2-year period and the remainder were examined on 3 occasions over an 18-month to 2-year period. Both right and left eye were examined (see §4.1). Corrected visual acuity was at least 6/6 in each eye. At the initial examination the mean emmetropic subjective refractive error was $+0.24 \pm 0.24D$ and mean myopic subjective refractive error was $-2.08 \pm 1.57D$.

Experimental procedure

Both subjective and objective refractive errors were recorded at each visit. The refractions were obtained after instillation of 2 drops of 1% tropicamide HCl (*Minims*[®], Chauvin) to each eye with a five-minute interval between drops to achieve mydriasis and cycloplegia (see §4.2). The refractive error data is expressed as mean spherical equivalent. Original data can be in appendix 6.

Keratometry measurements were taken on all subjects at all 3 examinations using a Rodenstock keratometer. Three measurements of corneal radius of curvature and axis were obtained along the two principal meridians for both eyes. Prior to taking the measurements, the subjects were positioned comfortably on the keratometer and the eyepiece focused in accordance to manufacturers guidelines.

The keratometer was calibrated using a precision 7.8mm spherical steel ball. The instrument was calibrated at regular intervals by the author or a member of the Optometry Division technical staff.

Corneal topography was measured at each visit by using the *EyeSys 2000* Corneal Analysis System (see §4.2.5). Subject name, gender and date of birth were entered into the program database before corneal image capture and analysis. The subjects were instructed to place their chin on the chinrest and place their forehead against the browbar and asked to fixate a green flashing central light within the placido rings. To

eliminate any nose shadow, the subject was advised to turn their head slightly so that the eye being captured faces the instrument directly. The videokeratoscope aligns itself with the eye automatically and a continuous video image of the eye is generated on a monitor. The image is adjusted until the pupil is centred within the central box. The subject is asked to blink and open their eye as wide as possible while the image is captured. The procedure was repeated three times on each eye at each visit.

The EyeSys 2000 was calibrated at regular intervals using the program and calibration sphere provided (55.06D).

6.7 Results

6.7.1 Validity and repeatability

The validity of keratometry and corneal topography measurements were investigated by taking 3 readings on each eye. A mean corneal curvature measurement was obtained from the 2 principal meridian curvature measurements for keratometry and videokeratoscopy. The validity is represented as the average standard deviation for all subjects. See table 6.1.

Table 6.1 Values of validity

<i>Instrument</i>	<i>Measurement</i>	<i>Validity</i>
Rodenstock Keratometer	Radius of curvature (mm)	±0.02mm (n=50)
EyeSys 2000 Corneal Topographer	Radius of curvature (mm)	±0.01mm (n=50)
EyeSys 2000 Corneal Topographer	Eccentricity value	±0.02mm (n=50)

Thirty eyes were analysed to provide values of repeatability. Repeatability is assessed on 2 separate measurement occasions. The time separation between measurements was approximately 6 months with minimal refractive error change in the subjects over this period. The method of repeatability is described in greater detail in appendix 5. See table 6.2 for repeatability results.

Table 6.2 Bias and limits of agreement for repeatability of ocular component measurements on two separate occasions.

<i>Instrument</i>	<i>Measurement</i>	<i>Bias</i>	<i>Standard deviation</i>	<i>95% Limits of Agreement</i>
Rodenstock Keratometer	Radius of curvature (mm)	-0.01	0.03	-0.07 to 0.05
EyeSys 2000	Radius of curvature (mm)	0.00	0.03	-0.06 to 0.06
EyeSys 2000	Eccentricity value	0.00	0.05	-0.10 to 0.10

6.7.2 Cross-sectional analysis

Central corneal curvature

Table 6.3 displays the information obtained by keratometry and corneal topography on the central 3mm of the cornea. The data is presented for both eyes on all three experimental occasions.

Table 6.3 Central corneal curvature for all subjects, right and left eyes and on all 3 visits.

	<i>Visit 1</i>		<i>Visit2</i>		<i>Visit3</i>	
	R	L	R	L	R	L
K mean	7.82±0.23	7.80±0.22	7.82±0.24	7.80±0.23	7.81±0.23	7.80±0.23
CT mean	7.91±0.23	7.89±0.23	7.91±0.24	7.88±0.24	7.91±0.24	7.89±0.23

K, keratometry; CT, corneal topography; all measurements are in mm; ± 1 sd

Correlation is positive, yet poor, between refractive error and central corneal curvature (right eye, initial visit), using the keratometer ($r = 0.06$, $p > 0.1$) and using the corneal topographer ($r = 0.08$, $p > 0.1$). See figures 6.2 and 6.3

Similar correlations were found for the left eyes and on the two subsequent visits. This data is shown in table 6.4.

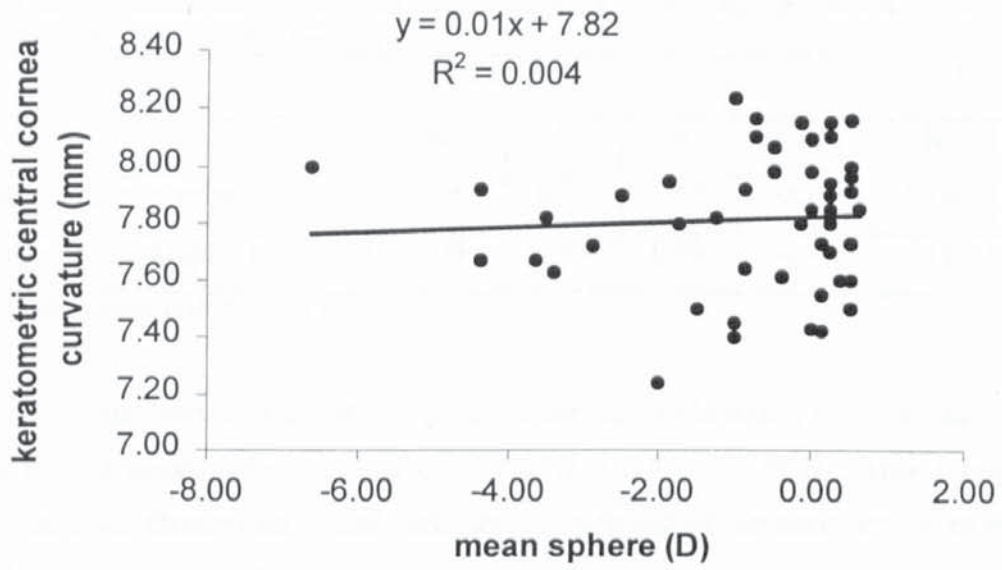


Figure 6.2 Keratometric central corneal curvature plotted against refractive error for the right eye on the first visit (n = 50).

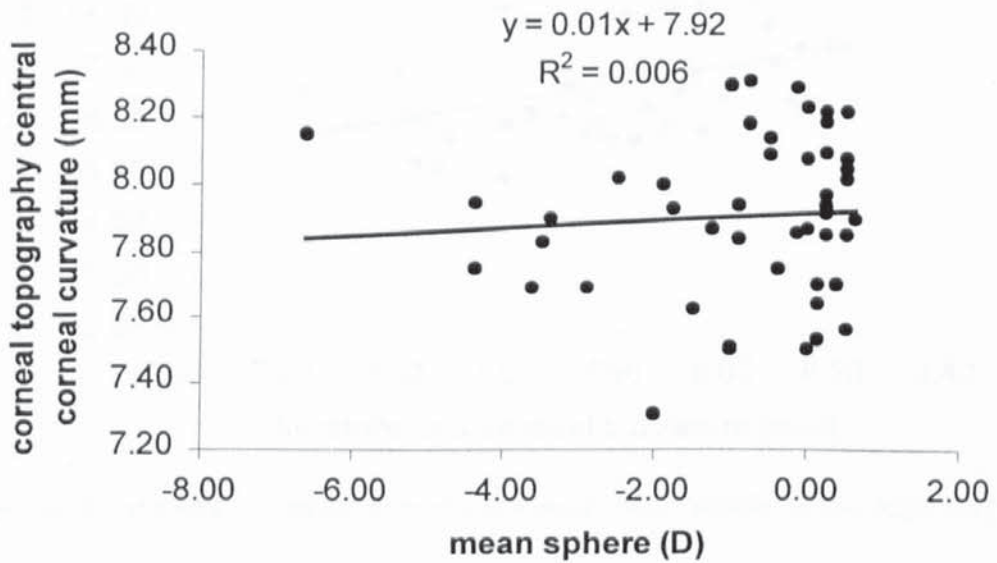


Figure 6.3 Corneal topography central corneal curvature plotted against refractive error for the right eye on the first visit (n = 50).

Table 6.4 Correlation coefficient values (r) for all subjects, at all visits, right and left eye separated, for both keratometry and corneal topography.

Eye	Visit 1		Visit 2		Visit 3	
	R	L	R	L	R	L
Keratometry r value	0.06	0.09	0.05	0.11	0.08	0.09
Corneal topography r value	0.08	0.08	0.08	0.09	0.06	0.07

All r values show probability of $p > 0.1$

However, the data shows a strong positive correlation between vitreous chamber depth and central keratometric corneal curvature ($r = 0.41$, $p < 0.002$). This relationship is present at all three visits, which indicates a flattening of the cornea with an elongation of the eye. See figure 6.4.

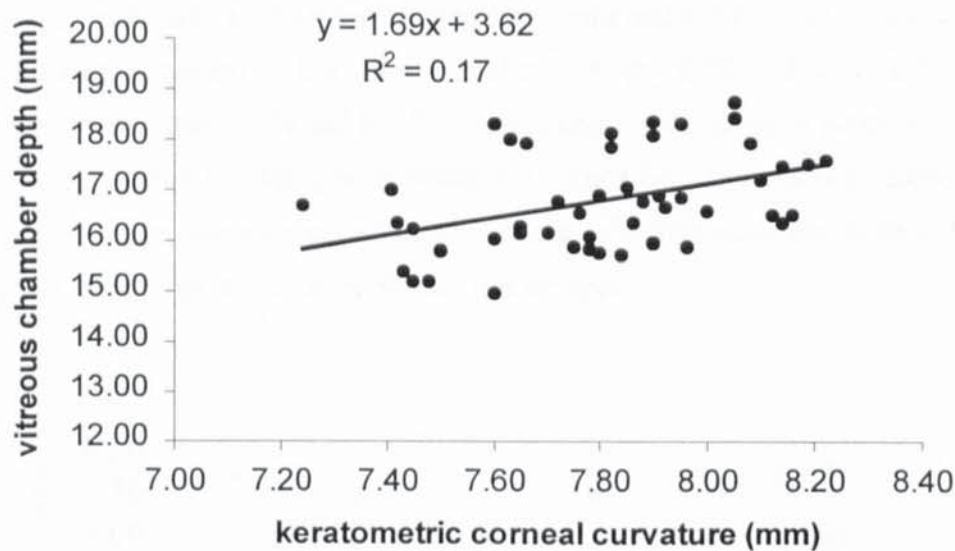


Figure 6.4 Keratometric corneal curvature plotted against vitreous chamber depth. Right eye ($n = 50$).

Central curvature in emmetropes and myopes

Twenty-six emmetropes took part in the experiment (13 right eyes and 13 left eyes) and 24 myopes (12 right eyes and 12 left eyes). Tables 6.5a and b display the information taken by keratometry and corneal topography on the central 3mm of the cornea. The data is presented for both eyes, all three experimental occasions and separated into emmetropic subjects and myopic subjects according to the results obtained by subjective refraction.

Table 6.5a Central corneal curvature for *emmetropic* subjects, right and left eyes on all 3 occasions.

	Visit 1		Visit 2		Visit 3	
	R	L	R	L	R	L
K mean	7.85±0.22	7.82±0.21	7.83±0.22	7.82±0.22	7.83±0.22	7.82±0.21
CT mean	7.93±0.22	7.90±0.21	7.92±0.23	7.90±0.22	7.92±0.22	7.90±0.22

K, keratometry; CT, corneal topography; all measurements are in mm; ± 1 sd

Table 6.5b Central corneal curvature for *myopic* subjects, right and left eyes on all 3 occasions.

	Visit 1		Visit 2		Visit 3	
	R	L	R	L	R	L
K mean	7.80±0.25	7.77±0.24	7.81±0.25	7.77±0.24	7.79±0.25	7.77±0.24
CT mean	7.89±0.25	7.87±0.24	7.89±0.25	7.87±0.25	7.90±0.26	7.87±0.24

K, keratometry; CT, corneal topography; all measurements are in mm; ± 1 sd

A weak correlation exists between refractive error and keratometric corneal curvatures for both emmetropes ($r = 0.03$, $p > 0.1$) and myopes ($r = 0.03$, $p > 0.1$), analysing the right eye only (see figures 6.5a and b). The correlation for the myopes is positive suggesting that as the amount of myopia increases the cornea becomes steeper. Low correlation coefficients are also apparent when correlating refractive error and corneal topography corneal curvatures in both emmetropes and myopes.

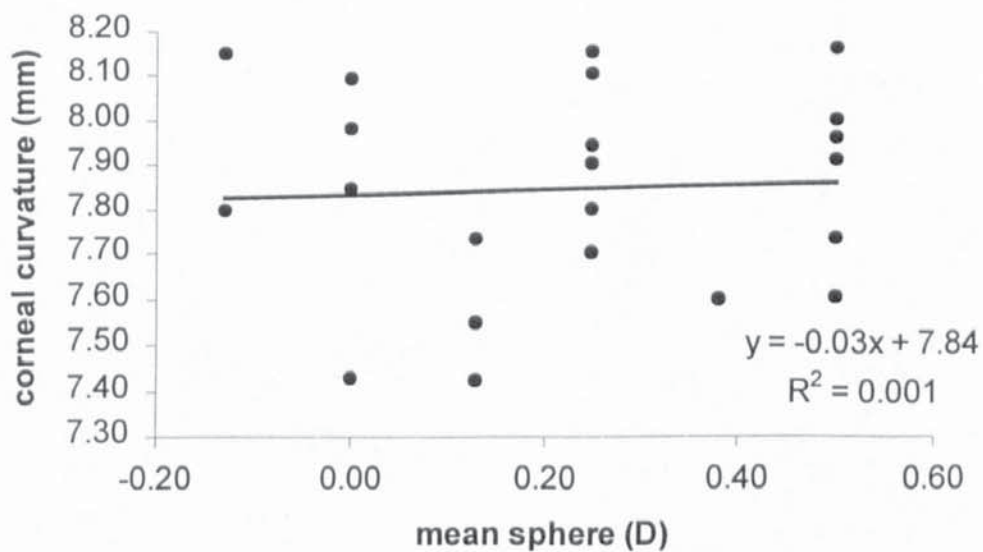


Figure 6.5a Keratometric central corneal curvature plotted against refractive error in emmetropes, for the right eye, on the first visit ($n = 26$).

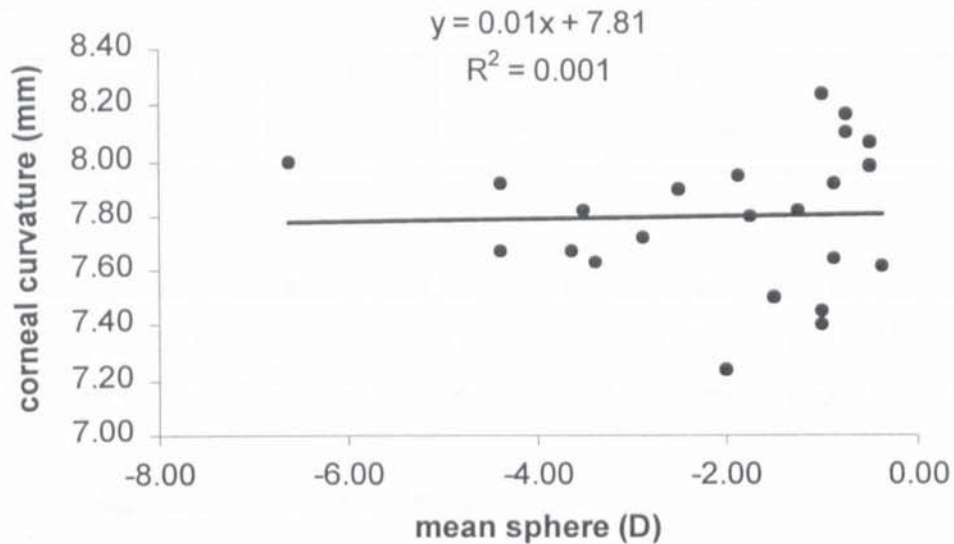


Figure 6.5b Keratometric central corneal curvature plotted against refractive error in myopes, for the right eye, on the first visit (n = 24).

A two-tailed, unmatched *t* test was applied to compare the means of the corneal curvatures in emmetropes and myopes (right eyes only) when measured by a keratometer and by a corneal topographer (see table 6.6).

Table 6.6 *t* Test probability (p value) for comparison of keratometric corneal curvatures in emmetropes and myopes. Right eye only.

	Visit 1	Visit 2	Visit 3
K p value	0.64	0.74	0.59
CT p value	0.57	0.71	0.79

The p value corresponds to a probability of chance occurrence. By convention, if $p < 0.05$ it is statistically significant. The results in table 6.6 demonstrate that there is no significant difference ($p > 0.05$) between the corneal curvature means in emmetropes and myopes when measured using a keratometer and a corneal topographer

Shape factor

The corneal contour and the amount of corneal flattening can be determined using the ρ -value, collected through corneal topography. Mean and standard deviations for corneal shape can be found in table 6.7.

Table 6.7 Corneal shape (ρ -value) for right and left eyes over 3 visits.

	Visit 1		Visit 2		Visit 3	
	R	L	R	L	R	L
Mean						
ρ -value	0.80±0.11	0.76±0.14	0.81±0.08	0.77±0.08	0.81±0.07	0.77±0.07

± 1 sd

Minimal positive correlation exists between refractive error and corneal shape when analysing purely the right eye on the first visit ($r = 0.04$, $p > 0.1$). Similar correlations are evident for the left eyes and when right and left eyes are examined on all 3 visits.

Corneal shape in emmetropes and myopes

Tables 6.8 displays the information regarding mean corneal shape in emmetropes and myopes.

Table 6.8 Mean corneal shape in emmetropes and myopes, right and left eyes on 3 visits.

	<i>Visit 1</i>		<i>Visit 2</i>		<i>Visit 3</i>	
	R	L	R	L	R	L
Emmetrope	0.80	0.72	0.82	0.76	0.81	0.77
ρ -value	±0.13	±0.17	±0.07	±0.08	±0.07	±0.08
Myope	0.80	0.79	0.79	0.77	0.82	0.77
ρ -value	±0.08	±0.08	±0.09	±0.08	±0.07	±0.07

± 1 sd

The ρ -value for emmetropes and myopes, both right and left eyes, appears to be greater than 0 and less than 1 suggesting that the cornea has an prolate ellipse shape.

A weak negative correlation was found between refractive error and corneal shape in emmetropes ($r = 0.17$, $p > 0.1$) and in myopes ($r = 0.16$, $p > 0.1$), right eye only. Similar results were also found for the left eyes and for right and left eyes over all 3 visits.

The results of a t test to compare the means of the corneal shape in emmetropes and myopes can be found in table 6.9 (right eyes only).

Table 6.9 *t* test probability (p value) for comparison of corneal shape (p-value) in emmetropes and myopes. Right eye only.

	<i>Visit 1</i>	<i>Visit 2</i>	<i>Visit 3</i>
Corneal shape probability value	0.98	0.27	0.53

The results demonstrate that there is no significant difference ($p > 0.05$) between the corneal shape means in emmetropes and myopes. Similar results were found when comparing the means for the left eyes.

6.7.3 Longitudinal analysis

Table 6.10 consists of values relating to the *change* in the parameters over the 18-month to 2-year period. The data depicts the numerical difference in the values between the initial visit and the final visit and thus represents the longitudinal change, i.e. with time. All the subjects have been separated into emmetropes and myopes, according to initial subjective refraction, to evaluate the changes within each refractive group.

Table 6.10 Numerical change in variables over an 18-month to 2-year period. Emmetropes $n = 26$, myopes $n = 24$.

	<i>Emmetropes</i>		<i>Myopes</i>	
	R	L	R	L
Δ Refractive error (D)	+0.03 \pm 0.24	+0.02 \pm 0.22	-0.24 \pm 0.25	-0.26 \pm 0.23
Δ K (mm)	0.00 \pm 0.05	0.00 \pm 0.03	-0.01 \pm 0.04	0.00 \pm 0.03
Δ CT (mm)	-0.01 \pm 0.02	0.00 \pm 0.02	+0.01 \pm 0.01	0.00 \pm 0.03
Δ Corneal shape (p-value)	+0.01 \pm 0.11	+0.04 \pm 0.16	+0.02 \pm 0.02	-0.02 \pm 0.06

K, corneal curvature measured by keratometry; CT corneal curvature measured by corneal topography. \pm 1 sd.

A weak positive correlation is evident between the refractive error change and the keratometric corneal curvature change for *myopes*, using data from the right eye only ($r = 0.22$, $p > 0.1$). See figure 6.6.

An insignificant negative correlation can be found between refractive error change and keratometric corneal curvature change for *emmetropes*, using right eye data only ($r = 0.02$, $p > 0.1$).

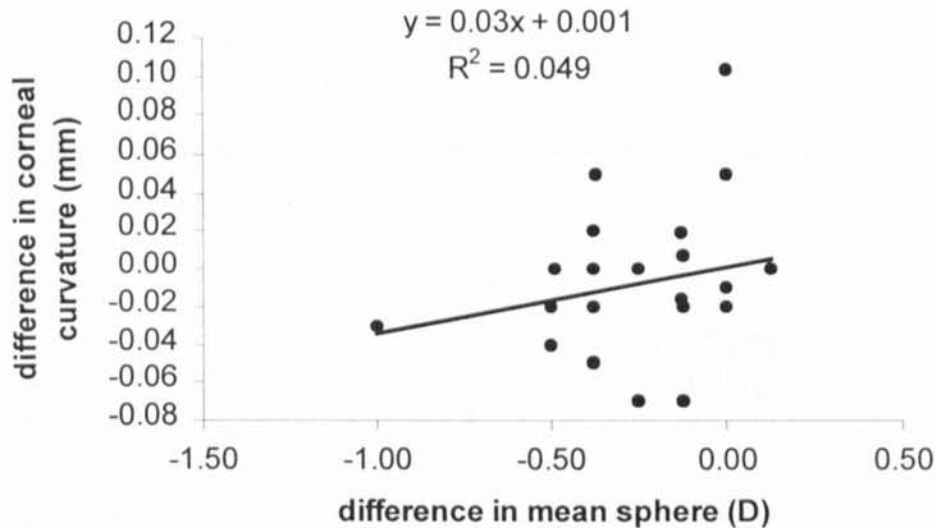


Figure 6.6 Change in refractive error, over an 18-month to 2-year period, plotted against change in keratometric corneal curvature. Myopes only, right eye (n = 24).

The positive correlation suggests that an increase in myopia (myopic shift) over a period of time could be associated with corneal steepening. However, the correlation is not significant.

Minimal correlation was also found between the change in axial length over time and the change in keratometric corneal curvature ($r = 0.15, p > 0.1$). This correlation was negative suggesting that an increase in axial length over time could also be associated with corneal steepening.

The association was investigated further by analysing the relationship between corneal curvature change and refractive error change in *late-onset* myopes only (n = 10). Data from the right eye only. A slight positive correlation was observed between the refractive error change over time and the corresponding change in keratometric corneal curvature ($r = 0.14, p > 0.1$). The results suggest that an increase in myopia in the late-onset myopia group, over time, is associated with a steepening in corneal curvature. No association was found between myopia increase over time and corneal steepening in *early-onset* myopes.

Longitudinal change in corneal shape

Figure 6.7 depicts the relationship between the change in refractive error and the change in corneal shape ($r = 0.11$, $p > 0.1$). The negative relationship demonstrates that a myopic shift in refractive error is associated with an increase in the ρ -value (peripheral corneal steepening).

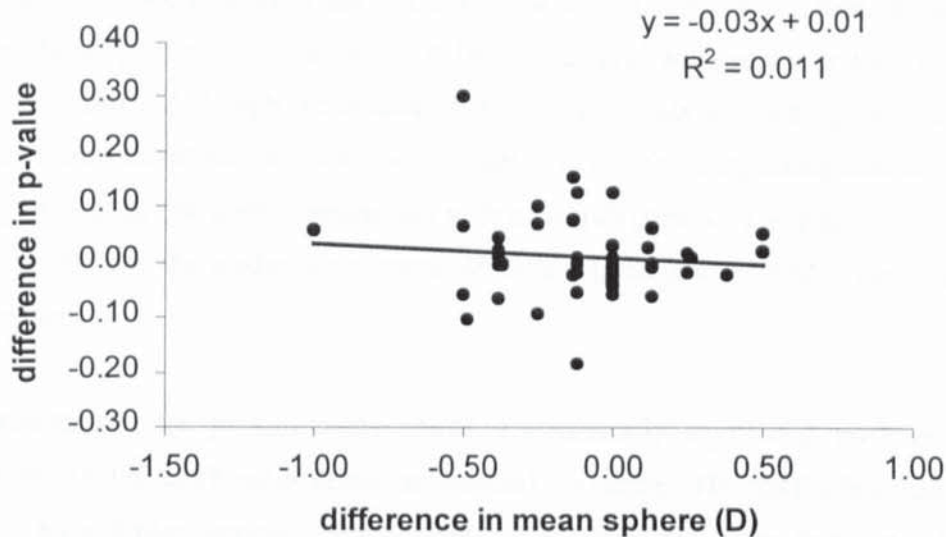


Figure 6.7 Change in refractive error, over an 18-month to 2-year period, plotted against change in corneal shape. Right eye only ($n = 50$).

6.8 Discussion

Cross-sectional analysis of central corneal curvature

The initial mean keratometric corneal curvature, for the complete data set (emmetropes and myopes), was 7.81 ± 0.23 mm. This value and its corresponding standard deviation is similar to corneal curvatures and standard deviations found in previous studies containing subjects within the same age range (Stenström, 1946; Fledelius, 1988; Carney *et al.*, 1997; McBrien and Millodot, 1987a and Guillon *et al.*, 1986).

The initial mean central corneal curvature, measured using the corneal topographer, for the complete data set, was 7.90 ± 0.23 mm. The value is slightly higher, yet similar, to the results from previous work. Guillon *et al.* (1986) found the apical radius of curvature, using a Wesley-Jessen Photo Electric Keratoscope, to be 7.79mm and Douthwaite *et al.* (1999) found it to be 7.86mm, using an EyeSys videokeratoscope.

The standard deviations, relating to the central corneal curvatures, appear to be alike in all studies.

Figures 6.1 and 6.2 show weak correlations between central corneal curvature and refractive error. Van Alphen (1961) re-analysed the data of Stenström (1946) in which 1000 right eyes were assessed in subjects aged between 20 and 35 years. Correlation coefficients were derived for a number of ocular variables. Van Alphen found a significant positive correlation ($r = 0.18$) between refractive error and the corneal radius of curvature. Although the results of this current study are not significant for corneal curvature and refractive error, the correlation is positive suggesting that an increasingly myopic refractive error is associated with a steeper cornea. The correlation coefficients vary between the studies as a result of differing subject refractive errors and subject number.

Interestingly, the present study shows a statistically significant positive correlation between vitreous chamber depth and corneal curvature. The results indicate that longer eyes have flatter corneae. Similar conclusions were drawn by Stenström (1946); van Alphen (1961) and Scott and Grosvenor (1993). Stenström found a positive correlation coefficient of 0.31 for these two variables and Scott and Grosvenor noted a positive correlation of 0.79. Correlation analysis describes the strength of the relationship between two variables but does not include the effect that other variables could have on the relationship. Consequently, Scott and Grosvenor hypothesise that different processes may underlie the elongation of the myopic eye compared to normal eyes.

Grosvenor and Scott (1991), in their study of myopes and emmetropes, found mean corneal power to be greater (steeper cornea) in myopes compared to emmetropes. Curtin (1985) reported on a number of studies which also revealed greater corneal power in myopes than in emmetropes. However, in the longitudinal study by McBrien and Adams (1997), no significant difference in corneal radius was found between emmetropes and any form of myopic group, i.e. early-onset myopia or late-onset myopia. In this study, the means of the corneal curvatures for emmetropes and myopes were compared using a *t* test: no significant difference was found.

When analysing the emmetropes and myopes separately, only a weak correlation exists between refractive error and corneal curvature. The correlation is positive for the myopes, which denotes corneal steepening with increasing amounts of myopic refractive error.

Shape factor

The initial mean shape factor value (ρ -value), for the complete data set (emmetropes and myopes), was 0.78 ± 0.13 . Douthwaite *et al.* (1999) measured apical radius and ρ -value in 200 normal corneae. The average ρ -value was calculated to be 0.76 using the *Eyesys* videokeratoscope, i.e. the same instrument as for this study. In a corneal asphericity study, conducted by Eghbali *et al.* (1995), the mean ρ -value was found to be 0.82, whereas Sheridan and Douthwaite (1989) found it to be 0.89 and Kiely *et al.* (1982) calculated the value to be 0.74.

Sheridan and Douthwaite (1989) also attempted to address the question of whether an association exists between corneal shape and refractive error. The subjects were divided into hyperopes, emmetropes and myopes. No significant difference was found for corneal shape in the three groups. Similar results were observed in the current data set, using a *t* test to compare means, between emmetropes and myopes.

Longitudinal analysis

The results show a minimal change in refractive error in the emmetropes and a myopic shift of approximately $0.25 \pm 0.24D$ in the myopes over the 18-month to 2-year longitudinal period of assessment. There is no corresponding change in corneal curvature (or corneal power) and minimal change in corneal shape. No significant correlation was detected between refractive error change and corneal curvature change. These results are in agreement with those of Grosvenor and Scott (1993) and McBrien and Adams (1997), who state that there is no evidence for corneal power or curvature change with a longitudinal change in refractive error. Contrasting results were obtained in a retrospective longitudinal study on young adults, aged 18 years and older, conducted by Goss (1987). The authors found a significant positive correlation between myopia progression rate and rate of keratometer power change (+0.70).

The data set was divided into emmetropes and myopes to determine whether the cornea affected the two groups differently in relation to refractive error change. A weak positive correlation was evident between the refractive error change and keratometric corneal curvature change in myopes. This, once again, links a myopic shift in refractive error with corneal steepening.

Further analysis revealed a low-level positive correlation among corneal curvature change and refractive error change in *late-onset* myopes but not in *early-onset* myopes. The interaction indicates that a myopic shift in myopia (late-onset) is associated with a steepening of the cornea. In support of this theory, Kent (1963) reported that corneal steepening accounted for over half of the refractive error changes in his single-case study.

Finally, the data shows a positive, albeit weak, correlation between change in refractive error and change in corneal shape over time. The movement of the cornea towards an increasingly oblate shape (steepening in the periphery) with increasing myopia agrees with the recent study (Horner *et al.*, 2000).

6.9 Summary

- Corneal curvature values are similar to those found by other investigators when measured by keratometry and corneal topography.
- A weak positive correlation was found between refractive error and corneal curvature. This suggests that a myopic refractive error is associated with a steep cornea.
- Paradoxically, there is a strong positive correlation between vitreous depth and corneal curvature suggesting that larger eyes have flatter corneae.
- When comparing corneal curvature values in emmetropes and myopes, no significant difference was noted between means, therefore, corneal curvatures for emmetropes and myopes are similar.
- Corneal shape values were similar to those found by other investigators and no significant difference was noted among means for emmetropes and myopes.
- An average myopic shift of -0.25D was found, for the myopic data set, over a period of 18-months to 2-years, though, no significant corresponding corneal change

was detected. However, the corneal change would probably be small and maybe masked by the level of resolution possible with keratometry measurements.

- Myopia progression, in *late-onset* myopes, appears to be weakly associated with corneal steepening. However, the same relationship could not be found in *early-onset* myopia.
- Corneal shape becomes increasingly oblate with increasing myopia.

CHAPTER 7

OCULAR COMPONENT ANALYSIS AND RETINAL SHAPE

7.1 Introduction

Peripheral refractive error can differ from that measured centrally with the amount depending upon the degree of eccentricity from the central fixation point (Ferree *et al.*, 1931 and Rempt *et al.*, 1971). Peripheral refractive error may also vary with the nasal and temporal visual fields (Ferree *et al.*, 1932). Ferree, Rand and Hardy (1931) classified peripheral refraction measurements into three different types corresponding to the amount of oblique astigmatism. Rempt, Hoogerheide and Hoogenboom (1971) extended this work to develop a graphical representation of the sagittal and tangential refractive errors against eccentricity, termed a skiagram, and further classified the peripheral refraction measurements into 5 types of skiagram (see § 3.2.1). The investigators demonstrated that the type I skiagram, that depicts eyes with low amounts of peripheral astigmatism, was often associated with myopic refractive errors. The type IV skiagram, represented by a large amount of peripheral astigmatism, was found more often in emmetropic eyes. Millodot (1981) investigated peripheral refraction and skiagrams and various researchers since have correlated central refractive error with peripheral refractive error (Logan, 1997; Love *et al.*, 2000; Mutti *et al.*, 2000 and Mutti *et al.*, 1997).

Ferree and Rand (1933) indicated that it may be possible to derive retinal contours using peripheral refraction measurements. This idea prompted Dunne (1995) to develop a computer-driven method of determining the retinal contour. The program is listed in appendix 4 and uses data from central and peripheral refraction and ocular biometry measurements.

7.2 Retinal shape assessment

Relative peripheral refractive error

The relative peripheral refractive error (PRE) can be used as an index of eye shape to compare eye contour in hyperopes, emmetropes and myopes. Mutti *et al.* (1997) and Mutti *et al.* (2000) assessed ocular shape in children by measuring the peripheral refractive error at 30° in nasal gaze. Love *et al.* (2000) also reported on the relative PRE in 40 myopic and 40 emmetropic eyes at 35° eccentricity in the nasal and temporal

meridia. The data was derived from the primary set of measurements taken from the 2-year longitudinal study described in this thesis. The relative PRE can be described as the peripheral equivalent mean sphere refractive error relative to the central equivalent mean sphere refractive error.

Calculation of retinal contour

The RetinaFit program, derived by Dunne (1995), produces X and Y co-ordinates to create a retinal contour for each subject. The retinal contour can be represented graphically by plotting a graph of the X and Y co-ordinates. The shape can be related to the length of the eye by plotting the co-ordinates against axial length. The derivation of retinal contour is explained in greater detail in §5.2.

The peripheral astigmatic factor

The mean amount of astigmatism was calculated at the corresponding nasal and temporal eccentricities. The peripheral astigmatic factor is explained in greater detail in §5.2.

7.3 Vergence contributions to emmetropia and myopia

The contribution of ocular components to the entire refractive system can be evaluated and expressed as ocular vergence (Erickson, 1984 and Leary, 1981). Figure 7.1 depicts how the vergence contributions are derived.

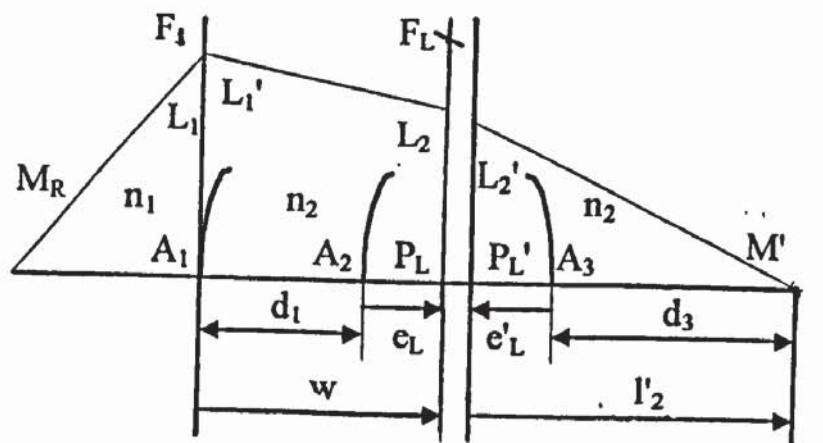


Figure 7.1 Formation of vergence contributions through the eye.

Where,

A_1	corneal apex
A_2	anterior lens surface apex
A_3	posterior lens surface apex
F_{sp}	spectacle power (D)
v	spectacle vertex distance (m)
F_1	corneal power (m)
d_1	anterior chamber depth (D)
d_2	lens thickness (m)
d_3	vitreous chamber depth (m)
$n_2 (= n_4)$	refractive index of humours (1.3333)

$L_1 = F_{sp}/(1-vF_{sp})$	vergence of light ray travelling from far point (M_R) to corneal surface (A_1)
$L'_1 = L_1 + F_1$	vergence of light after corneal refraction
$e_L = 0.596d_2$	distance of 1 st principal point of lens (P_L)
$e'_L = -0.358d_2$	distance of 2 nd principal point of lens (P'_L)
$w = d_1 + e_L$	distance from cornea (A_1) to 1 st principal point (P_L)
$L_2 = L'_1/(1-(w/n_2)L'_1)$	vergence of light at 1 st principal point of lens
$l'_2 = -e'_L + d_3$	distance from 2 nd principal point of lens (P'_L) to retina (M')
$L'_2 = n_2/l'_2$	vergence after lens refraction
$F_L = L'_2 - L_2$	equivalent lens power

7.4 Purpose

It is generally agreed that the main structural correlate of myopia is an increase in axial length and more specifically an increase in the vitreous chamber depth. In her cross-sectional study of retinal shape in anisomyopia, Logan (1997), discovered that myopia was a result of a longitudinal, rather than an equatorial, increase in dimension of the posterior globe. The results were computed using the same 'RetinaFit' computer program devised by Dr Mark Dunne. The purpose of the present study is to compare the retinal shape in emmetropes and myopes and to trace the change in retinal contour during myopia onset and progression, in young adults.

An alternative way to describe ocular shape is by using the relative PRE. In cross-sectional studies, a high percentage of emmetropic subjects show relative myopia in the periphery, indicating an oblate retinal shape and a high percentage of myopic subjects

show relative hyperopia in the periphery, indicating a prolate retinal shape. This relatively simple technique can also be applied to longitudinal data to assess the change in ocular shape during onset and progression of myopia.

The type I pattern of peripheral astigmatism has previously been linked to the myopic eye (Rempt *et al.*, 1971 and Hoogerheide *et al.*, 1971). The type I pattern is described by low values of peripheral astigmatism and the peripheral refraction becomes less myopic with increasing degrees of eccentricity. The paf ensures a definitive value of peripheral astigmatism. The data from the present study can be used to examine the association between myopia and low values of peripheral astigmatism and possibly provide a means of predicting myopia onset and progression in individuals.

7.5 Method

Subjects

The cohort consisted of 26 emmetropic subjects and 24 myopic subjects. The myopic group was also sub-divided into early-onset myopes (n = 14) and late-onset myopes (n = 10) and the emmetropic group was sub-divided into stable emmetropes (n = 22) and emmetropes that progressed into late-onset myopia (n = 4). The subjects ranged in age between 16 and 26 years and were divided into 23 males and 27 females.

Thirty-five subjects were examined on 3 occasions over a 2-year period and the remainder were examined on 3 occasions over an 18-month to 2-year period. Both right and left eye were examined (see §4.1). Corrected visual acuity was at least 6/6 in each eye. At the initial examination the mean emmetropic subjective refractive error was $+0.24 \pm 0.24D$ and mean myopic subjective refractive error was $-2.08 \pm 1.57D$.

Experimental procedure

A number of measurements were taken on all subjects and used in analysis for this chapter. Retinal shape data can be found in appendix 7. The same examiner obtained all the measurements. These measurements include: -

1. Full subjective refraction (checked using +1.00D blur test) and eye examination
2. Objective central refraction (Canon Autorefractometer R-1)
3. Objective peripheral refraction (Canon Autorefractometer R-1)
4. A-scan ultrasonography (Storz Omega)
5. Keratometry (Rodenstock, 2-position keratometer)

Subjective refraction (see § 4.2.1).

The subjective refractive error was found at each visit on all subjects and obtained after instillation of 2 drops of 1% tropicamide HCl (*Minims*[®], Chauvin) with a five-minute interval between drops to achieve cycloplegia. A 4m logmar chart was used to record the visual acuity and refractive error. The subjects were asked to sit in a chair located 4m from the chart whilst trial lenses were placed before their eyes until the best visual acuity and end-point was reached. The final refraction was checked using the +1.00D blur test. All refractive error measurements were converted from sphere, cylinder and axis into equivalent mean sphere using a specially designed computer program, written by Dr Mark Dunne in *Quickbasic*.

Objective central refraction (see §4.2.1)

Central and peripheral refractive error measurements were taken using the Canon Autorefractometer R-1. Two drops of 1% tropicamide HCl induced mydriasis and cycloplegia, as mentioned above. The subjects were instructed to place their chin on the chinrest and their forehead against the forehead bar. A strap was placed around the head to restrict head movement rather than eye movement. The subject's left eye was covered with an occluder while the right eye viewed a distant object. Five central refractive error readings were taken on each eye.

Objective peripheral refraction (see § 4.2.2)

An arc was placed on top of the main body of the Canon R-1 to allow peripheral refractive error measurements to be taken. Horizontal fixation targets were set at 5° intervals to a maximum of 35° both nasally and temporally. Five readings were taken at each eccentricity. The data was transferred to a personal computer, in conjunction with keratometry and A-scan ultrasound measurements, and entered into a specially devised computer program called RetinaFit, written by Dr Mark Dunne and modified by Chris Knight (Computer Science student, Aston University). The data was then manipulated in a number of ways to achieve different values including retinal contour and the peripheral astigmatic factor (paf).

A-scan ultrasonography (see § 4.2.3.)

The A-scan probe was sterilised with an alcohol wipe (*Medi-swab*, Seton Healthcare, England) before use on each subject. One drop of 0.4% benoxinate HCl (*Minims*[®], Chauvin) was instilled in each eye to induce corneal anaesthesia. The subject's pupils were dilated and accommodation was reduced owing to prior instillation of 2 drops of 1% tropicamide HCl. The probe was placed gently onto the cornea of one eye and ten measurements were taken while subjects fixated a distant spotlight with the other eye. Measurements were taken on both eyes in all subjects at all three visits.

Keratometry (see § 4.2.4)

Keratometry measurements were taken on all subjects at all three visits using a Rodenstock keratometer. Three measurements of corneal radius of curvature and axis were obtained along the two principal meridians for both eyes. Prior to taking the measurements, the subjects were positioned comfortably on the keratometer and the eyepiece focused in accordance with manufacturers guidelines.

The keratometer was calibrated using a precision 7.8mm spherical steel ball. The instrument was calibrated at regular intervals by the author or a member of the Optometry Division technical staff. See chapter 6 which describes the evaluation of corneal curvature in more depth.

7.6 Results

7.6.1 Validity and repeatability

Table 7.1 shows the validity data for the parameters discussed in this chapter. The validity results for corneal curvature and ultrasound measurements can be found in §5.5.1.

Table 7.1 Values of validity (n=50).

<i>Parameter</i>	<i>Validity</i>	
relative PRE	Nasal ± 0.38	Temporal ± 0.45
paf	± 12.28	
retp	± 0.53	
retr	± 0.85	

The repeatability values of the measurements can be found in table 7.2.

Table 7.2 Repeatability measurements for parameters (n=30).

<i>Parameter</i>	<i>Bias</i>	<i>Standard deviation</i>	<i>95% Limits of Agreement</i>
relative PRE nasal	0.30	1.05	-1.77 to 2.37
relative PRE temp	-0.13	1.24	-2.55 to 2.29
paf	10.08	34.30	-57.17 to 77.31
retp	-0.38	1.40	-3.13 to 2.37
retr	-0.50	2.36	-5.13 to 4.13

7.6.2 Relative PRE

A significant negative correlation was found between relative PRE at 35° and central subjective refraction in the nasal meridian ($r = 0.58, p < 0.002$). A significant negative correlation was also found between relative PRE at 35° and central subjective refraction in the temporal meridian ($r = 0.54, p < 0.002$). See figures 7.2a and b.

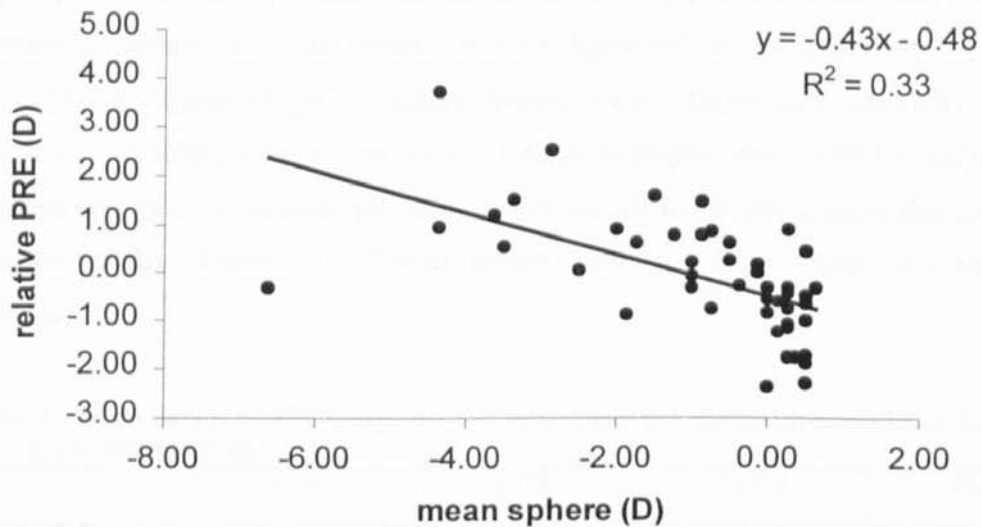


Figure 7.2a Subjective refractive error plotted against relative PRE at 35° in the nasal meridian. Right eye only (n=50).

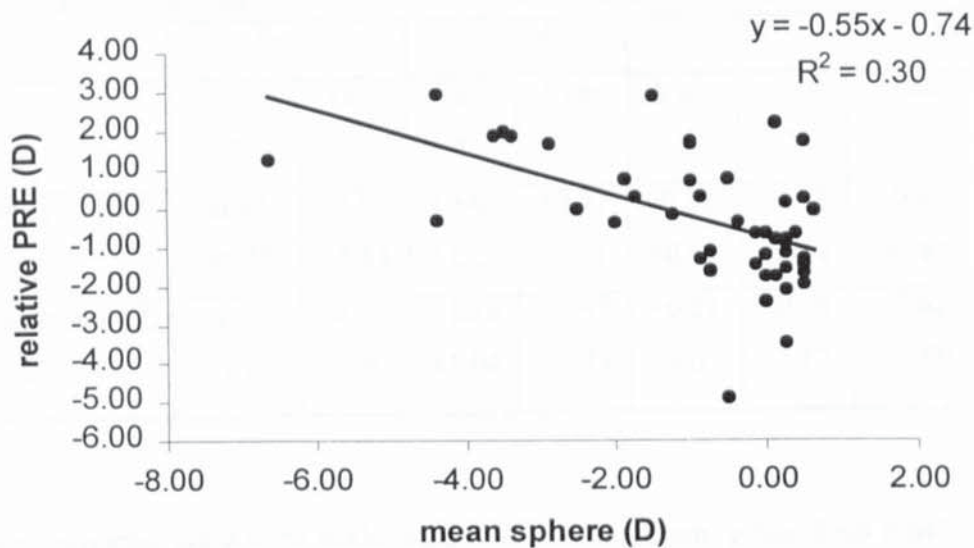


Figure 7.2b Subjective refractive error plotted against relative PRE at 35° in the temporal meridian. Right eye only (n=50).

Mutti *et al.* (1997) and Mutti *et al.* (2000) discovered that a high proportion of the *hyperopic* and *emmetropic* children showed relative *myopia* in the periphery and a large number of *myopic* subjects showed relative *hyperopia* in the periphery. Table 7.3 displays subject percentages of relative myopia in emmetropes and relative hyperopia in myopes. The subjects have been divided into emmetropes (emm^1), early- and late-onset myopes and initially emmetropic subjects whose refractive errors have shifted towards myopia in the 18-month to 2-year period (emm^2). Right eyes only have been considered.

Table 7.3 Percentages of relative myopia found in emmetropes and relative hyperopia found in myopes in nasal and temporal meridians.

	Emm^1		EOM		LOM		Emm^2	
	Visit 1	Visit 3						
Nasal (%)	82 rm	64 rm	71 rh	86 rh	70 rh	80 rh	100 rm	50 rh
Temporal (%)	82 rm	82 rm	79 rh	86 rh	60 rh	70 rh	75 rm	75 rh

Emm^1 = subjects emmetropic throughout examination period (n=22); EOM = early-onset myopes (n=14); LOM = late-onset myopes (n=10); Emm^2 = subjects initially emmetropic with myopic shift over examination period (n=4).

rm = relative myopia in periphery; rh = relative hyperopia in periphery.

The mean dioptric values of the relative PRE can be found in table 7.4.

Table 7.4 The dioptric values of relative PRE for emmetropes and myopes both nasally and temporally.

	<i>Emm</i> ¹		<i>EOM</i>		<i>LOM</i>		<i>Emm</i> ²	
	Visit 1	Visit 3	Visit 1	Visit 3	Visit 1	Visit 3	Visit 1	Visit 3
Nasal (D)	-0.80	-0.39	+0.81	+0.97	+0.37	+0.47	-0.80	+0.35
+ sd	±0.78	±0.64	±1.22	±1.01	±0.63	±0.72	±0.85	±1.30
Temporal (D)	-1.06	-0.19	+1.18	+0.95	+0.21	+0.49	-0.62	+0.62
+ sd	±1.23	±1.07	±1.04	±1.23	±1.07	±1.12	±0.69	±0.64

One interesting point to be made is the change in the *Emm*² group from relative myopia at the first visit to relative hyperopia at the final visit both nasally and temporally. At the initial visit the *Emm*² group were all emmetropic (mean refractive error = +0.41 ± 0.16D) and a high percentage demonstrated relative myopia in the periphery in a similar way to the *Emm*¹ group. However, at the final visit the mean refractive error for the subjects was -0.03 ± 0.11D (myopic shift) and relative hyperopia was noted in the periphery, similar to the *EOM* and *LOM* groups.

7.6.3 Ocular component analysis by vergence contribution

The descriptions below provide a guide for the analysis: -

$V_1 = F_1$	Cornea
$V_2 = L_2 - L'_1$	Separation between the cornea and the equivalent lens
$V_3 = F_L$	Equivalent lens
$V_A = V_1 + V_2 + V_3$	Anterior segment
$V_P = -L'_2$	Posterior segment
retr	Apical retinal radius (§7.2.2)
retp	Retinal asphericity (§7.2.2)
paf	Peripheral astigmatism factor (§7.2.3)
al/k	ratio reported to be a risk factor in the development of myopia

Ocular parameter variations in emmetropes, early- and late-onset myopes

Owing to the low number of subjects analysed in the subgroups (emmetropes, early-onset myopes and late-onset myopes), both right and left eyes have been considered. A two-tailed paired *t test* was used to compare the means of the right and left eyes in different refractive subgroups at the initial visit. The results indicate that there are no statistically significant differences between the means for the right and left eyes, therefore, the eyes can be pooled.

The calculated vergence contributions, retinal apical radius and shape (retr and retp), the peripheral astigmatic factor (paf) and the ratio of axial length to corneal radius of curvature (al/k) are shown in table 7.5 for emmetropes (n = 52), late-onset myopes (n = 20) and early-onset myopes (n = 28) at the initial visit.

Table 7.5 The calculated mean vergence contributions, retinal shape indicators (retr and retp) and indices for predicting myopia progression (paf and al/k) in emmetropia, late- and early-onset myopia. Mean and standard deviations are shown. All powers are expressed in dioptres and distances in millimeters.

<i>Parameter</i>	<i>Emmetropes</i>	<i>Late-onset myopes</i>	<i>Early-onset myopes</i>
F _{sp}	0.24 ± 0.24	-0.99 ± 0.62	-3.01 ± 1.57
F ₁ (V ₁)	42.62 ± 1.17	42.43 ± 1.37	43.20 ± 1.30
V ₂	10.13 ± 0.80	9.55 ± 0.74	8.87 ± 1.07
V ₃	23.95 ± 1.69	22.44 ± 2.39	21.76 ± 2.20
V _A	76.71 ± 2.45	74.42 ± 3.78	73.82 ± 2.69
V _P	-76.95 ± 2.49	-73.43 ± 3.60	-70.81 ± 3.01
retr	13.35 ± 2.65	15.00 ± 4.00	12.56 ± 1.96
retp	1.15 ± 1.51	1.79 ± 1.77	0.87 ± 0.88
paf	90.08 ± 30.05	75.96 ± 40.73	89.25 ± 26.53
al/k	3.00 ± 0.06	3.10 ± 0.05	3.24 ± 0.07

An ANOVA was used to assess whether the parameter means were significantly different in the three refractive groups. The results are shown in table 7.6. If the means were found to be significantly different, a post hoc test (Scheffé's) was applied for pairwise comparison.

Table 7.6 ANOVA and post hoc results to compare emmetrope, late- and early-onset myopia means for each parameter.

<i>Parameter</i>	<i>F – value</i>	<i>P – value</i>	<i>Post hoc results</i>	
F _{sp}	122.37	<0.0001	emm, lom emm, eom eom, lom	p<0.0001 p<0.0001 p<0.0001
F ₁ (V ₁)	2.64	0.08		ns
V ₂	18.84	<0.0001	emm, lom emm, eom eom, lom	p = 0.03 p<0.0001 p = 0.03
V ₃	11.78	<0.0001	emm, lom emm, eom eom, lom	p = 0.01 p<0.0001 ns
V _A	10.77	<0.0001	emm, lom emm, eom eom, lom	p = 0.01 p = 0.0003 ns
V _P	41.14	<0.0001	emm, lom emm, eom eom, lom	p<0.0001 p<0.0001 p = 0.01
retr	4.52	0.01	emm, lom emm, eom eom, lom	ns ns p = 0.02
retp	2.55	0.08		ns
paf	1.62	0.20		ns
al/k	130.09	<0.0001	emm, lom emm, eom eom, lom	p<0.0001 p<0.0001 p<0.0001

ns = not significant

Ocular parameter changes in myopia progression

To assess parameter change with myopia progression, the addition of ‘diff’ after each parameter indicates the change between the initial visit and the final visit.

A two-tailed paired *t test* was used to compare the mean changes for the right and left eyes, in different refractive subgroups, between the initial and final visit. The results

indicate that there are no statistically significant differences between the means for the right and left eyes, therefore, the eyes can be pooled.

Table 7.7 shows the calculated change in mean vergence contributions and retinal shape indicators (retr and retp), over the 18-month to 2-year study period, for emmetropes showing a myopic shift in refractive error (n = 8), late-onset myopes showing a myopic shift (n = 10) and early-onset myopes showing a myopic shift (n = 10).

Table 7.7 The calculated change in mean vergence contributions and retinal shape indicators (r_0 and ρ) in progressing emmetropia, late- and early-onset myopia. Mean and standard deviations are shown. All powers are expressed in dioptres and distances in millimeters.

<i>Parameter</i>	<i>Emm²</i>	<i>LOM prog</i>	<i>EOM prog</i>
F _{sp} diff	-0.33 ± 0.09	-0.38 ± 0.25	-0.29 ± 0.06
F ₁ (V ₁) diff	-0.07 ± 0.14	+0.02 ± 0.25	+0.02 ± 0.16
V ₂ diff	-0.65 ± 0.51	-0.25 ± 0.60	-0.09 ± 0.50
V ₃ diff	+0.65 ± 0.98	+0.39 ± 0.97	-0.42 ± 1.29
V _A diff	-0.07 ± 0.91	+0.15 ± 1.16	-0.49 ± 1.52
V _P diff	+0.40 ± 0.94	+0.22 ± 1.20	+0.78 ± 1.47

Emm² = initial emmetropes progressing into myopia, LOM prog = progressive late-onset myopes and EOM prog = progressive early-onset myopes.

Analysis, using an ANOVA, demonstrated no significant differences between the group means for any parameter.

Predictive indices in myopia

Rempt *et al.* (1971) suggested that a low amount of peripheral astigmatism, therefore a low paf, was indicative of a myopic subject and could be used as a predictive factor for myopia onset and progression. This theory was investigated by examining the change in refractive error (mean sphere difference) over the 18-month to 2-year period in relation to the initial paf values. See figure 7.3.

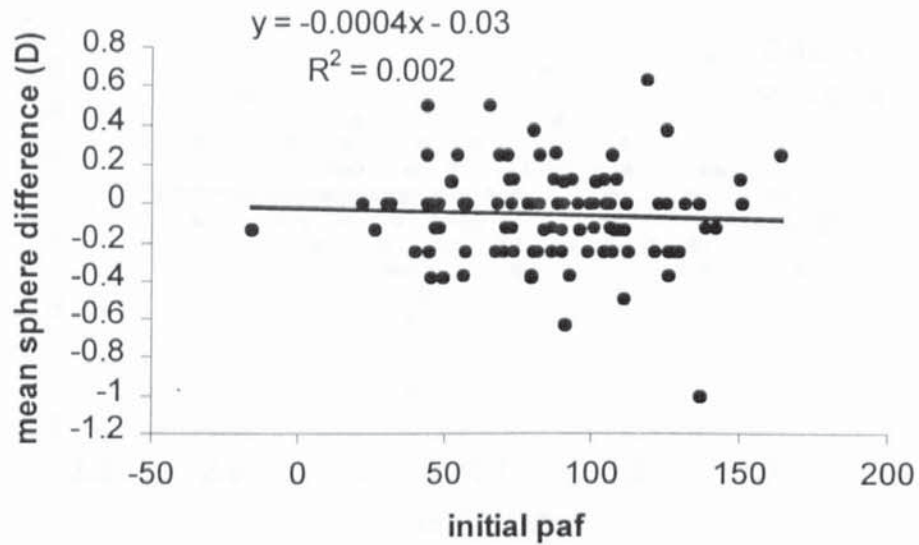


Figure 7.3 The initial paf values plotted against the change in refractive error over the study period (n = 100).

No significant correlation exists between initial paf and refractive error change ($r = 0.05$, $p = 0.64$). The data does not support the theory, proposed by Rempt, Hoogerheide and Hoogenboom, that paf can be used as a predictive factor for myopia onset and progression.

Grosvenor (1988) proposed that a high axial length/corneal radius ratio (al/k) could be a risk factor in the development of myopia. To test the hypothesis that the ratio could be used to predict myopia onset and progression, the initial al/k ratio was examined in relation to refractive error change (mean sphere difference) over the study period. See figure 7.4.

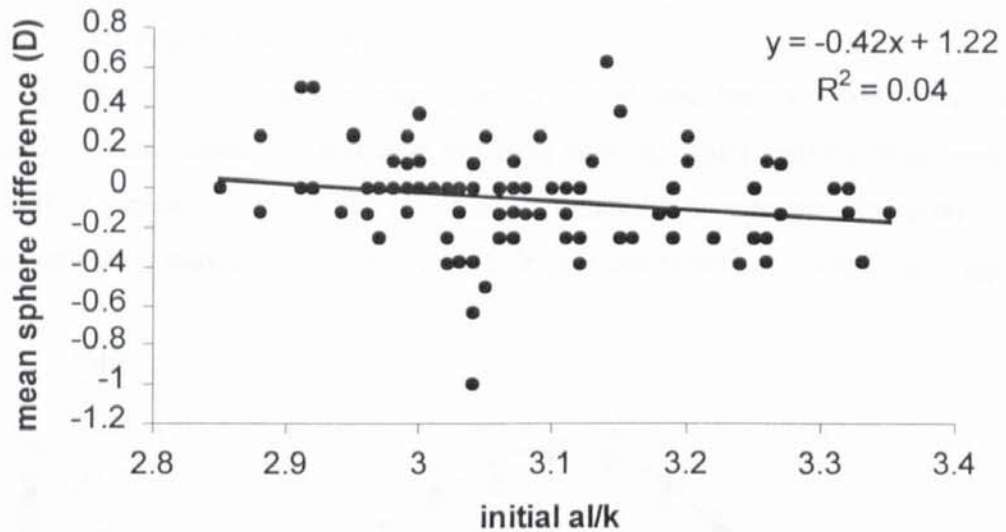


Figure 7.4 Initial al/k ratios plotted against the change in refractive error over the study period. N = 100.

There is a strong correlation between refractive error change and initial al/k ratio ($r = 0.21$, $p = 0.02$). The results indicate that a high initial al/k ratio produces a greater myopic shift in refractive error over an 18-month to 2-year study.

7.6.4 Retinal contour in myopia onset and progression

Repeatability of the technique

Peripheral refraction measurements, to 35° nasal and temporal along the horizontal meridian, were repeated 5 times on the same subject. The measurements were taken on a -3.00D female myope. Each set of measurements was separated by a day. The error bars represent standard errors based on 5 derivations of retinal contour. See figure 7.5.

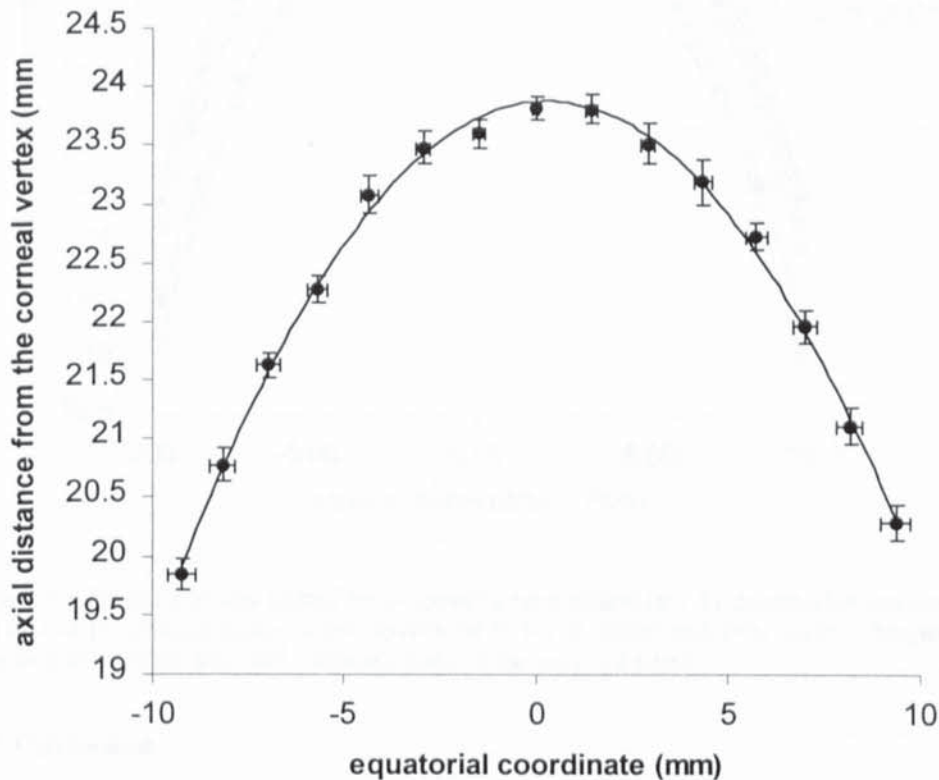


Figure 7.5 Mean retinal contour for a -3.00D myope derived from 5 separate set of peripheral refraction measurements. Error bars represent \pm SEM.

Retinal contour in early- and late-onset myopia

Figure 7.6 displays the retinal contours for progressive emmetropes (Emm²), late-onset myopes (LOM) and early-onset myopes (EOM). For each refractive group the contour is shown prior (initial visit) and post (final visit) myopia onset or progression. Mean shift in myopia (right and left eyes) for the progressive emmetrope group was -0.33 ± 0.09 , progressive late-onset myope group was -0.38 ± 0.25 and progressive early-onset myope group was -0.29 ± 0.06 .

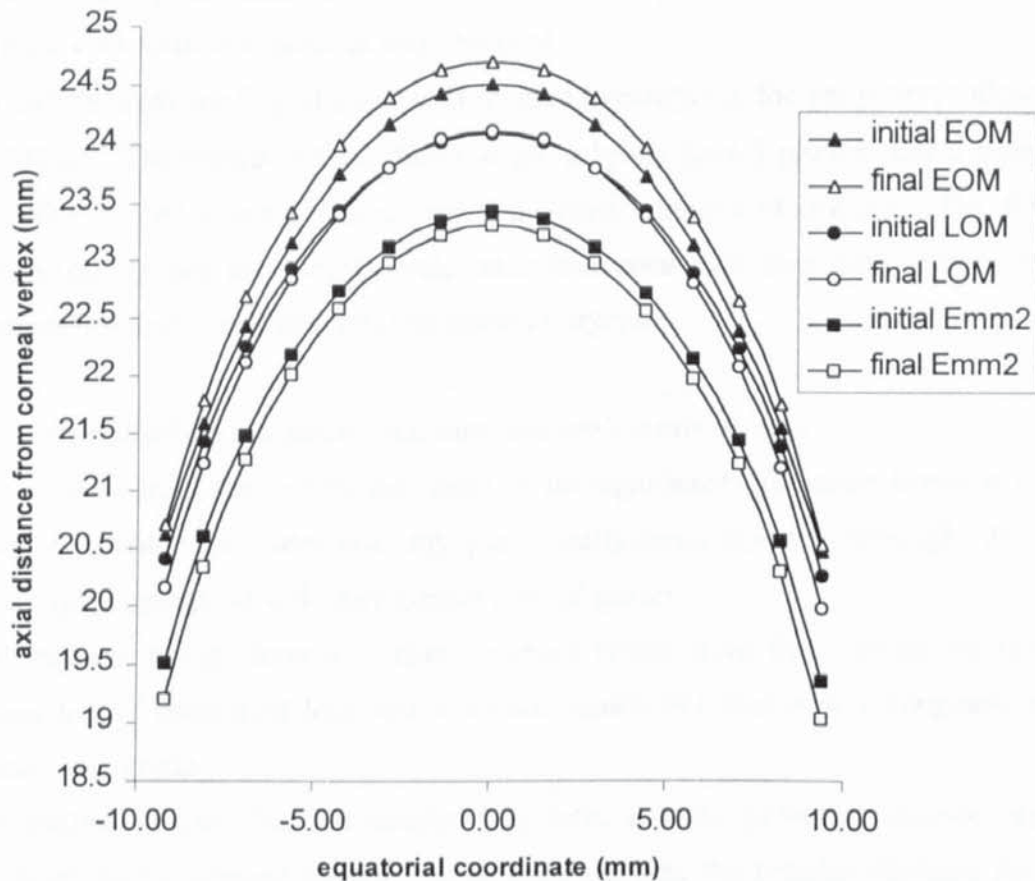


Figure 7.6 Retinal contours plotted for progressive emmetropes ($n = 8$), progressive late-onset myopes ($n = 10$) and progressive early-onset myopes ($n = 10$) at initial and final visits. Negative equatorial coordinates represent the nasal retina and positive the temporal retina.

7.7 Discussion

Relative PRE

On examining the relative PRE in children at 30° in nasal gaze, Mutti *et al.* (1997) and Mutti *et al.* (2000), found a high proportion of hyperopic children to demonstrate relative myopia in the periphery and myopic subjects to show relative hyperopia in the periphery. The examiners also noted relative myopia in emmetropic subjects. The current study assesses the relative PRE at 35° in the temporal and nasal meridia, on adults, and the findings agree with those of Mutti *et al.* The data demonstrates that refractive error is strongly correlated with relative PRE in both meridia.

Tables 7.3 and 7.4 display the mean relative PREs in stable emmetropes (Emm^1), early- (EOM) and late-onset (LOM) myopes and emmetropes that were emmetropic at the start of the study and showed a myopic shift (Emm^2). The Emm^1 group shows relative myopia in the periphery and both myopic groups show relative hyperopia. However,

the Emm² group demonstrated relative myopia in the periphery at the initial visit but by the final visit relative hyperopia was observed.

The EOMs show the largest amount of relative hyperopia in the periphery, followed by the LOMs. The results indicate that myopic subjects have a prolate retinal shape and the retina becomes more prolate with increasing amounts of myopia. The findings demonstrate further that longitudinal, rather than transverse stretching of the posterior segment is the principal structural correlate of myopia.

Component analysis in emmetropes, late- and early-onset myopes

It is evident from the results that there is no significant difference between corneal power in emmetropes, late-onset myopes or early-onset myopes, although, the early-onset myope group has a slightly greater corneal power.

Both myopic groups have a weaker vergence power from the distance between the cornea to the equivalent lens and a weaker equivalent lens power compared to the emmetropic group.

The analysis shows that the emmetropes have a more powerful anterior segment compared to the myopic groups. In the emmetropes, the anterior segment power is almost matched by the posterior segment power (derived from the axial length) which provides an overall emmetropic eye. The myopic eyes are the result of a low posterior segment power (long posterior segment) which has not been compensated for by the ocular components in the anterior segment, specifically anterior chamber depth and equivalent lens power.

The data from the thesis shows that there is a significant difference in apical radius (retr) means between the early- and late-onset myopes. The apical radii for both myopic groups are similar to that of the emmetropic group, however the early-onset myopes tend to have a steeper retinal apex than the late-onset myopes. The steep apical radius in conjunction with an asphericity value of 0.87 indicates a prolate ellipse shaped retina in the early-onset myopes. However, the retinal shape values are difficult to analyse owing to the relatively large standard deviations, low subject numbers and poor repeatability of the retinal contour technique.

The mean axial length to corneal radius ratio (al/k) is significantly different in emmetropes, late and early-onset myopes. Early-onset myopes have the highest ratio followed by late-onset myopes and emmetropes. The corneal powers (V_1) are similar

between all three groups, which indicates a long axial length in myopes. In agreement with the work of Grosvenor (1988) a high mean al/k ratio was found in myopes and a mean ratio of 3 was found for emmetropes. Also, Grosvenor and Scott (1994), suggest that eyes with a high al/k ratio will have a low powered lens. During emmetropization, the eye elongates which produces a high al/k ratio. To compensate, the lens decreases in power in an attempt to maintain emmetropia. Obviously, the decrease in lens power cannot decrease indefinitely, at which point myopia presents. The data reflects this theory in that the mean equivalent lens power, in early- and late-onset myopes, is significantly lower than that found in emmetropes.

Component analysis in myopia progression

In the emmetropic subjects that progress into myopia (Emm^2), it is apparent that the change in the distance between the cornea and equivalent lens (V_2) and the equivalent lens power (V_3) compensate each other. A small reduction in corneal power is also evident in this group with the myopic shift in refractive error. The vergence from the posterior segment (V_p) is generally negative in sign, owing to divergence, and the change in the posterior segment with myopia onset is positive (+0.40) indicating a less negative V_p and an increase in the length of the posterior segment.

The progressive late-onset myopes (LOM prog group) show an increase in the anterior segment vergence power (V_A), with myopia onset and progression, due largely to the increase in equivalent lens power. A more powerful anterior segment in conjunction with a longer posterior segment could explain the myopic shift in refractive error for the late-onset myopes.

The progressive early-onset myopes (EOM prog group) show a reduction in lens power, with myopia progression, rendering the anterior segment weaker. Without a change in the posterior segment, the eye would become more hyperopic; however, the change in the posterior segment power is greater than that of the anterior segment power, indicating a long posterior segment and an increase in myopia.

The data shows that the myopic shift in all three groups is a result of increased posterior segment length. In the Emm^2 and LOM prog myope groups the lens becomes more powerful, which adds to the myopic shift in refractive error, whereas, the lens weakens in power in the EOM prog myope group indicating that the myopic shift is due solely to an increase in posterior segment length.

Predictive indices

The results indicate that the initial peripheral astigmatic factor (paf) value is not an adequate predictive index for myopia onset and progression. However, the initial al/k value is a useful predictive index and could be utilised further in prospective myopia studies.

Retinal contour

Logan (1997) verified the computational retinal contour technique by comparing retinal contours with those derived by Laser Doppler interferometry (LDI). LDI is an *in vivo* technique, involving a beam from a laser diode, capable of determining the optical path length of the eye. Any discrepancy in measurements between the two techniques arise due to different layers of the retina.

Figure 7.6 displays the retinal contours for emmetropes (Emm^2), late and early-onset myopes (LOM and EOM) that progressed towards myopia. The Emm^2 group show a reduction in overall axial distance from the cornea. The axial distance at 0° eccentricity (axial length) reduces less than at the periphery suggesting some form of equatorial restriction or 'squeeze'. Similarly, the LOMs show minimal change in axial length, but display a reduction in axial distance at the periphery with myopia progression. The EOMs demonstrate that axial length at 0° eccentricity increases at a greater rate than axial distance in the periphery, denoting an increasingly prolate retinal shape with myopia progression. These investigations indicate that the eye stretches in the axial dimension during myopia onset and progression. Similar results were found by Logan (1997) in her study of retinal contour and anisomyopia and further evidence for axial, rather than equatorial expansion, can be found from the research on scleral stress in enucleated human eyes (van Alphen, 1986).

7.8 Summary

- Myopic subjects present with hyperopic relative peripheral refractive error (PRE) and emmetropic subjects present with myopic relative PRE. The data agrees with that of Mutti *et al* (1997) in their study on children. Stable emmetropic subjects (Emm¹) have myopic relative PRE. In the emmetropic subjects that show a shift towards myopia (Emm²), the relative PRE becomes increasingly hyperopic.
- Emmetropes have a more powerful anterior segment compared to the myopes, although, the emmetropes remain emmetropic owing to the shorter posterior segment. Myopic eyes are the result of a low posterior segment power (long posterior segment) that has not been compensated for by the power in the anterior segment.
- Early-onset myopes have a steeper retinal radius compared to the late-onset myopes indicating a more prolate shaped retina.
- Early-onset myopes have the highest ratio of al/k , followed by late-onset myopes and emmetropes. The corneal powers are similar between all three groups indicating that the high al/k ratio in myopes is the result of a long axial length. The data is in agreement with Grosvenor (1988).
- In the progressing emmetropes (Emm² group), the equivalent lens power increases with myopia onset, but is compensated for by the distance between the cornea and equivalent lens. The increase in myopia is primarily the result of posterior segment elongation.
- Myopia progression in late-onset myopes is the result of increased anterior segment power, due largely to an increase in the equivalent lens power in conjunction with posterior segment elongation.
- Myopia progression in early-onset myopes is the product of a long posterior segment which over-compensates for a weak anterior segment.
- Myopia onset and progression is the result of axial, not equatorial elongation.

CHAPTER 8

ACCOMMODATION IN EMMETROPIA AND MYOPIA

8.1 Introduction

Sustained nearwork and excessive closework demands have been implicated in the development of myopia in adults. A high lag of accommodation at near in conjunction with a reduced accommodative response will produce hyperopic defocus which may initiate axial elongation and induce myopia (Hung *et al.*, 1995; Wallman and McFadden, 1995, and Goss and Wickham, 1995). A number of research studies have investigated the link between refractive error and accommodation and particular attention has been given to accommodation in adult-onset myopia (McBrien and Millodot, 1986a; McBrien and Millodot, 1986b; McBrien and Millodot, 1987b; Strang *et al.*, 2000; Gilmartin and Bullimore, 1991; Abbott *et al.*, 1998 and Rosenfield and Gilmartin, 1987c).

Higher amplitudes of accommodation have been found in low myopes compared with high myopes and both myopic groups have been found to have higher amplitudes of accommodation than emmetropes and hyperopes (McBrien and Millodot, 1986a and Maddock *et al.*, 1981).

McBrien and Millodot (1986b) and Gwiazda *et al.* (1993b) reported higher mean accommodative response gradients in emmetropes compared to myopes. However, Abbott *et al.* (1998) did not find a significant difference when assessing accommodative responses in emmetropes, early-onset and late-onset myopes but did note a reduced accommodative response in progressing myopes compared to stable myopes.

8.2 Assessment of accommodation

Accommodation is a term used to describe an adjustment of the dioptric power of the eye to enable objects to be focused on the retina at any distance. In humans, accommodation is achieved by the change in shape of the crystalline lens. The dioptric power of the lens increases on accommodation due to a steepening of the crystalline lens surfaces (mainly anterior central), sagittal thickening of the lens and the forward translation of the lens into the anterior chamber (Brown, 1973). The main purpose of accommodation is to overcome a blurred retinal image of an object of regard and maintain equilibrium of the overall near vision triad of responses.

The amplitude of accommodation represents the maximum amount of accommodation an eye can exert. The amount of accommodation an eye produces declines with age. The near point advances towards the far point, with age, and by 50 years of age the two points are approaching coincidence. Accommodation has been found to decline from approximately 14D at 10 years of age to 0.50D by the age of 60 (Millodot, 1990 and Bennett and Rabbetts, 1989).

In young eyes, the accommodative mechanism is able to function over a wide range and the relationship between accommodative response and stimulus can be represented by the stimulus-response curve. Emmetropes or corrected ametropes will exert a level of accommodation less than the stimulus vergence, often referred to as the accommodative 'lag,' when viewing a near object. For distant objects, the response exceeds the stimulus vergence and a 'lead' of accommodation is demonstrated. At an intermediate stimulus vergence (approximately 1 to 2D), the 'lead' decreases to zero. The central portion of the stimulus response function is almost linear and its gradient provides a measure of the gain of the accommodative system. The linear regression slope of the function can be used as an indicator of the ability to accommodate to a known stimulus.

Accommodative error index

As previously mentioned, the slope of the linear regression line is often used to describe the stimulus-response function. However, a regression line is characterized by three separate quantities, which are: -

1. The slope of the regression line, m
2. The intercept on the y -axis, c
3. Pearson correlation coefficient, r^2

Chauhan and Charman (1995) argue that comparison of stimulus-response curves using the slope parameter solely, without incorporating the intercept and/or correlation coefficient, may be misleading. A new parameter, the accommodative error index, derived by Chauhan and Charman combines the three separate regression line parameters to provide a summary of the accuracy of the response over a given stimulus interval. The accommodative error index (I) is the mean of the magnitude of the response error (E) divided by r^2 .

$$I = E/r^2$$

The response error (E) is found by calculating the area between the best-fit curve and the unit ratio.

The present study uses the accommodative error index to compare stimulus response functions. However, reference will also be made to the slope parameter (m) for the comparison of the results with other studies.

8.3 Purpose

The majority of research studies on accommodation and refractive error have been cross-sectional in nature. In a longitudinal study, Gwiazda *et al.* (1995) reported shallow accommodative response gradients in myopic children compared to emmetropic children and the ability to accommodate to real targets at near distances reduced with progressing myopia.

The aim of the study is to assess the relationship between myopia and accommodation over an 18-month to 2-year period. Particular attention has been paid to changes in amplitude of accommodation and accommodative response between refractive groups and during the onset and progression of myopia.

8.4 Method

Subjects

The cohort consisted of 26 emmetropic subjects and 24 myopic subjects. The myopic group was also sub-divided into early-onset myopes ($n = 14$) and late-onset myopes ($n = 10$) and the emmetropic group was sub-divided into stable emmetropes ($n = 22$) and emmetropes that progressed into late-onset myopia ($n = 4$). The subjects ranged in age between 16 and 26 years and were divided into 23 males and 27 females.

Thirty-five subjects were examined on 2 occasions over a 2-year period and the remainder were examined on 2 occasions over an 18-month to 2-year period. Both right and left eye were examined (see §4.1). Corrected visual acuity was at least 6/6 in each eye. At the initial examination the mean emmetropic subjective refractive error was $+0.24 \pm 0.24D$ and mean myopic subjective refractive error was $-2.08 \pm 1.57D$.

Subjective refraction (see § 4.2.1).

The subjective refractive error was found at each visit on all subjects and obtained after instillation of 2 drops of 1% tropicamide HCl (*Minims*[®], Chauvin) with a five minute interval between drops to achieve cycloplegia. A 4m LogMar chart was used to record the visual acuity and refractive error. The subjects were asked to sit in a chair located 4m from the chart whilst trial lenses were placed before their eyes until an end-point was reached. The final refraction was checked using the +1.00D blur test. All refractive error measurements were converted from sphere, cylinder and axis into equivalent mean sphere using a specially designed computer program, written by Dr Mark Dunne in *Quickbasic*. Accommodation data can be found in appendix 8.

Assessment of amplitude of accommodation

Amplitudes were measured subjectively using an RAF near-point rule that had been modified to read to the nearest 0.50D. Target luminance was 80 cdm⁻². The subjects observed a high contrast (90%), black-on-white near-point card, with N5 print. The push-up method was used to assess the amplitude of accommodation. The RAF rule was placed on the subject's cheeks and the near-point card was held, at eye level, at a distance of 50cm from the subject. The near-point card was slowly moved in towards the subject. The subjects were asked to locate the position of first, slight, sustained blur of the target, as suggested by Rosenfield (1997), at which point the amplitude of accommodation was read from the RAF rule. This measurement was repeated three times and a mean value was calculated. Monocular and binocular measurements were taken.

Assessment of accommodative stimulus-response (see §4.2.6)

Drops were not used in the assessment of accommodation. The right eye only was assessed and the left eye was covered with an occluder. The subjects were positioned comfortably on the Canon R-1 and instructed to view an individual optotype in the lowest line of letters that they were able to see clearly. All myopic subjects were corrected with soft contact lenses and allowed to adapt to the lenses for 20 minutes prior to the accommodation measurements being taken. The subjects were encouraged to blink freely throughout the experiment.

The high contrast (90%), black-on-white Snellen acuity optotypes ranged from a size of 6/60 to 6/6. The optotypes were front-illuminated which gave a target luminance of 65cdm^{-2} . To maintain pupil sizes above 2.9mm and to prevent signal attenuation in the Canon R-1 Autoref, the room luminance was mesopic. The plate of letters was moved along the subject's midline and located at viewing distances from the subject of 6, 3, 2, 1, 0.50, 0.33, 0.25 and 0.20m. The subjects were allowed to adapt to each new stimulus level for 30 seconds before readings were taken.

The Canon R-1 Autoref was set in its single-shot mode and six readings were taken for each accommodative stimulus. All measurements were taken as ocular accommodative responses. Mean spheres were calculated for accommodation measures. The measurements were transferred to a personal computer via an interface connection (S. W. Spadafore, Franklin & Marshall college, Lancaster, USA) and entered into an Excel spreadsheet where a single figure index of accommodative response was calculated (Chauhan and Charman, 1995).

8.5 Results

8.5.1 Validity and repeatability

Table 8.1 shows the values of validity and table 8.2 shows the values of repeatability.

Table 8.1 Values of validity

<i>Measurement</i>	<i>Validity</i>
Accommodative error index	± 0.08
Amplitude of accommodation (D)	± 0.25

Table 8.2 Values of repeatability

<i>Measurement</i>	<i>Bias</i>	<i>Standard deviation</i>	<i>95% Limits of agreement</i>
Accommodative error index	-0.12	0.16	-0.42 to 0.18
Amplitude of accommodation	-0.15	0.48	-1.09 to 0.79

8.5.2 Amplitude of accommodation

A strong negative correlation was found between refractive error and the amplitude of accommodation on the initial visit ($r = 0.44$, $p < 0.002$). This relationship indicates an increase in the amplitude of accommodation with an increasingly myopic refractive error (see figure 8.1).

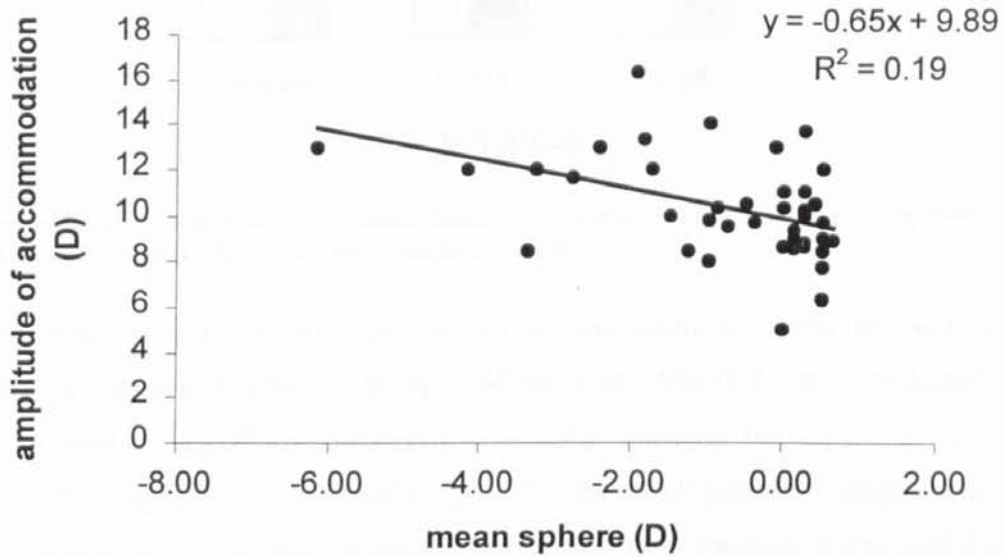


Figure 8.1 Amplitude of accommodation plotted against refractive error ($n = 50$).

Figure 8.2 presents the mean amplitudes of accommodation for emmetropes ($n = 26$), early-onset myopes ($n = 14$), and late-onset myopes ($n = 10$) at the initial and final visits.

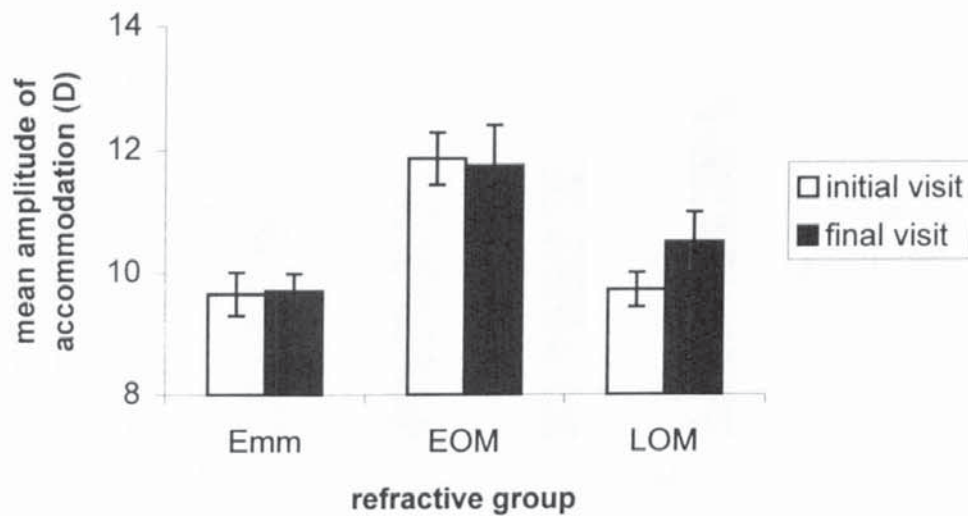


Figure 8.2 Mean amplitudes of accommodation in emmetropes (Emm), early-onset myopes (EOM) and late-onset myopes (LOM). Error bars represent ± 1 SEM.

To allow comparison of amplitude of accommodation means between the three refractive groups, a one-way analysis of variance (ANOVA) was conducted. At the initial visit, a significant difference was noted between the means $F_{2, 47} = 10.79$, $p < 0.0001$. Application of Scheffé's *post hoc* test to all pairwise comparisons between the means suggested that significant differences exist between *Emm* and *EOM* ($p = 0.0042$) and *EOM* and *LOM* ($p = 0.0012$).

A significant difference was also noted for the final visit $F_{2, 47} = 27.46$, $p < 0.0001$. Scheffé's test indicated significant differences again between *Emm* and *EOM* ($p < 0.0001$) and *Emm* and *LOM* ($p = 0.0002$).

Amplitude of accommodation data was also analysed in relation to stable emmetropes (*Emm1*, $n = 22$) and emmetropes shifting towards myopia (*Emm2*, $n = 4$) and stable myopes (*Myo1*, $n = 13$) and myopes progressing further into myopia (*Myo2*, $n = 11$) over the 2-year period (see figure 8.3). Subjects were deemed progressive if the refractive error shifted towards myopia by $-0.25D$ or more.

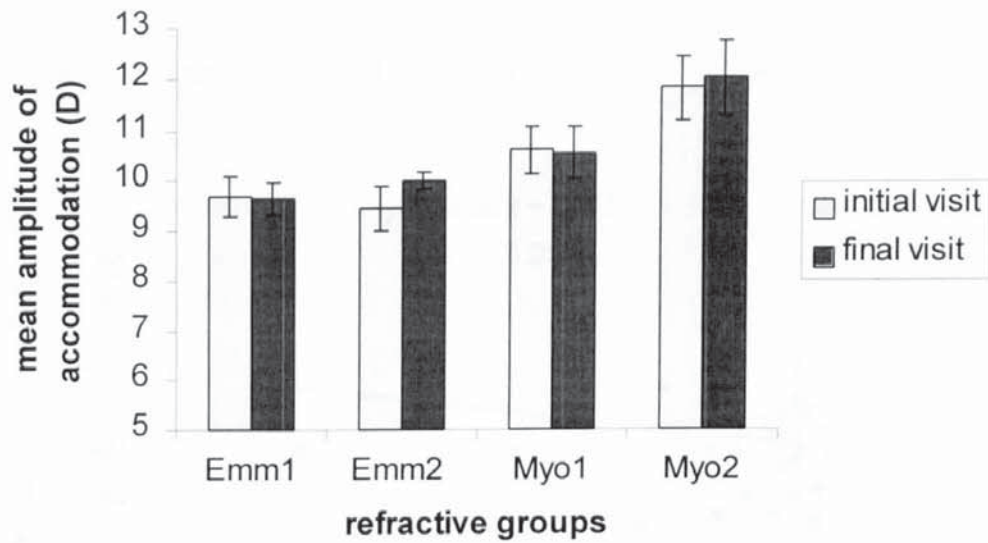


Figure 8.3 Mean amplitudes of accommodation for the stable emmetropic group (Emm1), progressing emmetropic group (Emm2), stable myopic group (Myo1) and progressing myopic group (Myo2). Error bars represent ± 1 SEM.

Figure 8.3 shows only a minimal shift in the amplitude of accommodation, over the study period, for the *Emm1* and *Myo1* groups, but a slight increase in the amplitude of accommodation for the *Emm2* and *Myo2* groups. A student's t-test was used to compare the means at the initial visit with that of the final visit in the *Emm2* group ($p = 0.35$) and in the *Myo2* group ($p = 0.83$). Both results indicate that the difference between the means is not significant and the amplitude of accommodation increased only slightly over the longitudinal study.

8.5.3 Accommodative error index

An insignificant negative correlation ($r = 0.22$, $p > 0.1$) was found between the accommodative error index and refractive error. See figure 8.4.

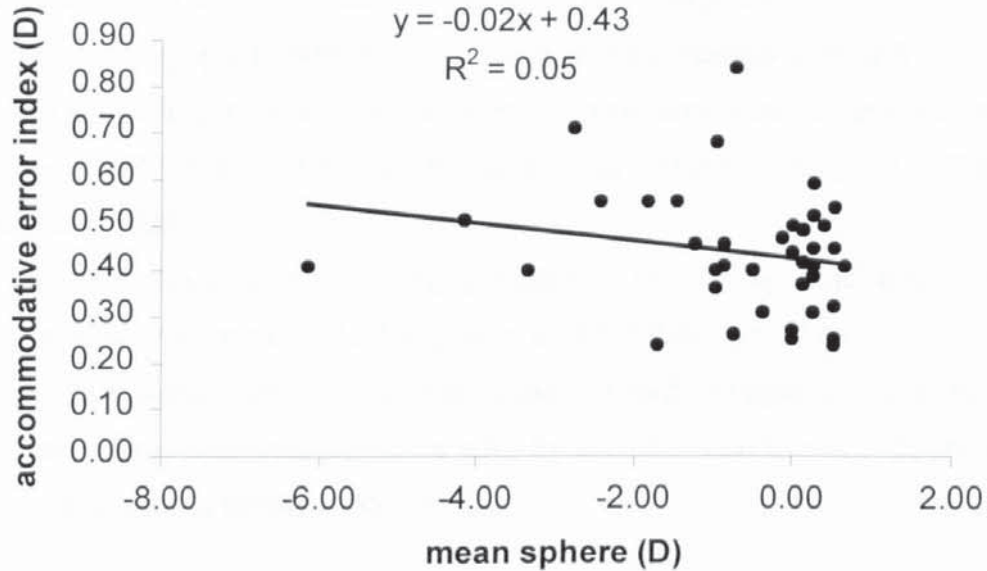


Figure 8.4 Accommodative error index plotted against refractive error ($n = 45$).

A column graph of mean accommodative error index plotted for emmetropes ($n = 24$), early-onset myopes ($n = 12$) and late-onset myopes ($n = 9$) at the initial and final visit can be seen in figure 8.5.

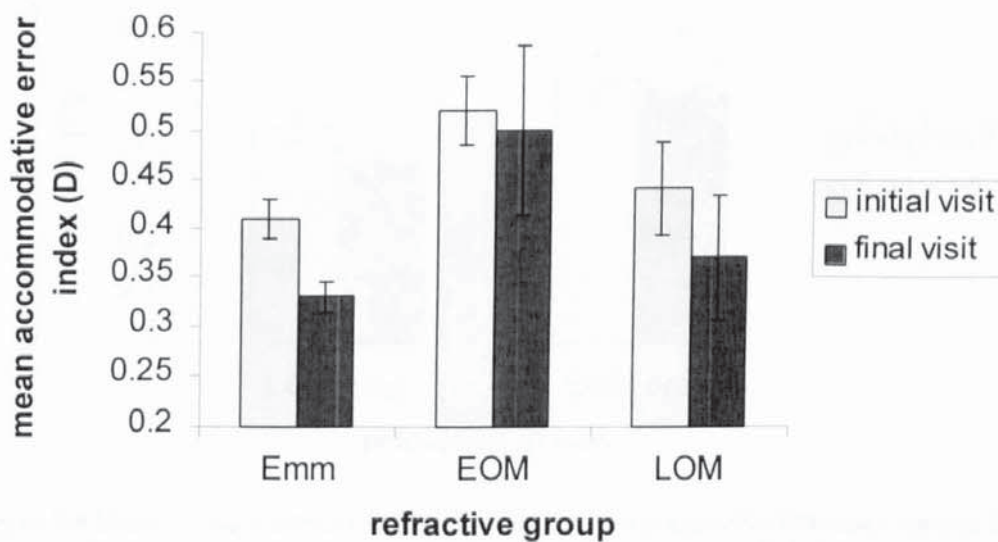


Figure 8.5 Mean accommodative error indices in emmetropes (Emm), early-onset myopes (EOM) and late-onset myopes (LOM). Error bars represent ± 1 SEM.

The results of a one-way ANOVA demonstrate that no significant difference was found between the means of the refractive groups at the initial visit ($F_{2, 42} = 2.10, p = 0.14$) or at the final visit ($F_{2, 42} = 2.87, p = 0.07$). However, it is apparent from the statistics and from the graph, especially at the final visit, that the mean accommodative error index is much higher for the *EOM* group compared to the *Emm* group.

To compare myopia progression in relation to accommodative error index over the 18-month to 2-year period, the refractive groups were separated into progressive late-onset myopes (LOM prog) and progressive early-onset myopes (EOM prog). The LOM prog group consisted of: -

1. myopes who presented with myopia after 15 years-of-age and demonstrated a shift in refractive error of 0.25D or greater over the study period ($n = 2$).
2. initially emmetropic subjects who shifted towards myopia by 0.25D or greater and ascertained a myopic refractive error by the final visit ($n = 4$). These subjects are also known as Emm2 in §8.5.2.

The EOM prog group consisted of subjects who presented with myopia prior to 15 years-of-age and progressed towards myopia by 0.25D or greater over the study period ($n = 9$). See figure 8.6.

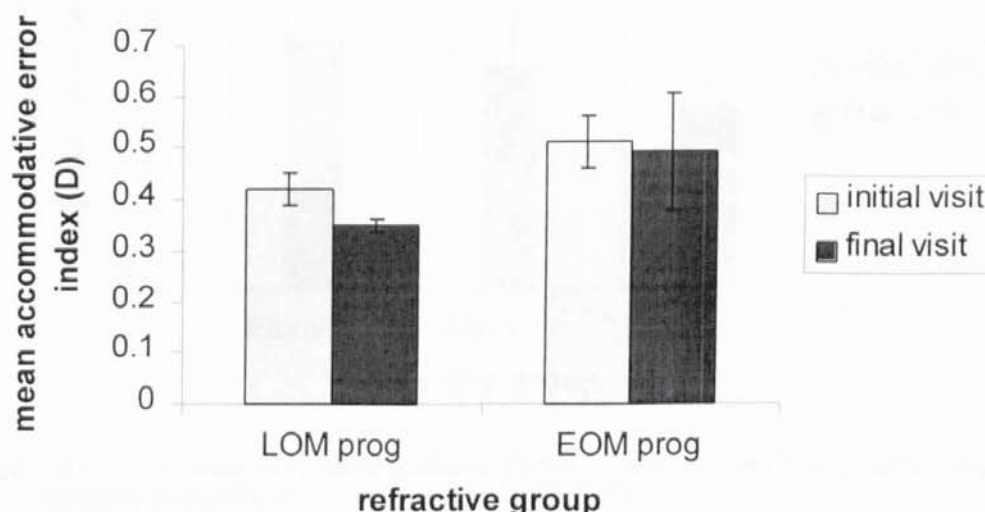


Figure 8.6 Mean accommodative error index plotted against progressive late-onset myopes (LOM prog) and progressive early-onset myopes (EOM prog). Error bars represent ± 1 SEM.

A student *t test* was employed to assess whether the *LOM prog* group and *EOM prog* group means were significantly different at the initial visit and the final visit. The means were not significantly different at the initial visit ($p = 0.18$) or at the final visit ($p = 0.33$).

Student *t tests* were also used to evaluate the difference between *LOM prog* means at the initial and final visit and *EOM prog* means at the initial and final visit. The *LOM prog* means were not significantly different ($p = 0.08$) and neither were the *EOM prog* means ($p = 0.89$).

8.5.4 Accommodation response gradient

Abbott *et al.* (1998) investigated the accommodative response gradients in emmetropes (Emm), progressing myopes (Myo2) and stable myopes (Myo1). The study demonstrated that the Myo2 group had shallower response gradients than the Emm group and Myo1. The accommodation response gradients for Emm ($n = 24$), Myo1 ($n = 11$) and Myo2 ($n = 10$) are shown in figure 8.7.

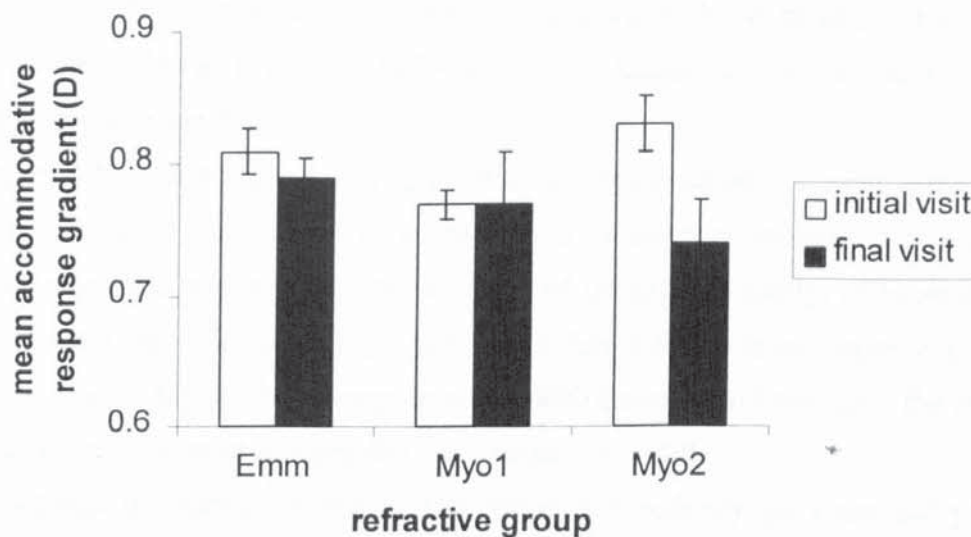


Figure 8.7 Accommodation response gradients plotted for emmetropes (Emm), stable myopes (Myo1) and progressive myopes (Myo2). Error bars represent ± 1 SEM.

The means of the groups were analysed using an ANOVA. No significant difference was noted between the means on the initial visit ($F_{2,42} = 2.04$, $p = 0.14$) or on the final visit ($F_{2,42} = 0.96$, $p = 0.39$).

Figure 8.7 demonstrates that the *Myo2* group has the greatest difference in means between the initial and final visits. A student's *t test* shows that there is no significant difference between the initial and final visit means for the *Myo2* group ($p = 0.06$), although, the result is close to being statistically significant.

8.6 Discussion

Amplitude of accommodation

The mean age of the subjects was 20.36 ± 2.73 years. The mean value for the push-up amplitude of accommodation was found to be $10.37 \pm 2.11D$ on the initial visit and $10.56 \pm 2.02D$ on the final visit. Duane (1922) measured amplitude of accommodation in over 4000 eyes and found the mean monocular amplitude of accommodation in 20 year-old subjects to be 11D.

Similarly, McBrien and Millodot (1986a) measured the amplitude of accommodation in eighty subjects, with a mean age of 19.82 years. The subjects were separated into refractive groups. Late-onset myopes were found to have the largest mean amplitude of accommodation (10.77D), followed by the early-onset myopes (9.87D), emmetropes (9.28D) and hyperopes (8.63D). The mean amplitudes of accommodation, for the current data set at the initial visit, are slightly higher than those found by McBrien and Millodot. The early-onset myope group were found to have the largest mean amplitude of accommodation (11.87D), followed by the late-onset myope group (9.72D) and emmetropic group (9.65D).

Figure 8.2 depicts the mean amplitude of accommodation for each refractive group. Analysis shows that there is a significant difference between the amplitude of accommodation means in the emmetropes and the myopes (early- and late-onset) at the initial and final visit. The graph also shows that both the emmetropes and early-onset myopes have only a small change in amplitude of accommodation over the study period whereas the late-onset myopes show an increase of 0.80D.

The change in mean amplitude of accommodation with myopia onset and progression, over the study period, is displayed in figure 8.3. It is apparent from the graph that both stable emmetropes (Emm1) and stable myopes (Myo1) show little or no change in amplitude of accommodation with respect to time. Progressive emmetropes (Emm2) show a slight increase in amplitude of accommodation (0.56D) as do the progressive myopes (Myo2). However, further evaluation on both groups indicates that the mean amplitudes are not significantly different between the initial and final visits.

Accommodation can be viewed with respect to dual innervation, autonomic nervous system control. Sympathetic innervation is responsible for negative accommodation and parasympathetic for positive. Two hypotheses exist to explain the findings that myopes tend to have higher amplitudes of accommodation compared to emmetropes. Charman (1982) suggests that myopes have a *strong parasympathetic* and *weak sympathetic* innervation, which would reduce the range of response in the sympathetic section of the response curve, resulting in reduced distance vision and high amplitude of accommodation at near. The second hypothesis is a result of pharmacological investigation. On evaluation of accommodation in monkeys, Tornqvist (1967) discovered that sympathetic mediated negative accommodation increased when the underlying level of parasympathetic accommodation increased and that sympathetic stimulation to the ciliary muscle is inhibitory. The hypothesis states that ocular focus in distance vision is dependent upon sympathetic activity while parasympathetic is responsible for near vision. If this were true, then at each measurement of amplitude of accommodation at near there would be sympathetic inhibitory effects. Maddock *et al.* (1981) propose that tonic accommodation (the resting position of focus the eye assumes in the absence of visual stimulation) is dioptrically lower in myopes compared to emmetropes and specifically in late-onset myopes. Myopes that present with dioptrically low values of tonic accommodation and low underlying parasympathetic tone would have a reduced inhibitory sympathetic effect and show higher amplitudes of accommodation (Gilmartin and Rosenfield, 1999).

Accommodative error index

Unlike amplitude of accommodation, the correlation between the accommodative error index and refractive error was insignificant suggesting that as the myopic refractive error increases, only a very small increase in the accommodative error index is evident (figure 8.4).

The mean accommodative error index for subjects with a mean age of 20.36 years was 0.44 ± 0.13 at the initial visit and 0.39 ± 0.21 at the final visit. Baker *et al.* (1998) found a similar result (0.39 ± 0.40) on subjects with a mean age of 23.5 years.

Statistical analysis indicates that no significant differences were noted between the mean accommodative error indices in emmetropes, early-onset myopes and late-onset myopes at either the initial and final visits. A closer look at figure 8.5 provides an

indication of the differences present between the refractive group means. At both the initial and final visit, the early-onset myope group has a greater mean accommodative error index followed by the late-onset myopes and the emmetropes. The data suggest that myopes have a more inaccurate accommodative response compared to emmetropes.

The accommodative error index in myopia progression, and more specifically late-onset myopia progression, was analysed and the results displayed graphically in figure 8.6. At the initial visit the early-onset myopes have a greater accommodative error index (more inaccurate accommodative response) compared to the late-onset myopes. By the final visit, after myopia progression, there is a small insignificant decrease in the accommodative error index for the early-onset myope group and a greater decrease, albeit insignificant, in the late-onset myope group. The results indicate that myopia onset and progression is accompanied with an increase in accommodative response accuracy.

Accommodation response gradient

Although data regarding the accommodative response gradient has not been displayed in the thesis, the data agrees with that of Ramsdale (1979); McBrien and Millodot (1986b) and Gwiazda *et al.* (1993b). The authors show that myopes have a lower accommodative response gradient than emmetropes and, therefore, myopes accommodate less than emmetropes to a near target.

Abbott *et al.* (1998) demonstrated that progressing myopes have shallower response gradients compared to emmetropes and stable myopes. This finding suggests that progressing myopes accommodate less to a near target. Accommodation response gradients, examined in the same refractive groups as those defined by Abbott *et al.*, were analysed in the current study. Unlike Abbott, Schmid and Strang, no significant difference was found between the three response gradient means. Figure 8.7 illustrates that the response gradient does not change significantly in the three groups between the initial and final visit, yet, there is a reduction in the response gradient for the progressive myope group, indicating a reduction in accommodation to near targets with myopia progression.

It has been suggested that a reduced accommodation response gradient could be related to myopia progression (Abbott *et al.*, 1998) and possibly acts as a predictive factor in myopia development (Gwiazda *et al.*, 1993b and Gwiazda *et al.*, 1995). Individuals

with low response gradients exhibit a high accommodative lag and a high degree of near blur which is the result of an inadequate accommodation system. The role of accommodation in the progression and onset of myopia is not yet fully understood (Gilmartin and Rosenfield, 1999). However, it is apparent from the results that sustained near work may contribute to myopia development

8.7 Summary

- Early-onset myopes were found to have the largest amplitudes of accommodation followed by late-onset myopes and emmetropes.
- Late-onset myopes show the largest increase in amplitude of accommodation over an 18-month to 2-year period.
- Emmetropes that progress into myopia, over the study period, and progressive myopes show an increase in amplitude of accommodation with respect to time.
- No significant correlation exists between the accommodative error index and refractive error.
- Early-onset myopes demonstrate a greater accommodative error index followed by late-onset myopes and emmetropes. The data indicates that myopes have an inaccurate accommodative response compared to emmetropes.
- Myopia onset and progression is accompanied with an increase in accommodative response accuracy
- No significant difference in accommodation response gradient means was noted between progressing myopes, stable myopes and emmetropes.

CHAPTER 9

OCULAR BLOOD FLOW IN EMMETROPES AND MYOPES

9.1 Introduction

Eye preservation depends on a constant supply of nutrient-rich blood. The retinal blood vessels are derived from the central retinal artery and provide blood for the inner layers of the retina. The choroid, iris and ciliary body are fed via the uveal blood vessels. A network of capillaries is located close to the retinal pigment epithelium. These capillaries are known as posterior choriocapillaries and evolve from the short posterior ciliary arteries. The long posterior ciliary arteries in conjunction with the anterior ciliary arteries provide blood to the anterior choriocapillaries. Choroidal blood flow represents 90-95% of the total blood flow to the eye and the remaining 5-10% can be accounted for by the retinal blood flow (Langham *et al.*, 1989). Previous research has shown that approximately 1ml of ocular blood flows per minute (Williamson and Harris, 1994).

9.2 Pulsatile ocular blood flow

Blood flow to the eye comprises two components: a steady continuous component and a pulsatile component, which varies with the cardiac cycle. The pulsatile component is also known as the pulsatile ocular blood flow (POBF). Blood flow increases during the systolic phase and decreases during the diastolic phase of the cardiac cycle (Silver *et al.*, 1989). Each contraction of the heart forces a bolus of blood into the ophthalmic artery which distributes blood across the ciliary and retinal vascular network. The living eye is not a simple elastic chamber and there are no valves to prevent back-flow of blood. The pulsatile component of the inflow to the eye is combined with a second steady and constant component. The flow of the blood out of the eye is assumed to be non-pulsatile (Riva *et al.*, 1985) and comprises 2 components: an outflow equal to the continuous inflow of blood into the eye and an outflow to compensate the average pulsatile component of inflow. The variation in ocular pulse, owing to systolic and diastolic phases, regularly disrupts the equilibrium producing a change in ocular volume. As a result of scleral rigidity and vascular network elasticity an increase in fluid volume induces a slight increase in ocular volume and a concomitant rise in IOP.

Manometric studies on human eyes have shown an increase in IOP to be a function of the increase in intraocular volume (Langham, 1966). However the relationship between IOP and volume for living eyes is non-linear due to changes in ocular rigidity at varying levels of IOP (Eisenlohr *et al.*, 1962). POBF is calculated from the relationship between the change in volume of blood and the ocular pulse. The relationship between volume and IOP is assumed to be linear, for calculation of POBF, owing to only small variations in IOP over a given pulse cycle. In a normal eye, the ocular pulse has an amplitude of 2 to 3 mmHg.

9.2.1 The Ocular Blood Flow Tonograph (OBF tonograph)

The OBF tonograph (OBF Labs, Cleverton, U.K.) is an instrument used to measure ocular blood flow. The instrument is described in more detail in §4.2.10. Langham *et al.* (1989) found the total vascular supply to the eye to be approximately 900 μ l per minute and the pulsatile component represents 590 to 724 μ l per minute for normal subjects. Normal mean POBF values have been recorded in males (669.90 μ l/min.) and females (841.90 μ l/min.) using the OBF tonograph (Yang *et al.*, 1997). The reproducibility of POBF measurements has been reported as satisfactory (Spraul *et al.*, 1998), although, measurements can vary between individual subjects owing to initial IOP level, scleral rigidity, pulse rate, axial length and refractive error. Jain and Marmion (1976) and Quigley and Langham (1975) compared the pneumatonograph with the Goldmann applanation tonometer and found the readings to be equivalent.

9.3 Purpose

James *et al.* (1991) indicated that the ocular pulse was influenced by axial length and Perkins (1981) noted dissimilar ocular pulse measurements between different refractive groups.

The variation in POBF measurements between subjects has been related to axial length and refractive error differences (Kothe *et al.*, 1992 and Price *et al.*, 1999).

The relationship between IOP and axial length and IOP and refractive error have been investigated by a number of researchers, although, the results are ambiguous. Tomlinson and Phillips (1970) found a positive correlation between long axial lengths and high IOP. Abdalla and Hamdi (1970) detected higher IOP values in myopes compared to emmetropes but only in subjects aged 40 years and above and in moderate myopes aged 11 to 20 years. Research on IOP in children indicated a weak correlation

between IOP and high myopia. However, Bengtsson (1972) found no significant difference in IOP between refractive groups and Bonomi *et al.* (1982) found no difference in IOP between a pair of eyes with unilateral high myopia.

The present study investigates the possible variations in POBF, pulse amplitude, pulse volume and IOP in relation to refractive error and axial length, specifically in emmetropes, early- and late-onset myopes.

9.4 Method

Subjects

The cohort consisted of 26 emmetropic subjects and 24 myopic subjects. The myopic group was also sub-divided into early-onset myopes (n = 14) and late-onset myopes (n = 10). The subjects ranged in age between 16 and 26 years and were divided into 23 males and 27 females.

All subjects were examined on the final visit. Both right and left eye were examined (see §4.1). Corrected visual acuity was at least 6/6 in each eye. At the final examination the mean emmetropic subjective refractive error was $+0.26 \pm 0.28\text{D}$ and mean myopic subjective refractive error was $-2.33 \pm 1.58\text{D}$.

Subjective refraction (see § 4.2.1).

The subjective refractive error was found at each visit on all subjects and obtained after instillation of 2 drops of 1% tropicamide HCl (*Minims*[®], Chauvin) with a five minute interval between drops to achieve cycloplegia. A 4m internally illuminated LogMar chart was used to record the visual acuity and refractive error. The subjects were asked to sit in a chair located 4m from the chart whilst trial lenses were placed before their eyes until an end-point was reached. The final refraction was checked using the +1.00D blur test. All refractive error measurements were converted from sphere, cylinder and axis into equivalent mean sphere using a specially designed computer program, written by Dr Mark Dunne in *Quickbasic*. IOP and OBF data can be found in appendix 9.

A-scan ultrasonography (see § 4.2.3.)

The A-scan probe was sterilised with an alcohol wipe (*Medi-swab*[®], Seton Healthcare, England) before use on each subject. One drop of 0.4% benoxinate HCl (*Minims*[®], Chauvin) was instilled to each eye to induce corneal anaesthesia. The subject's pupils were dilated and accommodation was reduced owing to prior instillation of 2 drops of

1% tropicamide HCl. The probe was placed gently onto the cornea of one eye and ten measurements were taken whilst subjects fixated a distant spotlight with the alternate eye. Measurements were taken on both eyes.

OBF Tonograph

The measurements were taken under corneal anaesthesia, using one drop of 0.4% benoxinate HCl (*Minims*[®], Chauvin). The subject's pupils were dilated and accommodation was reduced owing to prior instillation of 2 drops of 1% tropicamide HCl. Calibration was checked routinely using the instrument's own system. A new disposable tip was used for each subject. The OBF probe was mounted on a slit lamp and the subject was positioned and instructed to view a cross at 4m providing vertical and horizontal alignment of the eye. The base control unit was then instructed as to whether the subject was male or female and whether the right or left eye was being examined. On contact with the cornea, the airflow through the probe produces a whistling audio signal. Probe alignment and applanation of the cornea is demonstrated by an audio signal and the regular beat is synchronous with the heartbeat. The audio signal changes after approximately 15 seconds to indicate test completion. If an inadequate number of pulses are taken by the system, an error is registered and the test must be repeated.

9.5 Results

Table 9.1 shows the mean values and standard deviations of refractive error (Rx), axial length (AL), intraocular pressure (IOP), pulse amplitude (PA), pulse volume (PV) and ocular blood flow (OBF) in emmetropes (Emm), late-onset myopes (LOM) and early-onset myopes (EOM). Right eye only.

Table 9.1 Mean and standard deviations for refractive error, axial length, intraocular pressure, pulse amplitude, pulse volume and ocular blood flow measured with the OBF Tonograph.

<i>Parameter</i>	<i>Emm</i>	<i>LOM</i>	<i>EOM</i>
Rx (D)	+0.28 ± 0.26	-0.96 ± 0.33	-3.07 ± 1.47
AL (mm)	23.49 ± 0.52	24.51 ± 0.81	24.95 ± 0.81
IOP (mmHg)	12.53 ± 3.19	13.13 ± 2.30	14.17 ± 4.08
PA (mmHg)	3.62 ± 0.97	2.63 ± 0.83	1.90 ± 0.63
PV (µl)	8.24 ± 2.74	5.96 ± 1.46	4.16 ± 1.48
OBF (µl/min)	1150 ± 254	994 ± 249	766 ± 208

Emm, n = 25; LOM, n = 9 and EOM, n = 14

Variations in pneumatonograph data with refractive error and axial length

Figure 9.1 indicates that no statistically significant correlation was found between IOP and Rx ($r = 0.07$, $p = 0.64$). A similar result was found between IOP and AL ($r = 0.12$, $p = 0.43$).

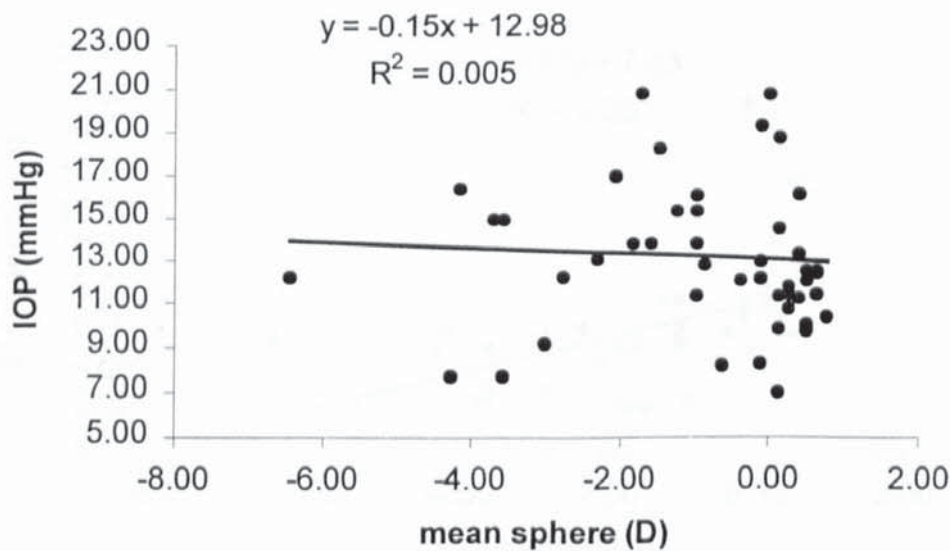


Figure 9.1 Intraocular pressure plotted against refractive error for all right eyes (n = 48).

A positive significant correlation was noted between PA and Rx ($r = 0.56, p < 0.0001$). See figure 9.2. A negative significant correlation was also found between PA and AL ($r = 0.53, p = 0.0001$).

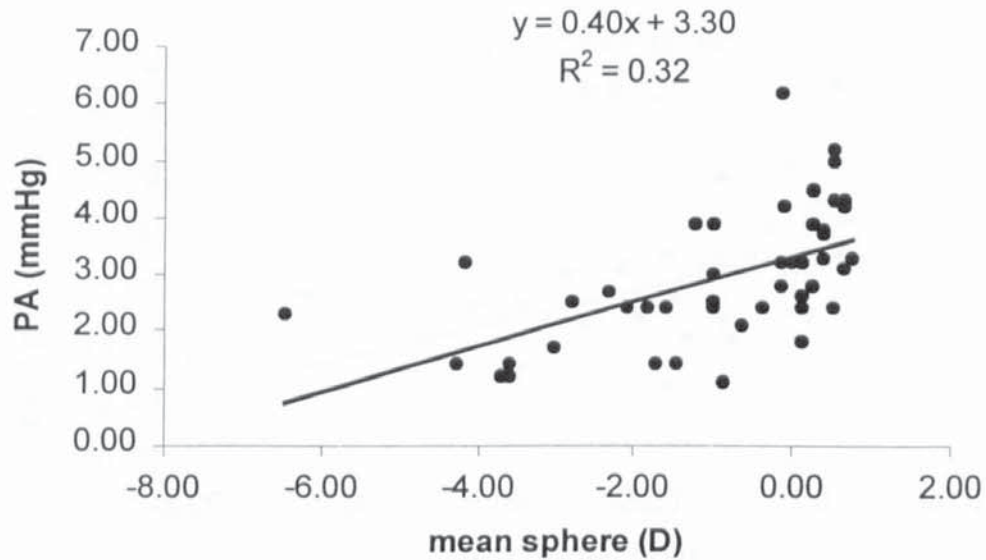


Figure 9.2 Pulse amplitude plotted against refractive error for all right eyes.

A positive significant correlation was found between PV and Rx ($r = 0.50, p = 0.0003$). See figure 9.3. A negative significant correlation demonstrated between PV and AL ($r = 0.49, p = 0.0004$).

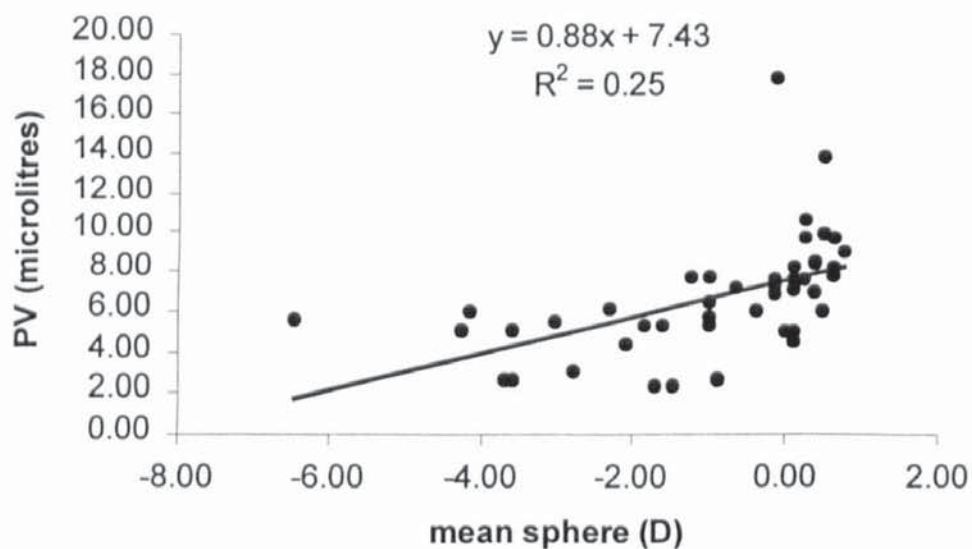


Figure 9.3 Pulse volume plotted against refractive error for all right eyes.

A significant positive correlation was found between OBF and Rx ($r = 0.52$, $p = 0.0002$). See figure 9.4. A negative significant correlation was noted between OBF and AL ($r = 0.54$, $p < 0.0001$).

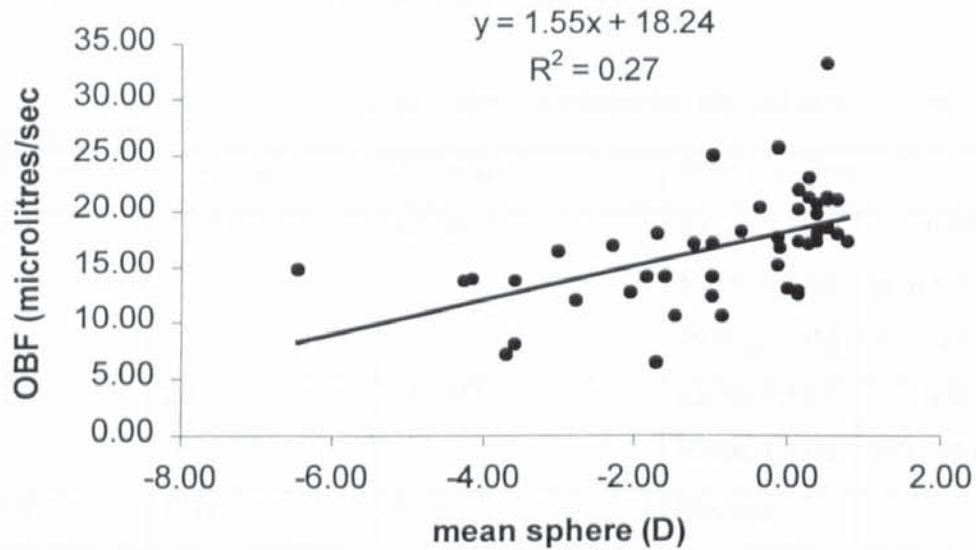


Figure 9.4 Ocular blood flow plotted against refractive error for all right eyes.

Mean pneumatonometer data in emmetropes, late- and early-onset myopes

An ANOVA was used to assess whether the tonography parameter means were significantly different between the three refractive groups. The results are shown in table 9.2. If the means were found to be significantly different, a post hoc test (Scheffé's) was applied for pairwise comparison.

Table 9.2 ANOVA and post hoc results to compare emmetrope, late- and early-onset myopia means for each parameter.

<i>Parameter</i>	<i>F – value</i>	<i>P – value</i>	<i>Post hoc results</i>	
Rx	82.73	<0.0001	Emm, LOM	p = 0.0007
			Emm, EOM	p<0.0001
			EOM, LOM	p<0.0001
AL	22.26	<0.0001	Emm, LOM	p = 0.002
			Emm, EOM	p<0.0001
IOP	1.02	0.37	Not sig	
PA	17.51	<0.0001	Emm, LOM	p = 0.02
			Emm, EOM	p<0.0001
PV	14.12	<0.0001	Emm, LOM	p = 0.05
			Emm, EOM	p<0.0001
OBF	10.74	0.0002	Emm, EOM	p = 0.0002

9.6 Discussion

Intraocular pressure

The mean value of IOP for emmetropes in the study was 12.53 ± 3.19 mmHg and 13.65 ± 3.20 mmHg for myopes (both LOM and EOM groups considered) using the OBF Tonograph. Abdalla and Hamdi (1970) studied IOP measurements, using applanation tonometry, in emmetropes (range $\pm 2D$ sphere) and myopes (range -2 to $-6D$ sphere) within different age groups. Between the ages of 11 to 20 years, the mean emmetrope IOP was 14.05 ± 2.24 mmHg and the mean myope IOP was 15.73 ± 1.92 mmHg. The mean emmetrope IOP decreased to 13.72 ± 2.40 mmHg and myope IOP to 14.53 ± 1.44 mmHg within the age group of 21 to 30 years. Similar result were found by Tomlinson and Phillips (1970) in their study of IOP in undergraduate students aged 18 to 27 years, using Goldmann applanation tonometry. The IOP measurements in the previous and

present studies are comparable, confirming the work of Quigley and Langham (1975) and Esgin *et al.* (1998) who state that IOP measurements obtained by the pneumatonograph are in close agreement to those obtained by Goldmann tonometry.

The present study found no statistically significant correlation between IOP and Rx or IOP and AL. Also, no significant difference in IOP means was found between emmetropes, late- and early-onset myopes when the data was analysed using an ANOVA. The results conflict with those of Tomlinson and Phillips (1970) who found a positive significant correlation between axial length and IOP and Abdalla and Hamdi (1970) who recorded higher IOP in myopes compared to emmetropes, although, statistical significance did vary between age groups. Edwards and Brown (1993) also found higher IOP values in myopic eyes compared to non-myopic eyes (in children). However, Bengtsson (1972), did not detect a significant difference in IOP between refractive groups when the influences of blood pressure, sex, season and time of day were accounted for. All three studies measured IOP with applanation tonometry and included hypermetropic refractive errors. Abdalla and Hamdi and Bengtsson assessed IOP according to various age groups. These differences in methodology may explain the discrepancies in IOP between studies.

High IOP has been indicated as a possible mechanism for myopia development (see §2.4.1). Although the data cannot be extrapolated to IOP values prior to myopia development in these subjects, it is apparent that the values are similar after onset and progression of myopia with those of emmetropes.

Pulse Amplitude

The results show a positive significant correlation between PA and Rx and a negative significant correlation between PA and AL. Statistical analysis using an ANOVA shows that there is a significant difference in the PA means between the Emm and LOM groups and the Emm and EOM groups. No significant difference was noted in the PA means between the LOM and EOM groups. The present study is in agreement with the findings of Perkins (1981); To'mey *et al.* (1981) and Logan (1997), who found the PA to be significantly lower in myopes compared to emmetropes.

Pulse Volume

The present study shows a positive significant correlation between PV and Rx and a negative significant correlation between PV and AL. Indicating that an increasingly

myopic refractive error is related to reduction in PV. Further analysis, using an ANOVA, demonstrates that there is a significant difference in the mean PV between emmetropes and the two myopic groups. The results agree with those of Logan (1997).

Ocular Blood Flow

A significant positive correlation exists between OBF and Rx and a significant negative correlation exists between OBF and AL. Similar results were found by Logan (1997) and Price *et al.* (1999). Yang *et al.* (1997) reported normal mean OBF values of 669.90 μ l/min in males and 841.90 μ l/min in females. Massey and O'Brien (1996) found a mean OBF value of 808 \pm 344 μ l/min and Ravalico *et al.* (1996) measured a mean OBF value of 819 \pm 212 μ l/min when studying 15 emmetropic subjects aged 10 to 20 years. A lower mean OBF value of 444 \pm 20 μ l/min [SEM] was reported by James *et al.* (1991) in their study of 34 subjects with a mean refractive error of -1.15 ± 0.28 D [SEM]. The mean OBF measurement for emmetropes, in the present study, is 1150 \pm 254 μ l/min and 880 \pm 228 μ l/min for myopes. A significant difference was noted in the OBF means between the Emm and EOM groups. No significant difference in the means was found between the Emm and LOM groups or the LOM and EOM groups. It is conceivable that the difference in mean OBF is a result of higher myopic refractive errors in the EOM group compared to the LOM, rather than an underlying difference in blood flow structure.

The highest mean values of PA, PV and OBF can be found in the Emm group followed by the LOM and then EOM groups. There is no significant difference in mean values of PA and PV in the LOM and EOM groups; yet, there is a significant difference in Rx. The results indicate that these two groups of myopes have similar PA and PV contributions that differ from that of the emmetropes. Once again, it is difficult to state whether the difference in the mean value of OBF between the LOM and EOM groups demonstrates a true distinction between the groups regarding blood flow in the eye, or if it is merely a result of higher refractive errors being present in the EOM group compared to the LOM. The theory could be examined further by matching the mean refractive error between the two groups and assessing the PA, PV and OBF means once again. Unfortunately, this was not possible in the current data set owing to low subject numbers.

9.7 Summary

- Mean IOP for emmetropes was 12.53 ± 3.19 mmHg and 13.65 ± 3.20 mmHg for myopes
- No significant correlation was found between IOP and Rx or IOP and AL.
- No significant difference in mean IOP was found between the Emm, LOM and EOM groups
- Positive significant correlations were found between PA and Rx, PV and Rx and OBF and Rx.
- Negative significant correlations were found between PA and AL, PV and AL and OBF and AL.
- A significant difference was found in PA means between the Emm and LOM groups and Emm and EOM groups
- A significant difference is apparent in PV means between the Emm and LOM groups and the Emm and EOM groups
- A significant difference was noted in the OBF means between the Emm and EOM groups.
- The highest mean values of PA, PV and OBF were found in the Emm group followed by the LOM group and then the EOM group.

Future work

Ocular volume. Calculations derived by Dr Nicola Logan. See appendix 12 for examples of emmetrope and myope ocular volumes.

CHAPTER 10

CRYSTALLINE LENS ASSESSMENT IN EMMETROPIA AND MYOPIA USING THE SCHEIMPFLUG CAMERA

10.1 Introduction

Analysis of the anterior segment of the eye can be facilitated by applying the Scheimpflug Principle. A focused, cross-sectional image of the anterior segment can be produced using a camera and slit-beam. The image of the crystalline lens permits examination of the lens radii of curvature in the sagittal plane.

The Scheimpflug Principle was derived by Theodor Scheimpflug, born in 1865 (Mayer, 1994). The first Scheimpflug camera consisted of a central camera surrounded by 7 fixed cameras all at angles of 45°. The film plane of each camera is positioned perpendicular to the optical axis of the objective to obtain focus throughout the image and this construction is known as the Scheimpflug Principle. The camera was used to produce accurate scale photomaps of land contours.

Scheimpflug cameras were introduced commercially in the late 1970s and have become valuable and effective tools in lens and cataract research. The Scheimpflug images can be used to examine cataracts (Qian *et al.*, 1997 and Goder and Huebscher, 1991), the anterior chamber (Boker *et al.*, 1995), lens thickness and volume (Kehrhahn and Olbert, 1992), biometry of the anterior segment (Olbert, 1995) and accommodation of the lens (Brown, 1973 and Brown, 1974).

10.2 The Scheimpflug Principle

It is known from paraxial optics that if the object plane is perpendicular to the optical axis, then the image produced is formed on the image plane (also perpendicular to the optical axis). However, if the object plane is tilted, with respect to the optical axis, and the image plane is perpendicular to the optical axis, the resulting image will not be focused and the degree of defocus will vary along the image plane. Tilting the image plane can focus the image and the amount of tilt is determined by the Scheimpflug Principle. If the lens plane, object plane and image plane are co-incident the image will be in focus along the entire image plane (see §4.2.9). Figure 10.1 demonstrates the Scheimpflug Principle. One important point to note is that although the image is in focus along the image plane, the magnification is not constant owing to different

locations of the plane being at different distance from the lens. Figure 10.2 shows an example of an image obtained using the Scheimpflug camera.

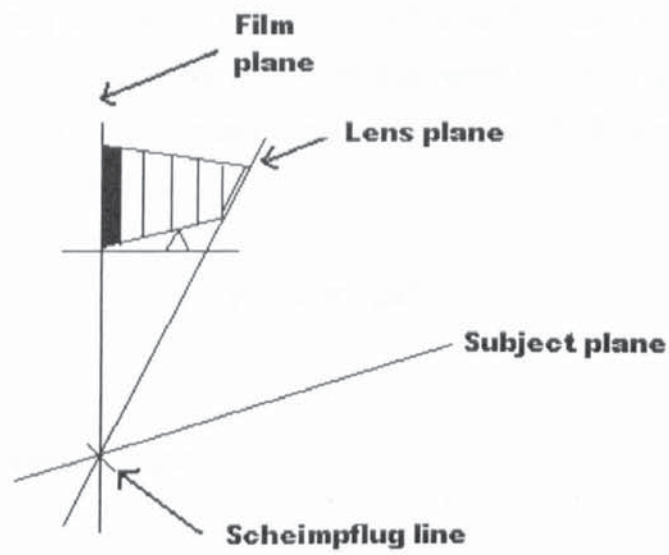


Figure 10.1 The Scheimpflug Principle

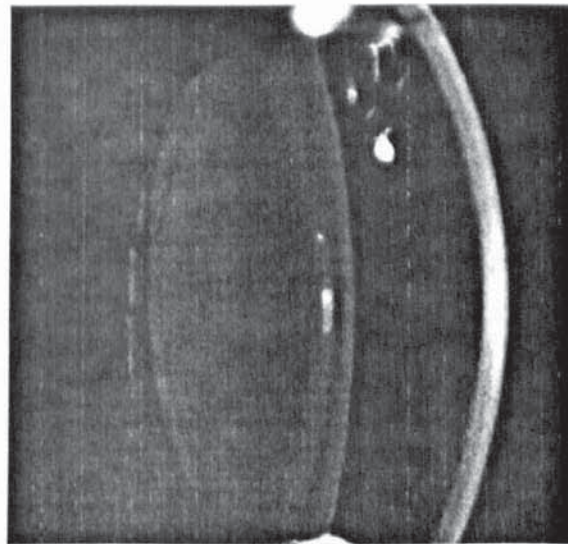


Figure 10.2 Image obtained using the Scheimpflug camera (after Harper, 1999).

10.3 Derivation of lens surface curvature

X and Y co-ordinates of the crystalline lens were estimated from images obtained from the Scheimpflug camera. The images were pasted into a custom computer program called *Extract* (written by Daniel Harris, Aston University, 1997), devised to locate points on a graph or image. Sets of co-ordinates were found for the front and rear crystalline lens surfaces. The lens surfaces are aspheric, so the following equation was used to describe a conic constant,

$$y^2 = 2r_0x - \rho x^2$$

Where,

r_0 = radius of curvature at the apex

ρ = asphericity.

This same equation has been used to determine the asphericity of the cornea and retina (see §6.4 and §7.2).

The laws of optical image formation state that 'when refraction or reflection takes place at two or more surfaces in succession, the image formed at the first, whatever its nature, becomes the object for the next' (Bennett and Rabbetts, 1989). The Scheimpflug image of the lens produces *apparent* lens curvatures and depths owing to refraction of light at the various optical surfaces and through optical media. Therefore, when the lens curvatures are assessed, the surfaces, depths and refractive indices prior to the one under examination must be taken into consideration. To assess the *real* curvature of the anterior lens surface, calculation of the corneal depth, *real* posterior corneal surface and *real* anterior chamber depth would be required (assuming the refractive indices). If the lens surfaces were spherical, step-along ray-tracing techniques would make this task feasible. However, owing to the aspheric nature of the lens surfaces the task is no longer simple and the calculation of the *real* posterior lens surface would be extremely difficult and tedious. The images also suffer from distortion owing to light absorption along the optical pathway (Huebscher *et al.*, 1999). The conversion of the anterior chamber depth from *apparent* to *real* was attempted by a final year optometry student (Leon Davies, Wellcome Vacation Scholarship. Unpublished report), although the results were inconsistent with those obtained by A-scan ultrasound. For this reason, ultrasound readings are used for anterior chamber depths and lens thickness and the lens

curvatures described in this chapter are *apparent* and are used merely for comparison between the emmetropic and myopia groups.

10.4 Purpose

The dioptric power of the lens decreases rapidly in childhood from approximately 23D at 3 years of age to 20D by the age of 14 (Sorsby *et al.*, 1961). In their study of the lens in 6 to 14 year olds, Zadnik *et al.* (1995) found the lens to thin between the ages of 6 to 10 years and then remain constant to 14 years of age. Similarly, McBrien and Millodot (1987a) noted thinner lenses in myopes compared to emmetropes in their biometric investigation of late-onset myopic eyes.

Calculation of vergence powers in emmetropes and myopes revealed a weaker vergence contribution from the anterior chamber depth and equivalent lens power in myopes compared to emmetropes (see Chapter 7). The purpose of this chapter is to evaluate lens curvatures and lens thickness, in order to help determine the origin of the difference in equivalent lens power between emmetropes and myopes.

10.5 Method

Subjects

The cohort consisted of 26 emmetropic subjects and 24 myopic subjects. The myopic group was also sub-divided into early-onset myopes (n = 13) and late-onset myopes (n = 10) and the emmetropic group was sub-divided into stable emmetropes (n = 21) and emmetropes that progressed into late-onset myopia (n = 4). The subjects ranged in age between 16 and 26 years and were divided into 23 males and 27 females.

Thirty-five subjects were examined on 3 occasions over a 2-year period and the remainder were examined on 3 occasions over an 18-month to 2-year period. Both right and left eye were examined (see §4.1). Corrected visual acuity was at least 6/6 in each eye. At the initial examination the mean emmetropic subjective refractive error was $+0.24 \pm 0.24$ D and mean myopic subjective refractive error was -2.08 ± 1.57 D.

Subjective refraction (see § 4.2.1).

The subjective refractive error was found at each visit on all subjects and obtained after instillation of 2 drops of 1% tropicamide HCl (*Minims*[®], Chauvin) with a five minute interval between drops to achieve cycloplegia. A 4m LogMar chart was used to record visual acuity and refractive error. The subjects were asked to sit in a chair located 4m

from the chart whilst trial lenses were placed before their eyes until an end-point was reached. The final refraction was checked using the +1.00D blur test. All refractive error measurements were converted from sphere, cylinder and axis into equivalent mean sphere using a specially designed computer program, written by Dr Mark Dunne in *Quickbasic*. Lens data can be found in appendix 10.

A-scan ultrasonography (see § 4.2.3)

The A-scan probe was sterilised with an alcohol wipe (*Medi-swab*, Seton Healthcare, England) before use on each subject. One drop of 0.4% benoxinate HCl (*Minims*[®], Chauvin) was instilled into each eye to induce corneal anaesthesia. The subject's pupils were dilated and accommodation was reduced owing to prior instillation of 2 drops of 1% tropicamide HCl. The probe was placed gently onto the cornea of one eye and ten measurements were taken while subjects fixated a distant spotlight with the alternate eye. Measurements were taken on both eyes in all subjects at all three visits.

Scheimpflug videography

Prior instillation of 2 drops of 1% tropicamide HCl induced mydriasis and reduced accommodation. Pupil dilation was required to enable full examination of both the anterior and posterior lens surfaces. The Marcher CASE-S Scheimpflug camera was used to take 5 images of the anterior segment in each eye. The subject was positioned comfortably in front of the camera and told to fixate the relevant flashing fixation light (red for right eye and green for left eye). The fixation target for each eye is positioned to the nasal side which allows the slit beam to pass along the optic axis of the eye. The camera was adjusted, using a joystick, to align the cross-hairs on the anterior lens surface and to position them at the apex of the lens surface curve.

The gain on the computer analysis system was set for 4.09 for both view and capture. This value was chosen as it supplied adequate amplification to the video signal without impairing the image. The reflected light from the cornea stimulates phototransistors, placed above and below the slit-beam aperture. The alignment indicator changing from red to green indicated perpendicular alignment of the slit-beam with the corneal apex. Once alignment was achieved the capture peddle was pressed and the image frozen.

10.6 Results

10.6.1 Validity and repeatability

The validity and repeatability values for the parameters measured are shown in tables 10.1 and 10.2. The validity results for ultrasound measurements can be found in §5.5.1.

Table 10.1 Values of validity for lens curvature calculations

<i>Measurement</i>	<i>Validity</i>
Lens asphericity ρ	± 0.01 mm (n = 50)
Lens apical radius r_0	± 0.08 mm (n = 50)

Table 10.2 Values of repeatability for lens curvature calculations

<i>Measurement</i>	<i>Bias</i>	<i>Standard deviation</i>	<i>95% Limits of Agreement</i>
Lens asphericity ρ	0.00	0.05	-0.09 to 0.09
Lens apical radius r_0	0.30	1.67	-2.98 to 3.58

10.6.2 Lens surface shape

No significant correlation was found between refractive error and the anterior lens surface asphericity ($r = 0.04$, $p = 0.80$) using data from the right eye only (see figure 10.3). No significant correlation was noted between the refractive error and the posterior lens asphericity either ($r = 0.004$, $p = 0.99$).

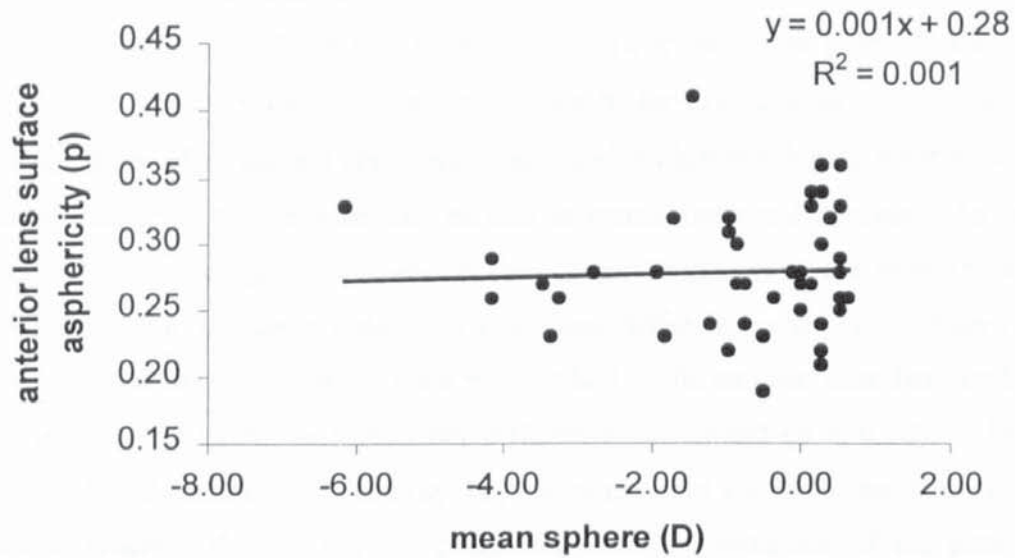


Figure 10.3 Refractive error plotted against asphericity for the anterior lens surface. Right eye only (n = 48).

Figure 10.4 shows the relationship between refractive error and the apical radius for the anterior lens surface.

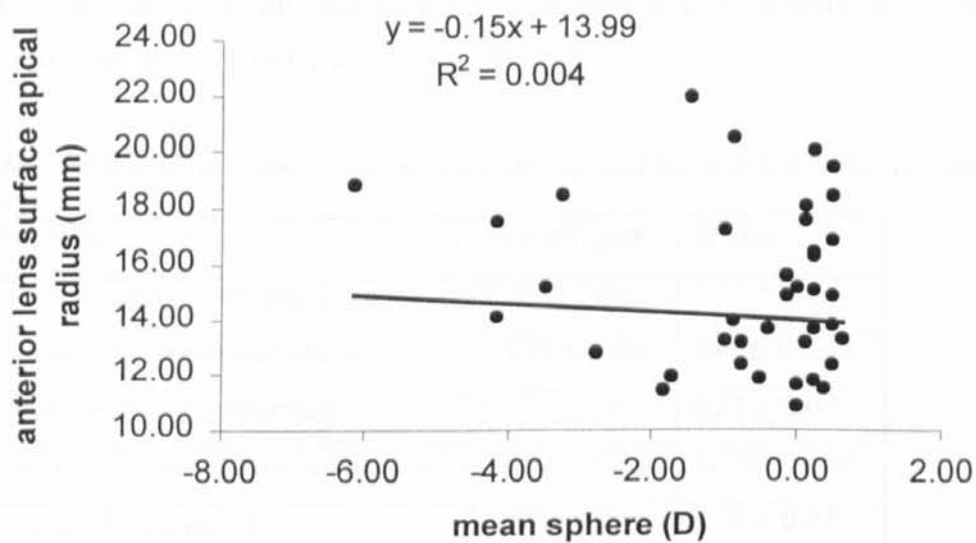


Figure 10.4 Refractive error plotted against apical radius for the anterior lens surface. Right eye only (n = 48).

A weak and insignificant negative correlation was found between refractive error and apical radius for the anterior lens surface ($r = 0.06$, $p = 0.65$) and posterior lens surface ($r = 0.04$, $p = 0.74$).

Lens shape in myopes and emmetropes

As mentioned previously, in §10.3, when the lens curvatures are assessed, the surfaces, depths and refractive indices prior to the one under examination must be taken into consideration. The corneal curvatures and anterior chamber depths must be evaluated before comparing the anterior lens surface in emmetropes and myopes. An unpaired student's *t test* was applied to compare the corneal curvatures of the emmetropes to the corneal curvatures of the myopes. No significant difference was noted between the two groups ($p = 0.78$). Similarly, a *t test* was applied to the anterior chamber depths in the two groups and again no significant difference was found ($p = 0.20$). The *t tests* indicate that the emmetropes and myopes examined have similar corneal curvatures and anterior chamber depths, thereby, permitting further comparison of the anterior lens surfaces. However, the *t test* shows a significant difference in lens thickness between emmetropes and myopes ($p = 0.03$), thereby, restricting further examination of the posterior lens surface and comparison between groups. Anterior chamber depth and lens thickness measurements were taken using the A-scan ultrasound.

Table 10.3 displays the lens parameter information and standard deviations in both emmetropes ($n = 25$) and myopes ($n = 23$).

Table 10.3 Anterior and posterior lens surface parameters and lens thickness (\pm S.D.) in emmetropes and myopes.

<i>Parameter</i>	<i>Emmetropes</i>	<i>Myopes</i>
Anterior surface asphericity, ρ	0.29 ± 0.04	0.27 ± 0.04
Anterior surface apical radius (mm)	13.89 ± 4.05	14.56 ± 3.55
Posterior surface asphericity, ρ	0.21 ± 0.04	0.21 ± 0.04
Posterior surface apical radius (mm)	10.02 ± 2.85	11.23 ± 3.59
Lens thickness (mm)	3.68 ± 0.22	3.54 ± 0.21

No significant differences were found for lens parameters, between emmetropes and myopes, using a student's unpaired *t test*, except for lens thickness. Myopes and emmetropes have a similar lens shape but myopes have a significantly thinner lens than emmetropes.

Lens shape during onset and progression of myopia

The mean shift in refractive error towards myopia in the late-onset myope group was $0.40 \pm 0.09D$ and in the early-onset group $0.38 \pm 0.09D$. Table 10.4 shows the lens parameters for the progressive late-onset myopes (including the emmetropes that progressed towards myopia) and the progressive early-onset myopes, over the study period. Right eyes only were assessed.

Table 10.4 Change in anterior and posterior lens surface parameters and lens thickness (\pm S.D.) in progressive late-onset (LOM prog) and progressive early-onset (EOM prog) myopes. Right eyes only (LOM prog $n = 7$ and EOM prog $n = 8$).

Parameter	LOM prog		EOM prog	
	Visit 1	Visit 3	Visit 1	Visit 3
Anterior surface ρ	0.27 ± 0.05	0.28 ± 0.04	0.29 ± 0.03	0.25 ± 0.04
Anterior surface r (mm)	12.89 ± 3.75	15.22 ± 1.22	14.93 ± 4.57	14.57 ± 2.30
Posterior surface ρ	0.19 ± 0.04	0.18 ± 0.05	0.23 ± 0.04	0.21 ± 0.07
Posterior surface r (mm)	9.44 ± 2.40	8.40 ± 2.05	11.95 ± 3.30	9.53 ± 3.57
Lens thickness (mm)	3.56 ± 0.14	3.60 ± 0.15	3.54 ± 0.18	3.51 ± 0.18

ρ = asphericity; r = apical radius.

The lens parameters were compared, between visit 1 and visit 3 for the LOM prog group, using a student's paired *t test*. No significant difference was found between the means for any parameter over the study period. Analysis was repeated on the EOM prog group. The only parameter to show a significant change over the study period was the anterior lens surface asphericity value, ρ . The ρ value reduced as the myopia increased which indicates a flattening of the conic curve in the periphery. Although no change was evident in lens thickness, the lens appeared to thin over time in the EOM prog group and thicken in the LOM prog group.

10.7 Discussion

Emsley (1936) combined values from two Gullstrand schematic eyes with his own values to present a new version of the three-surfaced schematic eye. The model eye was termed the Gullstrand – Emsley eye and assumed the anterior radius of the crystalline lens, in its relaxed state, to be 10mm and the posterior radius to be 6mm. The eye parameters were based on only a small number of experimental determinations, so new values were proposed for the lens. In a relaxed schematic eye, 11mm is assumed for the

anterior lens radius and 6.5mm for the posterior lens radius. Dubbelman and vanderHeijde (2000) corrected the Scheimpflug images using a ray-tracing technique and found the anterior lens surface radius to be 12.3mm and the posterior surface radius to be 6.1mm in subjects aged 16 years. Unfortunately, the refractive errors of the 102 subjects examined are unknown. The mean anterior lens surface apical radius, in the present study, was found to be 13.89 ± 4.05 mm in emmetropic subjects and 14.56 ± 3.55 mm in myopic subjects. The mean posterior apical radius was 10.02 ± 2.85 mm in emmetropes and 11.23 ± 3.59 mm in myopes. The radii appear to be much flatter than those found by Dubbelman and vanderHeijde, however, the radii are apparent in the present study and not real.

It is apparent from the present data that no significant correlation exists between refractive error and lens asphericity for either the anterior or posterior lens surfaces. Similarly, no significant correlation was noted between refractive error and lens apical radius for either the anterior or posterior surface. This suggests that lens surface shape and radius, both anterior and posterior, remains almost constant with an increasingly myopic refractive error.

Lens shape in emmetropes and myopes

A direct comparison of mean anterior and posterior lens surface asphericity in myopes and emmetropes revealed similar values in the two groups. The values of mean anterior and posterior lens apical radii were also alike between the two groups. Although lens shape appears to be similar in emmetropes and myopes, the data indicates that there is a significant difference in mean lens thickness. Myopes have thinner lenses than emmetropes. Ocular component analysis in emmetropes and myopes establishes that the myopic group has a weaker anterior segment, and specifically a weaker equivalent lens power, compared to the emmetropic group (See chapter 7). It is unlikely that there is a difference in the refractive index of the lens between the two groups, therefore, the findings suggest that myopes have a weaker lens power than emmetropes as a result of a thinner lens rather than a significant difference in lens shape.

Zadnik *et al.* (1995) and Mutti *et al.* (2000) found the crystalline lens to thin during childhood, specifically between the ages of 6 to 10 years. Prior to the age of 10 years, the lens curvature flattens, the equivalent refractive index decreases and the lens thins

resulting in a reduction in the equivalent power of the lens. During the rapid growth phase of the eye, there is an increase in the equatorial diameter of the globe which, in turn, increases the equatorial diameter of the lens and reduces the thickness. The reduction in lens power in early childhood permits the eye to remain emmetropic as the axial length increases. If axial length increases beyond that at which the optics of the eye can compensate, myopia occurs. After the age of 10 years, the lens refractive index begins to increase and the lens stops thinning so that the equivalent lens power remains constant. It has been seen in both children developing myopia (Zadnik *et al.*, 1995) and in adults developing myopia (McBrien and Millodot, 1987a) that the lens is thinner in myopes compared to emmetropes and the enlargement of the globe is responsible for this thinning of the lens.

Lens shape during onset and progression of myopia

No significant differences were found in lens shape, over the 18-month to 2-year study period, in the progressive late-onset myopia group. The lens thickness did increase, although, the change was not substantial. The only parameter to show a significant change over the study period in the progressive early-onset myopia group was the anterior lens surface asphericity, ρ . As myopia increased, the anterior ρ value decreased indicating a flattening of the conic curve in the periphery. Lens thickness decreased over time, in this group, but the change was not deemed significant. Ocular component analysis demonstrated an increase in equivalent lens power, in the progressive late-onset myopes, over the longitudinal study period (see chapter 7). This may be related to an increase in lens thickness. Component analysis shows a reduction in equivalent lens power in the progressive early-onset myopia group. The decrease in lens thickness, in conjunction with peripheral flattening of the anterior lens surface, might explain the reduction in lens power over time and with myopia increase. Lens thinning and flattening are likely to be consequences of myopia increase in the progressive early-onset myopia group, rather than a factor inducing myopia. The retinal contour in the progressive early-onset group shows an overall expansion of the globe with myopia increase, although, the axial length increases at a greater rate than axial distance in the periphery.

10.8 Summary

- The apparent mean anterior lens radii are flatter than the apparent mean posterior lens radii for both emmetropes and myopes
- The apparent lens radii are flatter than the real lens radii measured by Dubbelman and vanderHeijde (2000)
- Lens surface shape and radius, both anterior and posterior, remain constant with an increasingly myopic refractive error.
- Lens surface asphericity is similar in emmetropes and myopes
- Lens surface apical radii are similar in emmetropes and myopes
- Myopes have a weaker equivalent lens power and a thinner lens compared to emmetropes.
- Progressing early-onset myopes show a reduction in equivalent lens power owing to lens flattening and thinning. The equatorial diameter of the lens increases as the globe expands both axially and equatorially.
- Progressing late-onset myopia is related to an increase in lens thickness

CHAPTER 11

GENERAL DISCUSSION

The aim of this thesis was to investigate the ocular biometric correlates associated with myopia, specifically late-onset myopia, and to examine how these biometric correlates could be used as predictive indices for myopia onset and progression. There are a vast number of research studies and articles dedicated to myopia, which encompass many different aspects of the refractive condition. A high proportion of these studies has focused specifically on youth-onset myopia and its development and progression. This data set compiled is the first of its kind and has generated valuable information on ocular biometric changes and predictive factors associated with myopia onset and development in young adults. Statistical analysis of the data has produced interesting results in areas of myopia not yet fully investigated. The study incorporates both anterior and posterior segment biometric measurements in addition to a relatively new procedure, retinal contour. The computation of retinal contour provides a means of assessing retinal shape change and stretch during myopia onset and progression. The central feature of this thesis is the examination of interactions between various parameters, including retinal contour, in both early- and late-onset myope groups.

11.1 Classification of myopia

Myopia has been classified in many ways, yet, probably the most simple and widely adopted system has been proposed by Grosvenor (1987). Grosvenor examined myopia prevalence in British and North American populations and derived classification categories according to the age at which myopia first presents. The most common form of myopia is early-onset myopia (also known as youth-onset myopia) which presents around 6 years of age and persists throughout the teenage years and then stops. Approximately 25% of Western populations exhibit myopia by the late teens. Late-onset myopia (described by Grosvenor as early adult-onset myopia) generally occurs following physical maturity and between the ages of 20 to 40 years of age. Myopia prevalence peaks to approximately 30% in Western populations between 18 to 40 years of age. The myopia classification system, introduced by Grosvenor, was adopted for the thesis. However, Goss and Winkler (1983) found that the average age of cessation of myopia progression was 15.25 years in females and 16.66 years in males, which

corresponds with the approximate ages for the end of the adolescent growth spurt. This suggests that myopia onset after this date could be classified as late-onset myopia. Consequently, the age range for late-onset myopia classification was adjusted for the study to allow for the inclusion of undergraduate students (age range 16 to 26 years).

At the initial visit the subjects were divided into two refractive groups: emmetropes and myopes. Defining the range of refractive error, that constitutes myopia, is important in myopia onset and progression studies and varies between investigators. For this study, emmetropes were defined as subjects with a spherical equivalent refractive error of -0.24 to $+0.50$ D. Myopes were defined as subjects with a spherical equivalent refractive error of -0.25 D or greater. The change in refractive error that constitutes a myopic shift is also often difficult to define. For this project, a change in spherical refractive error of -0.25 D or greater was designated as a myopic shift in refractive error. A refractive error change of this degree is small but was considered appropriate owing to the relatively short period of study. The myopes were subdivided into early- and late-onset myopes according to the age at which myopia presented. The subjects were deemed early-onset myopes if myopia onset was prior to 16 years of age and late-onset myopes if myopia onset was after 16 years of age. The subjects were examined three times over the 18-month to 2-year period to assess the ocular biometric changes associated with onset and progression of myopia.

11.2 Predictive factors for myopia onset and progression

Ratio of axial length to corneal curvature

The thesis has shown that a myopic eye has a higher ratio of axial length to corneal curvature (al/k) compared to emmetropes and that onset and progression of myopia, in adults aged 16 to 26, is strongly correlated with an increase in al/k . Grosvenor (1988) and Grosvenor and Scott (1994) measured the mean al/k ratio in Melanesian and British school children aged 6 to 19 years. He proposed that an eye having a high al/k ratio was at risk of developing myopia. Grosvenor also suggests that an eye with a high al/k would have a low powered lens as a result of lens power reduction during emmetropization. The results of the thesis are in agreement with those of Grosvenor, in that, myopic eyes have higher al/k ratios and thinner lenses compared to emmetropic eyes. The ratio of al/k has a strong relationship with the final state of refractive error (maximum myopia), in the multiple stepwise regression analysis, and has been shown to be an adequate predictive index for myopia onset and progression. Subjects with a high

initial al/k ratio had a greater myopic shift in refractive error compared to the subjects with a low initial al/k ratio. Goss and Jackson (1993) found similar results in their study of ocular components in school children.

Retinal shape

Changes in retinal asphericity, apical retinal radius and relative peripheral refractive error (PRE) also appear to be related to a shift in myopia and with further investigation could be used as predictive indicators. Posterior segment elongation in conjunction with retinal apical steepening and peripheral retinal flattening describes a prolate shaped retina. Early changes in these factors, in association with a shift towards a more relative hyperopic PRE, could be used to predict onset and progression of myopia. Future work would involve the application of predictive indices for myopia development in children. Assessment of the retinal shape, the relative PRE and the al/k ratio could be further investigated as risk factors and developed to provide a method to determine myopia onset in children and young adults.

11.3 Cross-sectional analysis of biometric correlates in emmetropia and myopia

Cornea

Myopia develops because either the optical power of the eye is abnormally great or the eye is abnormally long. A number of investigators have found corneal curvature to be steeper and corneal power to be greater in myopes compared to emmetropes (Sorsby *et al.*, 1957; Curtin, 1985; Grosvenor and Scott, 1991; Grosvenor and Scott, 1993 and Goss *et al.*, 1997). Data analysis from the thesis indicates that myopes have slightly steeper corneae compared to emmetropes. However, the means of both corneal curvature and corneal shape factor were compared between emmetropes and myopes and found to be insignificant. The results indicate that emmetropes and myopes, aged 16 to 26 years, have similar corneal radii of curvature and a myopic eye is likely to be related to a long axial length. Yet, the data also shows that the cornea steepens with an increasingly myopic refractive error, demonstrating that advancing myopia is linked to both corneal curvature and axial length.

Anterior chamber

The findings of the thesis suggest that myopes have deeper anterior chamber depths compared with emmetropes and an increasingly myopic refractive error is weakly correlated with a deeper anterior chamber. The data also shows myopes to have thinner crystalline lenses compared to emmetropes, but similar values regarding lens surface radii and asphericity. Ocular component analysis demonstrates that myopes have a weaker anterior segment vergence power compared to emmetropes. The difference in anterior segment vergence power between the two groups is likely to be a result of the thinner lens, and corresponding lower lens power, found in myopes. Sheridan (1955) used phakometry to measure anterior lens surface radii in a comparison study of ocular parameters in emmetropes and myopes. In this thesis, lens thickness was measured using the A-scan ultrasound and the Scheimpflug camera was used to capture cross-sectional images of the lens. Further manipulation of these images provided valuable information regarding the lens radii of curvature and lens surface shape. This novel approach to lens assessment permits the examination of both the anterior and posterior lens surfaces.

Axial length

Erickson (1991) showed that the amount of myopic refractive error was directly related to an axial length, or more specifically, to an increase in the vitreous chamber depth. A number of comparison studies have shown that myopes have a greater axial length, or vitreous chamber depth, compared to emmetropes (Curtin, 1985; McBrien and Adams, 1997 and Sorsby *et al*, 1962). The results from the thesis are in agreement with these investigators. The data also exhibits a strong negative correlation between refractive error and axial length (and vitreous chamber depth) indicating that an increasingly myopic refractive error is related to a longer eye. Component vergence analysis, from the thesis, shows that the longer vitreous chamber depth in myopes is associated with a weak posterior segment vergence power. It may be assumed that a weak anterior segment power would compensate for a weak posterior segment power (elongated vitreous depth), thereby, producing an emmetropic eye. However, the data shows that the vitreous depth is longer than that for which that anterior segment can compensate, generating a myopic eye.

Scleral stretch

The ocular biometric correlates of myopia found in this thesis are similar to those found by other investigators and agrees with the theory of lens thinning in myopes (Mutti *et al*, 2000 and Zadnik *et al*, 1995) and the theory of emmetropization and ametropia proposed by van Alphen (1961) and van Alphen (1986). Mutti *et al*. (2000) propose that expansion of the globe in childhood produces a thinner and flatter lens in order to maintain emmetropia in the growing eye. In later childhood, the equatorial expansion is restricted by the orbit, which promotes expansion in the axial plane, resulting in myopia.

In van Alphen's detailed analysis of component values of refraction, using data derived from Stenström (1946), he concluded that three independent factors could provide all correlations between the optical elements. The *size* factor, which has loadings in corneal curvature and axial length (longer eyes have flatter corneae); the *stretch* factor, which has loadings in axial length, anterior chamber depth and lens thickness and the *derailment* factor, which has loadings in all variables. The *stretch* factor was found to be important when determining refractive error. It has been confirmed that an increase in axial length is accompanied by a thinning and stretching of the posterior sclera (Curtin, 1985 and Duke-Elder, 1949). Van Alphen hypothesised that the ciliary muscle-choroid layer acted like an elastic coat of smooth muscle around the eye. The tone of the ciliary muscle regulates the resistance of the ciliary-choroid capsule. Intraocular pressure (IOP) stretches the sclera in the growing eye producing a longer eye with a flatter cornea. However, the effect of IOP upon the sclera is resisted and counteracted by the ciliary-choroid layer, which is associated with the *derailment* factor. The ciliary muscle-choroid layer stretches, displacing the iris-lens diaphragm posteriorly, resulting in deeper anterior chambers and thinner lenses in larger eyes. Van Alphen stated that emmetropization was dependent upon the autonomic nervous system's control of the ciliary muscle-choroid layer and that ametropia was produced when factors interfered with this emmetropization mechanism, e.g. myopia is produced as a result of parasympathetic underactivity or excess sympathetic activity during ocular growth. Evidence suggests that the autonomic nervous system plays an important role in emmetropization and in the onset of early- and late-onset myopia, although, the strong genetic link associated with myopia cannot be ignored (Gilmartin, 1986).

Conclusions

The results from the thesis demonstrate that myopic eyes have deeper vitreous chambers, deeper anterior chambers and thinner crystalline lenses. Myopic eyes also present with a relative hyperopic peripheral refractive error (PRE) and emmetropic eyes present with a relative myopic PRE. The findings indicate that myopic subjects have a prolate retinal shape, which becomes more prolate with increasing amounts of myopia. A prolate shaped retina demonstrates that longitudinal, rather than transverse, stretching of the posterior segment is the principle structural correlate of myopia and corresponds with the findings of van Alphen, Mutti *et al.* and Logan (1997).

11.4 Cross-sectional analysis of biometric correlates in early- and late-onset myopia

Statistical analysis of the data from the present study found no significant difference in mean corneal curvature, mean anterior chamber depth or mean lens thickness between late-onset myopes (LOM) and early-onset myopes (EOM). Similar results were found by Bullimore *et al.* (1992) in their investigation of steady-state accommodation and ocular biometry in late-onset myopia. The vitreous chamber depth is longer in the EOM group compared to the LOM group; yet, the difference in mean values is not statistically significant. However, there is a significant difference in mean refractive error between the two groups with the EOM group presenting with a higher refractive error. The longer vitreous chamber depth must account for this difference, albeit not statistically different from the LOM group, and corresponding weaker posterior segment vergence power found in the EOM group.

High percentages of the EOM group and the LOM group show relative hyperopic PRE. The EOM group also present with greater dioptric values of relative hyperopic PRE, which, in conjunction with a longer vitreous chamber depth and steeper retinal apical radius denotes a more prolate shaped retinal contour compared to the LOM group. Figure 11.1 illustrates the retinal contours in the myopia-progressing LOM and EOM groups (also figure 7.6 from chapter 7). It is apparent from the retinal contours that, even prior to myopia progression, the EOM group has a slightly longer axial length and a more prolate shaped retina compared to the LOM group. This is to be expected owing to the greater myopic refractive error in the EOM group. These findings verify, once again, that myopia onset and progression is related to posterior segment elongation with

minimal effect in the transverse plane and the effects are intensified according to the age of myopia onset, i.e. early-onset myopes have a greater vitreous chamber depth and more prolate shaped retina.

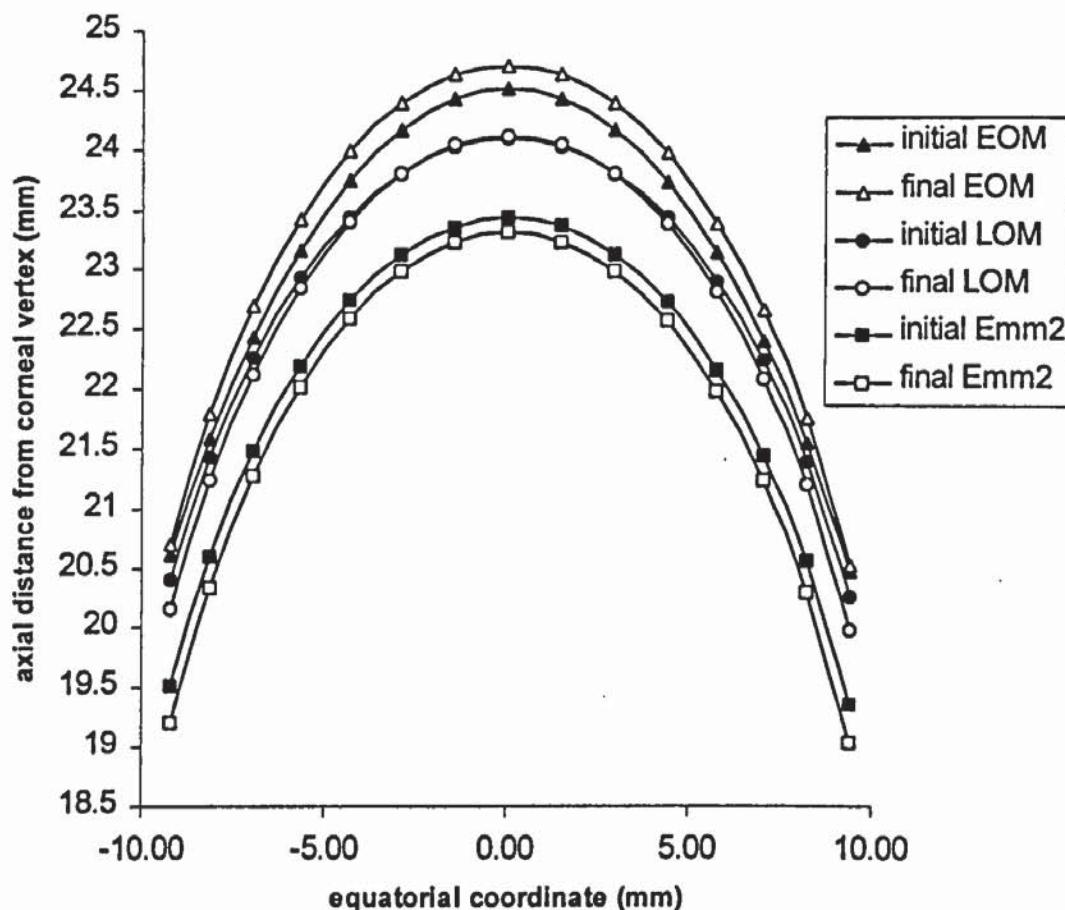


Figure 11.1 Retinal contours plotted for progressive emmetropes ($n = 8$), progressive late-onset myopes ($n = 10$) and progressive early-onset myopes ($n = 10$) at initial and final visits. Negative equatorial coordinates represent the nasal retina and positive the temporal retina.

11.5 Longitudinal ocular biometric changes in myopia onset and progression

The purpose of the thesis was not only to assess the ocular biometric differences between myopes and emmetropes and late-onset myopes and early-onset myopes, but also to investigate possible changes that occur with the onset of myopia. Previous longitudinal studies have found a change in corneal curvature and power with an increase in myopia (Goss *et al*, 1985; Goss, 1987; Kent, 1963 and Grosvenor and Scott, 1993). A very weak positive correlation was noted between myopia increase and corneal curvature change in the present data set. Both LOM and EOM subjects, especially LOM, who progressed towards myopia, showed a slight corneal steepening.

A weak negative correlation was also found with corneal asphericity, demonstrating an increase in corneal asphericity with an increase in myopia, i.e. more oblate. However, corneal vergence power did not change significantly with myopia progression in myopes or those emmetropes that showed a myopic shift in refractive error (Emm²). This finding substantiates the proposal that the cornea has minimal influence in myopic refractive error increase.

When analysing the ocular components separately, through component vergence power analysis, it is apparent that both the Emm² and LOM groups show an increase in the equivalent lens power with myopia onset and progression and the EOM group shows a decrease in the equivalent lens power. There appears to be minimal age-related alteration in the refractive index of the human lens, although, the cortical index gradient is thought to decrease slowly with age to counteract the increase in lens curvature (Pierscionek and Chan, 1989). In this thesis, it is presumed that the change in the equivalent lens power is not a consequence of changing lens refractive index. Accordingly, the axial measurement of the crystalline lens shows an increase in lens thickness in the Emm² and LOM groups and a decrease in lens thickness in the EOM group with a myopic shift in refractive error. All three refractive groups demonstrate posterior segment elongation, albeit only very slight in the Emm² group. Component vergence analysis provides an estimation of the proportion of power each separate ocular parameter contributes to the entire refractive system of the eye. Component vergence analysis demonstrates the following:

1. Emm² group - the increase in equivalent lens power with myopia onset is compensated for by a decrease in the power between the cornea and the equivalent lens, thereby, indicating a minimal change in anterior segment power. Myopia onset in this group is solely a result of posterior segment elongation.
2. LOM group - myopia progression is the result of an increase in the anterior segment power (primarily due to equivalent lens power increase) in conjunction with elongation of the posterior segment.
3. EOM group - myopia progression is the result of posterior segment elongation, which has not been compensated for by lens thinning and anterior segment power reduction.

Mechanisms for myopia onset and progression in late-onset myopes

The Emm² group consisted of 4 subjects (8 eyes), mean age 18.5 years at the start of the study, that were initially emmetropic and became myopic by the final visit. Owing to the age, the Emm² subjects can be counted as LOM. Myopia progression in the LOM group is associated with a slight increase in axial length and increase in lens thickness. The Emm² group and LOM group show mild equatorial retinal constriction, or 'squeeze', resulting in a more prolate shaped retina (see figure 11.1). The onset of myopia in the young adult eye and its increasing prevalence in developed countries is constantly linked with sustained or excessive nearwork (McBrien and Adams, 1997 and Rosenfield and Gilmartin, 1998). The necessity to see clearly at near relies on the near vision triad and specifically accommodation of the lens. Accommodation produces an increase in thickness of the lens. The increase in lens thickness and equatorial retinal constriction demonstrated in the Emm² and LOM groups with myopia onset and progression might, therefore, be related to the accommodation mechanism. The results of the present study show emmetropes and late-onset myopes to have lower amplitudes of accommodation compared to early-onset myopes. Sustained nearwork and reduced amplitudes of accommodation, in conjunction with a reduced stimulus-response gradient, may result in a defocused retinal image which could be a precursor to axial elongation and myopia onset. Contraction of the ciliary muscle releases tension on the zonular fibres allowing the lens to increase its curvature and thickness and reduce its equatorial diameter. One theory for late-onset myopia is that sustained nearwork could induce spasm of accommodation and continual contraction of the ciliary body could possibly translate to the retina resulting in a constriction at the equator.

Findl *et al* (1997) measured eye elongation during accommodation, using partial coherence interferometry and found the axial length to increase by $11 \pm 2.1\mu\text{m}$ in emmetropes and $5 \pm 1.9\mu\text{m}$ in myopes during maximum accommodation (amount not specified by authors). The investigators implied that accommodation could be a contributing factor to the development and progression of myopia.

Mechanisms for myopia onset and progression in early-onset myopes

Myopia progression in EOM is principally a result of posterior segment elongation. Figure 11.1 illustrates the increase in the EOM retina, both axially and equatorially, with myopia progression. The retina attempts to expand equatorially which reduces

lens thickness. The expansion axially exceeds the expansion equatorially resulting in posterior segment elongation and produces a more prolate shaped retina.

It is possible that two separate mechanisms are at work in the development of myopia. One mechanism induces myopia in an emmetropic eye, at an age when eye growth has ceased, as a result of inaccurate accommodation and retinal blur during periods of excessive and sustained nearwork. The other induces an increase in myopia in an already myopic eye as a continuation from the original breakdown in the emmetropization process in childhood. Goss *et al* (1985) describe the latter pattern of myopia as *adult continuation or acceleration*.

11.6 Future work

The thesis has provided an extensive data set allowing detailed cross-sectional and longitudinal analysis of a wide-range of biometry data on emmetropes and myopes. The analysis of longitudinal data was limited owing to the lack of repeatability of some parameters, high standard deviations and low numbers of subjects demonstrating myopia onset and progression during the study, although, this was not envisaged at the start of the study. Nevertheless, both cross-sectional and longitudinal data allows explanation of a number of theories in myopia development. Continuation of the study will involve greater subject numbers, reduction in the mean age of the subjects and an extension of the study period. This will provide a base of younger emmetropic subjects and a greater length of time over which to assess changes in refractive error. Greater rates of myopia progression will induce greater changes in the ocular biometry measurements and provide stronger statistical evidence for structural change. Analysis of family history of myopia, amount of time undertaking nearwork activity and further assessment of the accommodation system will help further our understanding of the increasingly common occurrence of late-onset myopia.

Myopia in children

Another interesting area of future study will involve children, aged 6 to 15, to examine the ocular biometric changes, and specifically the relatively novel technique of retinal contour, associated with myopia onset. It is apparent from eyecare practitioner records that once the refractive error in children has 'derailed' and myopia is present, a high percentage of subjects demonstrate a substantial shift in the refractive error towards

myopia during the ensuing years. The study will examine further the association between anterior and posterior segments during myopia onset using similar techniques and measurements to those exercised on adults in this thesis.

Crystalline lens assessment

One particular area of interest is the difference in crystalline lens power between emmetropes and myopes and the subsequent lens power change in early- and late-onset myopes with myopia onset and progression. Additional lens analysis, using data obtained from the Scheimpflug camera and ophthalmophakometer, will assist in further study of the anterior segment and its link with myopia. The ophthalmophakometer can provide accurate measurements of lens radii of curvature, which can then be used to verify the results from the Scheimpflug camera. The Scheimpflug camera can then be introduced as a new and useful instrument for ocular biometry studies.

Ocular blood flow and eye volume

Evidence shows that choroidal blood flow is reduced in myopia. The choroid of the myopic eye is also significantly thinner than the choroid of the emmetropic eye (Cheng *et al.*, 1992). Silver *et al* (1989) suggests that reduced blood flow is indicative of the large intraocular volume observed in myopic eyes. The longitudinal assessment of blood flow will assist in the evaluation of whether choroidal blood flow changes as a cause or an effect of myopia development.

An algorithm is currently being developed by Dr Logan (Aston University) to estimate total ocular volume. The calculation requires ocular biometry measurements that have already been recorded for this thesis. Ocular volume analysis in emmetropes and myopes will provide a greater understanding of globe size and will help to describe the changes that occur with increase in myopia. Van Alphen (1986) assessed changes in enucleated human eyes with increased IOP. The eyes demonstrated axial expansion rather than radial expansion. Axial expansion and prolate shaped retinæ were found in the present thesis in myopes and in myopia progression. Ocular blood flow, IOP and ocular biometry measurements in conjunction with ocular volume analysis during myopia progression will further test the theories of van Alphen.

REFERENCES

- Abbott, M. L., Schmid, K. L. and Strang, N. C. (1998). Differences in the accommodation stimulus response curves of adult myopes and emmetropes. *Ophthalmic and Physiological Optics*, **18**, 13-20.
- Abdalla, M. I. and Hamdi, M. (1970). Applanation ocular tension in myopia and emmetropia. *British Journal of Ophthalmology*, **54**, 122-125.
- Abrahamsson, M. and Sjostrand, J. (1992). Refraction changes in normal and amblyopic children. *Investigative Ophthalmology and Visual Science*, **33**, 1338.
- Adams, D. W. and McBrien, N. A. (1992). Prevalence of myopia and myopic progression in a population of clinical microscopists. *Optometry and Vision Science*, **69**, 467-473.
- Adams, D. W. and McBrien, N. A. (1993). A longitudinal study of the relationship between tonic accommodation (dark focus) and refractive error in adulthood. *Investigative Ophthalmology and Visual Science*, **34**, 1308.
- Ashton, G. C. (1985). Nearwork, school achievement and myopia. *Journal of Biosocial Science*, **17**, 223-233.
- Atkinson, J., Braddick, O. J. and French, J. (1980). Infant astigmatism: its disappearance with age. *Vision Research*, **20**, 891-893.
- Baker, F. J., Rappon, J. M., James, M. F., Rosenfield, M. and Portello, J. K. (1998). Form and repeatability of the accommodative stimulus-response function. *Investigative Ophthalmology and Visual Science*, **39**, s1048.
- Baldwin, W. R., West, D., Jolley, J. and Reid, W. (1969). Effects of contact lenses on refractive corneal and axial length changes in young myopes. *Journal of Optometry and Archives of American Academy of Optometry*, **46**.
- Bengtsson, B. (1972). Some factors affecting the distribution of intraocular pressures in a population. *Acta Ophthalmologica*, **50**, 33-45.
- Bennett, A. G. (1988a). Aspherical and continuous curve contact lenses. *Optometry Today*, **28**, 11-14, 140-142, 238-242, 433-444, 630-632.
- Bennett, A. G. (1988b). A method of determining the equivalent powers of the eye and its crystalline lens without the resort to phakometry. *Ophthalmic and Physiological Optics*, **8**, 53-59.
- Bennett, A. G. and Rabbetts, R. B. (1989). *Clinical Visual Optics*, Butterworths, Great Britain.

- Biggs, R. D., Alpern, M. and Bennett, D. R. (1959). The effect of sympathomimetic drugs upon the amplitude of accommodation. *American Journal of Ophthalmology*, **48**, 169-171.
- Blum, H. L., Peters, H. B. and Bettman, J. W. (1959). *Vision screening for elementary schools - The Orinda study*, University of California Press, Berkeley, CA.
- Boker, T., Sheqem, J., Rauwolf, M. and Wegener, A. (1995). Anterior chamber angle biometry: A comparison of Scheimpflug photography and ultrasound biomicroscopy. *Ophthalmic Research*, **27** (suppl. 1), 104-109.
- Bonomi, L., Mecca, E. and Massa, F. (1982). Intraocular pressure in myopic anisometropia. *Int. Ophthalmology*, **5**, 145-148.
- Borish, I. M. (1970). *Clinical Refraction*, Professional Press, Chigago.
- Brown, N. (1973). The change in shape and internal form of the lens of the eye on accommodation. *Experimental Eye Research*, **15**, 441-459.
- Brown, N. (1974). The changes in lens curvature with age. *Experimental Eye Research*, **19**.
- Bullimore, M. A., Gilmartin, B. and Royston, J. M. (1992). Steady-state accommodation and ocular biometry in late-onset myopia. *Documenta Ophthalmologica*, **80**, 143-155.
- Bylund, D. B. and Chacko, D. M. (1999). Characterization of alpha 2 adrenergic receptor subtypes in human ocular tissue homogenates. *Investigative Ophthalmology and Visual Science*, **40**, 2299-2306.
- Carney, L. G., Mainstone, J. C. and Henderson, B. A. (1997). Corneal topography and myopia. *Investigative Ophthalmology and Visual Science*, **38**, 311-320.
- Charman, W. N. (1972). Diffraction and the precision of measurement of corneal and other small radii. *American Journal of Optometry Archives of the American Academy of Optometry*, **49**, 672-679.
- Charman, W. N. (1982). The accommodative resting point and refractive error. *Ophthalmic Optics*, **21**, 469.
- Charman, W. N. (1983) In *Progress in Retinal Research*(Ed, Chandler, O. a.) Pergamon Press, Oxford.
- Charman, W. N. and Jennings, J. A. M. (1982). Ametropia and peripheral refraction. *American Journal of Optometry and Physiological Optics*, **59**, 922-923.
- Chauhan, K. and Charman, W. N. (1995). Single figure indices for the steady-state accommodative response. *Ophthalmic and Physiological Optics*, **15**, 217-221.

- Cheng, H., Singh, O. S., Kwong, K. K., Xiong, J., Woods, B. T. and Brady, T. J. (1992). Shape of the myopic eye as seen with high-resolution magnetic resonance imaging. *Optometry and Vision Science*, **69**, 698-701.
- Christensen, A. M. and Wallman, J. (1991). Evidence that increased scleral growth underlies visual deprivation myopia in chicks. *Investigative Ophthalmology and Visual Science*, **32**, 2143-2150.
- Clark, B. A. J. (1973). Keratometry: a review. *Australian Journal of Optometry*, **56**, 94-100.
- Cogan, D. G. (1937). Accommodation and the autonomic nervous system. *Archives of Ophthalmology*, **18**, 739-766.
- Cole, B. L., Maddocks, J. D. and Sharpe, K. (1996). Effect of VDUs on the eyes: report of a 6-year epidemiological study. *Optometry and Vision Science*, **73**, 512-528.
- Collins, G. (1937). The electronic refractionometer. *British Journal of Physiological Optics*, **11**, 30-42.
- Cook, R. C. and Glasscock, R. E. (1951). Refractive and ocular findings in the newborn. *American Journal of Ophthalmology*, **34**, 1407-1413.
- Culhane, H. M. and Winn, B. (1999). Dynamic accommodation and myopia. *Investigative Ophthalmology and Visual Science*, **40**, 1968-1974.
- Curtin, B. J. (1985). *The Myopias: Basic Science and Clinical Management*, Harper & Row, Philadelphia.
- Donders, F. C. (1864). *On the anomalies of accommodation and refraction of the eye.*, The New Sydenham Society, London.
- Douthwaite, W. A., Hough, T., Edwards, K. and Notay, H. (1999). The EyeSys videokeratoscopic assessment of apical radius and p-value in the normal human cornea. *Ophthalmic and Physiological Optics*, **19**, 467-475.
- Drasdo, N. and Fowler, C. W. (1974). Non-linear projection of the retinal image in a wide-angle schematic eye. *British Journal of Ophthalmology*, **58**, 709-714.
- Duane, A. (1922). Studies in monocular and binocular accommodation and their clinical applications. *American Journal of Ophthalmology*, **5**, 865-877.
- Dubbelman, M. and vanderHeijde, G. L. (2000). Undistorted acquisition of the curvature of the aging lens using Scheimpflug photography. *Investigative Ophthalmology and Visual Science*, **41**, 16.
- Duke-Elder, W. S. (1949). *Textbook of Ophthalmology*, C. V. Mosby.

- Dunne, M. C. M. (1995). A computing scheme for determination of retinal contour from peripheral refraction, keratometry and A-scan ultrasonography. *Ophthalmic and Physiological Optics*, **15**, 133-143.
- Dunne, M. C. M. and Barnes, D. A. (1987). Schematic modelling of peripheral astigmatism in real eyes. *Ophthalmic and Physiological Optics*, **7**, 235-239.
- Dunne, M. C. M. and Barnes, D. A. (1990). Modelling oblique astigmatism in eyes with known peripheral refraction and optical dimensions. *Ophthalmic and Physiological Optics*, **10**, 46-48.
- Dunne, M. C. M., Barnes, D. A. and Clement, R. A. (1987). A model for retinal shape changes in ametropia. *Ophthalmic and Physiological Optics*, **7**, 159-160.
- Ebenholtz, S. M. (1983). Accommodative hysteresis: a precursor for induced myopia? *Investigative Ophthalmology and Visual Science*, **24**, 513-515.
- Edwards, M. H. (1998) In *Myopia Updates - Proceedings of the 6th International Conference on Myopia*(Ed, Tokoro, T.) Springer-Verlag, Tokyo, pp. 48-52.
- Edwards, M. H. and Brown, B. (1993). Intraocular pressure in a selected sample of myopic and non-myopic Chinese children. *Optometry and Vision Science*, **70**, 15-17.
- Edwards, M. H. and Brown, B. (1996). IOP in myopic children: the relationship between increases in IOP and the development of myopia. *Ophthalmic and Physiological Optics*, **16**, 243-246.
- Egashira, S. M., Kish, L. L., Twelker, J. D., Mutti, D. O., Kadnik, K. and Adams, A. J. (1993). Comparison of cyclopentolate versus tropicamide cycloplegia in children. *Optometry and Vision Science*, **70**, 1019-1026.
- Eghbali, F., Yeung, K. K. and Maloney, R. K. (1995). Topographic determination of corneal asphericity and its lack of effect on the relative outcome of radial keratotomy. *American Journal of Ophthalmology*, **119**, 275-280.
- Ehinger, B. (1982). Neurotransmitter systems in the retina. *Retina*, **2**, 305-321.
- Ehrlich, D. L., Atkinson, J. and Braddick, O. J. (1995). Reduction of infant myopia: a longitudinal cycloplegic study. *Vision Research*, **35**, 1313-1324.
- Eisenlohr, J. E., Langham, M. E. and Maumenee, A. E. (1962). Manometric studies of the pressure volume relationships in living and enucleated eyes of individual human subjects. *British Journal of Ophthalmology*, **46**, 536-548.
- Emsley, H. H. (1936). *Visual Optics*, Hatton Press, London.
- Enoch, J. M. (1975). Marked accommodation, retinal stretch, monocular space perception and retinal receptor orientation. *American Journal of Optometry and Physiological Optics*, **52**, 376-392.

- Erickson, P. (1984). Complete ocular component analysis by vergence contribution. *American Journal of Optometry and Physiological Optics*, **61**, 469-472.
- Erickson, P. (1991) In *Refractive Anomalies: Research and Clinical Applications*. (Eds, Grosvenor, T. and Flom, M. C.) Butterworth-Heinemann, USA, pp. 199-218.
- Esgin, H., Alimgil, M. L. and Erda, S. (1998). Clinical comparison of the ocular blood flow tonograph and the Goldmann applanation tonometer. *European Journal of Ophthalmology*, **8**, 162-166.
- Ferree, C. E. and Rand, G. (1933). Interpretation of refractive conditions in the peripheral field of vision. *Archives of Ophthalmology*, **9**, 925-938.
- Ferree, C. E., Rand, G. and Hardy, C. (1931). Refraction for the peripheral field of vision. *Archives of Ophthalmology*, **5**, 717-732.
- Ferree, C. E., Rand, G. and Hardy, C. (1932). Refractive asymmetry in the temporal and nasal halves of the visual field. *American Journal of Ophthalmology*, **15**, 513-522.
- Findl, O., Drexler, W., Schmetterer, L. and Fercher, A. F. (1997). Eye elongation during accommodation assessed by partial coherence interferometry. *Investigative Ophthalmology and Visual Science*, **38**, 1349.
- Fisher, S. K., Ciuffreda, K. J. and Levine, S. (1987). Tonic accommodation, accommodative hysteresis and refractive error. *American Journal of Optometry and Physiological Optics*, **64**, 799-809.
- Fledelius, H. C. (1981). Changes in eye refraction and eyesize during adolescence - with special reference to the influence of low birth weight. *Documenta Ophthalmologica Proc.*, **28**, 63-69.
- Fledelius, H. C. (1982). Ophthalmic changes from age 10-18 years. A longitudinal study of sequels of low birth weight III. Ultrasound oculometry and keratometry of anterior eye segment. *Acta Ophthalmologica*, **60**, 393-420.
- Fledelius, H. C. (1988). Corneal curvature radius. *Acta Ophthalmologica*, **Suppl. 185**, 74-77.
- Fledelius, H. C. (1995a). Adult onset myopia- oculometric features. *Acta Ophthalmologica Scandinavica*, **73**, 397-401.
- Fledelius, H. C. (1995b). Myopia of adult onset. Can analyses be based on patient memory? *Acta Ophthalmologica*, **73**, 394-396.
- Fledelius, H. C. and Stubgaard, M. (1986). Changes in refraction and corneal curvature during growth and adult life. A cross sectional study. *Acta Ophthalmologica*, **64**, 487-491.

- Flitcroft, D. I. (1999). The lens paradigm in experimental myopia: oculomotor, optical and neurophysiological considerations. *Ophthalmic and Physiological Optics*, **19**, 103-111.
- Garner, L. F., Meng, C. K., Grosvenor, T. P. and Mohindin, N. (1990). Ocular dimensions and refractive power in Malay and Melanesian children. *Ophthalmic and Physiological Optics*, **10**, 234-238.
- Geyer, O., Neudorfer, M., Snir, T., Goldstein, M., Rock, T. and Bartov, E. (1999). Pulsatile ocular blood flow in diabetic retinopathy. *Acta Ophthalmologica Scandinavica*, **77**, 522-525.
- Gilmartin, B. (1986). A review of the role of sympathetic innervation of the ciliary muscle in ocular accommodation. *Ophthalmic and Physiological Optics*, **6**, 23-37.
- Gilmartin, B. and Bullimore, M. A. (1987). Sustained near-vision augments inhibitory sympathetic innervation of the ciliary muscle. *Clinical Vision Science*, **1**, 197-208.
- Gilmartin, B. and Bullimore, M. A. (1991). Adaptation of tonic accommodation to sustained visual tasks in emmetropia and late-onset myopia. *Optometry and Vision Science*, **68**, 22-26.
- Gilmartin, B., Bullimore, M. A., Rosenfield, M. and al, e. (1992). Pharmacological effects on accommodative adaptation. *Optometry and Vision Science*, **69**, 276-282.
- Gilmartin, B. and Rosenfield, M. (1999). Myopia and nearwork. *Optician*, **218**, 18-22.
- Goder, G. H. and Huebscher, H.-J. (1991) In *Distribution of Cataract in the Population and Influencing Factors*(Eds, Sasaki, K. and Hockwin, O.) Karger, Basel.
- Goldschmidt, E. (1968). On the etiology of myopia. *Acta Ophthalmologica*, **Suppl. 98**, 1-172.
- Goldschmidt, E. (1969). Refraction in the newborn. *Acta Ophthalmologica*, **47**, 570-578.
- Gordon, R. A. and Donzis, P. B. (1985). Refractive development of the human eye. *Archives of Ophthalmology*, **103**, 785-789.
- Goss, D. A. (1984). Overcorrection as a means of slowing myopic progression. *American Journal of Optometry and Physiological Optics*, **61**, 85-93.
- Goss, D. A. (1986). Effect of bifocal lenses on the rate of childhood myopia progression. *American Journal of Optometry and Physiological Optics*, **63**, 134-141.

- Goss, D. A. (1987). Meridional corneal components of myopia progression in young adults and children. *American Journal of Optometry and Physiological Optics*, 64, 475-481.
- Goss, D. A. (1990). Variables related to the rate of childhood myopia progression. *Optometry and Vision Science*, 67, 631-636.
- Goss, D. A. (1991). Clinical accommodation and heterophoria findings preceding juvenile onset myopia. *Optometry and Vision Science*, 68, 110-116.
- Goss, D. A. (1994). Effect of spectacle correction on the progression of myopia in children - a literature review. *Journal of the American Optometric Association*, 65, 117-128.
- Goss, D. A. and Cox, V. D. (1985). Trends in the change of clinical refractive error in myopes. *Journal of the American Optometric Association*, 56, 608-613.
- Goss, D. A. and Erickson, P. (1990). Effects of changes in the anterior chamber depth on refractive error in the human eye. *Optometry and Vision Science*, 5, 197-201.
- Goss, D. A., Erickson, P. and Cox, V. D. (1985). Prevalence and pattern of adult myopia progression in a general optometric practice population. *American Journal of Optometry and Physiological Optics*, 62, 470-477.
- Goss, D. A. and Grosvenor, T. (1999) In *Clinical Management of Myopia*, Vol. 2 , pp. 49-62.
- Goss, D. A., Hampton, M. J. and Wickham, G. (1988). Selected review on genetic factors in myopia. *Journal of the American Optical Association*, 59, 875-884.
- Goss, D. A. and Jackson, T. W. (1993). Cross-sectional study of changes in the ocular components in school children. *Applied Optics*, 32, 4169-4173.
- Goss, D. A. and Jackson, T. W. (1996a). Clinical findings before the onset of myopia in youth: 2. zone of clear single binocular vision. *Optometry and Vision Science*, 73.
- Goss, D. A. and Jackson, T. W. (1996b). Clinical findings before the onset of myopia in youth: 3. heterophoria. *Optometry and Vision Science*, 73, 269-278.
- Goss, D. A., van Veen, H. G., Rianey, B. B. and Feng, B. (1997). Ocular components measured by keratometry, phakometry and ultrasound in emmetropic and myopic optometry students. *Optometry and Vision Science*, 74, 489-495.
- Goss, D. A. and Wickham, M. G. (1995). Retinal-image mediated ocular growth as a mechanism for juvenile onset myopia and for emmetropization. *Documenta Ophthalmologica*, 90, 341-375.

- Goss, D. A. and Winkler, R. L. (1983). Progression of myopia in youth: Age of cessation. *American Journal Of Optometry and Physiological Optics*, 60, 651-658.
- Graves, B. (1926). Changes of tension of the lens capsule during accommodation and under the influence of various drugs. *British Medical Journal*, 1, 4-15.
- Gray, L. S., Gilmartin, B. and Winn, B. (2000). Accommodation microfluctuations and pupil size during sustained viewing of visual display terminals. *Ophthalmic and Physiological Optics*, 20, 5-10.
- Gray, L. S., Strang, N. C., Winfield, N., Gimartin, B. and Winn, B. (1998). The magnitude and distribution of open-loop accommdation using three different methods of opening the loop. *Optometry and Vision Science*, 75, 897.
- Gray, L. S., Winn, B. and Gilmartin, B. (1993). Accommodative microfluctuations and pupil diameter. *Vision Research*, 33, 2083-2090.
- Grosvenor, T. (1970). Refractive error distribution in New Zealand's Polynesian and European children. *Journal of Optometry and Archives of American Academy of Optometry*, , 673-679.
- Grosvenor, T. (1977). A longitudinal study of refractive changes between the ages of 20 and 40. Part 3: Statistical analysis. *Optometric Monthly*, 68, 455-457.
- Grosvenor, T. (1987). A review and a suggested classification system for myopia on the basis of age-related prevalence and age of onset. *American Journal of Optometry and Physiological Optics*, 64, 545-554.
- Grosvenor, T. (1988). High axial length/corneal radius ratio as a risk factor in the development of myopia. *American Journal of Optometry and Physiological Optics*, 65, 689-696.
- Grosvenor, T. (1994). Refractive component changes in adult-onset myopia: evidence from five studies. *Clinical and Experimental Optometry*, 77, 196-205.
- Grosvenor, T., Perrigin, D. M., Perrigin, J. and Maslovitz, B. (1987). Houston myopia control study: a randomized clinical trial. Part II. Final report by the patient care team. *American Journal of Optometry and Physiological Optics*, 64, 482-498.
- Grosvenor, T. and Scott, R. (1991). Comparison of refractive components in youth-onset and early adult-onset myopia. *Optometry and Vision Science*, 68, 204-209.
- Grosvenor, T. and Scott, R. (1993). Three-year changes in refraction and its components in youth-onset and early adult-onset myopia. *Optometry and Vision Science*, 70, 677-683.

- Grosvenor, T. and Scott, R. (1994). Role of the axial length/corneal radius ratio in determining the refractive state of the eye. *Optometry and Vision Science*, **71**, 573-579.
- Guillon, M., Lydon, D. P. M. and Wilson, C. (1986). Corneal topography: a clinical model. *Ophthalmic and Physiological Optics*, **6**, 47-56.
- Gullstrand, A. (1909) In *Physiological Optics*, Vol. 1 (Ed, Helmholtz, H. v.) Dover publications, New York, USA, pp. 350-358.
- Gwiazda, J., Bauer, J., Thorn, F. and Held, R. (1995). A dynamic relationship between myopia and blur-driven accommodation in school-aged children. *Vision Research*, **35**, 1299-1304.
- Gwiazda, J., Grice, K. and Thorn, F. (1999). Response AC/A ratios are elevated in myopic children. *Ophthalmic and Physiological Optics*, **19**, 173-179.
- Gwiazda, J., Thorn, F., Bauer, J. and Held, R. (1993a). Emmetropization and the progression of manifest refraction in children followed from infancy to puberty. *Clinical Visual Science*, **8**, 337-344.
- Gwiazda, J., Thorn, F., Bauer, J. and Held, R. (1993b). Myopic children show insufficient accommodative response to blur. *Investigative Ophthalmology and Visual Science*, **34**, 690-694.
- Heath, P. (1936). Neosynephrin hydrochloride: some uses and effects in ophthalmology. *Archives of Ophthalmology*, **16**, 839.
- Hemenger, R. P., Garner, L. F. and Ooi, C. S. (1995). Change with age of the refractive index gradient of the human ocular lens. *Investigative Ophthalmology and Visual Science*, **36**, 703-707.
- Hennessey, R. T. (1975). Instrument myopia. *Journal of the Optical Society of America*, **65**, 1114-1120.
- Hirsch, M. J. (1950). An analysis of inhomogeneity of myopia in adults. *American Journal of Optometry Archives of the American Academy of Optometry.*, **27**, 562-571.
- Hirsch, M. J. (1952). The changes in refraction between the ages of 5 and 14 - theoretical and practical considerations. *American Journal of Optometry Archives of the American Academy of Optometry.*, **29**, 445-459.
- Hirsch, M. J. (1958). Changes in refractive state after the age of forty-five. *American Journal of Optometry Archives of the American Academy of Optometry.*, **35**, 229-237.
- Hirsch, M. J. (1964). Predictability of refraction at age 14 on the basis of testing at age 6 - interim report from the Ojai longitudinal study of refraction. *American Journal of Optometry Archives of the American Academy of Optometry.*, **41**, 567-573.

- Hitzenberger, C. K. (1991). Optical measurement of the axial eye length by laser doppler interferometry. *Investigative Ophthalmology and Visual Science*, **32**, 616-624.
- Hodos, W. and Kuenzel, W. J. (1984). Retinal-image degradation produces ocular enlargement in chicks. *Investigative Ophthalmology and Visual Science*, **25**, 652-659.
- Hofstetter, H. W. (1969). Emmetropization - biological process or mathematical artifact? *American Journal of Optometry Archives of the American Academy of Optometry*, **46**, 447-450.
- Hoogerheide, J., Rempt, F. and Hoogenboom, W. P. H. (1971). Acquired myopia in young pilots. *Ophthalmologica*, **163**, 209-215.
- Horner, D. G., Soni, P. S., Vyas, N. and Himebaugh, N. L. (2000). Longitudinal changes in corneal asphericity in myopia. *Optometry and Vision Science*, **77**, 198-203.
- Hosking, S. L., Roff, E. J. and Hirst, A. D. (2000). Ocular blood flow and pulsatility in glaucoma. *Continuing Education optometry*, **3**, 25-29.
- Howland, H. C. and Sayles, N. (1985). Photokeratometric and photorefractive measurements of astigmatism in infants and young children. *Vision Research*, **25**, 73-81.
- Hoyt, G. S., Stone, R. D., Fromer, C. and Billson, F. A. (1981). Monocular axial myopia associated with neonatal eyelid closure in human infants. *American Journal of Ophthalmology*, **91**, 197-200.
- Huebscher, H. J., Fink, W., Steinbruck, D. and Seiler, T. (1999). Scheimpflug records without distortion - A mythos? *Ophthalmic Research*, **31**, 134-139.
- Hung, L. F., Crawford, M. L. J. and Smith, E. L. (1995). Spectacle lenses alter eye growth and refractive status of young monkeys. *Nature Med.*, **1**, 761-765.
- Inagaki, Y., Tanaka, M., Hirano, A., Magatani, H., Kato, K. and Nakajima, A. (1985). Rearranged automated keratometer for newborn infants and patients in the supine position. *American Journal of Ophthalmology*, **99**, 664-666.
- Irving, E. L., Callender, M. G. and Sivak, J. G. (1995). Inducing ametropias in hatchling chicks by defocus - aperture effects and cylindrical lenses. *Vision Research*, **35**, 1165-1174.
- Irving, E. L., Sivak, J. G. and Callender, M. G. (1992). Refractive plasticity of the developing chick eye. *Ophthalmic and Physiological Optics*, **12**, 448-456.
- Jain, M. R. and Marmion, V. J. (1976). A clinical evaluation of the applanation pneumatonograph. *British Journal of Ophthalmology*, **60**, 107-110.

- James, C. B., Trew, D. R., Clark, K. and Smith, S. E. (1991). Factors influencing the ocular pulse - axial length. *Graefe's Archive of Clinical and Experimental Ophthalmology*, 229, 341-344.
- Jensen, H. (1991). Myopia progression in young schoolchildren. A prospective study of myopia progression and the effect of a trial with bifocal lenses and beta blocker eye drops. *Acta Ophthalmologica*, Suppl. 200.
- Jensen, H. (1995). Myopia in teenagers. *Acta Ophthalmologica*, 73, 389-393.
- Jiang, B.-C. (1995). Parameters of accommodative and vergence systems and the development of late-onset myopia. *Investigative Ophthalmology and Visual Science*, 36, 1737-1742.
- Kehrhahn, O.-H. and Olbert, D. (1992). Nonlinear equations for calculating lens parameters based on Scheimpflug photographs: preliminary results. *Ophthalmic Research*, 24 (suppl. 1), 63-68.
- Kent, P. R. (1963). Acquired myopia of maturity. *American Journal of Optometry Archives of the American Academy of Optometry*, 40, 247-256.
- Kiely, P. M., Smith, G. and Carney, L. G. (1982). The mean shape of the human cornea. *Optica Acta*, 39, 1027-1040.
- Kinge, B. and Midelfart, A. (1999). Refractive changes among Norwegian university students - a three year longitudinal study. *Acta Ophthalmologica Scandinavica*, 77, 302-305.
- Kinge, B., Midelfart, A., Jacobsen, G. and Rystad, J. (1999). Biometric changes in the eyes of Norwegian university students - a three year longitudinal study. *Acta Ophthalmologica Scandinavica*, 77, 648-652.
- Kinney, J. A. S., Luria, S. M., Ryan, A. P., Schlichting, C. L. and Paulson, H. M. (1980). The vision of submariners and national guardsmen: A longitudinal study. *American Journal of Optometry and Physiological Optics*, 57, 469-478.
- Koretz, J. F., Rogot, A. and Kaufman, P. L. (1995). Physiological strategies for emmetropia. *Transactions of the American Ophthalmology Society*, 93, 105-122.
- Kothe, A. C., Vachon, N. and Woo, S. (1992). Factors affecting pulsatile ocular blood flow: axial length and ocular rigidity. *Optometry and Vision Science*, 69 (suppl.), 74.
- Krakau, C. E. T. (1992). Calculation of the pulsatile ocular blood flow. *Investigative Ophthalmology and Visual Science*, 33, 2754-2756.
- Laatikainen, L. and Erkkila, H. (1980). Refractive errors and other ocular findings in school children. *Acta Ophthalmologica*, 58, 129-136.

- Lam, C. S. Y., Edwards, M., Millodot, M. and Goh, W. S. H. (1999). A 2-year longitudinal study of myopia progression and optical component changes among Hong Kong schoolchildren. *Optometry and Vision Science*, **76**, 370-380.
- Langham, M. E. (1966) In *Glaucoma Symposium* Tuzing.
- Langham, M. E., Farrell, R. A., O'Brien, V., Silver, D. M. and Schilder, P. (1989). Blood flow in the human eye. *Acta Ophthalmologica*, **67**, 9-13.
- Langham, M. E., Grebe, R., Hopkins, S., Marcus, S. and Sebag, M. (1991). Choroidal blood flow in diabetic retinopathy. *Experimental Eye Research*, **52**, 167-173.
- Langham, M. E. and Kramer, T. (1990). Decreased choroidal blood flow associated with retinitis pigmentosa. *Eye*, .
- Larsen, J. S. (1971a). The sagittal growth of the eye. 1. Ultrasonic measurement of the depth of the anterior chamber from birth to puberty. *Acta Ophthalmologica*, **49**, 239-262.
- Larsen, J. S. (1971b). The sagittal growth of the eye. III. Ultrasonic measurement of the posterior segment (axial length of the vitreous) from birth to puberty. *Acta Ophthalmologica*, **49**, 441-453.
- Larsen, J. S. (1971c). The sagittal growth of the eye. IV. Ultrasonic measurement of the axial length of the eye from birth to puberty. *Acta Ophthalmologica*, **49**, 873-887.
- Larsen, J. S. (1971d). The sagittal growth of the eye. II. Ultrasonic measurement of the axial diameter of the lens and the anterior segment from birth to puberty. *Acta Ophthalmologica*, **49**, 427-440.
- Le Grand, Y. (1967). *Form and Space Vision*, University Press, Bloomington, Indiana.
- Leary, G. A. (1981). Ocular component analysis by vergence contribution to the back vertex power of the anterior segment. *American Journal of Optometry and Physiological Optics*, .
- Leary, G. A. and Young, F. A. (1968). A set of equations for computing the components of ocular refraction. *American Journal of Optometry Archives of the American Academy of Optometry*, **45**, 743-759.
- Lin, L. L., Chen, C., Hung, P. and Ko, L. (1988a). Nationwide survey of myopia among schoolchildren in Taiwan, 1986. *Acta Ophthalmologica*, **Suppl. 185**, 29-33.
- Lin, L. L., Hung, L., Shih, Y., Hung, P. and Ko, L. (1988b). Correlation of optical components with ocular refraction among teen-agers in Taipei. *Acta Ophthalmologica*, **Suppl. 185**, 69-73.
- Linfield, P. B. (1993). Myopia and the trend towards emmetropia in new born premature babies. *Investigative Ophthalmology and Visual Science*, **34 (suppl.)**, 1353.

- Littman, H. (1951). Grundlegende betrachtungen zur ophthalmometrie. *Albrecht von Graefes Archiv für Klinische und Experimentelle Ophthalmologie*, **133**, 152-156.
- Logan, N. S. (1997) In *Vision Sciences* Aston University, Birmingham, pp. 236.
- Logan, N. S., Gilmartin, B. and Dunne, M. C. M. (1995). Computation of retinal contour in anisomyopia. *Ophthalmic and Physiological Optics*, **15**, 363-366.
- Lotmar, W. (1971). Theoretical eye models with aspherics. *Journal of the Optical Society of America*, **61**, 1522-1529.
- Love, J., Gilmartin, B. and Dunne, M. C. M. (2000). Relative peripheral refractive error in adult myopia and emmetropia. *Investigative Ophthalmology and Visual Science*, **41**.
- Maddock, R. J., Millodot, M., Leat, S. and Johnson, C. A. (1981). Accommodation responses and refractive error. *Investigative Ophthalmology and Visual Science*, **20**, 387-391.
- Maguire, L. J., Singer, D. E. and Klyce, S. D. (1987). Graphic presentations of computer-analyzed keratoscope photographs. *Archives of Ophthalmology*, **105**, 223-230.
- Mantjarvi, M. (1983). Incidence of myopia in a population of Finnish school children. *Acta Ophthalmologica*, **61**, 417-423.
- Mantjarvi, M. I. (1985). changes in refraction in schoolchildren. *Archives of Ophthalmology*, **103**, 790-792.
- Massey, A. D. and O'Brien, C. (1996). Pulsatile ocular blood flow: a population study of normals. *Investigative Ophthalmology and Visual Science*, **37**, S31.
- Matsumura, I., Maruyama, S., Ishikawa, Y., Hirano, R., Kobayashi, K. and Kohayakawa, Y. (1983) In *Advances in diagnostic visual optics*(Eds, Breinin, G. M. and Siegel, I. M.) Springer, Berlin.
- Mauger, R. R., Likens, C. P. and Applebaum, M. (1984). Effects of accommodation and repeated applanation tonometry on intraocular pressure. *American Journal of Optometry and Physiological Optics*, **61**, 28-30.
- Mayer, H. (1994). Theodor Scheimpflug. His personality and lifework. *Ophthalmic Research*, **26**, 3-9.
- McBrien, N. and Barnes, D. A. (1984). Review and evaluation of theories of refractive error development. *Ophthalmic and Physiological Optics*, **4**, 201-213.
- McBrien, N. A. and Adams, D. W. (1997). A longitudinal investigation of adult-onset and adult progression of myopia in an occupational group. *Investigative Ophthalmology and Visual Science*, **38**, 321-333.

- McBrien, N. A. and Millodot, M. (1986a). Amplitude of accommodation and refractive error. *Investigative Ophthalmology and Visual Science*, **27**, 1187-1190.
- McBrien, N. A. and Millodot, M. (1986b). The effect of refractive error on the accommodative response gradient. *Ophthalmic and Physiological Optics*, **6**, 145-149.
- McBrien, N. A. and Millodot, M. (1987a). A biometric investigation of late onset myopic eyes. *Acta Ophthalmologica*, **65**, 461-468.
- McBrien, N. A. and Millodot, M. (1987b). The relationship between tonic accommodation and refractive error. *Investigative Ophthalmology and Visual Science*, **28**, 997-1004.
- McBrien, N. A. and Norton, T. T. (1992). The development of experimental myopia and ocular component dimensions in monocularly lid-sutured tree shrews (*Tupaia belangeri*). *Vision Research*, **32**, 843-852.
- Medina, A. and Fariza, E. (1993). Emmetropization as a first-order feedback system. *Vision Research*, **33**, 21-26.
- Midelfart, A., Aamo, B., Sjøhaug, K. A. and Dysthe, B. E. (1992). Myopia among medical students in Norway. *Acta Ophthalmologica*, **70**, 317-322.
- Millodot, M. (1981). Effect of ametropia on peripheral refraction. *American Journal of Optometry and Physiological Optics*, **58**, 691-695.
- Millodot, M. (1990). *Dictionary of Optometry*, Butterworth & Co Ltd.
- Millodot, M. and Lamont, A. (1974). Refraction of the periphery of the eye. *Journal of the Optical Society of America*, **64**, 110-111.
- Mohindra, I. (1977). A non-cycloplegic refraction technique for infants and young children. *Journal of the American Optometric Association*, **48**, 518-523.
- Mohindra, I. and Held, R. (1981). Refractions in human from birth to five years. *Documenta Ophthalmol. Proc. Ser.*, **28**, 19-27.
- Moses, R. A. (1981) In *Adler's Physiology of the Eye. Clinical Application* (Ed, Moses, R. A.) C. V. Mosby, , pp. 304-325.
- Mutti, D. O., Sholtz, R. I., Friedman, N. E. and Zadnik, K. (1997). Peripheral refraction and ocular shape in children. *Investigative Ophthalmology and Visual Science*, **38**, 1157.
- Mutti, D. O., Sholtz, R. I., Friedman, N. E. and Zadnik, K. (2000). Peripheral refraction and ocular shape in children. *Investigative Ophthalmology and Visual Science*, **41**, 1022-1030.

- Mutti, D. O. and Zadnik, K. (1995). How applicable are animal models to human juvenile onset myopia? *Vision Research*, **35**, 1283-1288.
- Mutti, D. O. and Zadnik, K. (1996). Is computer use a risk factor for myopia? *Journal of the American Optometric Association*, **67**, 521-530.
- Nathan, J., Kiely, P. M., Crewther, S. G. and Crewther, D. P. (1985). Disease-associated visual image degradation and spherical refractive errors in children. *American Journal of Optometry and Physiological Optics*, **62**, 680-688.
- Olbert, D. (1995). The use of Scheimpflug photography in the documentation of clinical states and in the biometry of the anterior eye segment. *Ophthalmic Research*, **27** (suppl. 1), 20-24.
- O'Neal, M. R. and Connon, T. R. (1987). Refractive error change at the United States Air Force Academy - class of 1985. *American Journal of Optometry and Physiological Optics*, **64**, 344-354.
- Ong, E. and Cuiffreda, K. J. (1995). Nearwork-induced transient myopia. *Documenta Ophthalmologica*, **91**, 57-85.
- Owens, D. A. and Wolf-Kelly, K. (1987). Near work, visual fatigue and variations of oculomotor tonus. *Investigative Ophthalmology and Visual Science*, **28**, 743-749.
- Parssinen, O., Hemminki, E. and Klemetti, A. (1989). Effect of spectacle use and accommodation on myopic progression: final results of a three-year randomised clinical trial among schoolchildren. *British Journal of Ophthalmology*, **73**, 547-551.
- Peckham, C. S., Gardiner, P. A. and Goldstein, H. (1977). Acquired myopia in 11-year-old children. *British medical Journal*, **1**, 542-544.
- Pendse, G. S., Dan de Kar, V. M. and Bhave, L. S. (1951). Preliminary note on study of the refractive state, with special reference to myopia. *Archives of Ophthalmology*, **45**, 168.
- Perkins, E. S. (1981). The ocular pulse. *Current Eye Research*, **1**, 19-23.
- Pierscionek, B. K. and Chan, D. Y. (1989). Refractive index gradient of human lenses. *Optometry and Vision Science*, **66**.
- Portello, J. K. and Rosenfield, M. (1997). Clinical characteristics of pre-myopic individuals. *Optometry and Vision Science*, **74** (suppl.), 176.
- Price, E. L., Gray, L. S. and Button, N. F. (1999). Sources of variation in the measurement of pulsatile ocular blood flow. *Investigative Ophthalmology and Visual Science*, **40**, S507.

- Pruett, R. C. (1988). Progressive myopia and intraocular pressure: what is the linkage? *Acta Ophthalmologica*, **185 (suppl.)**, 117-127.
- Pugh, J. R. and Winn, B. (1988). Modification of the Canon Auto Ref R1 for use as a continuously recording infra-red optometer. *Ophthalmic and Physiological Optics*, **8**.
- Qian, W., Soderberg, P. G., Chen, E. and Philipson, B. (1997). An external standard for Scheimpflug slit-lamp microscopy. *Investigative Ophthalmology and Visual Science*, **38**, 1612.
- Quigley, H. A. and Langham, M. E. (1975). Comparative intraocular pressure measurements with the pneumatonograph and the Goldmann tonometer. *American Journal of Ophthalmology*, **80**, 266-273.
- Ramsdale, C. (1979). Monocular and binocular accommodation. *Ophthalmic Optics*, **19**, 606-622.
- Ravalico, G., Toffoli, G., Pastori, G., Croce, M. and Calderini, S. (1996). Age-related ocular blood flow changes. *Investigative Ophthalmology and Visual Science*, **37**, 2645-2650.
- Rempt, F., Hoogerheide, J. and Hoogenboom, W. P. H. (1971). Peripheral retinoscopy and the skiagram. *Ophthalmologica*, **162**, 1-10.
- Riva, C. E., Cranstoun, S. D., Grunwald, J. E. and Petrig, B. L. (1994). Choroidal blood-flow in the foveal region of the human ocular fundus. *Investigative Ophthalmology and Visual Science*, **35**, 4273-4281.
- Riva, C. E., Grunwald, J. E., Sinclair, S. H. and Petrig, B. L. (1985). Blood velocity and volumetric flow-rate in human retinal vessels. *Investigative Ophthalmology and Visual Science*, **26**, 1124-1132.
- Robb, R. M. (1977). Refractive errors associated with hemangiomas of the eyelids and orbit in infancy. *American Journal of Ophthalmology*, **83**, 52-58.
- Roberts, W. L. and Banford, R., D. (1967). Evaluation of bifocal correction technique in juvenile myopia. *Optometric Weekly*, .
- Rosenfield, M. (1994). Accommodation and myopia - are they related? *Journal of Behavioral Optometry*, **5**, 3-11.
- Rosenfield, M. (1997) In *The ocular examination: measurements and findings* (Ed, Zadnik, K.) W. B. Saunders and company, Philadelphia, pp. 88-109.
- Rosenfield, M., Ciuffreda, K. J., Hung, G. K. and Gilmartin, B. (1993). Tonic accommodation: a review. I. Basic aspects. *Ophthalmic and Physiological Optics*, **13**, 266-284.

- Rosenfield, M., Ciuffreda, K. J. and Novogrodsky, L. (1992). Contribution of accommodation and disparity-vergence to transient nearwork-induced myopic shifts. *Ophthalmic and Physiological Optics*, **12**, 433-436.
- Rosenfield, M. and Gilmartin, B. (1987a). Beta-adrenergic receptor antagonism in myopia. *Ophthalmic and Physiological Optics*, **7**, 359-364.
- Rosenfield, M. and Gilmartin, B. (1987b). Effect of a near-vision task on the response AC/A of a myopic population. *Ophthalmic and Physiological Optics*, **7**, 225-233.
- Rosenfield, M. and Gilmartin, B. (1987c). Synkinesis of accommodation and vergence in late-onset myopia. *American Journal of Optometry and Physiological Optics*, **64**, 929-937.
- Rosenfield, M. and Gilmartin, B. (1988). Accommodative adaptation induced by sustained disparity-vergence. *American Journal of Optometry and Physiological Optics*, **65**, 118-126.
- Rosenfield, M. and Gilmartin, B. (1998). *Myopia and Nearwork*, Butterworth-Heinemann, Oxford.
- Royston, J. M., Dunne, M. C. M. and Barnes, D. A. (1989). Calculation of crystalline lens radii without resort to phakometry. *Ophthalmic and Physiological Optics*, **9**, 412-414.
- Saunders, K. J., Woodhouse, M. and Westall, C. A. (1995). Emmetropisation in human infancy: rate of change is related to initial refractive error. *Vision Research*, **35**, 1325-1328.
- Schaeffel, F., Glasser, A. and Howland, H. C. (1988). Accommodation, refractive error and eye growth in chickens. *Vision Research*, **28**, 639-657.
- Scheiman, M. and Wick, B. (1994). *Clinical management of binocular vision - heterophoric, accommodative and eye movement disorders.*, Lippincott.
- Schmid, G. F., Petrig, B. L., Riva, C. E., Laties, A. M., Mendel, M. J. and Dunne, M. C. M. (1994) In *Vision Science and its application* Santa Fe, New Mexico.
- Schmid, K. L. and Wildsoet, C. F. (1997). The sensitivity of the chick eye to refractive defocus. *Ophthalmic and Physiological Optics*, **17**, 61-67.
- Scott, R. and Grosvenor, T. (1993). Structural model for emmetropic and myopic eyes. *Ophthalmic and Physiological Optics*, **13**, 41-47.
- Septon, R. D. (1984). Myopia among Optometry students. *American Journal of Optometry and Physiological Optics*, **61**, 745-751.
- Sheridan, M. (1955). The crystalline lens in myopia. *Optician*, **129**, 447-450, 456.

- Sheridan, M. and Douthwaite, W. A. (1989). Corneal asphericity and refractive error. *Ophthalmic and Physiological Optics*, **9**, 235-238.
- Silver, D. M., Farrell, R. A., Langham, M. E., O'Brien, V. and Schilder, P. (1989). Estimation of pulsatile ocular blood flow from intraocular pressure. *Acta Ophthalmologica*, **67**, 25-29.
- Silver, D. M. and Geyer, O. (2000). Pressure-volume relation for the living human eye. *Current Eye Research*, **20**, 115-120.
- Simensen, B. and Thorud, L. A. (1994). Adult-onset myopia and occupation. *Acta Ophthalmologica*, **72**, 469-471.
- Smith, E. L., Bradley, D. V., Fernandes, A. and Boothe, R. G. (1999). Form deprivation myopia in adolescent monkeys. *Optometry and Vision Science*, **76**, 428-432.
- Smith, E. L., Harwerth, R. S., Crawford, M. L. J. and van Noorden, G. K. (1987). Observations on the effects of form deprivation on the refractive status of the monkey. *Investigative Ophthalmology and Visual Science*, **28**, 1236-1245.
- Smith III, E. L., Huang, J. and Hung, L.-F. (1997) In *Proceedings of the 6th international congress on myopia*(Ed, Tokoro, T.) Springer, .
- Sorsby, A. (1967). *The nature of spherical refractive errors*, US Department of Health, education and Welfare, Washington, DC.
- Sorsby, A., Benjamin, B., Davey, J. B., Sheridan, M. and Tanner, J. M. (1957). Emmetropia and its aberrations. *Medical Research Council*, No. 293.
- Sorsby, A., Benjamin, B. and Sheridan, M. (1961). Refraction and its components during the growth of the eye from the age of three. *Medical Research Council*, No. 301.
- Sorsby, A. and Leary, G. A. (1970). A longitudinal study of refraction and its components during growth. *Medical Research Council*, No. 309.
- Sorsby, A., Leary, G. A. and Richards, M. J. (1962a). Correlation ametropia and component ametropia. *Vision Research*, **2**, 309-313.
- Sorsby, A., Sheridan, M. and Leary, G. A. (1962b). Refraction and its components in twins. *Medical Research Council*, No. 303.
- Sorsby, A., Sheridan, M., Leary, G. A. and Benjamin, B. (1960). Vision, visual acuity and ocular refraction in young men. *British Medical Journal*, **1**, 1394-1398.
- Sperduto, R. D., Seigal, D., Roberts, J. and Rowland, M. (1983). Prevalence of myopia in the United States. *Archives of Ophthalmology*, **101**, 405-407.
- Spraul, C. W., Lang, G. E., Hogel, J. and Lang, G. K. (1998). Reproducibility of measurements with a new slit lamp-mounted ocular blood flow tonograph. *Graefe's Archive of Clinical and Experimental Ophthalmology*, **236**, 274-279.

- Stansbury, F. C. (1948). Pathogenesis of myopia. *Archives of Ophthalmology*, 39, 273-299.
- Steele, C. F., Crabb, D. P. and Edgar, D. F. (1992). Effects of different ocular fixation conditions on A-scan ultrasound biometry measurements. *Ophthalmic and Physiological Optics*, 12, 491-495.
- Stenstrom, S. (1946). Untersuchungen über die variation und kovariation der optischen elemente des menschlichen auges. *Acta Ophthalmologica*, suppl. 26.
- Stone, J. (1962). The validity of some existing methods of measuring corneal contour with suggested new methods. *British Journal of Physiological Optics*, 19, 25-230.
- Storey, J. K. (1982). Measurement of the eye with ultrasound. *The Ophthalmic Optician*, Feb 27, 150-160.
- Strang, N. C., Gilmartin, B., Gray, L. S., Winfield, N. R. and Winn, B. (2000). Open-loop accommodation in emmetropia and myopia. *Current Eye Research*, 20, 190-194.
- Thompson, C. (1987) In *Vision Sciences* Aston University, Birmingham.
- To'mey, K. F., Faris, B. M., Jalkh, A. E. and Nasr, A. M. (1981). Ocular pulse in high myopia: a study of 40 eyes. *Annals of Ophthalmology*, May, 569-571.
- Tomlinson, A. and Phillips, C. I. (1970). Applanation tension and axial length of the eyeball. *British Journal of Ophthalmology*, 54, 548-553.
- Tornqvist, G. (1967). The relative importance of the parasympathic and sympathetic nervous systems for accommodation in monkeys. *Investigative Ophthalmology*, 6, 612.
- Troilo, D. and Wallman, J. (1991). The regulation of eye growth and refractive state: an experimental study of emmetropization. *Vision Research*, 31, 1237-1250.
- Trolio, D. and Wallman, J. (1987). Changes in corneal curvature during accommodation in chicks. *Vision Research*, 27, 241-247.
- van Alphen, G. W. H. M. (1961). On emmetropia and ametropia. *Ophthalmologica (suppl.)*, 124, 1-92.
- van Alphen, G. W. H. M. (1976). The adrenergic receptors of the intraocular muscles of the human eye. *Investigative Ophthalmology*, 15, 502-505.
- van Alphen, G. W. H. M. (1986). Choroidal stress and emmetropization. *Vision Research*, 26, 723-734.
- van Alphen, G. W. H. M., Kern, R. and Robinette, S. L. (1965). Adrenergic receptors of the intraocular muscles. *Archives of Ophthalmology*, 74, 253-259.

- Wallman, J. (1991) In *Refractive Anomalies: Research and Clinical Applications*. (Eds, Grosvenor, T. and Flom, M. C.) Butterworth-Heinemann, USA, pp. 268-286.
- Wallman, J. and Adams, J. I. (1987). Developmental aspects of experimental myopia in chicks: susceptibility, recovery and relation to emmetropization. *Vision Research*, **27**, 1139-1163.
- Wallman, J., Adams, J. I. and Trachtman, J. N. (1981). The eyes of young chickens grow towards emmetropia. *Investigative Ophthalmology and Visual Science*, **20**, 557-561.
- Wallman, J. and McFadden, S. (1995). Monkey eyes grow into focus. *Nature Med.*, **1**, 737-739.
- Wallman, J., Xu, A., Wildsoet, C., Krebs, W., Gottlieb, M., Marran, L. and Nickla, D. (1992). Moving the retina: a third mechanism for focusing the eye. *Investigative Ophthalmology and Visual Science*, **ARVO**, 1053.
- Wang, F. R., Zhou, X. D. and Zhou, S. Z. (1994). A CT study of the relation between ocular axial biometry and refraction. *Chinese Journal of Ophthalmology*, **30**, 39-40.
- Ward, P. A. and Charman, W. N. (1985). Effect of pupil size on steady-state accommodation. *Vision Research*, **25**, 1317-1326.
- Ware, J. (1813). Observations relative to the near and distant sight of different persons. *Philosophic Transcripts of the Royal Society, London*, **1**, 31.
- Wildsoet, C. The aetiology of myopia - A review of results from animal studies and their implications for the clinical management of human myopia. .
- Wildsoet, C. and Wallman, J. (1992). Optic nerve section affects ocular compensation for spectacle lenses. *Investigative Ophthalmology and Visual Science*, **ARVO**, 1053.
- Wildsoet, C. and Wallman, J. (1995). Choroidal and scleral mechanisms of compensation for spectacle lenses in chicks. *Vision Research*, **35**, 1175-1194.
- Wildsoet, C. F. (1997). Active emmetropization - evidence for its existence and ramifications for clinical practice. *Ophthalmic and Physiological Optics*, **17**, 279-290.
- Wildsoet, C. F. and Pettigrew, J. (1988). Experimental myopia and anomalous eye growth patterns unaffected by optic nerve section in chickens: evidence for local control of eye growth. *Clinical Vision Science*, **3**, 99-107.
- Wildsoet, C. F. and Pettigrew, J. (1988). Kianic acid-induced eye enlargement in chickens, differential effects on anterior and posterior segments. *Investigative Ophthalmology and Visual Science*, **29**, 311-319.

- Williamson, T. H. and Harris, A. (1994). Ocular blood flow measurement. *British Journal of Ophthalmology*, 78, 939-945.
- Winn, B., Pugh, J. R., Gilmartin, B. and Owens, H. (1989). The effect of pupil size on static and dynamic measurements of accommodation using an infra-red optometer. *Ophthalmic and Physiological Optics*, 9, 277-283.
- Wold, K. C. (1949). Hereditary myopia. *Archives of Ophthalmology*, 42, 225-237.
- Wood, I. C. J. and Hodi, S. (1992). Refractive findings of a longitudinal study of infants from birth to one year of age. *Investigative Ophthalmology and Visual Science*, 33, 971.
- Wood, I. C. J., Hodi, S. and Morgan, L. (1995). Longitudinal changes in the refractive error in infants during the first year of life. *Eye*, 9, 551-557.
- Wood, I. C. J., Mutti, D. O. and Zadnik, K. (1996). Crystalline lens parameters in infancy. *Ophthalmic and Physiological Optics*, 16, 310-317.
- Yang, Y. C., Hulbert, M. F. G., Batterbury, M. and Clearkin, L. G. (1997). Pulsatile ocular blood flow measurements in healthy eyes: reproducibility and reference values. *Journal of Glaucoma*, 6, 175-179.
- Young, F. A. (1955). Myopes versus nonmyopes - a comparison. *American Journal of Optometry Archives of the American Academy of Optometry*, 32, 180-191.
- Young, F. A. (1961). The effect of restricted visual space on the primate eye. *American Journal of Ophthalmology*, 52, 799-806.
- Young, F. A. (1963). Reading, measures of intelligence and refractive errors. *American Journal of Optometry Archives of the American Academy of Optometry*, 40, 257-264.
- Young, F. A. (1977). The nature and control of myopia. *Journal of the American Optometric Association*, 48, 451-457.
- Young, F. A. and Leary, G. A. (1991) In *Refractive Anomalies. Research and Clinical Applications*(Ed, Flom, T. G. a. M. C.) Butterworth-Heinemann, , pp. 301-309.
- Young, F. A., Leary, G. A., Baldwin, W. R., West, D. C., Box, R. A., Harris, E. and Johnson, C. (1969). The transmission of refractive errors within Eskimo families. *American Journal of Optometry Archives of the American Academy of Optometry*, 46, 676-685.
- Young, T. (1801). *Phil. Trans. R. Soc. Lond*, 91.
- Zadnik, C., Mutti, D. O., Friedman, N. E. and Adams, A. J. (1993). Initial cross-sectional results from the Orinda longitudinal study of myopia. *Optometry and Vision Science*, 70, 750-758.

- Zadnik, K. and Mutti, D. O. (1998) In *Myopia and Nearwork* (Eds, Rosenfield, M. and Gilmartin, B.) Butterworth-Heinemann, Oxford, U.K., pp. 13-30.
- Zadnik, K., Mutti, D. O. and Adams, A. J. (1992). The repeatability of measurement of the ocular components. *Investigative Ophthalmology and Visual Science*, **33**, 2325-2333.
- Zadnik, K., Mutti, D. O. and Adams, A. J. (1995). Longitudinal evidence of crystalline lens thinning in children. *Investigative Ophthalmology and Visual Science*, **36**, 1581-1587.
- Zylbermann, R., Landau, D. and Berson, D. (1993). The influence of study habits on myopia in Jewish teenagers. *Journal of Pediatric Ophthalmology and Strabismus*, **30**, 319-322.

APPENDICES

APPENDIX 1 – Biometric measurements

Px	Eye	Age	Es1	Es2	Es3	ACD1	ACD2	ACD3	LT1	LT2	LT3	VD1	VD2	VD3
AB	r	18	0.63	0.38	0.13	3.88	3.78	3.44	3.46	3.43	3.48	16.60	16.61	16.77
	l	18	0.50	0.38	0.25	3.60	3.93	3.64	3.43	3.35	3.35	16.99	16.83	16.84
AT	r	27	-1.00	-1.00	-1.00	3.94	3.90	3.81	3.53	3.68	3.67	17.75	18.02	17.58
	l	27	-1.00	-1.13	-1.13	3.23	3.95	3.93	4.18	3.68	3.64	17.78	17.45	17.68
AK	r	21	0.00	0.00	0.13	3.88	3.86	3.65	3.44	3.48	3.54	17.53	17.12	17.19
	l	21	0.25	0.25	0.25	3.86	3.96	3.51	3.59	3.50	3.70	17.01	16.94	16.94
AD	r	19	-0.50	-0.63	-0.63	3.72	3.96	3.98	3.92	3.31	3.27	18.75	17.98	18.42
	l	19	-0.88	-0.88	-0.88	3.79	3.92	3.96	3.46	3.41	3.36	18.32	17.63	18.11
BS	r	19	0.25	0.25	0.25	3.86	3.90	3.57	4.20	3.77	3.86	15.86	16.11	16.04
	l	19	0.13	0.38	0.50	3.75	3.95	3.76	4.01	3.86	3.86	15.50	15.72	15.81
BG	r	16	-0.50	-1.50	-1.50	3.95	3.93	3.65	3.52	3.55	3.74	16.82	16.81	16.84
	l	16	-0.25	-0.88	-1.38	3.93	3.86	3.38	3.67	3.65	3.60	16.57	16.49	16.98
DP	r	19	0.25	0.75	0.75	3.86	3.76	3.72	3.85	3.79	3.86	16.11	16.17	16.31
	l	19	0.13	0.63	0.38	3.77	3.42	3.59	3.84	3.93	3.95	16.23	16.52	16.39
DW	r	20	-1.00	-1.00	-1.00	3.82	3.56	3.73	3.78	3.88	3.91	15.32	15.38	15.22
	l	20	-0.88	-1.13	-1.13	3.79	3.99	3.75	3.82	3.81	3.91	15.19	15.16	15.19
DL	r	19	-2.88	-3.13	-3.13	3.92	3.81	3.75	3.70	3.65	3.84	16.36	16.45	16.26
	l	19	-2.38	-2.63	-2.75	4.01	3.89	3.80	3.65	3.88	3.82	16.01	15.56	16.08
GC	r	18	-0.38	-0.38	-0.38	3.88	3.68	3.83	3.27	3.25	3.37	16.63	16.71	16.74
	l	18	-0.38	-0.63	-0.63	3.91	3.92	4.01	3.21	3.50	3.35	16.83	16.54	16.64
GK	r	19	-0.88	-0.88	-1.00	3.92	3.92	3.94	3.35	3.36	3.40	17.09	16.71	17.03
	l	19	-1.50	-1.50	-1.50	3.99	3.96	3.88	3.48	3.44	3.32	16.89	16.88	17.54
Gke	r	23	-3.50	-3.38	-3.75	3.97	4.03	3.95	3.48	3.54	3.54	18.13	17.89	18.10
	l	23	-3.63	-3.50	-3.88	3.95	4.12	3.94	3.45	4.41	3.54	18.16	17.71	18.34
HS	r	18	-0.13	0.00	-0.13	3.77	3.91	3.92	3.34	3.25	3.24	17.02	17.23	17.44
	l	18	-0.13	0.00	0.00	3.79	3.96	3.97	3.27	3.22	3.18	17.19	17.26	17.44
IP	r	24	0.50	0.50	0.63	3.83	3.51	3.60	3.69	3.80	3.73	16.36	16.38	16.57
	l	24	0.63	0.50	0.50	3.74	3.70	3.72	3.84	3.78	3.79	16.13	16.24	16.40
JS	r	21	0.50	0.38	0.38	3.48	3.88	3.44	3.80	3.73	3.74	16.08	15.43	15.84
	l	21	0.50	0.50	0.75	3.56	3.85	3.60	3.45	3.78	3.65	15.78	15.15	15.70
KR	r	19	-6.63	-7.00	-7.00	3.82	3.72	3.46	3.74	3.77	3.86	18.50	18.54	18.74

	I	19	-7.38	-7.63	-7.88	3.84	3.76	3.51	3.81	3.76	3.77	18.45	18.63	19.00
KJ	r	19	-1.25	-1.50	-1.63	3.54	3.85	3.78	3.65	3.78	3.77	17.19	16.55	16.88
	I	19	-1.25	-1.25	-1.38	3.58	3.80	3.79	4.08	3.66	3.66	15.87	16.39	16.58
LP	r	21	-1.00	-1.25	-1.50	3.87	3.95	3.73	3.26	3.27	3.19	16.60	16.74	16.99
	I	21	-2.00	-2.38	-2.25	3.61	3.45	3.93	3.28	3.35	3.34	17.07	17.71	16.85
LD	r	19	-2.50	-2.50	-2.88	3.91	3.84	3.94	3.66	3.72	3.35	18.09	18.26	18.35
	I	19	-2.25	-2.00	-2.38	3.81	3.81	3.92	3.24	3.24	3.33	17.94	17.94	17.59
LT	r	19	0.25	0.25	0.25	3.95	3.95	3.99	3.67	3.69	3.52	15.66	15.66	16.12
	I	19	0.13	0.13	0.13	3.95	3.81	3.94	3.66	3.28	3.62	15.56	15.96	15.44
MS	r	21	-1.50	-1.75	-1.88	3.68	3.73	3.46	3.79	3.67	3.83	16.13	15.80	16.20
	I	21	-1.25	-1.38	-1.38	3.42	3.45	3.45	3.93	4.09	4.04	16.20	15.84	15.89
MSh	r	19	0.50	0.13	0.25	3.64	3.55	3.44	3.73	3.80	3.91	14.94	15.15	15.19
	I	19	0.63	0.38	0.38	3.64	3.43	3.02	3.89	3.90	3.98	14.94	15.05	15.01
MA	r	27	0.00	-0.25	0.38	3.82	3.88	3.73	3.31	3.42	3.47	16.28	16.08	16.32
	I	27	-0.25	-0.12	0.38	3.83	3.79	3.52	3.46	3.51	3.59	16.27	16.10	16.22
RB	r	22	0.13	0.13	0.13	3.85	3.75	3.58	3.69	3.70	3.74	15.32	15.69	15.79
	I	22	0.13	0.13	0.00	3.77	3.64	3.58	3.78	3.76	3.75	15.74	15.53	15.44
SD	r	18	0.25	0.25	0.25	3.83	3.78	3.91	3.64	3.50	3.70	15.52	15.80	15.72
	I	18	0.25	0.25	0.25	3.75	3.79	3.66	3.59	3.46	3.64	15.69	15.85	15.82
SCr	r	19	-1.75	-2.00	-2.13	3.60	3.60	3.60	3.51	3.51	3.53	17.56	17.60	17.82
	I	19	-1.75	-1.88	-2.13	3.80	3.55	3.62	3.53	3.59	3.64	17.49	17.45	17.45
SJo	r	18	0.13	0.13	0.38	3.82	3.80	3.42	3.69	3.55	3.59	15.15	15.19	15.41
	I	18	0.13	0.25	0.38	3.73	3.62	3.43	3.83	3.50	3.65	15.30	15.25	15.11
SG	r	19	-2.00	-2.25	-2.38	3.95	3.97	3.99	3.35	3.20	3.20	16.26	16.40	16.66
	I	19	-2.25	-2.50	-2.63	3.79	3.97	3.92	3.16	3.28	3.32	16.44	16.37	16.72
SJ	r	19	-0.13	0.25	0.13	3.62	3.85	3.48	3.82	3.69	3.96	15.59	15.91	15.73
	I	19	0.13	0.38	0.13	3.80	3.74	3.48	3.66	3.96	3.74	15.96	15.50	16.01
SZ	r	21	-1.88	-1.75	-1.75	4.00	3.86	3.86	3.21	3.35	3.21	18.21	18.52	18.30
	I	21	-1.88	-1.88	-2.00	3.89	3.96	3.73	3.93	3.21	3.33	18.34	18.05	18.44
SV	r	19	-3.38	-3.75	-3.87	3.22	3.80	3.78	3.48	3.46	3.36	18.68	17.88	18.00
	I	19	-4.13	-4.38	-4.38	3.85	3.69	3.66	3.47	3.84	3.76	17.37	17.67	17.99
SC	r	19	0.38	0.50	0.50	3.97	3.63	3.50	3.50	3.73	3.72	15.61	15.86	16.01
	I	19	0.50	0.38	0.50	3.76	3.79	3.60	3.76	3.59	3.66	15.58	15.65	15.95
SM	r	21	-0.75	-1.00	-1.25	3.76	3.92	3.73	3.39	3.67	3.40	17.74	17.42	17.93
	I	21	-0.75	-1.13	-1.25	3.99	3.93	3.80	3.51	3.47	3.50	17.49	17.58	18.12

SiJ	r	20	-0.88	-0.88	-1.00	3.93	3.94	3.95	3.77	3.71	3.83	16.07	15.99	16.15
	l	20	-0.50	-0.75	-0.88	3.62	3.87	3.94	3.82	3.67	3.86	16.42	15.83	16.10
SG	r	19	0.00	0.25	0.00	3.87	3.85	3.66	3.70	3.59	3.67	16.25	16.36	16.51
	l	19	-0.25	0.00	-0.38	3.65	4.01	3.89	3.71	3.63	3.76	16.78	16.42	16.61
VP	r	25	-1.88	-1.75	-1.75	4.00	3.86	3.86	3.21	3.35	3.21	18.21	18.52	18.30
	l	25	-1.88	-1.88	-2.00	3.89	3.96	3.73	3.93	3.21	3.33	18.34	18.05	18.44
ZB	r	20	0.50	0.38	0.38	3.71	3.99	3.86	3.85	3.64	3.72	15.54	15.81	15.88
	l	20	0.50	0.50	0.50	3.85	4.02	3.85	3.68	3.50	3.72	15.75	16.02	16.07
CF	r	23	0.50	0.50	0.50	3.66	3.70	3.70	3.73	3.62	3.62	16.45	16.48	16.48
	l	23	0.38	0.50	0.38	3.56	3.55	3.55	3.57	3.45	3.45	16.95	17.00	17.00
HN	r	18	-4.38	-4.50	-4.38	3.80	3.42	3.42	5.04	3.78	3.78	16.63	17.91	17.91
	l	18	-4.13	-4.25	-4.13	3.80	3.98	3.98	5.04	3.76	3.76	16.63	16.65	16.65
KM	r	18	0.25	0.50	0.50	3.28	3.25	3.14	3.79	3.79	3.82	16.25	16.10	16.49
	l	18	0.50	0.50	0.50	3.21	3.12	3.09	3.85	3.79	3.86	15.96	16.15	15.99
JC	r	18	0.25	0.25	-0.13	3.67	3.71	3.40	3.77	3.63	3.71	16.18	15.97	16.31
	l	18	-0.25	-0.25	-0.37	3.67	3.58	3.67	3.55	3.81	3.53	16.29	15.71	16.16
CJ	r	23	0.00	0.00	-0.13	3.70	3.49	3.46	3.97	3.85	3.87	15.98	15.65	15.85
	l	23	0.00	-0.13	-0.25	3.58	3.77	3.50	4.09	3.87	4.09	15.74	15.26	15.46
DT	r	28	0.50	0.50	0.63	3.86	3.80	3.86	4.14	4.14	4.14	15.73	15.76	15.93
	l	28	0.50	0.50	0.50	3.89	3.85	3.89	4.07	4.10	4.07	15.47	15.50	15.67
JF	r	24	-4.38	-4.50	-4.50	3.95	3.90	3.88	3.54	3.49	3.56	17.75	17.59	18.07
	l	24	-3.63	-3.50	-4.00	3.97	3.96	3.85	3.47	3.51	3.37	17.48	17.47	17.79
DS	r	27	-0.75	-0.88	-0.88	4.02	4.02	3.88	3.95	3.92	3.88	17.05	17.14	17.49
	l	27	-1.13	-1.13	-1.13	3.93	4.01	3.93	4.12	3.96	4.09	17.28	17.24	17.44
EM	r	20	0.13	0.63	0.63	3.83	3.76	3.76	3.78	3.83	3.83	14.92	14.98	14.98
	l	20	0.25	0.50	0.50	3.79	3.80	3.80	3.73	3.84	3.84	15.32	15.04	15.04
At	r	20	-3.63	-3.75	-3.75	3.98	3.93	3.78	3.34	3.42	3.41	18.13	17.98	18.31
	l	20	-3.63	-3.63	-3.88	3.95	3.91	4.02	3.54	3.42	3.55	17.81	17.97	18.17
RC	r	19	0.25	0.00	-0.12	3.77	3.97	3.68	3.41	3.36	3.25	16.58	16.69	16.86
	l	19	0.00	-0.25	-0.37	3.93	3.89	3.87	3.30	3.46	3.42	16.73	16.62	16.94
AM	r	18	0.25	0.38	0.13	3.59	3.52	3.12	3.59	3.63	3.66	16.15	16.43	16.55
	l	18	0.25	0.38	0.13	3.25	3.25	3.38	3.72	3.61	3.65	15.93	16.18	16.48
ND	r	19	0.50	0.50	0.50	3.90	3.90	3.81	3.42	3.33	3.40	16.45	16.43	16.65
	l	19	0.38	0.38	0.50	3.91	3.84	3.80	3.35	3.45	3.42	16.43	16.21	16.53

Es (D) = subjective refractive error; ACD (mm) = anterior chamber depth (ultrasound); Lr (mm) = lens thickness (ultrasound) and VD (mm) = vitreous depth (ultrasound).

Division of Optometry
Aston University
Birmingham, B4 7ET
0121 359 3611 x 5100

10th July 1998

Dear Dr Trafford,

The purpose of this letter is to seek your advice and request permission to include some of the children, at Wolverhampton Grammar School, in a research study on the development of short-sightedness (myopia). The study requires the participation of children aged between 11-14 years who currently do not wear any spectacles or have only recently started to wear spectacles for myopia.

The aim of the study is to monitor the progression of myopia and to find out whether it can be related to particular eye measurements. Previous research has demonstrated that a link exists between the length of the eye and the curvature of the front surface of the eye. The results of the study will help our understanding of how certain eye measurements can be used to predict which children may become myopic. A number of basic eye measurements will have to be taken, including a full eye examination. The measurements will be taken and supervised by qualified optometrists, using conventional procedures, and some procedures will involve the use of eye drops.

The study has been given approval by the Human Science Ethical Committee of Aston University and a parallel study is being carried out on the first year Optometry undergraduates at the university.

We hope to follow the progression of the children over a 2 year period. The following is a list of measurements to be recorded:-

1. Shape of the front of the eye

Several instruments, which are regularly used in general optometric practice, will be used to assess the curve and the shape of the front of the eye.

2. Refractive power of the eye

The test will measure the amount of long- or short-sightedness using the same tests used in a normal eye examination.

3. Length of the eye

A standard clinical technique will be performed to measure the length of the eyes.

We envisage that the children would find the instruments and the taking of measurements both interesting and informative. Professor Gilmartin and I would appreciate the opportunity to arrange a meeting with you, to explain in more detail the techniques and instruments to be used. If you have any queries, please contact Professor Gilmartin or myself on the above telephone number.

Yours sincerely,

Miss Justine Love Bsc (Hons), MCOptom. - Clinical Demonstrator.
Bernard Gilmartin PhD; Bsc (Hons); FCOptom; F.A.A.O. - Professor of Optometry.

1st July 1998

Dear Parent,

The purpose of this letter is to request permission to include your child in a research study on the development of short-sightedness (myopia).

The study requires the participation of children aged between 6-11 years who currently do not wear any spectacles or have only recently started to wear spectacles for myopia. The aim of the study is to monitor the progression of myopia and to find out whether it can be related to particular eye measurements.

The study has been given approval by the Human Science Ethical Committee of Aston University and a parallel study is being carried out on the first year Aston optometry undergraduates. A number of basic eye measurements will be taken, including a full eye examination. The measurements will be taken and supervised by qualified optometrists (opticians), using conventional procedures, and will involve the use of eye drops. We will be following the progression of the children over a 2 year period. The following measurements will be recorded:-

1. Shape of the front of the eye

Several instruments, which are regularly used in general optometric practice, will be used to assess the curve and the shape of the front of the eye.

2. Refractive power of the eye

The test will measure the amount of long- or short-sightedness using the same tests used in a normal eye examination.

3. Length of the eye

A standard clinical technique will be performed to measure the length of the eyes.

We envisage that the children will find the instruments and the taking of measurements both interesting and informative. The research will help our understanding of how certain eye measurements can be used to predict which children may become myopic. Professor Gilmartin and I are planning to visit the school on Thursday 9th July (7.00-8.00pm) to explain fully, with a demonstration, the techniques and measurements to be used. We trust that you will be able to join us and to ask any questions that you may feel appropriate. Please complete the reply slip enclosed, on behalf of your child, and return it to the school. Please return the reply slip by Wednesday 8th July.

Thankyou
Yours sincerely,

Miss Justine Love Bsc (Hons), MCOptom. - Clinical Demonstrator.
Bernard Gilmartin PhD; Bsc (Hons); FCOptom; F.A.A.O. - Professor of Optometry.

REPLY SLIP

I will/will not be attending the meeting to discuss the myopia research project on
Thursday 9th July at 7.00pm

NAME OF PARENT.....

NAME OF CHILD.....

CLASS.....

APPENDIX 3 – University Ethical Committee forms and consent forms

ASTON UNIVERSITY

PROJECT NO.....

THE SENATE

REG/97/130

HUMAN SCIENCE ETHICAL COMMITTEE

Application for approval of a research project involving human volunteers

Please read the enclosed guidelines before completing this form - in typescript or black ink - and return the form to: The Secretary of the Human Science Ethical Committee, Registry. If you intend to administer or expose subjects to a physical procedure other than simple venepuncture you must also submit an experimental protocol.

Project title:

Ocular biometric correlates of early- and late-onset myopia in young adults.

Investigators:	Department /address:	Telephone:
Justine Love	Vision Sciences	0121 359 3611 x 5175
.....	
Dr B Gilmartin	Vision Sciences	0121 359 3611 x 5159
.....	
.....	
.....	
.....	

A

Details of sponsoring/collaborating organisation (if any)

1. Name: Not Applicable
2. Does the sponsoring/collaborating organisation provide insurance?
YES/NO*
3. If drugs are used, do any require a clinical trials certificate or clinical trials exemption certificate?
YES/NO*

***If yes, please provide a copy of the certificate**

B

Summary of project

1. Starting date: 01/01/98
2. Duration: 2.5 years
3. Location: Division of Optometry, Aston University.
4. Physical procedures:

Myopia occurs when axial elongation is not fully compensated for by the flattening of the cornea or lens, or both. A relationship has been previously reported between myopia, axial length and the corneal radius of curvature.

Biometric measurements will be taken during the period when myopic changes in children are most probable, that is between 8 and 13 years of age. The following measurements will be taken:-

1. *Corneal radius of curvature* - assessed using the Bausch and Lomb keratometer.
2. *Corneal topography* - using the EyeSys 2000 Corneal Analysis System.
3. *Peripheral refraction* - assessed with the Canon IR autorefractor.
4. *Objective and subjective refraction* - using the topically applied ocular drug aqueous tropicamide (1%) in single-dose applicators (*Minims*, Chauvin Pharmaceuticals).
5. *A-Scan ultrasound* - readings produced by 10Mhz A-Scan ultrasound. Recordings are taken through the subject's cornea and hence a topical anaesthetic (0.4% Benoxinate) will be required.
6. *Scheimpflug slit lamp camera* - for comparison of cross-sectional images of the anterior chamber with the ultrasound results.
7. *Oculomotor assessment* - subjective measurements of accommodation and convergence using the RAF rule.

5. Substances to be administered (a substance is anything other than normal food. Chemical constituents of food stuffs, ethanol and variation of the diet should be included here):

- 1) Tropicamide which is a topically applied ocular drug. The drug is a synthetic antimuscarinic which has been used routinely in general optometric practice for many years and produces mydriasis and cycloplegia. Two drops of 1% tropicamide will be administered with a five minute period between the drops. Mild cycloplegia occurs after approximately 15 minutes and the full amplitude of accommodation returns after 6 hours although mydriasis may remain for another hour or two.

- 2) Benoxinate which is a topically applied ocular drug. The drug produces corneal anaesthesia, for use with the A-scan ultrasound, and is used routinely in general optometric practice. One drop of 0.4% benoxinate will be administered to both eyes and anaesthesia occurs after 30 seconds and recovers after 20 minutes.

6. Psychological assessment: Not Applicable

7. Questionnaires: (only to be completed when project contains questionnaire(s) which fall within the types of questionnaire requiring HSEC approval [Guidelines D(3)])

A history will be taken of any first degree relatives who suffer with myopia and the subjects will be asked to provide an estimate of the number of hours per week undertaking close work.

C

Subjects

1. Number of subjects to be used: 100
2. Over what time span? 2.5 years
3. Age of subjects: 16-28 years
4. Sex of subjects: Male and Female
5. Source:
Undergraduate students in the Division of Optometry
6. Will payments be made to the subjects and if so, how much will each be paid?
There will be no payment: subjects will receive a standard eye test and ocular health check..
7. Are the subjects patients or healthy volunteers? (If patients, give diagnosis, clinic/responsible practitioner).
Healthy volunteers.
8. Will any subjects be excluded and if so, on what grounds?

Subjects will be excluded if they present with the following:-

1. Hypermetropia - where the spherical equivalent refraction is greater than +0.50D
 2. Astigmatism greater than -2.00D
 3. Strabismus or amblyopia
 4. Gas permeable or hard contact lens wearers
 5. Ocular disease
 6. Systemic disease that may influence the results.
 7. Prescribed medication that may influence the results.
9. Is the activity of the subject to be restricted in any way before or after the procedure? (e.g. diet, driving).

Owing to the mydriasis and cycloplegia, induced by the instillation of tropicamide (mentioned previously), the subjects may observe slight blurring of vision. Extra care will be suggested to the subjects when undertaking their normal activities during the rest of the day, e.g. driving and cycling.

The subjects will be advised not to rub their eyes or to go into any windy or dusty environments for 20 minutes after the anaesthetic, benoxinate, has been instilled because the subject will not be able to feel any foreign bodies entering the eye.

10. Consent: Please attach a copy of the consent form you intend to use, detailing how procedures and hazards will be explained.
Consent form is attached.

D

Hazards

1. Please give full details of any hazards which could affect the health, safety or welfare of any subject.

The induced mydriasis and cycloplegia may produce blurred vision and photophobia (glare). There is also a minimal risk of causing acute closed angle glaucoma. However, this condition has an incidence of 1 in 10000 people over the age of 40. Driving is prohibited for at least 2 hours after the session has concluded.

Benoxinate produces a short-lived slight stinging on instillation. In around 1 in 1000 subjects (usually over 50 years of age) a localised or diffuse corneal desquamation may occur reducing visual acuity. However, the corneal epithelium regenerates spontaneously.

2. How do you propose to minimise these hazards?

To overcome the blurred vision and glare, the subjects will be advised to rest for a 1/2 to 1 hour after the drops are instilled.

To minimise the very small risk of acute closed angle glaucoma, the subject's intraocular pressure and anterior chamber angles will be assessed before the drops are instilled. The intraocular pressure will be recorded again after the drops have been instilled. An increase in the intraocular pressure of more than 5 mmHg indicates a possibility of acute angle glaucoma. In this case the subject would be closely monitored and referred immediately to the eye department located at the nearest hospital, if required.

The visual acuity and corneal integrity will be checked after benoxinate has been instilled, and before proceeding with A-scan ultrasounography, to check for corneal desquamation. A drop will only be placed in one eye, and the eye will be checked, before continuing on the other eye. The recovery from corneal desquamation can be helped with artificial tears.

3. Is there any precedent for these experiments? If so, please give details with references if possible.

Instillation of tropicamide has been a standard procedure in the optometric teaching programme and general open clinic for many years. Please see previous Ethical Committee records for acceptance of 87(vii) June 1987; 86B/87(x) February 1986 and 87(xi) June 1987.

4. Has this project been considered/is it being considered by any other Ethical Committee? If so, please give details and decision made.

No

**E
STATEMENT BY NAMED INVESTIGATORS, HEAD OF DEPARTMENT AND (if necessary) RESEARCH SUPERVISOR**

I consider that the details given constitute a true summary of the projects and that the hazards and potential risks to any subject are accurately described.

Investigator.....
date.....

HUMAN SCIENCE ETHICAL COMMITTEE

CONSENT FORM FOR VOLUNTEER SUBJECTS

PROJECT TITLE

Ocular biometric correlates of early- and late-onset myopia in young adults.

RESEARCH WORKERS AND DEPARTMENT RESPONSIBLE

Miss J Love BSc (Hons) MCOptom, Division of Optometry.
Dr B Gilmartin PhD; BSc (Hons); FCOptom; FAAO, Division of Optometry.

EXPLANATION OF ANY POSSIBLE HAZARDS AND THE PROCEDURES TO BE USED

The purpose of the study is to take a series of eye measurements during the period when children are most likely to develop myopia (short-sightedness). Measurements will be taken every 5-6 months over a 2 year period. The following measurements will be recorded:-

1. *Corneal radius of curvature* - this will require the patient to sit in front of an instrument which can measure the radius of curvature of the cornea (the front surface of the eye) using reflected light. The instrument does not touch the eye or induce any discomfort and provides an accurate and repeatable measure of the central 3mm of the cornea. The procedure is simple and is commonly used in general optometric practice.
2. *Corneal topography* - this instrument measures both the central and peripheral (beyond the central 3mm) radii of curvature of the cornea. An accurate and repeatable map of the corneal shape can be produced. The instrument does not touch the eye or induce any discomfort.

3. *Objective and subjective refraction* - refraction is the process of measuring and correcting any short-sightedness or long-sightedness in the eyes. Subjective refraction requires the subject to read letters on a chart whilst looking straight ahead and answering simple questions about the clarity of the letters. The routine is the same as that demonstrated in a general eye examination. The subject also looks straight ahead during an objective refraction but an automated refracting machine measures the amount of short- or long-sightedness in the eyes. The instrument does not touch the eye or induce any discomfort, although eye drops will have to be used during this part of the test to enlarge the pupils.
4. *Peripheral refraction* - as mentioned above, normal refraction requires the subject to look straight ahead whereas peripheral refraction requires the subject to look off-centre and slightly to one side by varying amounts. Measurements are taken using an automated refracting machine. The instrument does not touch the eye or induce any discomfort, although eye drops will have to be used during this part of the test to enlarge the pupils.
5. *A-Scan ultrasound* - this technique is used to take measurements of the eye, such as, the length from the front surface of the eye to the back surface. One drop of 0.4% benoxinate will be administered to both eyes. Benoxinate is a corneal anaesthetic which allows the ultrasound probe to be placed lightly on the front surface of the eye for measurements to be taken.
6. *Scheimpflug slit lamp camera assessment* - this instrument provides an image of the front section of the eye allowing ocular measurements to be taken. The subject will look towards a small target light on the instrument while the measurements are being taken. The instrument does not touch the eye or induce any discomfort, although eye drops will have to be used during this part of the test to enlarge the pupils.
7. *Oculomotor assessment* - these are measurements pertaining to the movement of the eyes. The subject will observe a number of simple instruments and tests which will allow the assessment of how well the eyes work together and on their own. The tests and instruments are exactly the same as those demonstrated in a general eye examination.

The above measurements will be taken using instruments and techniques that are used regularly in general optometric practice and in other research projects. For an accurate measurement of the refraction to be obtained, the pupil must be dilated with two drops of 1% tropicamide. The drops are instilled into the eye using sterile single-dose applicators (*Minims*). Previous studies and trials with this substance indicate that the risks associated with it are minimal (especially in children). Tropicamide is used regularly in general optometric practice and may produce slightly blurred vision for approximately 45 minutes after the drops have been instilled. The blurred vision improves after 45 minutes although the pupil remains dilated for approximately 6-8 hours and this may cause mild sensitivity to bright lights. For these reasons, it is advisable for the subject to rest after the measurements have been taken for $\frac{1}{2}$ to 1 hour. There is a minimal risk of inducing acute closed angle glaucoma. However, this

condition has an incidence of 1 in 10000 people over the age of 40. Driving is prohibited for at least 2 hours after the session has concluded.

For accurate ultrasound measurements to be taken, one drop of the corneal anaesthetic benoxinate must be administered to each eye. Anaesthesia occurs after 30 seconds and recovers after 20 minutes. Benoxinate is used regularly in general optometric practice for measuring intraocular pressure in the eye. It is advisable not to enter windy or dusty environments or rub the eyes up to 20 minutes after the drops have been instilled because subjects will not feel dust or fragments in the eye.

You will be asked about any allergy or hypersensitivity to any general medication or ophthalmic drugs before the measurements are taken or drops instilled. Medication being taken by the subject must also be reported at the first visit.

Please ensure that you have read all of the information on this sheet and ask any questions before signing the consent form.

CONFIDENTIALITY OF INFORMATION

The confidentiality of personal information and the anonymity of all subjects involved in this investigation will be preserved in the following way:

All subjects will be numbered rather than named. Data will be stored on computer and comply with the Data Protection Act.

VOLUNTEER'S STATEMENT

I have read and understood the above explanation. I have had the opportunity to discuss it with the investigators and to ask any questions. I agree _____ to take part in the above project and I understand that I am free to withdraw at any time.

Signed:

Dated:

JGW/HSEC
1.10.97

APPENDIX 4 – Calculations and computer programs relating to the thesis

Calculation of mean refractive error from repeat readings

REM calculation of mean refractive errors

REM automatic calculation of sturm's interval and sagittal rx

start:

CLS

INPUT "number of repeat readings (maximum 9)"; rep

summre = 0: sumc0 = 0: sumc45 = 0

FOR doop = 1 TO rep

REM input data

CLS

PRINT "reading"; doop: PRINT

INPUT "sphere (D)"; s

INPUT "cylinder (D)"; c

INPUT "axis"; a

REM astigmatism decomposition

mre(doop) = s + (c / 2)

c0(doop) = c * COS((2 * a) * .0174532)

c45(doop) = c * SIN((2 * a) * .0174532)

REM sum data

REM calculate mean

summre = summre + mre(doop)

sumc0 = sumc0 + c0(doop)

sumc45 = sumc45 + c45(doop)

NEXT doop

REM calculate mean

meanmre = summre / rep

meanc0 = sumc0 / rep

meanc45 = sumc45 / rep

REM astigmatism recomposition

c = -SQR(meanc0 ^ 2 + meanc45 ^ 2)

a = (ATN((c - meanc0) / meanc45)) / .0174532

IF a < 0 THEN a = a + 180

s = meanmre - (c / 2)

REM printout

CLS

PRINT "mean sphere="; s

PRINT "mean cylinder="; c

PRINT "mean axis="; a

REM automatic conversion to sturm's interval and sag rx

REM convert to crossed cyl

cyla = s

cylob = s + c

REM locate sag rx

sagrx = cyla

```

tanrx = cylb
IF a < 45 THEN sagrx = cylb
IF a < 45 THEN tanrx = cyla
IF a > 135 THEN sagrx = cylb
IF a > 135 THEN tanrx = cyla

REM find sign of sturm's interval
IF sagrx > tanrx THEN c = -c
IF sagrx < tanrx THEN c = c

REM printout
PRINT
PRINT "sturm's interval="; c
PRINT "sagittal refraction="; sagrx

PRINT : INPUT "another set of values(press return) or no (press 1)"; xyz
IF xyz = 0 THEN GOTO start
END

```

Calculation of mean tangential 'K' from repeat measurements

```

REM calculation of mean k readings
REM automatic derivation of tangential k

start:
CLS
INPUT "number of repeat readings (maximum 9)"; rep
summre = 0: sumc0 = 0: sumc45 = 0
FOR doop = 1 TO rep

REM input data
CLS
PRINT "reading"; doop: PRINT

REM data entered in x-cyl form
INPUT "flattest k"; fk
INPUT "along axis"; fa
INPUT "steepest k"; sk
INPUT "along axis"; sa

REM convert to spherocylinder
s = fk
c = sk - fk

REM calculate mean axis
IF fa > sa THEN sa = sa + 90
IF fa < sa THEN sa = sa - 90
a = (fa + sa) / 2
IF a <= 0 THEN a = a + 180

REM astigmatic decomposition
mre(doop) = s + (c / 2)
c0(doop) = c * COS((2 * a) * .0174532)
c45(doop) = c * SIN((2 * a) * .0174532)

REM sum data
summre = summre + mre(doop)
sumc0 = sumc0 + c0(doop)
sumc45 = sumc45 + c45(doop)

```

NEXT doop

REM calculate mean
meanmre = summre / rep
meanc0 = sumc0 / rep
meanc45 = sumc45 / rep

REM astigmatic decomposition
c = -SQR(meanc0 ^ 2 + meanc45 ^ 2)
a = (ATN((c - meanc0) / meanc45)) / .0174532
IF a < 0 THEN a = a + 180
s = meanmre - (c / 2)

REM convert to x-cyl
cyla = s
cylb = s + c

REM locate tangential k
tank = cylb
IF a < 45 THEN tank = cyla
IF a > 135 THEN tank = cyla

REM printout
PRINT
PRINT "tangential k="; tank

PRINT : INPUT "another set of values (press return) or no (press 1)"; xyz
IF xyz = 0 THEN GOTO start
END

RetinaFit

REM incorporates meridional coddinton backtrace as in (8)
REM setup for all multiple field angles as in (8)
REM automatic peripheral astigmatism/refraction as in (7)
REM set up for direct biometry entry as in (5)
REM trace specific field angles as in (3)
REM set up for raytrace as in (2)
REM incorporates ray/aspheric (1)
REM finds retinal coordinates

REM input biometric parameters

INPUT "refractive error(sagittal meridian)[D]"; s11
INPUT "cylinder(wtr=-ve)[D]"; cyl

REM adjust value for central astigmatism
l1 = s11 - cyl: PRINT "adjust refractive error"; l1

INPUT "radius of cornea (tangential meridian) [mm]"; r1
f1 = 333.3 / r1
INPUT "anterior chamber depth[mm]"; dd1
d1 = dd1 / 1000

REM routine to deal with low acd's
changegain = .9975
IF dd1 < 3 THEN INPUT "change acd gain (suggest 0.8)"; changegain

INPUT "lens thickness [mm]"; dd3
d2 = dd2 / 1000

```
INPUT "vitreous chamber depth [mm]"; dd3
d3 = dd3 / 1000
```

REM assumed refractive indices

```
n1 = 1
n2 = 1.3333
n3 = 1.416
n4 = 1.3333
```

REM bennett (1988) computing scheme

```
mrX = l1
l1b = l1 + f1
c = l1b
e1 = .596 * d2
e1b = -.358 * d2
w = d1 + e1
l2 = l1b / (1 - ((w / n2) * l1b))
s = l2
o = -e1b + d3
l2b = n2 / o
l = l2b
cc = (c / l) * 100
ss = ((s - c) / l) * 100
ll = ((l - s) / l) * 100
f1 = l2b - l2
m = (w / n2) * (f1 * f1)
n = f1 + f1
fe = n - m
```

REM royston (1990) addition

```
f2 = .38 * f1
r2 = 82.7 / f2
f3 = -(f2 * e1) / e1b
r3 = -82.7 / f3
```

```
pi = 3.1415926535897#
```

REM calculation of peripheral refraction

REM communication for main program

```
r = r1
acd = dd1
alr = r2
lt = dd2
plr = r3
vitr = dd3
```

REM allow multiple field angles
REM field angle input cycle

```
fieldangle:  
CLS
```

```
faloop = 1  
rerun1 = 0: retrun = 0  
INPUT "external angle"; U(faloop)  
INPUT "measured interval of sturm at this angle (D)"; msturm(faloop)  
msturm(faloop) = msturm(faloop) - cyl
```

```

INPUT "measured sagittal refraction at this angle (D)"; msagrx(falooop)
msagrx(falooop) = msagrx(falooop) - cyl

REM field angle computation cycle

falooop = 1
U = U(falooop): msturm = msturm(falooop): msagrx = msagrx(falooop)
CLS : PRINT "altering corneal conic constant to match interval of sturm"

REM set up initial ocular parameters
REM conic constant of cornea (adjusted to match sturm)

REM set conic values
conagain = 0
setconic:
conicnmax = 9

conicspan = 6
IF conagain = 1 THEN INPUT "default conic span=6,input new value"; conicspan

conicstart = 3
IF conagain = 1 THEN INPUT "default conic start value=3, input new value"; conicstart

conicincr = conicspan / conicnmax
FOR conicloop = 1 TO conicnmax
p(conicloop) = conicstart - (conicloop * conicincr)
p = p(conicloop)

REM retinal radius (adjusted to match sagittal)
retr = -12

rollonloop = -1
rollon:
rollonloop = rollonloop + 1
REM set initial ray parameters
d = -10000
h = TAN(U / (180 / pi)) * 10003.026649#
REM speeds up convergence for field angles
IF SQR(U ^ 2) = 10 THEN h = 1763.806885#
IF SQR(U ^ 2) = 20 THEN h = 3640.803952#
IF SQR(U ^ 2) = 30 THEN h = 5775.230872#
IF SQR(U ^ 2) = 40 THEN h = 8393.466582999999#
IF SQR(U ^ 2) = 50 THEN h = 11920.963276#
IF SQR(U ^ 2) = 60 THEN h = 17325.332731#

IF rollonloop > 0 THEN h = halter

REM loop for x until ray and surface y values equal

REM calculate start value for x (based upon spherical surface)
REM use ray tracing scheme of w.j.smith (1966)

searchloop = -1
search:
searchloop = searchloop + 1
sinu = SIN(U / (180 / pi))
cosu1 = SQR(1 - (sinu ^ 2))
s = d
q = (h * cosu1) + (s * sinu)
sini = (q * (1 / r)) - sinu

```

```

cosi = SQR(1 - (sinu ^ 2))
sinuplusi = (sinu * cosi) + (cosu1 * sini)
x = (q * sinuplusi) / (cosu1 + cosi)
IF searchloop > 0 THEN x = xalter

round:
REM equation of ray
yray = h + (TAN(-U / (180 / pi)) * (-d + x))

REM equation of aspheric surface
ysurf = SQR((2 * r * x) - (p * (x ^ 2)))

REM compare ray from ray and surface
ydiff = yray - ysurf
absydiff = SQR(ydiff ^ 2)
IF absydiff < .000001 THEN GOTO printout

GOSUB fastloop1

REM printout
printout:
xalter = x

REM trace meridional ray through cornea
REM initial q and sinu known
REM need to find curvature at intersection point (sagittal)
rsag = SQR(r ^ 2 + ((1 - p) * (ysurf ^ 2)))
csag = 1 / rsag
rtan = (rsag ^ 3) / (r ^ 2)
ctan = 1 / rtan

REM refraction at cornea
c = ctan
n = n1
nn = n2

GOSUB refract
cosi1 = cosi
cosii1 = cosii
cosuu1 = cosuu
x1 = x

REM modified coddington trace for aspheric cornea
REM oblique surface powers (sagittal and tangential)
ospsag = csag * ((n2 * cosii) - (n1 * cosi))
flospsag = ospsag
osptan = ctan * ((n2 * cosii) - (n1 * cosi))
flosptan = osptan

REM intercept with optic axis
ll = qq / sinuu

REM compare intercept with acd
intdiff = acd - ll
absintdiff = SQR(intdiff ^ 2)
IF absintdiff < .000001 THEN GOTO printout2

GOSUB fastloop2

REM printout2
printout2:

```

```

REM printout internal angle (inverse sine)
intang = (ATN((SQR(1 - cosuu ^ 2)) / cosuu)) * (180 / pi)
halter = h

```

```

REM transfer to anterior lens
t = acd
GOSUB transfer

```

```

REM refraction at anterior lens
c = 1 / alr
n = n2
nn = n3
GOSUB refract
cosi2 = cosi
cosii2 = cosii
cosuu2 = cosuu
x2 = (q * sinuplusi) / (cosu1 + cosi)
d = (acd - x1 + x2) / cosuu1
dcal = d
osp = c * ((n3 * cosii) - (n2 * cosi))
f2ospsag = osp
f2osptan = osp

```

```

REM transfer to posterior lens
t = lt
GOSUB transfer

```

```

REM refraction at posterior lens
c = 1 / plr
n = n3
nn = n4
GOSUB refract
cosi3 = cosi
cosii3 = cosii
cosuu3 = cosuu
x3 = (q * sinuplusi) / (cosu1 + cosi)
d = (lt - x2 + x3) / cosuu2
dalpl = d
osp = c * ((n4 * cosii) - (n3 * cosi))
f3ospsag = osp
f3osptan = osp

```

```

REM transfer to retina
t = vitr
GOSUB transfer

```

```

REM calc retinal intersection coordinates

```

```

seelight:
c = 1 / retr
sini = (q * c) - sinu
cosi = SQR(1 - (sini ^ 2))
sinuplusi = (sinu * cosi) + (cosu1 * sini)
cosuplusi = (cosu1 * cosi) - (sinu * sini)
x4 = (q * sinuplusi) / (cosu1 + cosi)
y = (q * (1 + cosuplusi)) / (cosu1 + cosi)
d = (vitr - x3 + x4) / cosuu3
dplr = d

```

```

REM peripheral refraction calc (mer/codd backtrace)

```

REM start from retina

```
s = dplr
t = dplr
ss = n3 / ((n4 / s) - f3ospsag)
tt = (n3 * (cosi3 ^ 2)) / (((n4 * (cosii3 ^ 2)) / t) - f3osptan)
```

```
s = ss + dalpl
t = tt + dalpl
ss = n2 / ((n3 / s) - f2ospsag)
tt = (n2 * (cosi2 ^ 2)) / (((n3 * (cosii2 ^ 2)) / t) - f2osptan)
```

```
s = ss + dcal
t = tt + dcal
ss = n1 / ((n2 / s) - f1ospsag)
tt = (n1 * (cosi1 ^ 2)) / (((n2 * (cosii1 ^ 2)) / t) - f1osptan)
```

```
sagrx = 1000 / ss: sagrx(retinaloop) = sagrx
tanrx = 1000 / tt
sturm = sagrx - tanrx
```

```
IF retrun = 2 GOTO printout4
IF retrun = 1 GOTO retina
```

```
IF rerun1 = 0 THEN GOSUB conicloopdata
```

REM now think about retina

```
retagain = 0
setret:
retnmax = 9
```

```
retspan = 10
IF retagain = 1 THEN INPUT "default retina span=10,input new value"; retspan
```

```
retstart = -8
IF retagain = 1 THEN INPUT "default retina start value=-8,input new value"; retstart
```

```
retincr = retspan / retnmax
FOR retinaloop = 1 TO retnmax
retr(retinaloop) = retstart - (retinaloop * retincr)
retr = retr(retinaloop)
retrun = 1
GOTO seelight
retina:
NEXT retinaloop
GOSUB retinastuff
```

printout4:

REM fix decimal places and store data

```
sagrx(falooop) = (INT(sagrx * 10)) / 10
tanrx(falooop) = (INT(tanrx * 10)) / 10
sturm(falooop) = (INT(sturm * 10)) / 10
x4(falooop) = (INT(x4 * 100)) / 100
y(falooop) = (INT(y * 100)) / 100
p(falooop) = (INT(p * 10)) / 10
retr(falooop) = (INT(retr * 10)) / 10
```

REM field angle output cycle

```

CLS
REM print headings
fa$ = "angle"
sag$ = "sagittal"
tang$ = "tangential"
sturm$ = "sturm's interval"
x$ = "x retinal intercept"
y$ = "y retinal intercept"
p$ = "corneal conic constant"
r$ = "retinal radius"

REM peripheral refraction output
PRINT fa$, sag$, tang$, sturm$
PRINT U(falooop), sagrx(falooop), tanrx(falooop), sturm(falooop)
PRINT "", msagrx(falooop), "<measured>", msturm(falooop)

REM conic/retina output
PRINT fa$, p$, r$
PRINT U(falooop), p(falooop), "", retr(falooop)

REM retinal intercept output
PRINT fa$, x$, y$
PRINT U(falooop), x4(falooop), "", y(falooop)
PRINT : INPUT "another field angle (return) or stop (press 1)"; choice
IF choice = 0 THEN GOTO fieldangle
PRINT : PRINT : PRINT

END

REM subroutine:fastloop 1 (ray intercept with aspheric)
fastloop1:
diff1(count1) = ydiff
parameter = x
gain = changegain
accuracy = .000001
increment = .0000001#
IF count1 = 1 THEN GOSUB speedup1
IF count1 = 2 THEN GOSUB speedup1
GOSUB convergence1
RETURN

REM subroutine:speedup1
speedup1:
deltay = diff1(count1 - 1) - diff1(count1)
multipleparameter = diff1(1) / deltay
deltaparameter = (multipleparameter * gain) * increment
RETURN

REM subroutine:convergence1
convergence1:
IF count1 = 0 THEN deltaparameter = increment
count1 = count1 + 1
IF count1 > 2 THEN count1 = 0
IF diff1(count1) > accuracy THEN GOTO option11
IF diff1(count1) < -accuracy THEN GOTO option21
option11:
parameter = parameter + deltaparameter
x = parameter
GOTO round
option21:

```

```

parameter = parameter - deltaparameter: x = parameter
x = parameter
GOTO round
RETURN

```

```

REM subroutine:fastloop2 (ray intercept with pupil)

```

```

fastloop2:
diff2(count2) = intdiff
parameter = h
gain = 1
accuracy = .000001
increment = .0000001#
IF count2 = 1 THEN GOSUB speedup2
IF count2 = 2 THEN GOSUB speedup2
GOSUB converge2
RETURN

```

```

REM subroutine: speedup2

```

```

speedup2:
deltay = diff2(count2 - 1) - diff2(count2)
multipleparameter = diff2(1) / deltay
deltaparameter = (multipleparameter * gain) * increment
RETURN

```

```

REM subroutine:converge2

```

```

converge2:
IF count2 = 0 THEN deltaparameter = increment
count2 = count2 + 1
IF count2 > 2 THEN count2 = 0
IF diff2(count2) > accuracy THEN GOTO option12
IF diff2(count2) < accuracy THEN GOTO option22
option12:
parameter = parameter + deltaparameter
h = parameter
GOTO search
option22:
parameter = parameter - deltaparameter: x = parameter
h = parameter
GOTO search
RETURN

```

```

REM subroutine for conicloopdata

```

```

conicloopdata:
REM storage of conicloopdata
sturm(conicloop) = sturm
NEXT conicloop

```

```

REM conicloop printout

```

```

FOR conicloop = 1 TO conicnmax
xa(conicloop) = sturm(conicloop)
ya(conicloop) = p(conicloop)
PRINT "conic,sturm="; (INT(p(conicloop) * 10)) / 10, (INT(sturm(conicloop) * 10)) / 10
NEXT conicloop

```

```

PRINT "now check for extrapolation-required interval of sturm:"; msturm(falooop)

```

```

INPUT "alter conic values[press 1] or go ahead [return]"; conagain
IF conagain = 1 THEN GOTO setconic

```

```

CLS : PRINT "altering retinal curvature to match sagittal refraction"

```

```

REM curve fit sturm
REM polint prog
x = msturm
n = conicmax
DIM c(n), d(n)
ns = 1
dif = ABS(x - xa(1))
FOR i = 1 TO n
  dift = ABS(x - xa(i))
  IF dift < dif THEN
    ns = i
    dif = dift
  END IF
  c(i) = ya(i)
  d(i) = ya(i)
NEXT i
y = ya(ns)
ns = ns - 1
FOR m = 1 TO n - 1
  FOR i = 1 TO n - m
    ho = xa(i) - x
    hp = xa(i + m) - x
    w = c(i + 1) - d(i)
    den = ho - hp
    IF den = 0! THEN PRINT "abnormal exit"
    den = w / den
    d(i) = hp * den
    c(i) = ho * den
  NEXT i
  IF 2 * ns < n - m THEN
    dy = d(ns)
  ELSE
    dy = c(ns + 1)
  END IF
  ns = ns + 1
  y = y + dy
NEXT m
ERASE d, c

REM required conic constant
p = y

REM rerun to calc interval of sturm
rerun = 1
GOTO rollon

RETURN

REM subroutine for retina stuff
retinastuff:
REM printout retinaloop
FOR retinaloop = 1 TO retnmax
  xa(retinaloop) = sagrx(retinaloop)
  ya(retinaloop) = retr(retinaloop)
  PRINT "retina, sagittal="; (INT(retr(retinaloop) * 10)) / 10, (INT(sagrx(retinaloop) * 10)) / 10
NEXT retinaloop

PRINT "now check for extrapolation -required sagittal rx:"; msagrx(falooop)
INPUT "alter retina values [press 1] or go ahead [return]"; retagain
IF retagain = 1 THEN GOTO setret

```

```

REM curve fit sagittal refraction
REM polint prog
x = msagrx
n = retmax
DIM c(n), d(n)
ns = 1
dif = ABS(x - xa(1))
FOR i = 1 TO n
dift = ABS(x - xa(i))
IF dift < dif THEN
ns = i
dif = dift
END IF
c(i) = ya(i)
d(i) = ya(i)
NEXT i
y = ya(ns)
ns = ns - 1
FOR m = 1 TO n - 1
FOR i = 1 TO n - m
ho = xa(i) - x
hp = xa(i + m) - x
w = c(i + 1) - d(i)
den = ho - hp
IF den = 0! THEN PRINT "abnormal exit"
den = w / den
d(i) = hp * den
c(i) = ho * den
NEXT i
IF 2 * ns < n - m THEN
dy = d(ns)
ELSE
dy = c(ns + 1)
ns = ns - 1
END IF
y = y + dy
NEXT m
ERASE d, c

REM required retinal radius
retr = y

REM rerun to calc sagittal refraction
retrun = 2
GOTO seelight

RETURN

REM subroutine : refraction
refract:
sini = (q * c) - sinu
cosi = SQR(1 - (sini ^ 2))
sinuplusi = (sinu * cosi) + (cosu1 * sini)
cosuplusi = (cosu1 * cosi) - (sinu * sini)
sinii = (n * sini) / nn
cosii = SQR(1 - (sinii ^ 2))
sinuu = (sinuplusi * cosii) - (cosuplusi * sinii)
cosuu = (cosuplusi * cosii) + (sinuplusi * sinii)
qq = (q * (cosuu + cosii)) / (cosu1 + cosi)

```

RETURN

REM subroutine: transfer to next surface

transfer:

$q = qq - (t * \sin u)$

$\sin u = \sin uu$

$\cos u = \cos uu$

RETURN

APPENDIX 5 – Statistical analysis

In order to manage information efficiently, basic statistical analysis can be used to interpret the results and to derive conclusions. Information regarding statistical analysis was obtained from Hatch (1998), Norman and Streiner (1994), Fleming and Nellis (1994) and Armstrong *et al.* (2000) and personal communication with Dr R. A. Armstrong, lecturer, Aston University.

T test

A *t* test is a simple way of comparing the means of two groups. The test uses the *t* probability distribution, which is a set of distributions for sample sizes between 5 and infinity, instead of the normal distribution. The null hypothesis is used for the test which states that *there is no difference between the two means*. If two independent groups are compared, the *unmatched* formula must be used. The *matched* formula is used if the same group is examined before and after clinical intervention. A two-tailed statistical test is one that tests for difference in both directions. In the majority of cases the two-tailed approach is preferred. The *t* test provides a *p* value which corresponds to the probability of chance occurrence. If $p < 0.05$, the value is taken as statistically significant and there is a difference between the two means. If $p > 0.05$, the value is insignificant and there is no difference between the two means.

Simple regression and correlation analysis

Regression analysis deals with the *nature* of the relationship between variables. Correlation analysis is concerned with measuring the *strength* of the relationship between variables. Regression analysis can be applied in its simplest form to a scatter diagram consisting of a set of points of paired observations on two variables *x* and *y*. The aim of regression analysis is to derive an equation that describes a line that 'best fits' each set of plotted points. The aim of correlation analysis is to determine a summary measure of degree of correlation, i.e. amount of association between the two variables *x* and *y*. If the *y* variable increases as the *x* variable increases, *positive* correlation is evident. If the *y* variable decreases as the *x* variable increases, *negative* correlation is evident.

Regression analysis

Linear regression lines can be described by the equation for a straight line:

$$y = a + bx$$

Where,

y = dependent variable

x = independent variable

b = gradient

a = intercept (point at which the best fit line passes through the y axis)

The relationship between the x and y variables are rarely precise and the *best fitting regression line* between the points must be utilised. The best fitting regression line is determined using the criterion of *least squares* and the regression line is expressed as the *average* relationship between the two variables and is fitted as close as possible to the plotted points. The gradient coefficient b is then referred to as the *regression coefficient*.

Correlation analysis

Correlation is very closely linked to regression analysis. Whether the correlation is positive or negative depends upon whether the straight line (regression) through the points has a positive or negative slope. Correlation analysis provides a summary measure of the degree of correlation between x and y . This degree of correlation is denoted by r which is known as the *correlation coefficient*. The squared value of the correlation coefficient is the *coefficient of determination*, r^2 . This value describes the closeness of the relationship between the x and y variables, i.e. how closely do the points cluster around the regression line and provides an estimate of variation. Consequently, r^2 measures the proportion of total variation in y that is explained by the regression equation. The question of whether a strong or weak correlation exists between x and y cannot be simply answered by noting the size of r or r^2 ; a statistical table is required. Pearson's correlation coefficient table provides a numerical value of probability that the result occurred by chance.

Limitations of regression and correlation analysis

1. In the calculation of a regression equation, changes in x should not be necessarily taken as a *cause* for changes in y . Also a significant r value does not imply a causal relationship between the variables
2. The correlation coefficient, r , only tests whether a linear relationship is present. Some curved relationships may not produce a significant r value.
3. With a large number of variables (n), low values of r can still be significant.

Multiple regression analysis

Multiple regression analysis is an extension of the basic regression model but involves two or more independent variables to estimate the value of y . The multiple regression equation is described below,

$$y = a + b_1x_1 + b_2x_2 + b_3x_3 \dots + b_kx_k$$

Where,

y = dependent variable

$x_1, x_2, x_3 \dots x_k$ = independent variables

a = intercept

$b_1, b_2, b_3, \dots b_k$ = regression coefficients

Owing to the number of independent variables, the regression line is a line in multi-dimensional space and the calculations required for determining regression coefficients are complex. A solution to this problem is to use a computerised statistical program, such as, StatView.

As with simple regression, the coefficient of determination (r^2) provides a measure of information. An r^2 value of 0.45 would indicate that 45% of the variation in the dependent variable y is explained by variation in the independent variable x . In the case of multiple regression analysis a similar measure can be found which describes the *joint* variation of all the independent variables. This measure is known as the *multiple coefficient of determination* (R^2). The coefficient of multiple regression, denoted by R , is a measure of degree of association. However, R is rarely used and most attention is paid to R^2 .

The statistical significance of the multiple regression model can be tested using an F test and involves the R^2 value. The F statistic is explained as the ratio of the explained to the unexplained *variance*. The F test describes the overall explanatory power. The F test can be assessed, using critical F value tables, to find the probability of that value occurring by chance. If the F test value exceeds the critical F value, then we reject the null hypothesis, i.e. no difference and conclude that the overall regression is significant.

Limitations of multiple linear regression

1. Degree of intercorrelation between x variables – refers to the situation when some or all of the variables are highly correlated with one another and are therefore not independently distributed. A high degree of intercorrelation may result in the following:-
 - a) estimated regression coefficients may not be solely determined.
 - b) coefficients may fluctuate between samples
 - c) relative importance of individual variables may be less reliable.

Intercorrelation is inevitable in most regression analysis.

2. Errors in variables – refers to the case where measurement errors are included in the regression model. Measurement errors in the dependent variable are part of the error term and do not create a problem but errors in the independent variables can lead to bias and inconsistent parameter estimates.
3. Correlation does not necessarily imply causation.
4. Sample size – the ideal sample size (subject number) should be at least 5 to 10 times the number of independent variables. If the subject number is greater than the number of independent variables there is a high probability that a variable may be selected by chance Norman and Streiner, 1994.

Stepwise multiple regression analysis

The purpose of stepwise multiple regression analysis is to discover whether the introduction of another variable is statistically significant and clinically important. Statistical significance can be explained by the F test and clinical importance can be obtained by the new R^2 value that results from including the new variable. The simplest way of applying stepwise multiple regression is to set-up a database to include the y variable and the corresponding x variables and analyse using the specialist program, i.e. *StatView*. Variables are selected in the order of their power to explain additional

variance. At the end of every step, the program calculates the next best step for all variables not yet included in the equation. Ideally, stepwise multiple regression should only be used for exploratory investigations or as a screening exercise. Once significant variables have been detected, an hypothesis can be generated and further study or future projects are then required.

Correlation matrix

When a number of parameters need to be correlated against each other, a simple solution is to design a tabular matrix arrangement of the data. This can be produced in *Statview*.

Analysis of variance (ANOVA)

This test compares means, or more specifically variability, in 2 or more groups and is an extension of the *t* test. If the ratio of variability is high, there is a significant difference of variation between the groups. If the ratio is low, there is little difference of variation between groups. The test uses the null hypothesis which states that there is no significant difference between the group means. An ANOVA can be easily applied to data using the *Statview* computer software. If the results of the ANOVA show that the group means are significantly different, pairwise comparison of the data is advised in the form of a *post-hoc* test. A variety of methods are available for making *post-hoc* tests and they vary in sensitivity. A critical mistake is to make Type 1 error, i.e. to reject the null hypothesis when it is true.

Scheffé's 'S' test was used for statistical analysis in this thesis to assess pairwise comparisons for the following reasons:

1. Groups with unequal number of replicates can be assessed
2. The method does not assume equal variances in the groups
3. Protects against Type 1 error
4. Provides a conservative result

Measurement of repeatability

The current study involves detailed measurements of a number of ocular parameters. The issue of the repeatability of these measurements must not be ignored, especially in a study of longitudinal design. Repeatability can be assessed by calculating the difference in a measurement reading obtained on two separate occasions followed by analysis of distribution of the differences. The mean of the differences provides the *bias* and the degree of repeatability, also known as *limits of agreement*, is the mean difference ± 1.96 multiplied by the standard deviation of the differences (Zadnik *et al.*, 1992).

References:

- Armstrong, R. A., Slade, S. V. and Eperjesi, F. (2000). An introduction to analysis of variance (ANOVA) with special reference to data from clinical experiments in optometry. *Ophthalmic and Physiological Optics*, **20**, 235-241.
- Fleming, M. C. and Nellis, J. G. (1994). *Principles of Applied Statistics*, Routledge, London.
- Hatch, S. W. (1998). *Ophthalmic Research and Epidemiology*, Butterworth-Heinemann, Boston.
- Norman, G. R. and Streiner, D. L. (1994) In *Biostatistics: the bare essentials* Mosby, St Louis, USA.
- Zadnik, K., Mutti, D. O. and Adams, A. J. (1992). The repeatability of measurement of the ocular components. *Investigative Ophthalmology and Visual Science*, **33**, 2325-2333.

APPENDIX 6 – Data relating to corneal curvature and shape

Px	Eye	Age	Esc1	Esc2	Esc3	KJ	K2	K3	Ke1	Ke2	Ke3	ρ_1	ρ_2	ρ_3	Al/k1	Al/k2	Al/k3
AB	r	18	0.46	-0.01	-0.44	7.85	7.80	7.88	7.90	7.88	7.87	0.26	0.71	0.77	3.05	3.05	3.01
	l	18	0.25	0.34	0.31	7.83	7.86	7.82	7.98	7.91	7.93	0.00	0.75	0.75	3.07	3.07	3.05
AT	r	27	-1.08	-1.17	-1.15	8.24	8.22	8.22	8.30	8.29	8.29	0.82	0.82	0.82	3.06	3.11	3.05
	l	27	-1.21	-0.81	-0.72	8.15	8.13	8.13	8.22	8.22	8.23	0.76	0.75	0.70	3.09	3.08	3.11
AK	r	21	-0.23	-0.19	-0.28	8.09	8.09	8.10	8.23	8.22	8.27	0.79	0.79	0.73	3.07	3.02	3.01
	l	21	-0.20	0.01	-0.17	8.15	8.15	8.15	8.26	8.25	8.26	0.80	0.77	0.81	3.00	2.99	2.96
AD	r	19	-0.33	-1.26	-0.97	8.07	8.07	8.05	8.14	8.19	8.16	0.84	0.90	0.92	3.27	3.13	3.19
	l	19	-1.16	-1.01	-1.09	8.02	8.02	8.05	8.16	8.15	8.16	0.81	0.80	0.81	3.19	3.11	3.16
BS	r	19	-0.52	0.11	-1.15	7.80	7.80	7.78	7.92	7.89	7.88	0.94	0.90	0.90	3.07	3.05	3.02
	l	19	-1.06	-0.23	-0.66	7.75	7.72	7.72	7.79	7.75	7.80	0.86	0.87	0.83	3.00	3.05	3.03
BG	r	16	-1.13	-1.31	-1.66	7.98	7.95	7.95	8.09	8.09	8.11	0.71	0.70	0.77	3.04	3.06	3.05
	l	16	-0.68	-1.07	-1.28	7.95	7.94	7.94	8.06	8.12	8.07	0.77	0.59	0.81	3.04	3.01	3.02
DP	r	19	0.54	0.63	0.35	8.15	8.12	8.14	8.22	8.27	8.25	0.69	0.70	0.71	2.92	2.92	2.93
	l	19	-0.83	0.15	-0.31	8.07	8.07	8.09	8.16	8.17	8.16	0.75	0.77	0.63	2.95	2.96	2.96
DW	r	20	-1.25	-1.25	-1.25	7.40	7.40	7.45	7.50	7.48	7.46	0.76	0.71	0.88	3.10	3.10	3.07
	l	20	-1.21	-1.05	-1.23	7.45	7.40	7.40	7.56	7.48	7.51	0.59	0.60	0.69	3.06	3.08	3.09
DL	r	19	-2.58	-2.40	-2.76	7.72	7.66	7.65	7.69	7.69	7.68	0.69	0.72	0.76	3.11	3.12	3.12
	l	19	-2.16	-1.58	-2.01	7.62	7.64	7.65	7.66	7.68	7.72	0.80	0.70	0.66	3.11	3.05	3.10
GC	r	18	-0.48	-0.62	-0.65	7.62	7.67	7.72	7.75	7.76	7.78	0.83	0.83	0.83	3.12	3.08	3.10
	l	18	-0.41	-0.78	-0.89	7.60	7.64	7.67	7.73	7.72	7.75	0.75	0.79	0.84	3.15	3.14	3.13
GK	r	19	-0.79	-0.72	-0.91	7.92	7.84	7.85	7.94	7.95	7.99	0.78	0.90	0.90	3.08	3.06	3.10
	l	19	-1.85	-1.24	-1.43	7.80	7.81	7.79	8.00	7.94	7.91	0.91	0.86	0.81	3.12	3.11	3.18
Gke	r	23	-3.96	-3.28	-3.30	7.82	7.82	7.82	7.83	7.88	7.85	0.66	0.70	0.76	3.27	3.26	3.27
	l	23	-4.10	-3.33	-3.50	7.84	7.84	7.82	7.96	7.96	7.92	0.72	0.66	0.62	3.26	3.35	3.30
HS	r	18	-0.39	-0.56	-0.78	8.15	8.18	8.14	8.29	8.30	8.26	0.69	0.75	0.72	2.96	2.98	3.02
	l	18	-0.79	-0.62	-0.48	8.13	8.22	8.20	8.30	8.31	8.34	0.52	0.59	0.71	2.98	2.97	3.00
IP	r	24	0.73	0.62	0.69	8.00	8.02	8.00	8.08	8.10	8.10	0.88	0.90	0.88	2.99	2.95	2.99
	l	24	0.69	0.61	0.62	8.00	8.04	8.00	8.09	8.07	8.09	0.83	0.80	0.87	2.96	2.95	2.99
JS	r	21	0.29	0.10	0.25	7.60	7.79	7.78	7.85	7.85	7.87	0.86	0.85	0.86	3.03	2.96	2.96
	l	21	0.07	-0.20	0.49	7.73	7.76	7.75	7.83	7.82	7.83	0.76	0.60	0.68	2.95	2.94	2.96
KR	r	19	-6.04	-5.77	-5.97	8.00	8.10	8.05	8.15	8.15	8.14	0.81	0.88	0.81	3.26	3.21	3.24
	l	19	-6.71	-6.11	-6.54	8.00	8.00	8.00	8.10	8.12	8.11	0.85	0.86	0.80	3.26	3.27	3.29

KJ	r	19	-1.23	-1.22	-1.70	7.82	7.93	7.80	7.87	7.86	7.88	0.86	0.82	0.88	3.12	3.05	3.13
	l	19	-1.52	-1.06	-1.93	7.80	7.70	7.70	7.78	7.77	7.76	0.82	0.79	0.87	3.02	3.10	3.12
LP	r	21	-0.71	-0.52	-0.62	7.45	7.44	7.41	7.51	7.53	7.56	0.73	0.79	0.80	3.19	3.22	3.23
	l	21	-1.58	-1.87	-1.15	7.40	7.40	7.40	7.46	7.48	7.47	0.72	0.77	0.77	3.28	3.32	3.26
LD	r	19	-1.89	-2.17	-1.86	7.90	7.90	7.90	8.02	8.05	8.06	0.73	0.75	0.74	3.25	3.27	3.25
	l	19	-1.66	-1.76	-1.65	7.82	7.82	7.80	7.97	7.96	7.96	0.75	0.81	0.71	3.20	3.20	3.19
LT	r	19	0.56	0.41	0.30	7.70	7.71	7.70	7.85	7.86	7.81	0.96	0.96	0.90	3.02	3.02	3.07
	l	19	0.75	-0.09	0.25	7.70	7.69	7.70	7.77	7.77	7.75	0.78	0.86	0.85	3.01	3.13	2.99
MS	r	21	-1.54	-1.70	-1.79	7.50	7.50	7.45	7.62	7.58	7.57	0.75	0.73	0.69	3.15	3.09	3.15
	l	21	-1.48	-1.29	-1.43	7.57	7.57	7.54	7.65	7.63	7.65	0.70	0.66	0.69	3.11	3.09	3.10
MSh	r	19	0.44	0.30	-0.12	7.50	7.48	7.48	7.56	7.55	7.56	0.79	0.81	0.70	2.97	3.01	3.01
	l	19	0.58	0.11	-0.13	7.45	7.49	7.45	7.54	7.54	7.55	0.60	0.58	0.58	3.02	2.99	2.95
MA	r	27	-0.43	-0.62	-0.89	7.43	7.43	7.42	7.50	7.49	7.51	0.88	0.88	0.86	3.15	3.15	3.17
	l	27	-0.42	-0.31	-0.66	7.50	7.50	7.52	7.59	7.58	7.60	0.89	0.85	0.87	3.14	3.12	3.10
RB	r	22	-0.25	-0.35	-0.58	7.55	7.50	7.50	7.64	7.57	7.63	0.75	0.73	0.71	3.06	3.09	3.08
	l	22	-0.23	0.22	-0.31	7.50	7.50	7.50	7.60	7.58	7.60	0.69	0.72	0.71	3.11	3.06	3.04
SD	r	18	-0.25	-0.40	-0.25	7.90	7.90	7.84	7.97	7.95	7.95	0.88	0.88	0.86	2.91	2.92	2.98
	l	18	-0.52	0.04	0.22	7.90	7.89	7.87	7.94	7.93	7.92	0.79	0.76	0.82	2.92	2.93	2.94
SCr	r	19	-1.35	-1.64	-1.78	7.80	7.86	7.82	7.93	7.99	7.97	0.82	0.80	0.86	3.17	3.15	3.19
	l	19	-2.14	-1.57	-1.97	7.80	7.86	7.83	7.95	7.99	7.97	0.86	0.81	0.80	3.18	3.13	3.16
SJo	r	18	-0.45	-0.09	-0.56	7.43	7.43	7.43	7.53	7.51	7.51	0.95	0.91	0.93	3.05	3.03	3.02
	l	18	-0.33	0.21	-0.37	7.40	7.40	7.40	7.47	7.49	7.48	0.78	0.76	0.84	3.09	3.02	3.00
SG	r	19	-1.85	-1.87	-2.05	7.24	7.24	7.24	7.31	7.32	7.36	0.82	0.87	0.82	3.25	3.26	3.30
	l	19	-2.39	-2.01	-2.59	7.20	7.20	7.20	7.32	7.30	7.30	0.95	0.77	0.84	3.25	3.28	3.33
SJ	r	19	0.35	0.08	0.30	7.80	7.75	7.80	7.86	7.86	7.86	0.74	0.77	0.75	2.95	3.03	2.96
	l	19	0.16	0.15	0.42	7.87	7.85	7.85	7.92	7.93	7.93	0.84	0.77	0.77	2.98	2.96	2.96
SZ	r	21	-1.93	-1.76	-1.83	7.95	7.96	7.95	8.00	8.06	8.06	0.86	0.89	0.92	3.20	3.23	3.19
	l	21	-1.99	-1.61	-1.92	7.90	7.88	7.90	7.96	7.99	7.99	0.88	0.89	0.81	3.19	3.20	3.23
SV	r	19	-3.06	-3.10	-3.36	7.63	7.61	7.63	7.90	7.88	7.88	0.79	0.55	0.69	3.33	3.30	3.29
	l	19	-3.72	-3.72	-3.72	7.67	7.65	7.67	7.79	7.75	7.76	0.73	0.74	0.72	3.22	3.29	3.31
SC	r	19	0.62	-0.01	-0.81	7.60	7.60	7.60	7.70	7.69	7.71	0.78	0.77	0.81	3.04	3.06	3.06
	l	19	0.09	0.15	-0.98	7.60	7.60	7.60	7.73	7.67	7.67	0.74	0.82	0.75	3.04	3.03	3.05
SM	r	21	-1.12	-1.09	-1.53	8.10	8.08	8.08	8.18	8.18	8.19	0.95	0.88	0.89	3.07	3.10	3.10
	l	21	-1.21	-1.10	-1.59	8.00	8.04	8.03	8.09	8.11	8.13	0.87	0.88	0.84	3.12	3.11	3.17
SiJ	r	20	-1.02	-0.87	-1.60	7.64	7.64	7.65	7.84	7.83	7.81	0.98	0.85	0.80	3.11	3.09	3.13

	I	20	-0.58	-0.59	-1.43	7.66	7.66	7.70	7.78	7.78	7.80	0.88	0.86	0.86	3.11	3.05	3.10
SG	r	19	-0.49	-0.32	-0.63	7.85	7.77	7.76	7.87	7.88	7.90	0.72	0.72	0.73	3.03	3.06	3.07
	I	19	-0.37	-0.13	-0.59	7.85	7.71	7.75	7.87	7.84	7.85	0.56	0.65	0.74	3.08	3.12	3.13
VP	r	25	-1.93	-1.76	-1.83	7.95	7.96	7.95	8.00	8.06	8.06	0.86	0.89	0.92	3.20	3.23	3.19
	I	25	-1.99	-1.61	-1.92	7.90	7.88	7.90	7.96	7.99	7.99	0.88	0.89	0.81	3.31	3.20	3.23
ZB	r	20	0.54	0.49	-0.06	7.73	7.77	7.75	7.85	7.83	7.82	0.85	0.78	0.80	2.99	3.02	3.03
	I	20	0.86	0.91	0.54	7.85	7.85	7.85	7.94	7.94	7.92	0.82	0.78	0.64	2.96	3.00	3.01
CF	r	23	0.40	0.45	0.45	8.16	8.15	8.16	8.22	8.22	8.23	0.76	0.77	0.75	2.92	2.92	2.92
	I	23	0.50	0.51	0.52	8.07	8.08	8.08	8.12	8.15	8.15	0.73	0.76	0.75	2.98	3.07	3.07
HN	r	18	-3.89	-3.97	4.56	7.67	7.72	7.66	7.75	7.75	7.75	0.79	0.77	0.78	3.32	3.25	3.28
	I	18	-3.56	-3.44	-3.44	7.60	7.65	7.60	7.68	7.65	7.70	0.79	0.80	0.84	3.35	3.19	3.21
KM	r	18	0.18	-0.53	-0.12	8.10	8.12	8.12	8.19	8.21	8.20	0.83	0.90	0.85	2.88	2.85	2.89
	I	18	0.10	0.78	-0.26	8.09	8.10	8.10	8.17	8.21	8.17	0.73	0.85	0.79	2.85	2.85	2.83
JC	r	18	-0.16	0.08	0.06	7.83	7.80	7.86	7.93	7.93	7.92	0.75	0.74	0.76	3.02	2.99	2.98
	I	18	-0.78	-0.44	-0.72	7.77	7.80	7.78	7.88	7.88	7.87	0.77	0.79	0.75	3.02	2.96	3.00
CJ	r	23	-0.33	-1.00	-0.50	7.98	7.96	7.96	8.08	8.08	8.08	0.88	0.86	0.86	2.92	2.93	2.95
	I	23	-0.35	-0.91	-0.90	7.89	7.90	7.90	7.93	7.93	7.93	0.70	0.79	0.79	2.96	2.90	2.93
DT	r	28	0.54	0.55	0.58	7.91	7.90	7.90	8.02	8.00	7.97	0.80	0.80	0.79	3.00	3.00	3.03
	I	28	0.37	0.40	0.40	7.85	7.85	7.85	7.91	7.92	7.93	0.75	0.80	0.82	2.98	2.99	3.01
JF	r	24	-3.79	-4.03	-3.87	7.92	7.90	7.90	7.95	7.95	7.99	0.84	0.84	0.84	3.19	3.16	3.23
	I	24	-3.49	-3.51	-3.57	7.95	7.92	7.90	7.97	7.96	7.96	0.73	0.76	0.77	3.13	3.15	3.17
DS	r	27	-0.74	-0.82	-0.82	8.17	8.20	8.19	8.31	8.26	8.34	0.69	0.69	0.84	3.06	3.06	3.08
	I	27	-0.72	-0.80	-1.02	8.25	8.27	8.24	8.32	8.34	8.32	0.66	0.75	0.72	3.07	3.05	3.09
EM	r	20	0.61	0.59	0.60	7.73	7.60	7.60	7.70	7.72	7.70	0.78	0.83	0.83	2.91	2.98	2.98
	I	20	0.13	0.50	0.55	7.63	7.60	7.60	7.68	7.68	7.68	0.71	0.75	0.75	2.99	2.98	2.98
Atr	r	20	-3.72	-3.63	-3.89	7.67	7.67	7.60	7.69	7.69	7.66	0.76	0.76	0.74	3.32	3.30	3.36
	I	20	-3.83	-3.75	-3.77	7.63	7.65	7.61	7.71	7.70	7.67	0.75	0.76	0.70	3.31	3.31	3.38
RC	r	19	-0.80	-1.01	-0.84	7.85	7.92	7.91	7.94	7.94	7.93	0.90	0.90	0.90	3.03	3.03	3.01
	I	19	-1.05	-1.18	-1.14	7.88	7.90	7.89	7.98	7.97	7.98	0.89	0.88	0.94	3.04	3.03	3.07
AM	r	18	0.45	0.61	0.79	7.94	7.99	8.00	8.10	8.09	8.08	0.77	0.85	0.78	2.94	2.95	2.92
	I	18	0.71	0.52	0.30	7.95	8.00	8.00	8.02	8.06	8.08	0.75	0.72	0.73	2.94	2.88	2.94
ND	r	19	-0.41	0.42	0.34	7.96	7.95	7.92	8.05	8.05	8.02	0.86	0.86	0.83	2.99	2.98	3.01
	I	19	-0.02	0.56	0.30	7.91	7.90	7.90	8.00	8.01	7.99	0.79	0.78	0.79	2.99	2.98	3.01

Esc (D) = objective refractive error (Canon Autorefr R-1); K (mm) = central corneal radius of curvature measurements (Rodenstock); Ke (mm) = central corneal radius of curvature measurements (EyeSys); ρ = corneal asphericity (EyeSys) and Al/k (mm) = ratio of axial length to corneal curvature (ultrasound and Rodenstock keratometer).

APPENDIX 7 – Data relating to peripheral refractive error, retinal curvature and retinal shape

<i>Px</i>	<i>Eye</i>	<i>Age</i>	<i>PAF1</i>	<i>PAF3</i>	<i>Retp1</i>	<i>Retp2</i>	<i>Retp3</i>	<i>Retr1</i>	<i>Retr2</i>	<i>Retr3</i>	<i>PRE1</i>		<i>PRE3</i>	
											<i>t</i>	<i>n</i>	<i>t</i>	<i>n</i>
AB	r	18	110.66	117.03	1.31	1.34	1.56	14.51	12.54	12.81	-0.02	-0.31	1.19	-0.33
	l	18	98.37	114.70	1.61	1.69	0.68	13.71	13.30	12.77	0.19	-0.75	0.41	0.5
AT	r	27	124.99	39.65	2.07	6.57	5.69	15.54	25.29	21.72	1.69	0.23	0.01	0.15
	l	27	83.46	33.85	1.83	3.33	3.60	15.90	17.43	18.62	-1.56	-0.43	-0.21	-0.28
AK	r	21	73.30	76.85	0.55	0.22	2.49	13.83	12.52	15.89	-1.19	-0.84	-1.22	-0.97
	l	21	79.34	80.81	0.64	-1.61	0.75	14.36	8.73	13.61	-1.01	-0.80	-0.95	-1.11
AD	r	19	-15.80	12.01	7.22	0.51	-0.76	27.46	13.70	11.72	0.77	0.27	0.62	0.33
	l	19	56.11	49.57	0.33	0.95	1.07	12.43	13.35	13.72	0.42	0.53	0.39	0.75
BS	r	19	43.53	49.53	2.18	2.29	2.05	15.43	15.30	14.27		-0.75	0.78	-0.18
	l	19	80.44	74.64	1.10	1.92	1.24	13.07	14.46	13.64	0.04	-1.21	-0.48	-0.41
BG	r	16	136.67	119.15	2.22	3.37	0.63	15.90	18.39	13.36	-4.88	0.60	-5.02	0.02
	l	16	90.81	112.37	3.55	0.98	0.65	19.86	16.25	14.89	-5.28	-0.82	-4.74	-0.44
DP	r	19	65.01	40.92	4.89	1.45	0.31	20.50	13.07	13.24	-2.11	-1.74	0.55	-0.59
	l	19	70.89	79.67	2.71	2.24	1.69	14.96	14.33	13.28	-0.33	-1.36	0.53	-0.45
DW	r	20	106.25	29.65	-1.04	2.61	4.15	9.27	14.90	16.41	1.75	-0.29	3.05	-0.25
	l	20	112.17	50.35	-0.92	3.51	1.37	10.49	16.96	13.48	0.13	-0.21	-1.13	-0.96
DL	r	19	129.56	85.42	1.82	-0.35	3.20	13.22	8.91	14.56	1.68	2.51	3.05	2.1
	l	19	107.02	231.61	0.92	2.41	2.11	11.69	15.08	11.64	1.29	1.46	2.23	2.51
GC	r	18	90.49	44.96	1.44	1.49	2.49	13.52	14.51	15.66	-0.34	-0.25	0.12	0.21
	l	18	73.58	45.90	1.68	0.47	0.58	14.58	12.27	12.55	-0.19	-0.58	-0.06	-0.21
GK	r	19	31.20	94.77	3.21	3.38	2.86	18.04	17.23	16.20	-1.29	0.79	-0.87	0.63
	l	19	45.37	28.38	1.74	0.72	1.04	14.39	12.79	8.97	0.27	1.49	0.81	1.17
Gke	r	23	101.10	-8.74	0.95	2.63	3.93	11.95	16.84	19.57	1.98	0.54	3.1	0.83
	l	23	87.06	50.84	2.01	1.49	1.63	14.46	14.44	13.52	3.87	0.54	2.76	0.67
HS	r	18	30.38	67.70	2.20	1.66	2.63	16.45	15.06	16.18	-1.45	0.18	-1.12	-1.25
	l	18	71.83	75.66	1.76	2.82	2.28	14.92	16.80	15.86	-0.56	-0.10	-0.47	-0.43
IP	r	24	108.41	88.36	-0.03	-0.15	-0.16	11.04	11.49	12.93	-1.96	-1.88	-1.21	-1.85
	l	24	107.23	80.52	2.03	1.21	1.46	15.55	13.78	14.38	-1.63	-2.18	-1.11	-1.46
JS	r	21	138.26	115.31	0.27	0.08	-0.11	11.30	9.79	9.91	-1.65	-1.71	-0.1	-1.02
	l	21	163.95	116.54	0.50	6.79	0.78	9.18	21.21	10.85	-0.95	-1.65	-0.82	-0.72
KR	r	19	126.05	82.03	1.22	1.21	1.15	13.15	12.43	11.50	1.29	-0.31	1.1	0.47

	l	19	121.23	104.86	-0.07	2.04	1.37	11.02	14.48	12.85	0.38	-1.06	1.72	0.06
KJ	r	19	103.80	69.09	2.04	1.33	1.06	13.82	13.32	12.24	-0.15	0.77	0.27	2.18
	l	19	122.66	97.88	0.02	1.29	0.54	9.62	13.40	10.78	0.52	0.85	-0.31	-0.66
LP	r	21	80.07	78.65	0.48	1.09	1.20	12.23	12.99	13.45	0.70	-0.07	0.39	-0.18
	l	21	79.67	88.20	2.02	1.48	1.51	14.33	13.39	13.59	0.83	-0.07	0.72	0.48
LD	r	19	81.50	48.06	0.72	2.04	2.78	13.01	15.56	17.13	0.00	0.06	1.82	1.21
	l	19	54.35	46.55	1.37	1.66	1.57	14.51	14.43	14.50	0.39	1.04	0.14	1.08
LT	r	19	57.53	49.74	0.45	1.56	1.59	12.52	13.87	13.11	-0.90	-0.42	1.85	0.52
	l	19	78.03	100.33	-0.80	0.87	0.68	11.11	12.59	11.63	1.75	0.05	0.81	0.13
MS	r	21	70.07	38.02	0.99	1.79	1.80	12.03	14.19	14.21	2.91	1.58	1.95	1.19
	l	21	95.80	47.29	0.37	2.56	1.97	10.03	15.07	13.80	0.86	0.50	2.14	1.25
MSh	r	19	89.75	54.31	1.64	1.69	1.27	14.46	13.46	12.79	-1.45	-2.27	-0.46	-0.16
	l	19	127.52	47.98	1.36	2.03	1.52	13.74	14.05	13.68	-0.77	-2.35	0.15	-1.44
MA	r	27	125.52	82.28	1.08	1.03	1.87	13.54	12.96	13.78	-1.74	-2.36	0.19	-0.67
	l	27	118.50	103.27	1.99	1.30	0.63	15.20	14.55	12.94	-1.23	-3.18	-1.14	-1.59
RB	r	22	131.69	69.29	0.34	3.03	2.39	11.71	15.69	13.72	2.17	-1.25	-0.62	-0.41
	l	22	110.86	57.25	0.37	3.11	0.56	12.21	16.01	12.43	0.56	-1.56	0.47	-0.45
SD	r	18	111.52	61.45	-2.19	-0.61	-0.35	8.35	9.10	10.99	-1.56	-1.17	1.12	-1.01
	l	18	99.92	80.28	-1.12	-0.29	1.90	10.61	10.77	15.09	-1.52	-1.06	-1.3	-0.84
SCr	r	19	86.57	77.54	1.58	0.42	0.94	13.44	10.19	12.10	0.29	0.60	0.35	0.88
	l	19	111.19	73.54	0.32	1.02	0.73	10.80	11.67	11.62	0.52	1.77	0.41	0.72
SJo	r	18	106.66	96.15	-1.61	2.97	2.65	9.05	15.30	14.53	-0.80	-0.61	1.257	-0.1
	l	18	68.19	69.42	-0.11	2.91	3.60	11.05	15.37	15.88	-0.58	-0.83	0.87	0.1
SG	r	19	56.76	53.94	0.71	3.35	0.96	12.66	16.67	14.15	-0.34	0.89	0.22	0.87
	l	19	81.54	68.27	-0.73	0.95	1.90	10.67	12.70	14.39	0.09	0.62	0.76	0.64
SJ	r	19	87.79	34.91	1.36	1.71	2.94	12.95	13.52	16.39	-0.64	0.03	0.42	0.15
	l	19	72.81	57.74	1.93	2.24	1.45	14.08	14.16	13.81	-0.89	-0.05	-0.59	0.23
SZ	r	21	104.33	74.68	0.95	1.12	1.40	13.26	13.90	14.15	0.79	-0.88	-1.1	0.03
	l	21	82.03	37.73	1.74	1.99	2.97	16.17	15.38	17.34	0.66	-1.63	1.01	1.2
SV	r	19	56.02	34.83	1.61	1.95	1.34	14.32	15.59	14.16	1.90	1.50	0.34	2.1
	l	19	39.81	27.85	0.95	0.66	1.90	12.40	12.43	14.04	1.20	1.08	0.79	1.92
SC	r	19	90.41	53.04	1.19	1.13	2.29	14.49	12.53	14.04	-0.65	-1.77	-0.1	-0.39
	l	19	88.08	31.73	2.08	2.24	2.56	13.94	14.36	14.58	-0.40	-0.69	0.31	1.86
SM	r	21	67.09	45.00	2.07	4.45	2.49	16.81	22.34	16.48	-1.63	-0.75	0.18	-0.09
	l	21	45.33	40.51	2.99	4.94	2.35	17.37	20.75	15.92	-0.14	-0.41	0.6	0.41

Sij	r	20	68.03	55.00	-0.61	4.13	0.52	10.80	13.41	10.12	0.33	1.47	1.61	1.39
	l	20	44.26	60.00	1.70	1.99	-0.17	15.20	14.57	10.71	0.06	0.62	0.75	0.97
SG	r	19	99.59	50.76	-1.30	1.42	1.21	11.40	14.96	15.01	-2.39	-0.56	-0.46	-0.67
	l	19	89.79	44.55	0.22	0.95	1.08	14.34	15.35	16.32	-2.86	-1.22	-1.64	-0.18
VP	r	25	104.33	74.68	0.95	1.12	1.40	13.26	13.90	14.15	0.79	-0.88	-1.1	0.03
	l	25	82.03	37.73	1.74	1.99	2.97	16.17	15.38	17.34	0.66	-1.63	1.01	1.2
ZB	r	20	100.61	91.67	2.83	1.79	-0.66	15.73	13.16	10.34	-1.35	-0.64	-0.58	-0.63
	l	20	48.06	125.03	6.83	2.29	-0.16	23.08	13.74	10.00	-1.01	-0.69	-0.81	-0.22
CF	r	23	95.10	100.32	1.09	1.00	1.15	12.22	12.01	12.35	0.24	-0.48	-0.3	-0.55
	l	23	150.63	84.60	0.27	0.89	1.05	10.22	11.75	12.20	0.27	0.42	-0.28	-0.19
HN	r	18	72.36	67.21	1.04	1.47	0.96	11.73	11.10	11.94	2.92	3.71	1.41	3.28
	l	18	70.36	76.11	0.72	4.18	0.52	11.05	17.75	11.14	2.63	3.72	2.42	2.05
KM	r	18	43.73	139.98	1.52	-0.39	0.01	13.70	9.40	9.86	-0.77	0.92	-0.93	0.99
	l	18	136.59	91.79	0.18	0.67	2.07	11.61	12.72	14.09	-0.80	0.24	-0.82	1.19
JC	r	18	49.25	26.17	1.88	2.00	2.50	14.21	14.50	14.97	0.14	-0.30	0.71	-0.7
	l	18	47.65	11.52	2.38	2.89	2.26	15.06	15.31	15.22	0.68	-0.34	0.91	-0.41
CJ	r	23	108.90	48.80	0.99	0.93	0.34	12.13	12.08	11.13	-0.67	-0.31	0.47	0.24
	l	23	125.81	95.75	0.88	1.79	0.04	12.06	11.94	9.79			1.29	1.45
DT	r	28	93.43	86.85	0.33	-0.52	0.89	10.65	8.99	12.37	-1.28	-1.01	-1.03	-0.35
	l	28	105.06	102.78	-0.35	1.04	-1.87	9.75	12.33	8.26	-0.93	-0.43	-0.45	-2.53
JF	r	24	106.41	93.92	-0.61	-0.02	0.06	9.68	10.62	11.18	-0.27	0.95	0.61	1.41
	l	24	149.98	130.71	-1.52	0.17	-1.17	7.78	9.38	5.26	-1.10	0.55	2.39	1.28
DS	r	27	26.05	23.15	1.80	2.47	4.64	15.55	16.83	20.39	-1.08	0.87	-0.55	0.11
	l	27	22.13	-2.65	3.33	3.01	4.33	18.49	17.68	19.47	-0.64	1.14	-0.31	0.16
EM	r	20	43.73	5.84	2.99	3.18	1.01	16.56	16.82	14.28	-1.75	-0.60	-1.12	0.74
	l	20	82.28	31.97	0.70	1.08	0.82	12.37	12.87	12.99	-1.47	1.31	-1.48	1.41
Atr	r	20	141.69	24.95	1.01	3.26	2.63	12.05	18.57	17.20	1.90	1.20	1.13	-0.65
	l	20	78.07	127.85	2.17	1.52	1.13	14.40	13.22	12.59	1.24	1.55	1.86	-1.62
RC	r	19	92.37	52.43	2.23	1.48	2.11	14.69	14.51	15.42	-1.13	-0.31	1.02	2.58
	l	19	79.42	68.11	1.53	1.74	1.80	13.82	14.15	14.28	-1.57	-0.15	-0.16	0.61
AM	r	18	46.39	98.74	3.16	3.20	0.17	16.42	17.93	12.84	-3.46	-1.07	-2.99	-0.29
	l	18	86.57	56.88	0.77	1.42	2.02	13.39	14.80	15.69	-2.23	0.61	-3.04	-0.1
NID	r	19	100.90	76.20	0.00	1.43	1.47	10.17	13.38	13.86	1.74	0.45	0.99	-0.25
	l	19	51.78	61.09	0.91	2.75	1.73	12.75	14.83	13.78	1.71	0.69	0.35	0.02

PAF = peripheral astigmatic factor; retp = retinal asphericity; retr (mm) = retinal apical radius and PRE (D) = relative peripheral refractive error.

APPENDIX 8 – Data relating to accommodation

<i>Px</i>	<i>Eye</i>	<i>A of A1</i>	<i>A of A3</i>	<i>AEI1</i>	<i>AEI3</i>	<i>SR slope1</i>	<i>SR slope3</i>
AB	r	8.92	10.17	0.88	0.18	0.98	0.87
AT	r	9.83	12	0.16		0.84	
AK	r	8.67	7.83	0.78	0.28	0.82	0.85
AD	r	10.5	12	0.40	0.15	0.71	0.85
BS	r	10.25	9.25	0.59	0.32	0.75	0.71
DP	r	8.67	11	0.41	0.39	0.84	0.74
DW	r	8	7.67	0.40	0.32	0.79	0.8
DL	r	11.67	11.67	0.71	0.35	0.73	0.81
GC	r	9.75	10	0.21	0.30	0.79	0.79
GKe	r	10.33	12	0.41	0.31	0.76	0.78
GK	r	8.5	9.5	0.40	0.26	0.74	0.75
HS	r	13	12.25	0.47	0.53	0.77	0.8
IP	r	9.67	8.5	0.24	0.30	0.8	0.75
JS	r	7.75	7	0.32	0.28	0.9	0.8
KR	r	13	15	0.41	0.26	0.82	0.73
KJ	r	8.5	11	0.46	0.39	0.74	0.73
LP	r	14	13	0.68	0.83	0.92	0.81
LD	r	13	13	0.55	0.40	0.75	0.96
LT	r	10	10.5	0.39	0.42	0.86	0.74
MS	r	10	9.5	0.55	0.49	0.89	0.75
MSh	r	9	10		0.30		0.81
MA	r	5	7.25	0.27	0.26	0.77	0.78
RB	r	8.58	9	0.37	0.24	0.82	0.78
SD	r	11	10.33	0.52	0.36	0.73	0.77
SCr	r	12	9.17	0.24	0.25	0.84	0.79
SJo	r	9	10.5	0.42	0.28	0.73	0.75
SG	r	16.33	16		1.31		0.4
SZ	r	13.33	11.5	0.55	0.70	0.62	0.52
SV	r	12	12.67		0.25		0.89
SC	r	10.5	10	0.50	0.36	0.86	0.88
SM	r	9.5	10.83	0.26	0.35	0.78	0.83
Sij	r	10.33	9	0.46	0.26	0.8	0.75
SGr	r	11	11	0.44	0.27	0.74	0.78
VP	r	13.33	11.5	0.55	0.70	0.62	0.52
ZB	r	6.33	6.5	0.67	0.28	0.71	0.8
KM	r	10.17	10.66	0.45	0.26	0.87	0.74
JC	r	8.83	10.33	0.45	0.34	0.69	0.83
CJ	r	10.33	8.75	0.50	0.44	1.03	1.06
DT	r	8.5	8	0.84	0.43	0.71	0.68
JF	r	12	15	0.51	0.22	0.93	0.82
DS	r	9.5	12	0.84	0.87	0.8	0.94
EM	r	9.33	11	0.49	0.53	0.81	0.82
RC	r	11	9.5	0.41	0.33	0.78	0.83
AM	r	13.67	11.5	0.31	0.30	0.75	0.79
ND	r	12	10.5	0.54	0.36	0.81	0.71

A of A (D) = amplitude of accommodation (RAF rule); AEI = accommodative error index and SR slope (D) = accommodative stimulus response curve gradient.

APPENDIX 9 – Data relating to intraocular pressure and ocular blood flow

<i>Px</i>	<i>Eye</i>	<i>IOP</i>	<i>PA</i>	<i>PR</i>	<i>PV</i>	<i>OBF</i>
AB	r	11.30	3.20	68.00	8.10	20.20
AT	r	15.30	3.90	70.00	7.60	17.20
AK	r	14.50	2.40	73.00	5.00	12.50
AD	r	8.20	2.10	61.00	7.10	18.20
DP	r	10.40	3.30	55.00	8.90	17.40
DW	r	11.30	2.50	84.00	6.40	25.00
DL	r	9.20	1.70	75.00	5.50	16.50
GC	r	12.00	2.40	75.00	6.00	20.40
GKe	r	13.70	2.40	68.00	5.30	14.10
GK	r	14.90	1.20	80.00	2.60	8.00
HS	r	12.10	2.80	67.00	7.50	15.20
IP	r	12.40	4.20	67.00	9.60	21.00
JS	r	13.30	3.80	72.00	8.40	18.10
KR	r	12.20	2.30	63.00	5.60	14.90
KJ	r	13.70	2.40	68.00	5.30	14.10
LP	r	18.20	1.40	66.00	2.30	10.50
LD	r	12.20	2.50	71.00	3.00	12.00
LT	r	10.70	2.80	63.00	7.50	17.10
MS	r	13.70	2.40	68.00	5.30	14.10
MSh	r	11.70	4.50	63.00	10.60	23.00
MA	r	11.20	3.30	67.00	8.30	19.90
RB	r	7.00	1.80	77.00	7.00	22.00
SD	r	11.40	3.90	59.00	9.60	21.20
SCr	r	16.90	2.40	81.00	4.40	12.70
SJo	r	16.10	3.70	70.00	6.90	17.30
SG	r	13.00	2.70	78.00	6.10	16.90
SJ	r	18.70	3.20	69.00	4.50	12.80
SZ	r	20.70	1.40	66.00	2.30	6.50
SV	r	14.90	1.20	82.00	2.60	7.10
SC	r	12.00	2.40	70.00	6.00	18.60
SM	r	15.30	3.90	70.00	7.60	17.20
SiJ	r	16.00	3.00	64.00	5.70	12.30
SGr	r	20.70	3.20	69.00	5.00	13.00
VP	r	20.70	1.40	66.00	2.30	18.00
ZB	r	13.30	3.80	72.00	8.40	20.70
CF	r	10.00	5.00	72.00	6.00	21.00
HN	r	16.40	3.20	65.00	6.00	13.90
KM	r	9.70	5.20	70.00	13.80	33.20
JC	r	12.90	3.20	63.00	7.20	17.70
CJ	r	8.30	6.20	41.00	17.80	25.70
DT	r	11.40	3.10	70.00	7.70	18.00
JF	r	7.70	1.40	76.00	5.10	13.80
DS	r	12.70	1.10	105.00	2.60	10.60
EM	r	12.50	4.30	65.00	8.10	18.00
ATr	r	7.70	1.40	72.00	5.10	13.80
RC	r	19.30	4.20	71.00	6.80	16.70
AM	r	9.80	2.60	68.00	7.50	17.40
ND	r	12.50	4.30	59.00	9.80	21.30

IOP (mmHg) = intraocular pressure; PA (mmHg) = pulse amplitude; PV (μ l) = pulse volume; PR (beats/min) = pulse rate and OBF (μ l/s) = ocular blood flow.

APPENDIX 10 – Data relating to crystalline lens curvature and shape

<i>Px</i>	<i>Eye</i>	<i>Antp1</i>	<i>Antr1</i>	<i>Postp1</i>	<i>Postr1</i>	<i>Antp3</i>	<i>Antr3</i>	<i>Postp3</i>	<i>Postr3</i>
AB	r	0.26	13.30	-0.22	-9.35	0.25	14.49	-0.24	-11.32
AT	r	0.22	9.92	-0.18	-9.22	0.19	9.56	-0.19	-9.51
AK	r	0.28	10.89	-0.23	-11.92				
AD	r	0.23	11.86	-0.20	-11.49	0.22	11.12	-0.17	-8.27
DP	r	0.36	20.12	-0.26	-11.19				
DW	r	0.31	13.26	-0.19	-9.89	0.31	17.77	-0.19	-8.92
DL	r	0.28	12.81	-0.25	-15.99	0.24	14.43	-0.17	-6.56
GC	r	0.26	13.67	-0.24	-10.81	0.19	9.98	-0.17	-7.16
GKe	r	0.27	13.98	-0.18	-11.85	0.29	16.92	-0.18	-8.42
GK	r	0.23	9.46	-0.24	-14.73	0.21	12.28	-0.19	-8.17
HS	r	0.28	14.88	-0.27	-11.84				
IP	r	0.26	16.94	-0.18	-9.61				
JS	r	0.33	18.53	-0.19	-8.19				
KR	r	0.33	18.85	-0.17	-7.12	0.32	17.46	-0.19	-9.21
KJ	r	0.24	16.75	-0.20	-10.54	0.23	13.36	-0.18	-7.10
LP	r	0.32	17.30	-0.21	-7.52	0.25	14.60	-0.21	-8.81
LD	r								
LT	r	0.22	11.80	-0.18	-10.04				
MS	r	0.41	22.02	-0.36	-17.76	0.29	16.17	-0.38	-18.43
MSh	r	0.36	19.55	-0.22	-11.28	0.33	16.56	-0.21	-10.48
MA	r	0.28	11.69	-0.21	-12.27				
RB	r	0.27	17.68	-0.21	-11.28				
SD	r	0.34	15.15	-0.22	-11.63				
SCr	r	0.32	11.94	-0.21	-9.36	0.29	16.17	-0.38	-18.43
SJo	r	0.33	13.14	-0.26	-13.38				
SG	r	0.25	10.90	-0.19	-10.04				
SJ	r	0.28	15.63	-0.18	-8.21				
SZ	r	0.23	11.44	-0.17	-8.51	0.23	12.49	-0.18	-7.97
SV	r	0.26	18.49	-0.30	-15.33	0.25	14.80	-0.22	-9.72
SC	r	0.32	11.52	-0.25	-14.02				
SM	r	0.27	13.17	-0.19	-12.00	0.28	15.76	-0.19	-8.15
SiJ	r	0.30	20.53	-0.23	-11.71	0.28	15.13	-0.18	-8.65
SGr	r	0.28	8.62	-0.23	-13.31	0.17	9.99	-0.16	-6.21
VP	r	0.23	11.47	-0.17	-8.52	0.23	12.51	-0.18	-7.97
ZB	r	0.29	12.40	-0.25	-13.53				
CF	r								
HN	r	0.29	17.57	-0.17	-7.93	0.28	16.31	-0.17	-7.84
KM	r	0.24	13.65	-0.25	-10.03				
JC	r	0.24	9.81	-0.18	-8.66	0.28	15.96	-0.21	-9.50
CJ	r	0.27	15.18	-0.12	-6.57				
DT	r	0.28	14.91	-0.18	-8.29				
JF	r	0.26	14.14	-0.20	-8.22	0.24	13.00	-0.17	-7.79
DS	r	0.24	12.35	-0.18	-8.16	0.27	14.51	-0.22	-10.19
EM	r	0.34	18.15	-0.30	-14.28				
ATr	r	0.27	15.19	-0.23	-11.71	0.19	9.61	-0.21	-10.64
RC	r	0.30	16.47	-0.22	-10.10	0.25	13.86	-0.18	-7.46
AM	r	0.34	16.34	-0.23	-8.11				
ND	r	0.25	13.85	-0.19	-8.87				

Antp1 and 3 = anterior lens surface asphericity at initial and final visit; Postp1 and 3 = posterior lens surface asphericity at initial and final visit; Antr1 and 3 (mm) = anterior lens surface apical radius at initial and final visit and Postr1 and 3 (mm) = posterior lens apical radius at initial and final visit.

RELATIVE PERIPHERAL REFRACTIVE ERROR IN ADULT MYOPIA AND EMMETROPIA

((J.Love, B.Gilmartin, M.C.M.Dunne)) Neurosciences Research Institute, Aston University, Birmingham, U.K.

Purpose. Mutti *et al.* (1997; ARVO, 5399) assessed retinal shape in children by measuring relative peripheral refractive error (PRE) at 30° in nasal gaze. We report here on the equivalent mean sphere PRE relative to central equivalent mean sphere refractive error measured in adults, at 35°, in both the nasal and temporal meridia. PRE is used as an index of eye shape to compare eye shape in emmetropia and myopia. **Methods.** Measurements were obtained using an open-view objective IR autorefractor and mean spheres derived by a matrix transformation. Two drops of 1% tropicamide were instilled to induce cycloplegia and mydriasis. The relative PREs were compared in 20 young adult myopes, i.e. 40 eyes [mean (D sph.equiv.) = -2.23 ± 1.60 ; range -0.50 to -7.38] and 20 emmetropes, i.e. 40 eyes [mean (D sph.equiv.) = $+0.21 \pm 0.26$; range +0.50 to -0.25]. **Results.** Eighty-five percent of emmetropic subjects showed relative myopia in both the nasal meridian ($-0.89 \pm 0.93D$) and temporal meridian ($-0.94 \pm 1.09D$). Seventy-eight percent of myopic subjects showed greater relative hyperopia in both nasal meridian ($+0.64 \pm 1.12D$) and seventy percent in the temporal meridian ($+0.52 \pm 1.71D$). A significant positive correlation was found between relative PRE at 35° and central subjective refraction both nasally ($r=0.53$, $p<0.002$) and temporally ($r=0.55$, $p<0.002$). A two-factor split-plot ANOVA indicated that the difference in PREs between myopes and emmetropes was significant ($p<0.001$). **Conclusions.** The data suggest that emmetropic subjects have an oblate retinal shape and myopic subjects have a prolate retinal shape and that the retina becomes more prolate with increasing myopia. The findings demonstrate further that longitudinal, rather than transverse, stretching of the posterior segment is the principle structural correlate of myopia.

None.

Appendix 12 – Ocular volume

The eye is divided into 5 parts

Total volume is the sum of:

V1 = volume of corneal section of the eye

V2 = volume of the anterior nasal part

V3 = volume of the anterior temporal part

V4 = volume of the posterior nasal part

V5 = volume of the posterior temporal part

INPUT PARAMETERS	EMMETROPE	MYOPE
Refractive error (D)	+0.13	-4.13
Horizontal visible iris diameter (mm)	11.71	11.61
Corneal apical radius (mm)	7.57	7.79
Corneal asphericity	0.73	0.73
Nasal retinal contour	$y = -0.045 - 0.032 + 23.08$	$y = -0.056 + 0.028 + 23.15$
Temporal retinal contour	$y = -0.064 + 0.169 + 24.63$	$y = -0.041 + 0.044 + 24.67$

RESULTS

Emmetrope volume (mm^3) = 5.30×10^3

Myope volume (mm^3) = 5.91×10^3

Calculation for eye volume

The eye is divided into 5 parts

Total volume is the sum of:

V1 = volume of corneal section of eye

V2 = volume of the anterior nasal part

V3 = volume of the anterior temporal part

V4 = volume of the posterior nasal part

V5 = volume of the posterior temporal part

Horizontal visible iris diameter = I

r_0 = apical radius

The cornea is defined by the equation

$$y^2 = 2r_0x - px^2$$

For posterior nasal part of eye

$$y = gx^2 + hx + i$$

For posterior temporal part of eye

$$y = jx^2 + kx + l$$

INPUT PARAMETERS

$$I := 12$$

$$r_0 := 7.72$$

$$g := -0.089$$

$$j := -0.076$$

$$p := 0.79$$

$$h := -0.431$$

$$k := 0.258$$

$$i := 23.72$$

$$l := 23.685$$

$$x_1 := \frac{I}{2}$$

$$r := \frac{r_0}{p}$$

$$a := 0.269$$

$$d := 0.398$$

$$b := 3.609$$

$$e := -5.409$$

$$x_1 = 6$$

$$r = 9.772$$

$$c := 16.395 - 15$$

$$f := 23.134 - 15$$

$$c = 1.395$$

$$f = 8.134$$

To calculate the volume of the corneal section of the eye

$$V1 := \pi \cdot \sqrt{p} \cdot \left[\left[r(r+x_1) \cdot \sqrt{2 \cdot x_1 \cdot r - (x_1)^2} \right] - \frac{\left[2 \cdot x_1 \cdot r - (x_1)^2 \right]^{\frac{3}{2}}}{3} - \left(r^3 \cdot \operatorname{asin} \left(\frac{x_1 - r}{r} \right) \right) - \frac{\pi \cdot r^3}{2} \right]$$

$$V1 = 137.384$$

To calculate the volume of the front nasal part of the eye

$$y_1 := 0.269 \cdot x^2 + 3.609 \cdot x + 16.395 - 15$$

$$x_3 := \frac{-b + \sqrt{b^2 - 4 \cdot a \cdot c}}{2 \cdot a}$$

$$x_4 := \frac{-b - \sqrt{b^2 - 4 \cdot a \cdot c}}{2 \cdot a}$$

$$x_3 := -0.398$$

$$x_4 := -13.081$$

$$x_2 := x_4$$

$$x_2 = -13.081$$

$$V2 := \frac{\pi}{12} \cdot \left[3 \cdot a \cdot \left[(x_2)^4 - (x_1)^4 \right] + \left[(x_2)^3 - (x_1)^3 \right] \cdot 2 \cdot b \right]$$

$$V2 = 1.217 \cdot 10^3$$

To calculate volume of the front temporal part of the eye

$$y_2 := 0.398 \cdot x^2 - 5.409 \cdot x + 23.134 - 15$$

$$x_5 := \frac{-e + \sqrt{e^2 - 4 \cdot d \cdot f}}{2 \cdot d}$$

$$x_6 := \frac{-e - \sqrt{e^2 - 4 \cdot d \cdot f}}{2 \cdot d}$$

$$x_5 := 11.868$$

$$x_6 := 1.722$$

$$x_{23} := x_5$$

$$x_{23} := 11.868$$

$$V3 := \frac{\pi}{12} \cdot \left[3 \cdot d \cdot \left[(x_{23})^4 - (x_1)^4 \right] + \left[(x_{23})^3 - (x_1)^3 \right] \cdot 2 \cdot e \right]$$

$$V3 = 1.674 \cdot 10^3$$

To calculate volume of the back nasal part of the eye

$$x_{24} := 0 \quad m := i - 15 \quad m := 8.72$$

$$x_7 := \frac{-h + \sqrt{h^2 - 4 \cdot g \cdot m}}{2 \cdot g}$$

$$x_8 := \frac{-h - \sqrt{h^2 - 4 \cdot g \cdot m}}{2 \cdot g}$$

$$x_7 := -12.612$$

$$x_8 := 7.769$$

$$x_{14} := x_7$$

$$x_{14} := -12.612$$

$$V_4 := \frac{\pi}{12} \cdot \left[3 \cdot g \cdot \left[(x_{24})^4 - (x_{14})^4 \right] + \left[(x_{24})^3 - (x_{14})^3 \right] \cdot 2 \cdot h \right]$$

$$V_4 = 1.316 \cdot 10^3$$

To calculate volume of the back temporal part of the eye

$$x_{25} := 0$$

$$n := 1 - 15$$

$$n = 8.685$$

$$x_9 := \frac{-k + \sqrt{k^2 - 4 \cdot j \cdot n}}{2 \cdot j}$$

$$x_9 = -9.127$$

$$x_{10} := \frac{-k - \sqrt{k^2 - 4 \cdot j \cdot n}}{2 \cdot j}$$

$$x_{10} = 12.521$$

$$x_{15} := x_{10}$$

$$x_{15} = 12.521$$

$$V_5 := \frac{\pi}{12} \cdot \left[3 \cdot j \cdot \left[(x_{25})^4 - (x_{15})^4 \right] + \left[(x_{25})^3 - (x_{15})^3 \right] \cdot 2 \cdot k \right]$$

$$V_5 = 1.202 \cdot 10^3$$

Total volume of eye = V

$$V := V_1 + V_2 + V_3 + V_4 + V_5$$

$$V = 5.546 \cdot 10^3$$